NASA TECHNICAL MEMORANDUM

NASA TM X-1415

NASA TM X-1415

GPO PRICE $ _____

CFSTI PRICE(S) $ 3.00

Hard copy (HC) _____

Microfiche (MF) _____

ff 653 July 65

FACILITY FORM 602

N67-27306 (ACCESSION NUMBER)

44 (PAGES)

(NASA CR OR TMX OR AD NUMBER)

1 (THRU)

(CODE)

2 (CATEGORY)

PROJECT FIRE FLIGHT 1 VIBRATION DATA

by

Herbert A. Leybold and Henry T. Thornton, Jr.

Langley Research Center
Langley Station, Hampton, Va.

and

Robert N. Hancock and E. D. Griffith

Ling-Temco-Vought, Inc., Vought Aeronautics Division
Dallas, Texas

NATIONAL AERONAUTICS AND SPACE ADMINISTRATION • WASHINGTON, D. C. • OCTOBER 1967

NASA TM X-1415

PROJECT FIRE FLIGHT 1 VIBRATION DATA

By Herbert A. Leybold and Henry T. Thornton, Jr.

Langley Research Center
Langley Station, Hampton, Va.

and

Robert N. Hancock and E. D. Griffith

Ling-Temco-Vought, Inc., Vought Aeronautics Division
Dallas, Texas

NATIONAL AERONAUTICS AND SPACE ADMINISTRATION

For sale by the Clearinghouse for Federal Scientific and Technical Information
Springfield, Virginia 22151 – CFSTI price $3.00

PROJECT FIRE FLIGHT 1 VIBRATION DATA

By Herbert A. Leybold and Henry T. Thornton, Jr.
Langley Research Center

and

Robert N. Hancock and E. D. Griffith
Ling-Temco-Vought, Inc., Vought Aeronautics Division

SUMMARY

Three channels of vibration data were recorded during Project Fire Flight 1. An analog type reduction of the data was made under NASA contract NAS1-1946 and consisted of determining, in engineering units, such quantities as power spectral density, average spectral density, probability density, auto-correlation, cross-correlation, and cross-power spectral density for significant events during the flight. The results of this analysis are presented.

INTRODUCTION

The first Project Fire space vehicle was launched at Cape Kennedy, Florida. The primary purpose of the flight was to measure convective and radiative heating during reentry into the Earth's atmosphere at a velocity of approximately 37 000 feet per second (11.3 km/sec). Of secondary interest was the measurement of shock and vibration environments during the launch phase of the flight. The purpose of these measurements was to obtain data for evaluation of preflight test levels used for qualification and flight acceptance testing of the spacecraft and its subsystems. In addition, the data are useful in determining realistic test levels for future spacecraft, similar in configuration and mounting, when flown on the same launch vehicle. The purpose of this paper is to present the inflight data in a form amenable to further evaluation rather than to present an interpretation of the vibration data obtained. As a reference for the data presented, the launch vehicle is described and significant events during the flight are noted.

Reduction of the flight data was performed by Ling-Temco-Vought Aeronautics Acoustic Laboratory under NASA Contract NAS1-1946. The results of the reduction of the flight data have been reproduced in this paper.

SPACE VEHICLE AND MISSION PROFILE

The space vehicle consisted of an Atlas D launch vehicle, a velocity package (V/P) to achieve the correct attitude and reentry speed, and a reentry package (R/P) to record and transmit data during reentry. A photograph of the space vehicle at lift-off is shown in figure 1. A schematic of the three major systems in the space vehicle is shown in figure 2. The mission profile is shown in figure 3. Significant events during the boost stage of the flight are as follows:

Event	Nominal time, sec
Lift-off	0
Booster engine cutoff (BECO)	133.0
Booster jettison	136.0
Sustainer engine cutoff (SECO)	288.5
Shroud separation	298.0
Vernier engine cutoff (VECO)	306.0
Spacecraft separation	311.5

Because the vibration measuring subsystems were located in the velocity package shell, the significant data period is limited to the boost phase from lift-off to separation of the spacecraft from the Atlas booster. Vibration data were not obtained during the velocity phase of Antares II-A5 motor burning or the reentry phase.

VIBRATION MEASURING SYSTEM

The vibration measuring system consisted of standard commercial instrumentation and hardware necessary for recording, simultaneously, three independent channels of vibration data during the flight. The measuring system was divided into three subsystems, one for each data channel. Each channel consisted of one piezoelectric transducer, one isolation stud, one low-noise cable assembly, one charge amplifier, necessary mounting hardware, and interconnecting wiring to the velocity package telemeter and power source. The subsystems were designated A, B, and C, and associated with inter-range instrumentation group (IRIG) telemeter channel numbers 16 (40 kc), 17 (52.5 kc), and 18 (70 kc), respectively. The output stage of each charge amplifier contained an internal Gaussian-type low pass filter with nominal cutoff frequency of 3 kc. This filter was used to prevent possible excessive overloading of the telemetry channels used. Physical locations of the three transducers are as shown in figure 4. The sensitive axis of each transducer was along the longitudinal, or thrust, axis of the vehicle. The transducer for subsystem A (channel 16, 40 kc) had a dynamic range of ±25g and was mounted

at the velocity package – Antares II-A5 separation ring, on the underside of the velocity package ring. The transducer for subsystem B (channel 17, 52.5 kc) had a dynamic range of ±15g and was mounted at the outer shell, on the ring at station 439.25. The transducer for subsystem C (channel 18, 70 kc) had a dynamic range of ±30g and was mounted on the upper ring of the velocity package shell at station 468.65, the separation plane between the velocity package and the Atlas D booster vehicle.

CALIBRATION OF VIBRATION MEASURING SYSTEM

Each vibration measuring subsystem was calibrated separately during prelaunch checkout of the velocity package at the launch site. A schematic of the calibration setup is shown in figure 5. Each subsystem was calibrated at 16 discrete frequencies ranging from 5 to 5000 cps at each of four different amplitude levels representing 25, 50, 75, and 100 percent of the dynamic range of the subsystem. The input signal was obtained from an audio signal generator, the amplitude being monitored on a voltmeter. The calibration constant was 1 mV/peak g. The output signal was transmitted, by telemetry, to a receiving ground station where the telemeter mixed signal was recorded on magnetic tape. The calibration procedure was also monitored on a scope. A playback of the calibrations for each of the three subsystems is shown in figures 6 to 8. The rolloff at the lower frequencies is caused by a 20 cps (Hz) cutoff of the strip chart recorder.

A phase check was also made by recording all three channels simultaneously during the calibration procedure by using the same exciting sinusoidal signal. Oscilloscope photographs showed that all three channels were in phase up to 1200 cps. At 1500 cps the 70 kc channel lagged the 40 kc channel by 20^{o}, the 52.5 kc channel being approximately halfway between the other two channels. Similarly, at 2000 cps the lag was approximately 30^{o}, and at 2500 cps the lag was approximately 45^{o}. A sample of the three simultaneous calibrations at 200 cps is shown in the upper right-hand portion of figure 9.

FLIGHT DATA

Flight data were transmitted by telemetry and the mixed signal per interrange instrumentation group format was recorded on magnetic tape at receiving ground stations. Telemeter channels 3 to 15 were utilized for other data within the velocity package and channels 16, 17, and 18 were utilized for the vibration measuring subsystems. The flight-data tapes and prelaunch-calibration tapes were played back through the NASA Langley Research Center ground station where the mixed signal was discriminated for channels 16, 17, and 18. The discriminators for each channel were filtered with 5 kc Gaussian output filters. The data signal for each channel was rerecorded on magnetic tape by using a wide band frequency modulated (FM) format (15 in./sec, 27 kc carrier at

±40 percent deviation). Calibration data from the prelaunch calibrations were transcribed on to the appropriate tracks during rerecording. These rerecorded FM data were used for reduction and analysis purposes.

DATA REDUCTION AND ANALYSIS

The analysis procedure consisted essentially of preliminary quantitative analyses of the overall flight data period, qualitative selection of significant data periods, and then a more detailed quantitative analysis of the selected data. A descriptive schematic of the types of analyses performed on a single data channel signal is shown in figure 10.

The preliminary analyses consisted of obtaining records of the variation of overall amplitude levels with time on a true-root-mean-square level recorder for the entire data period. These records were supplemented by various examinations of tape loops of the signals at different discrete time periods by using the true-root-mean-square voltmeter, the strip recorder, the period or frequency counter, and pictures of the representative wave shapes. The purpose of these preliminary quantitative and qualitative analyses was

(1) to select intervals of data having fairly constant root-mean-square amplitudes

(2) to make a preliminary classification of these intervals as stationary

(3) to identify obvious sinusoidal wave energy and to classify these signals by period or frequency, amplitude, and time duration and

(4) to make a preliminary judgment on the energy in each selected interval with regard to randomness and periodicity.

From these analyses the data were evaluated and discrete time periods were selected for more detailed analyses and for reference points.

The detailed analyses consist of one-third-octave band analyses, narrow-band spectral analyses, and amplitude probability density analyses. For the narrow-band spectral analyses, upper and lower frequency limits of the data sample were selected, an appropriate filter bandwidth was selected to reduce the noise effects from outside the selected frequency limits, and detailed records were made of the spectral distribution of the energy within the selected intervals by using both 10 cps and 2 cps bandwidth filters. From the one-third-octave band records and these records, judgments were made of the stationary conditions within the time intervals selected and, where necessary, adjustments were made in the selected time intervals to assure that the adjusted intervals contained only data which appeared to be nearly stationary. Also, obvious periodicities were identified and classified as to frequency, amplitude, and time duration. Amplitude probability density analyses were performed on some of the data samples used in these analyses.

In addition to these analyses, auto-correlation and dual signal analyses were performed on selected data samples. The dual signal analyses consisted of cross-correlation, cross-spectral density, and coherency. A descriptive schematic of types of analysis performed on dual signals is shown in figure 11. Calibration and setup procedures for each of the instruments employed are outlined in the appendix.

In addition, significant shock pulses during various stages of the flight were played back through a series of low pass, Gaussian, constant-delay filters. Amplitude response and phasing information for these filters are shown in figure 12.

RESULTS AND DISCUSSION

The results of the analyses performed are presented in graphical form in figures 13 to 91. The figures have been arranged with regard to type of analyses and data channel and are discussed in subsequent paragraphs.

Time histories from lift-off through spacecraft separation (rms g values as functions of time) for each of the three data channels are presented in figures 13 to 15. A band-pass filter from 100 to 2000 cps was utilized to produce an acceptable signal-noise ratio over the widest possible band of frequencies. These figures also show inset photographs of the real-time signal during prelaunch, launch, and transonic portions of the flight. Real-time signals of several shock pulses occurring in the later stages of flight are shown and discussed in a subsequent paragraph.

The results for several types of analysis for the 40.0, 52.5, and 70 kcps data channels are presented in figures 16 to 57. These analyses consist of overall level, one-third-octave level, spectral density, and probability density. The one-third-octave plots were taken at center frequencies ranging from 25 cps to 5000 cps by utilizing a 100 mm/sec writing speed and a 1 mm/sec chart speed. Spectral density analyses were made with both a 10 cps and a 2 cps narrow band filter. The results were plotted as the variation of acceleration density with frequency. Sweep rates and averaging time constants for the spectral analyses are indicated in each plot. Data sample time intervals are also indicated in each plot. The predominant spikes on each of the spectral plots are the result of deviated carrier data for several different subcarrier oscillator frequencies. The spikes are not the result of discrete sinusoids mixed in the data as can be clarified by the probability density plots. On several of the spectral plots, a comparison is made between the data signal and the prelaunch noise. These plots were primarily used to determine the optimum band-pass filter to be used on the data sample in order to obtain the highest signal-noise ratio. In general, the vibration was predominantly of a random nature with significant amplitudes only in the lift-off and transonic phases of flight. The maximum overall root-mean-square amplitude levels were approximately 1.5g rms during the transonic phase of the flight.

Figures 58 to 83 present the results of several types of correlation analyses between the 40.0 and 52.5 kcps, 52.5 and 70 kcps, and 40 and 70 kcps data channels. These analyses consist of auto- and cross-correlation, cross-spectral density, and power spectral density analyses, respectively, for each of these three combinations of data channels and for each of three different time intervals. The auto- and cross-correlation plots are self-explanatory. Included on these plots are the averaging time constants used and the calculated cross-correlation coefficient between channels. The cross-power spectral density plots are presented on a linear scale with an arbitrary vertical scale of unity. The arbitrary scale was used because the calibration methods were much simpler to use than absolute methods, and the data yield the same correlation information. This is explained further in the appendix. Spectral density plots have been replotted with the same arbitrary scale so that they can be used in conjunction with the cross-spectral density plots for a more detailed analysis and evaluation of the data.

Figures 84 to 86 show spectral analyses for each of the data channels during the start of the transonic portion of the flight where the data are nonstationary (that is, ascending portion of time history). No significant discrete-frequency vibrations were noted except for short-time-period transients following lift-off, booster engine cutoff, sustainer engine cutoff, and spacecraft separation events. These transients, which are of a relatively low amplitude, have been filtered with several different low pass filters for each of the data channels and events and are recorded in figures 87 to 90.

The data for this particular flight showed that the measured vibration environment was significantly lower than the preflight predicted environment.

CONCLUDING REMARKS

The results of a fairly detailed analog analysis of the Project Fire Flight 1 vibration data have been presented. These analyses show data characteristics for each of the three data channels and some of the correlation characteristics between channels. The data showed that for this particular flight, the measured vibration environment was significantly lower than the preflight predicted environment. In general, the vibration was predominantly of a random nature with significant amplitudes only in the lift-off and transonic phases of flight. The maximum overall root-mean-square amplitude levels were approximately 1.5g root mean square during the transonic phase of the flight. No significant discrete-frequency vibrations were noted except for short-time-period transients following lift-off, booster engine cutoff, sustainer engine cutoff, and spacecraft separation events. These discretes were also of relatively low amplitude.

No attempt was made to obtain transfer functions between the data channels, although these functions can be obtained from the data presented. Also, no attempt has been made to evaluate or to extrapolate the data obtained for use on other spacecraft configurations.

Langley Research Center,
National Aeronautics and Space Administration,
Langley Station, Hampton, Va., April 24, 1967,
714-00-00-01-23.

APPENDIX

ANALYSIS EQUIPMENT CALIBRATION PROCEDURES

Calibration Ratio

Between 20 and 2000 cps the 52.5 kcps calibration voltages played back from the broadband magnetic tape were approximately 0.23 volt (rms). Between these frequency limits the average deflection was 1.5 cm during calibration at the launch site. The calibration ratio was 5.0 cm per ±15.0g (peak).

Therefore,

$$\frac{1.5}{5.0} = \frac{x}{15.0}$$

$$x = \frac{1.5 \times 15.0}{5}$$

$$x = 4.5g \text{ (peak)}$$

Where x is the g value. Converting to g (rms) yields

$$x = 4.5 \times 0.707$$

$$x = 3.18g \text{ (rms)}$$

One-Third-Octave Plots

On the one-third-octave plots, the "heavy" lines are 10 dB apart. A reference voltage of 0.23 volt (rms) indicated a level of 3.18g (rms) and the appropriate scale was established.

Narrow Band Plots

The narrow band analysis plots utilized band-pass filters of 2 and 10 cps nominal which had effective bandwidths of 3.4 and 14.0 cps, respectively. The bandwidths are illustrated in the response curves in figure 92. Band limits were considered when calibrating the analyzer with a sine-wave signal.

From the one-third-octave analysis the frequency bandwidth (BW) of interest is known to be about 2000 cps and the overall acceleration level is about 3.0g rms. These parameters are related by the following equation for a flat spectrum:

$$g \text{ (rms)} = (g^2/\text{cps})(\text{BW})$$

where g^2/cps is the acceleration density. The average acceleration density for the data is

$$g^2/cps = g\ (rms)^2/BW$$

$$g^2/cps = 9.0/2000$$

$$g^2/cps = 0.0045$$

Because the spectrum was not flat, the analyzer was arbitrarily set for an acceleration density of 0.010 g^2/cps. For the average spectral density plots the square root of this value (that is, 0.10) was used.

Within the 14 cps filter bandwidth, the overall g value (rms) for an acceleration density of 0.010 g^2/cps was

$$g\ (rms) = \sqrt{0.010 \times 14}$$

$$g\ (rms) = \sqrt{0.14}$$

$$g\ (rms) = 0.374$$

And, from the previous discussion, the calibration factor was

$$0.23V\ (rms) = 3.18g\ (rms)$$

or

$$0.0725V\ (rms) = 1.0g\ (rms)$$

Therefore, the equivalent sinusoidal calibration voltage V_s is

$$\frac{1g\ (rms)}{0.374g\ (rms)} = \frac{0.0725V\ (rms)}{V_s\ (rms)}$$

$$V_s = 0.0725 \times 0.374 = 0.028V\ (rms)$$

The loop tape recorder used in the narrow band analysis had an output/input ratio of 5.66. The sinusoidal calibration voltage V_s was multiplied by this factor to obtain the actual calibration voltage, V_a

$$V_a = V_s \times 5.66$$

$$V_a = 0.028 \times 5.66$$

$$V_a = 0.152V\ (rms)$$

APPENDIX

Amplitude Probability Density, p(x)

The sigma scales on the amplitude probability density plots were normalized by equating 1σ to the true-root-mean-square level of the signal input to the analyzer. For each analysis a calibration curve was also plotted by using the band limited output of a random noise generator applied to the analyzer with the same true-root-mean-square level as the signal. The band limits of this calibration voltage were identical with the signal because the same band-pass filters were used.

Maximum $p(x)$ value of the calibration voltage was taken as 0.4 which is the maximum value on a normal Gaussian curve. This value along with the minimum values of $p(x)$ at $\pm 5.0\sigma$ establish the amplitude probability density scale on the right-hand side of the plots. The relation of the arbitrary scale y on the left to the $p(x)$ scale is shown on the plots.

On top of each plot, "best judgment" was used to locate an amplitude scale in sigma units. Small direct-current voltage bias components on the signal and calibration voltage may shift these plots to the left or right. For this reason an arbitrary scale was used.

Auto and Cross Correlation

In auto- and cross-correlation analyses, arbitrary calibration methods are much simpler to use than absolute methods, and yield the same correlation information. Arbitrary methods were used in these analyses. The auto- and cross-correlation systems shown in figures 10 and 11 were used with the addition of band-pass filters on the outputs of the tape recorder. These filters whose responses are shown in figure 9 were used to limit all signals to the frequencies between 100 and 2000 cps.

For auto correlation, the signal was directed into both channels of a time-delay tape recorder. Signal levels into the time delay recorder were adjusted to arbitrary levels of equal value. A sweep of the range of time delay τ was made, and the maximum correlation amplitude $R_{XX}(0)$ was adjusted for approximately 2 inches by using the variable gain control on the X,Y recorder. At this peak value, the amplitude scale on the multiplier is 100 percent or less. Both channels of the time delay recorder used the same arbitrary scale. For cross correlation of two signals, the arbitrary levels are maintained except that the integer multiplier scale adjustment on the X,Y plotter is used to obtain magnification of the cross-correlation scale $R_{XZ}(\tau)$ if correlation values are low. The time delay scale τ is compared with a 1000 cps calibration signal in figure 93.

APPENDIX

Power-Spectral and Cross-Spectral Density

A similar arbitrary calibration method was used for power-spectral density and cross-spectral density analyses. A 1000 cps sinusoid of arbitrary level (that is, 0.150V (rms)) was applied to the multiplier and the gain was adjusted for 100-percent meter indication. The gain of the X,Y plotter was then adjusted for 4 inches deflection on the co-spectrum, as shown in figure 94. Signals A and B are applied to the multiplier and equal levels are adjusted for reasonable deflection at the frequency where maximum deflection occurs. This was 1.00V (rms) for the 40.0 and 52.5 kcps channels at -2 to 3 seconds.

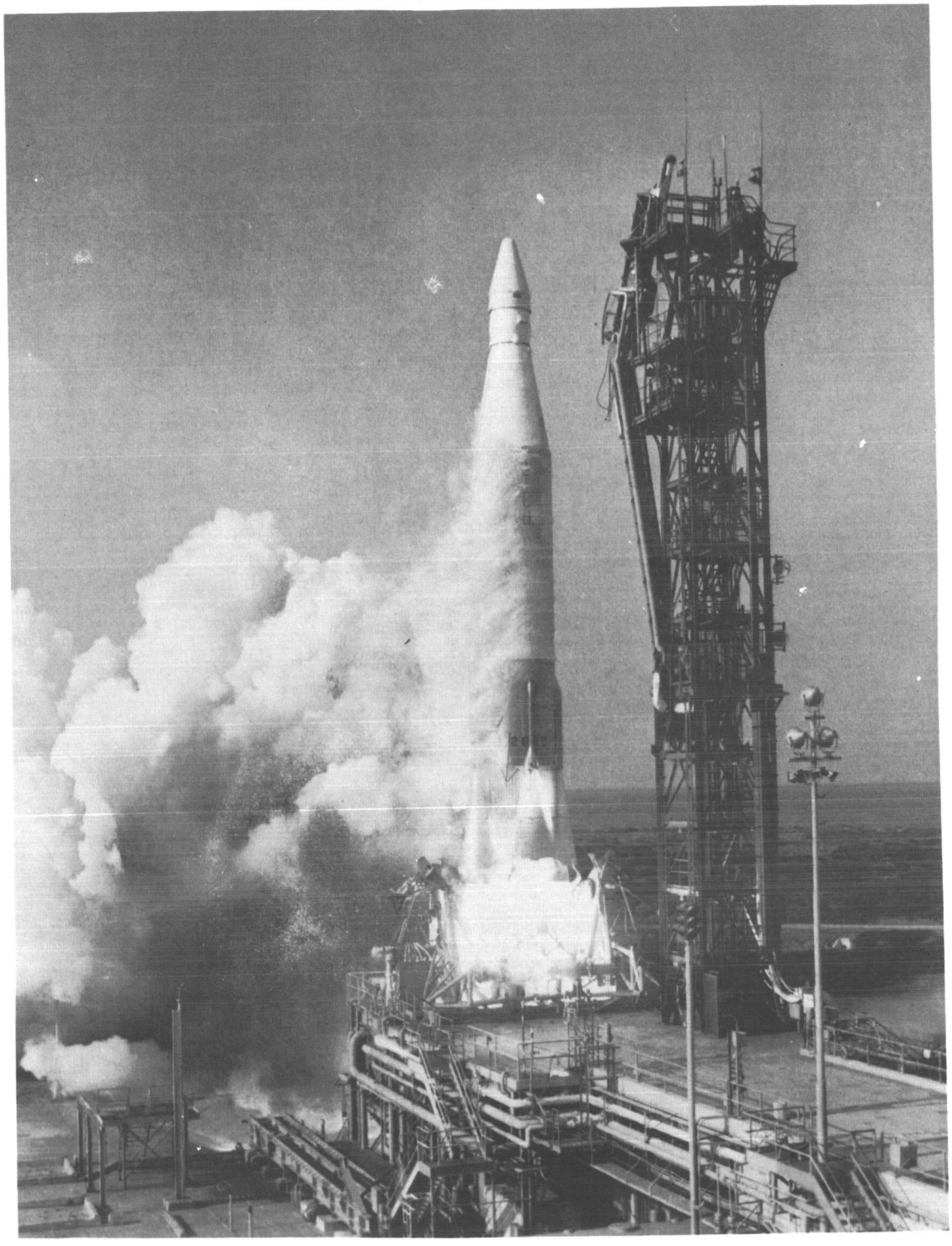

Figure 1.- Project Fire spacecraft at lift-off. L-65-139

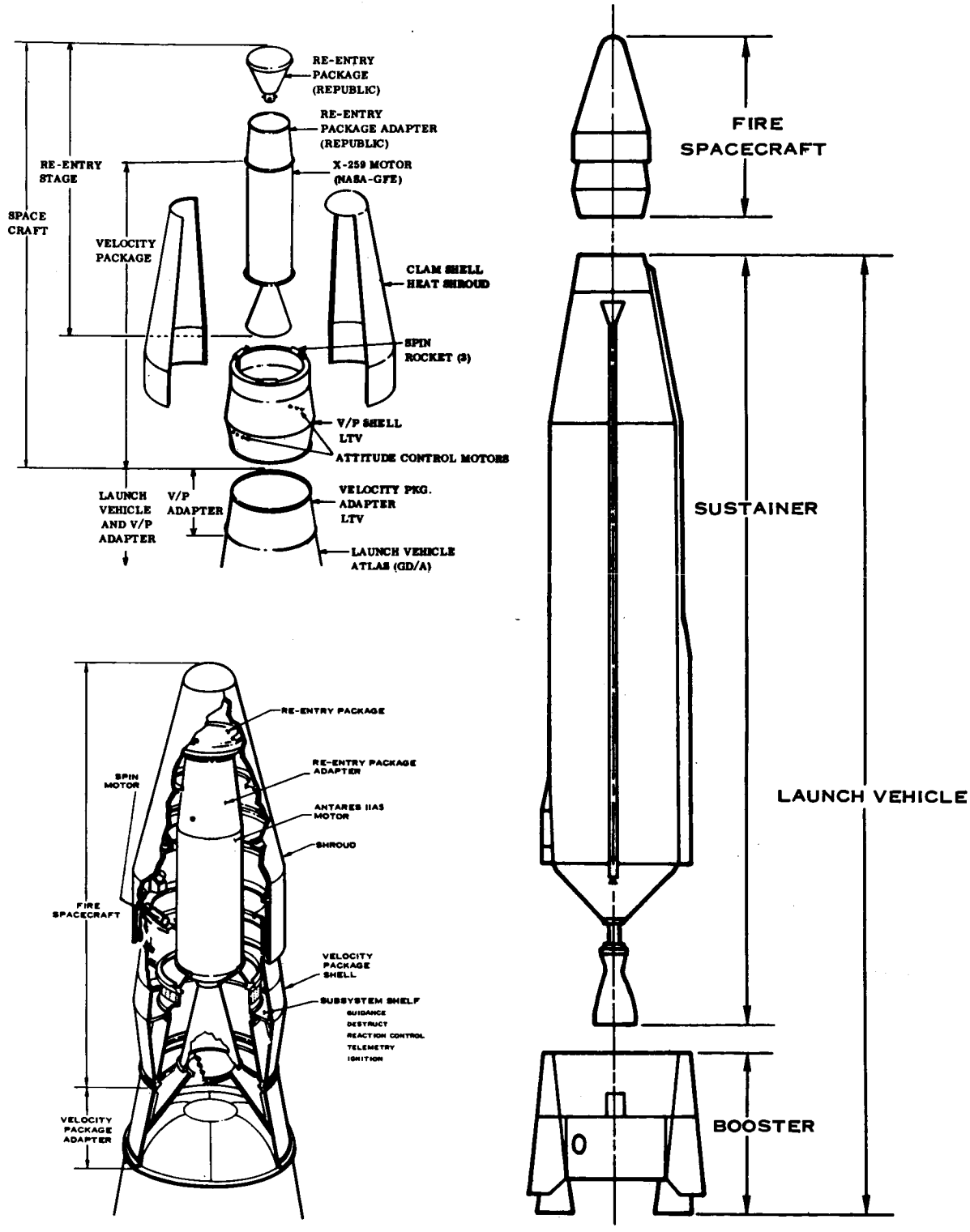

Figure 2.- Launch vehicle and spacecraft.

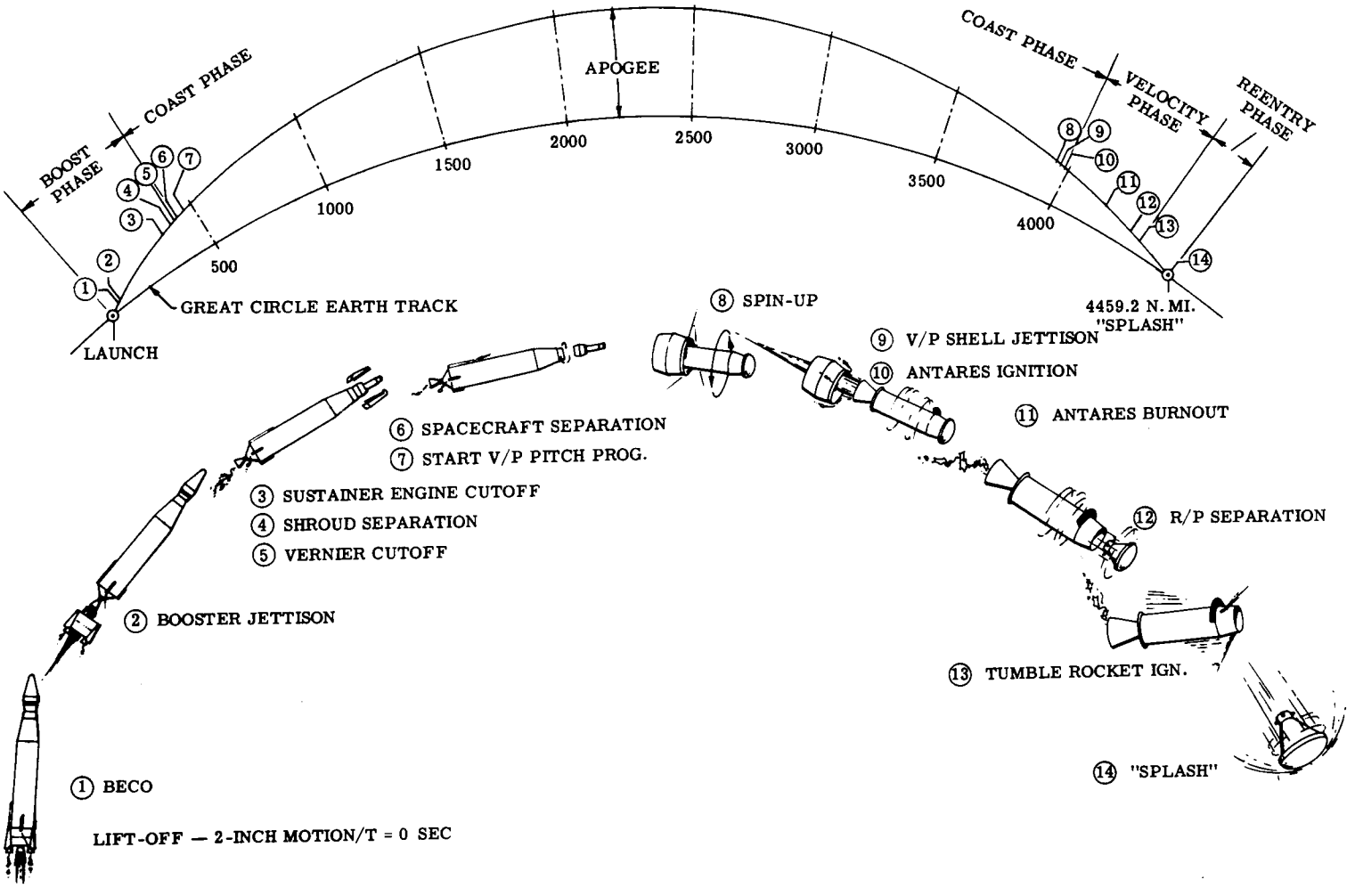

Figure 3.- Mission profile.

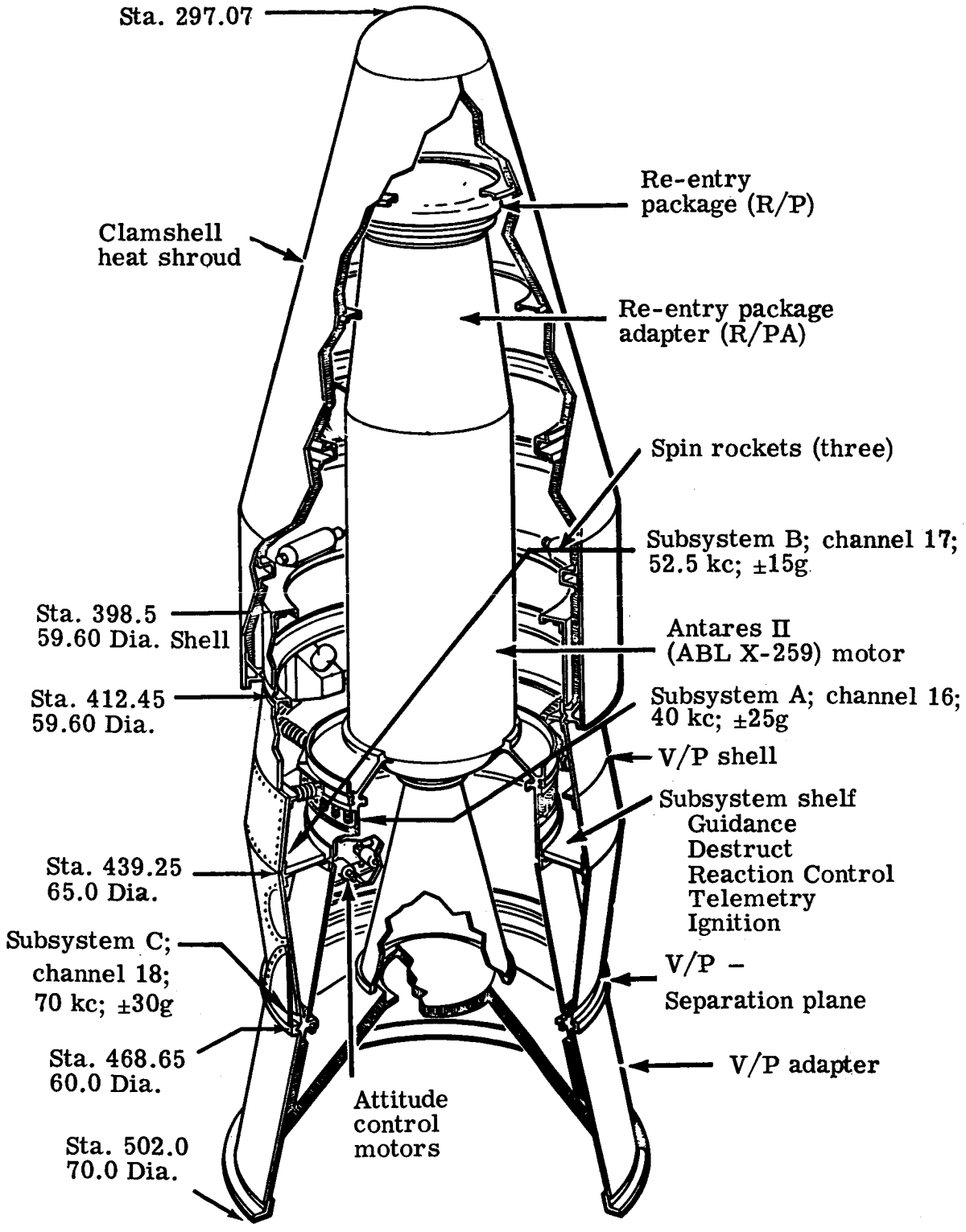

Figure 4.- Location of vibration measuring subsystems A, B, and C within the velocity package.

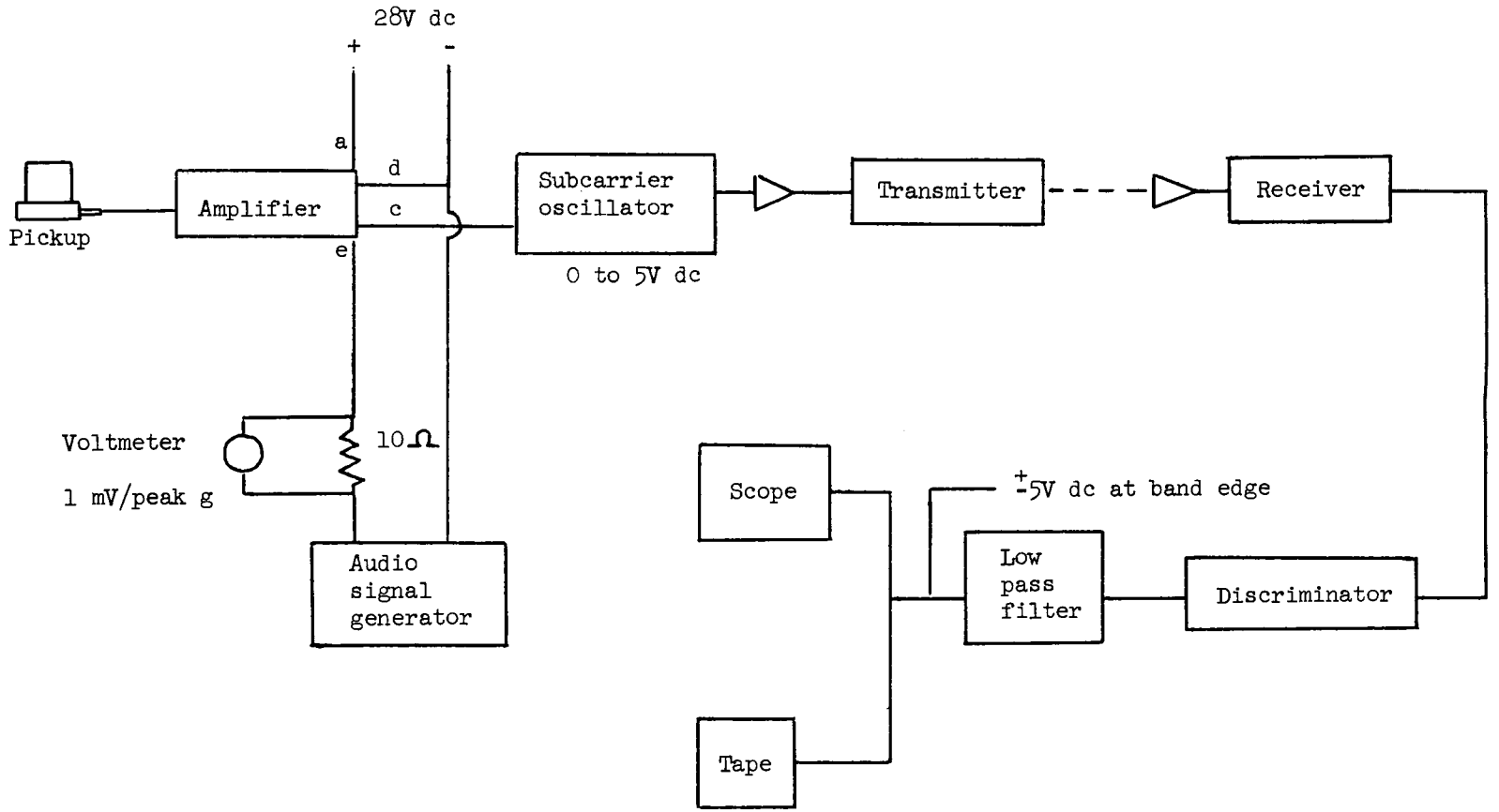

Figure 5.- Schematic of calibration for vibration measuring subsystems A, B, and C.

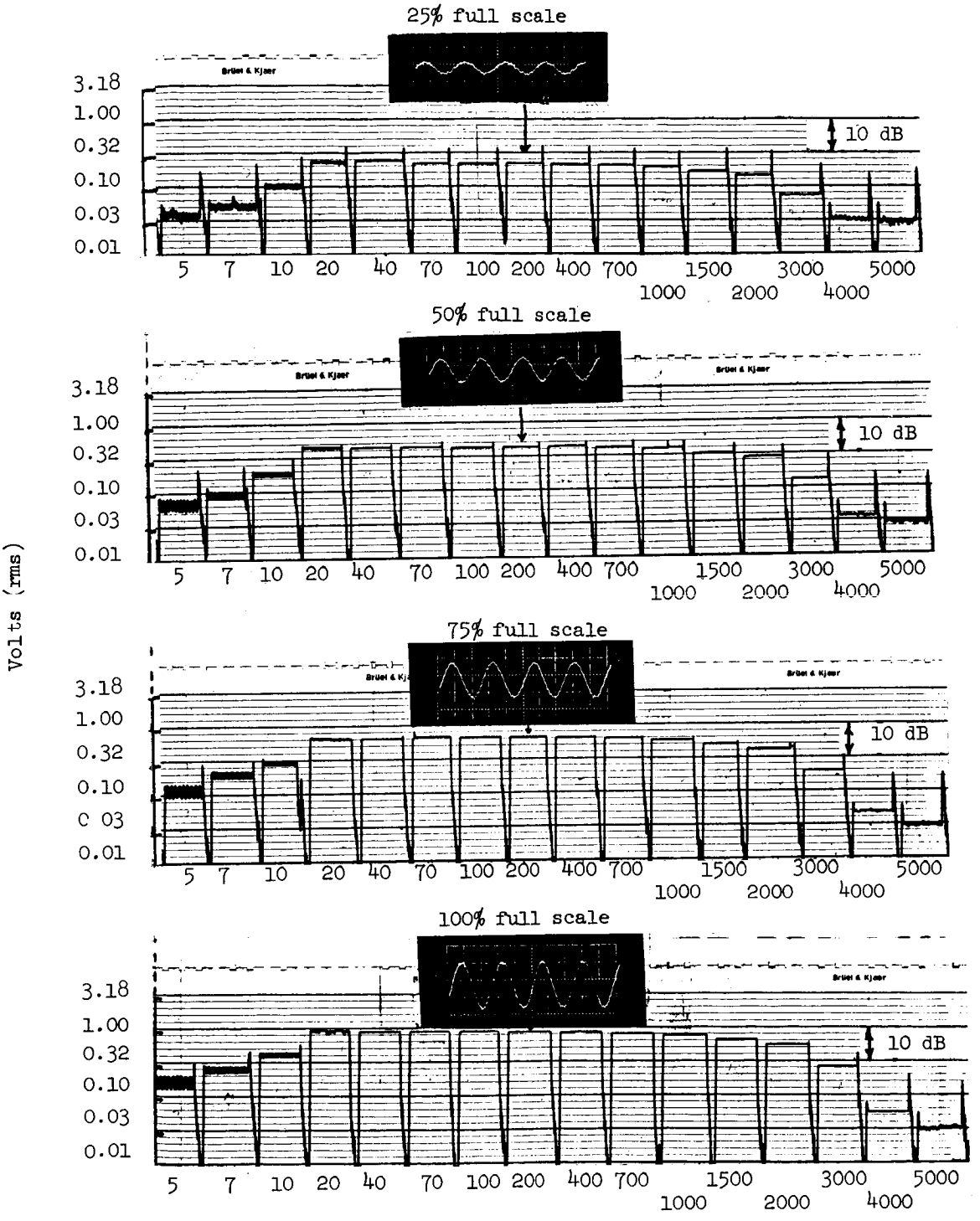

Figure 6.- Calibration curves for vibration monitoring subsystem A (±30g).

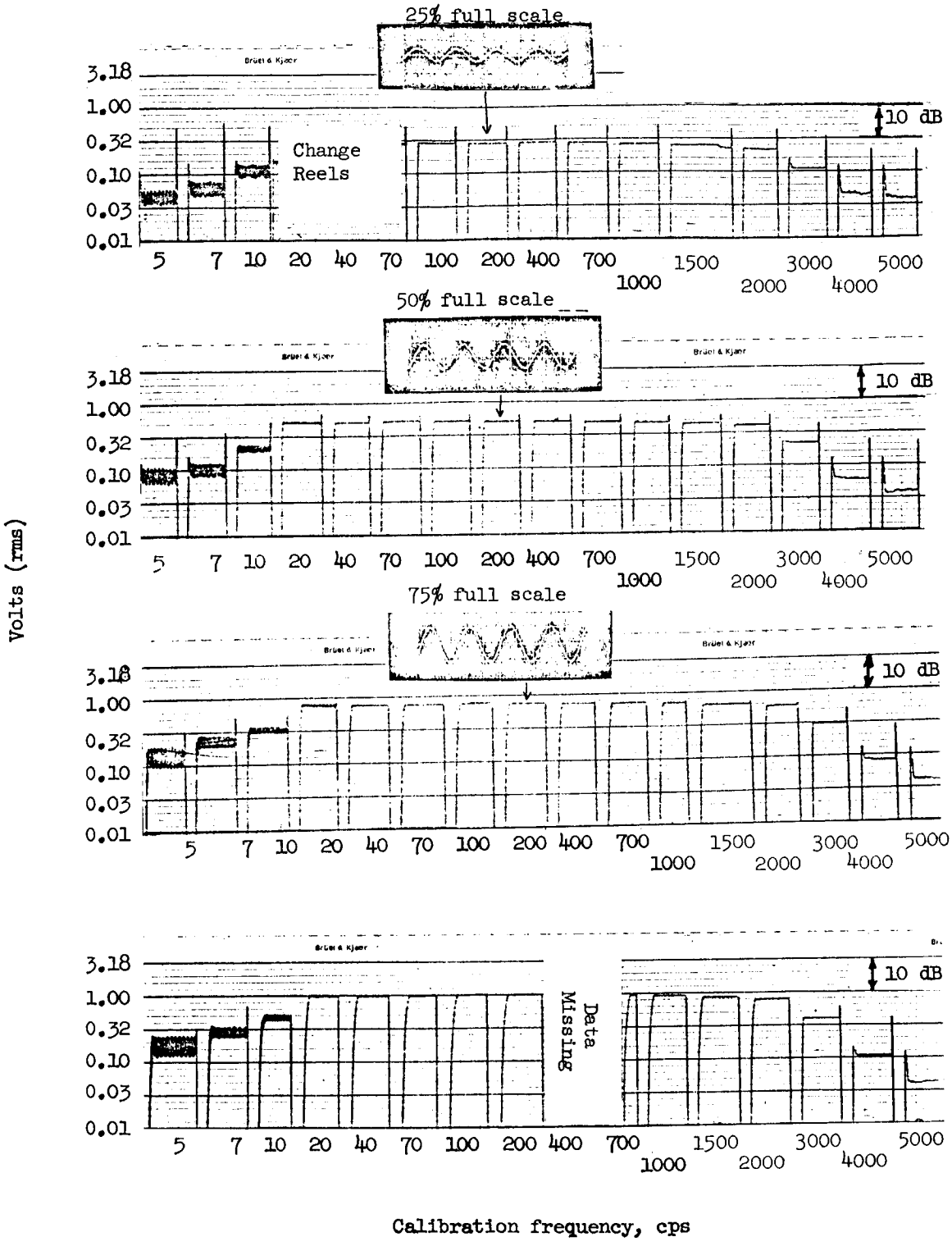

Figure 7.- Calibration curves for vibration monitoring subsystem B (±15g).

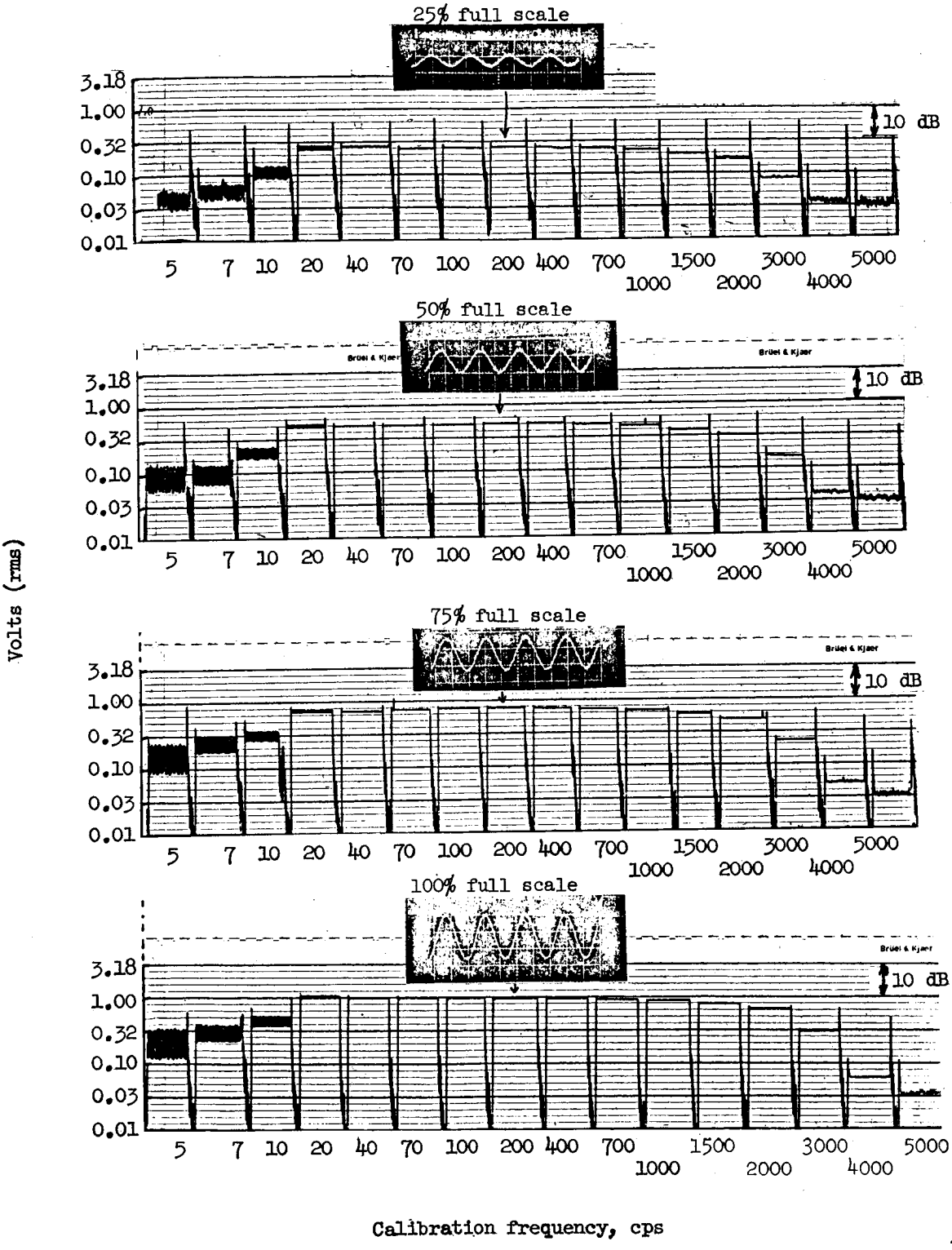

Figure 8.- Calibration curves for vibration monitoring subsystem C, ±30g full scale; 70 kcps channel; 5 kcps output filter.

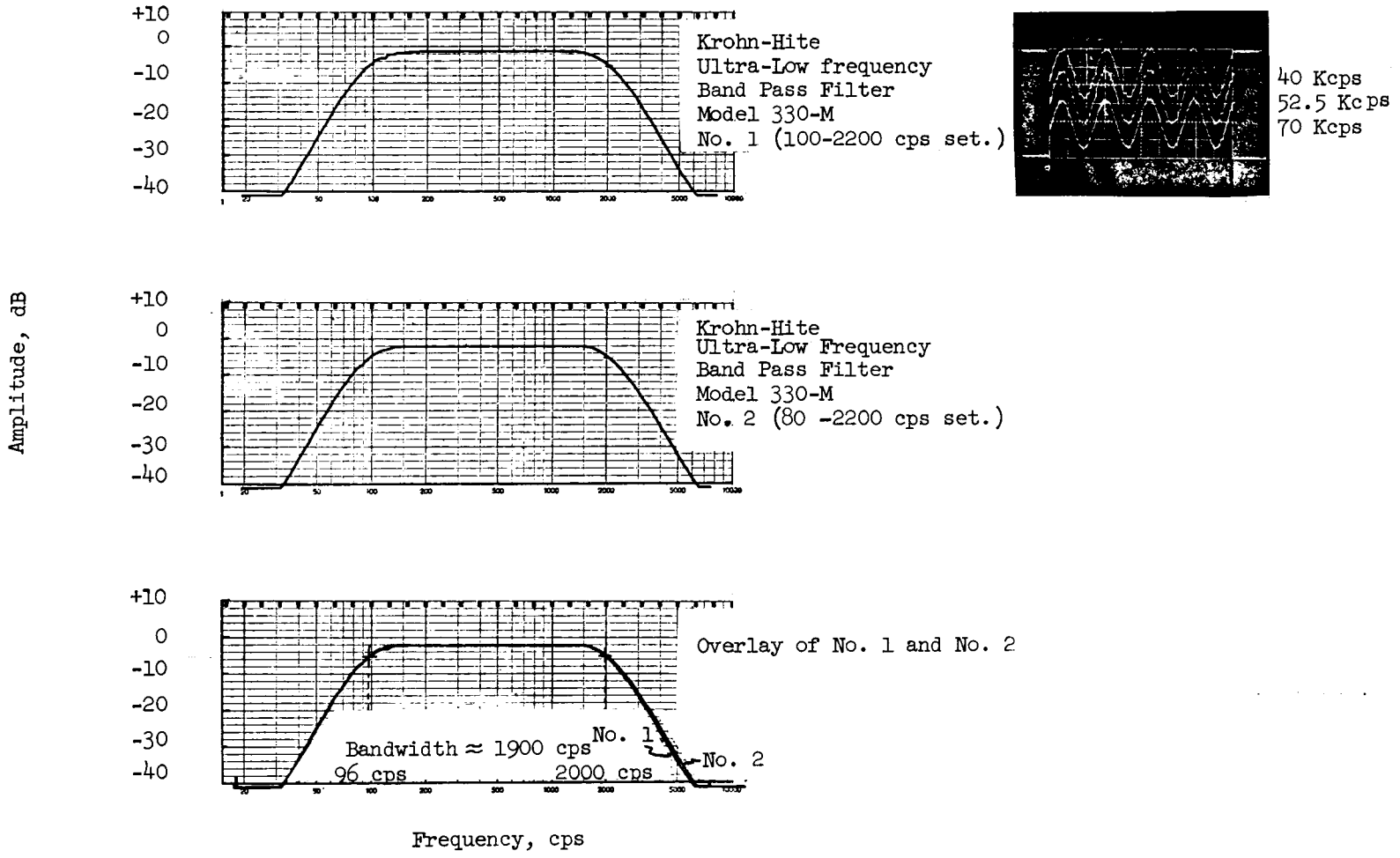

Figure 9.- Band-pass filter response curves and relative phase of sinusoidal (200 cps) calibration signals. 40, 52.5, and 70.0 kcps channels.

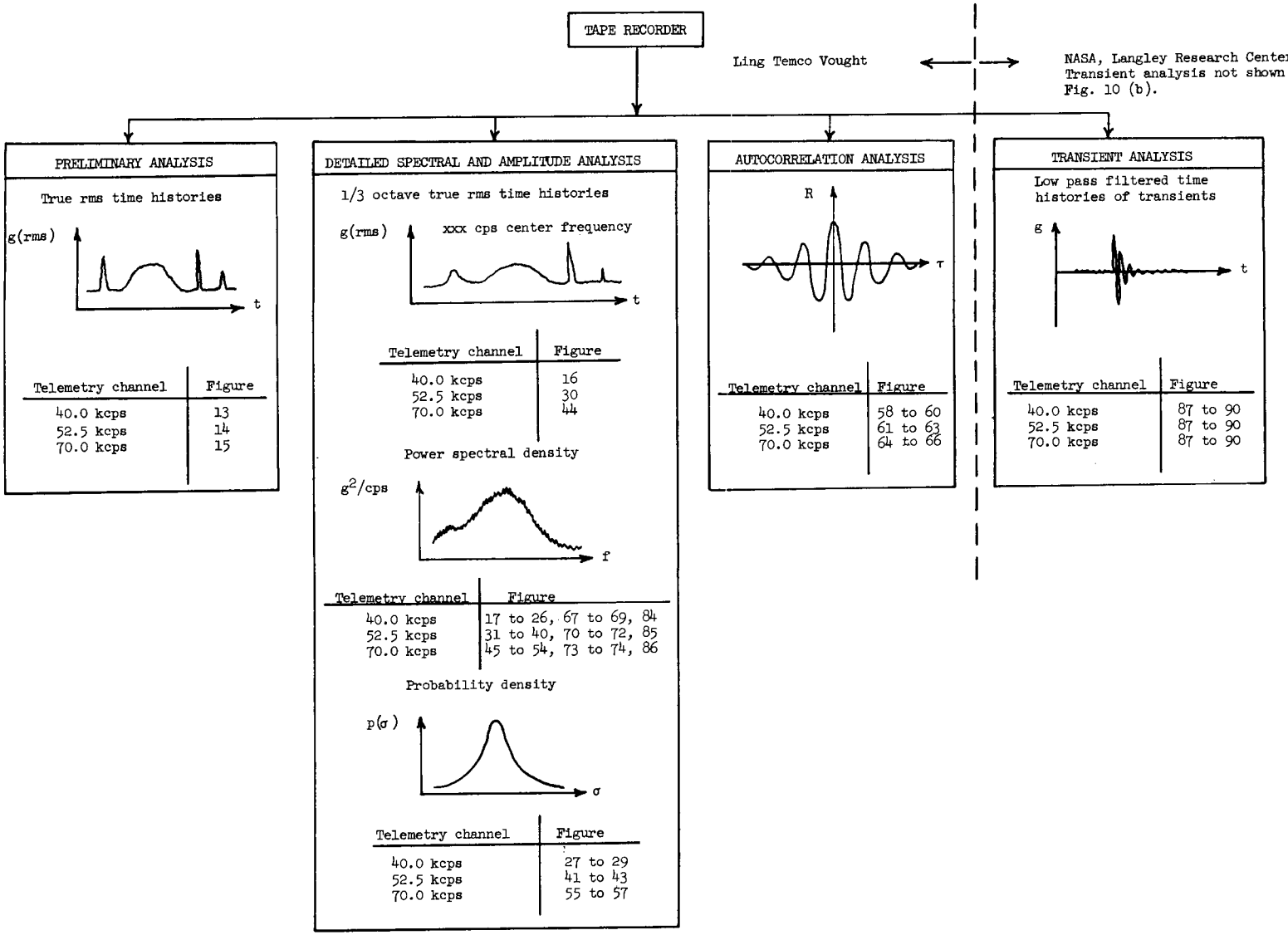

(a) Typical output signal and location according to figure.

Figure 10.- Flow chart of single signal data analysis.

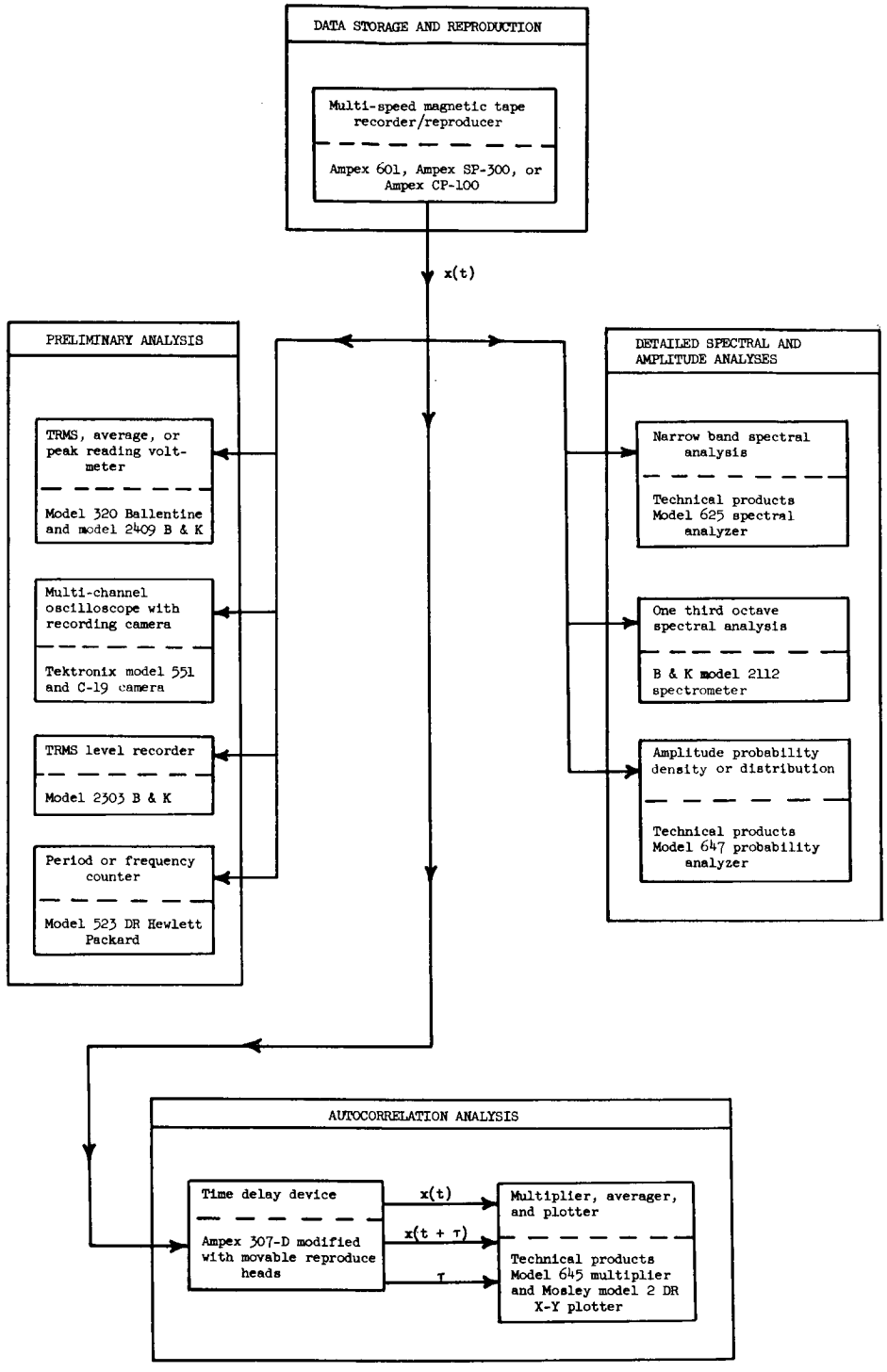

(b) Equipment for analysis.

Figure 10.- Concluded.

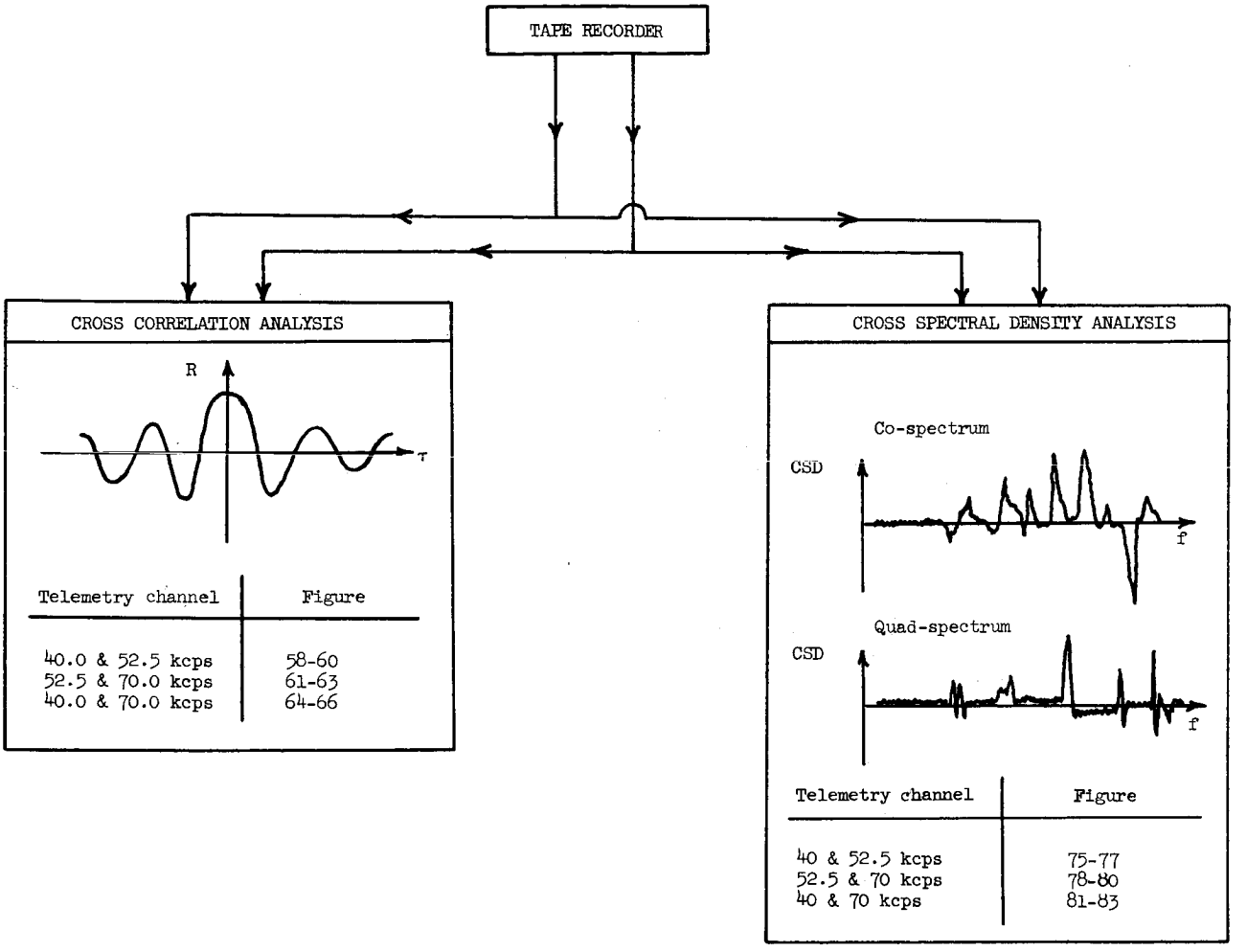

(a) Typical output signal and location by figure.

Figure 11.- Flow chart of dual signal data analysis.

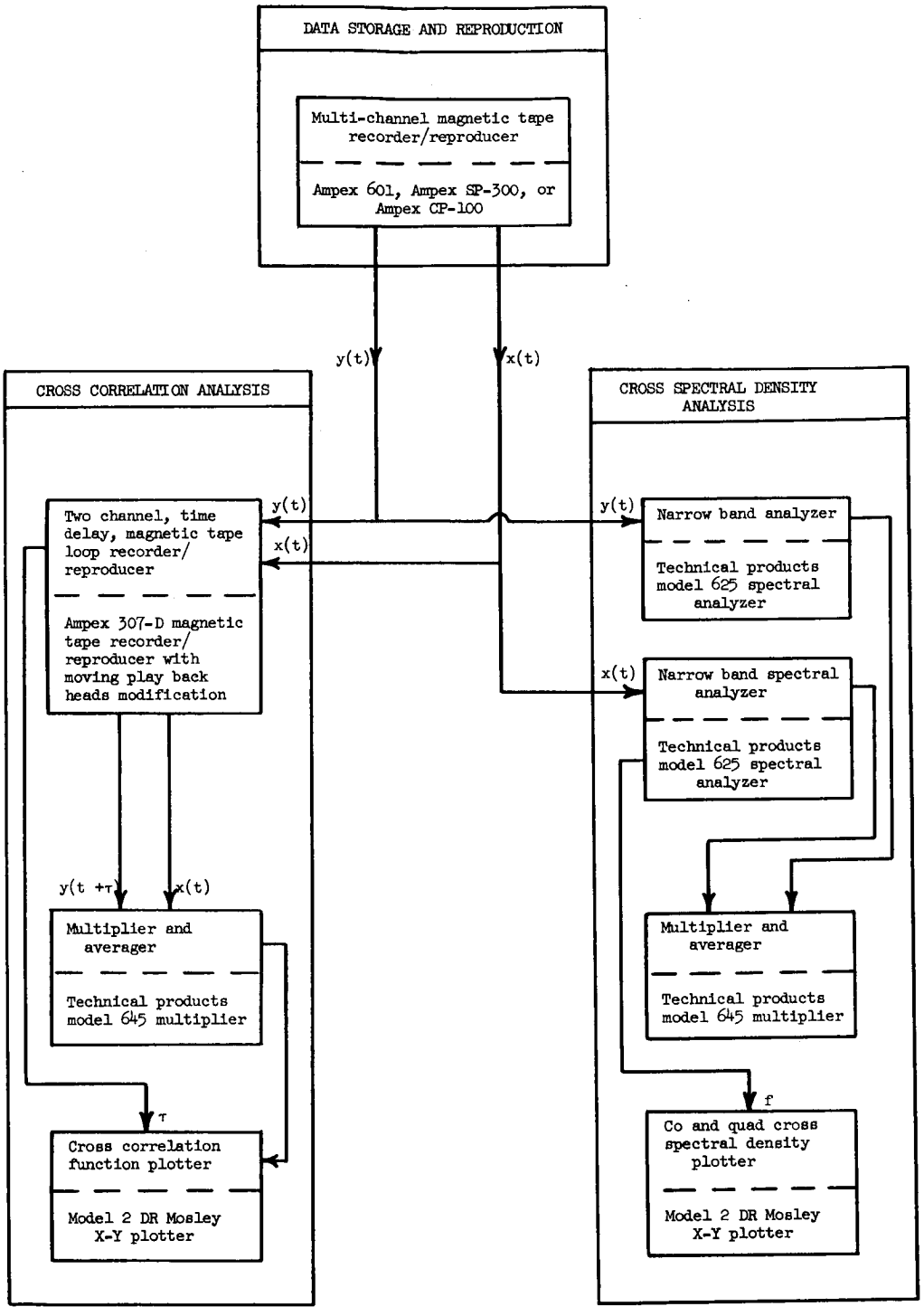

(b) Equipment used in analysis.

Figure 11.- Concluded.

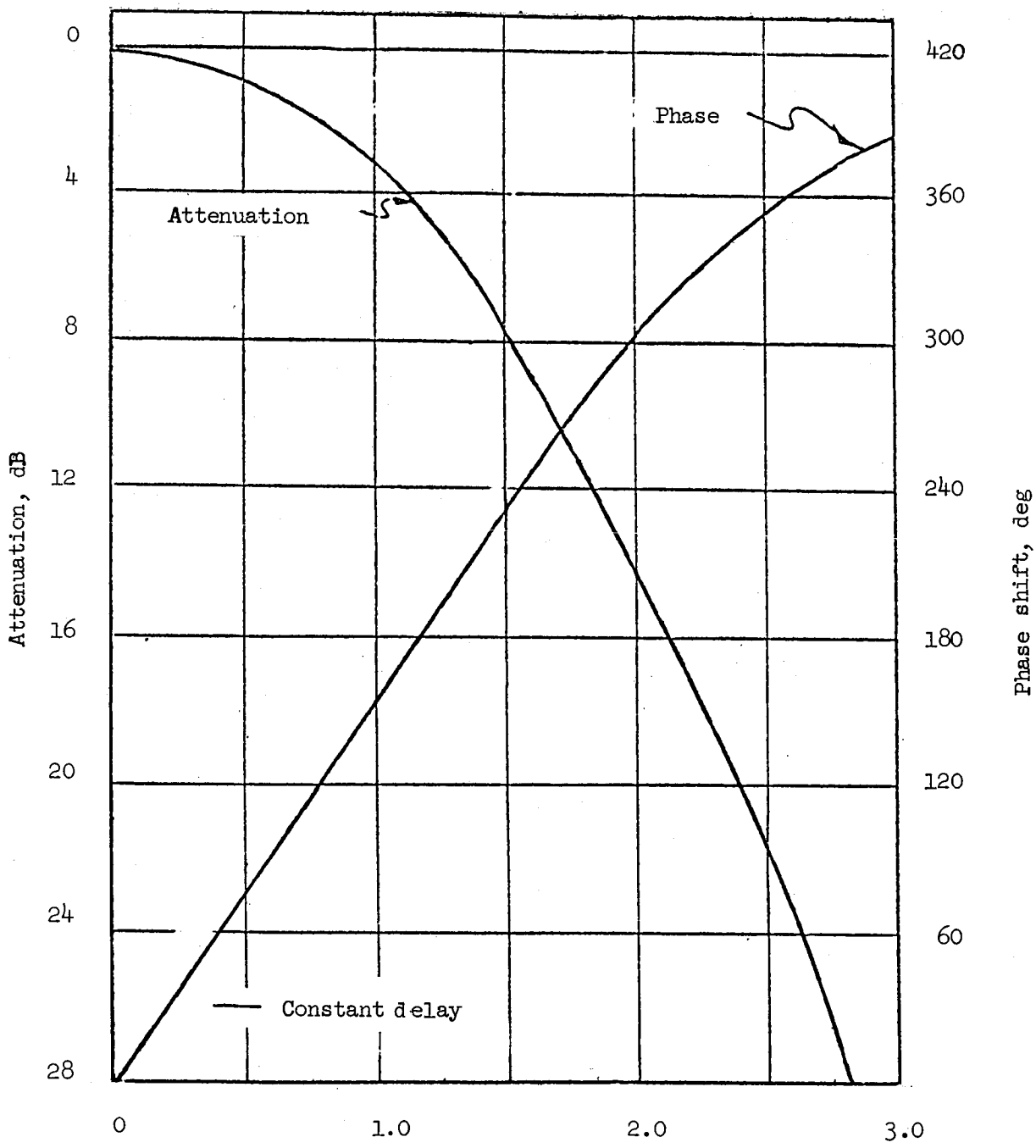

Figure 12.- Amplitude and phase response of Gaussian filter used at Langley Research Center.

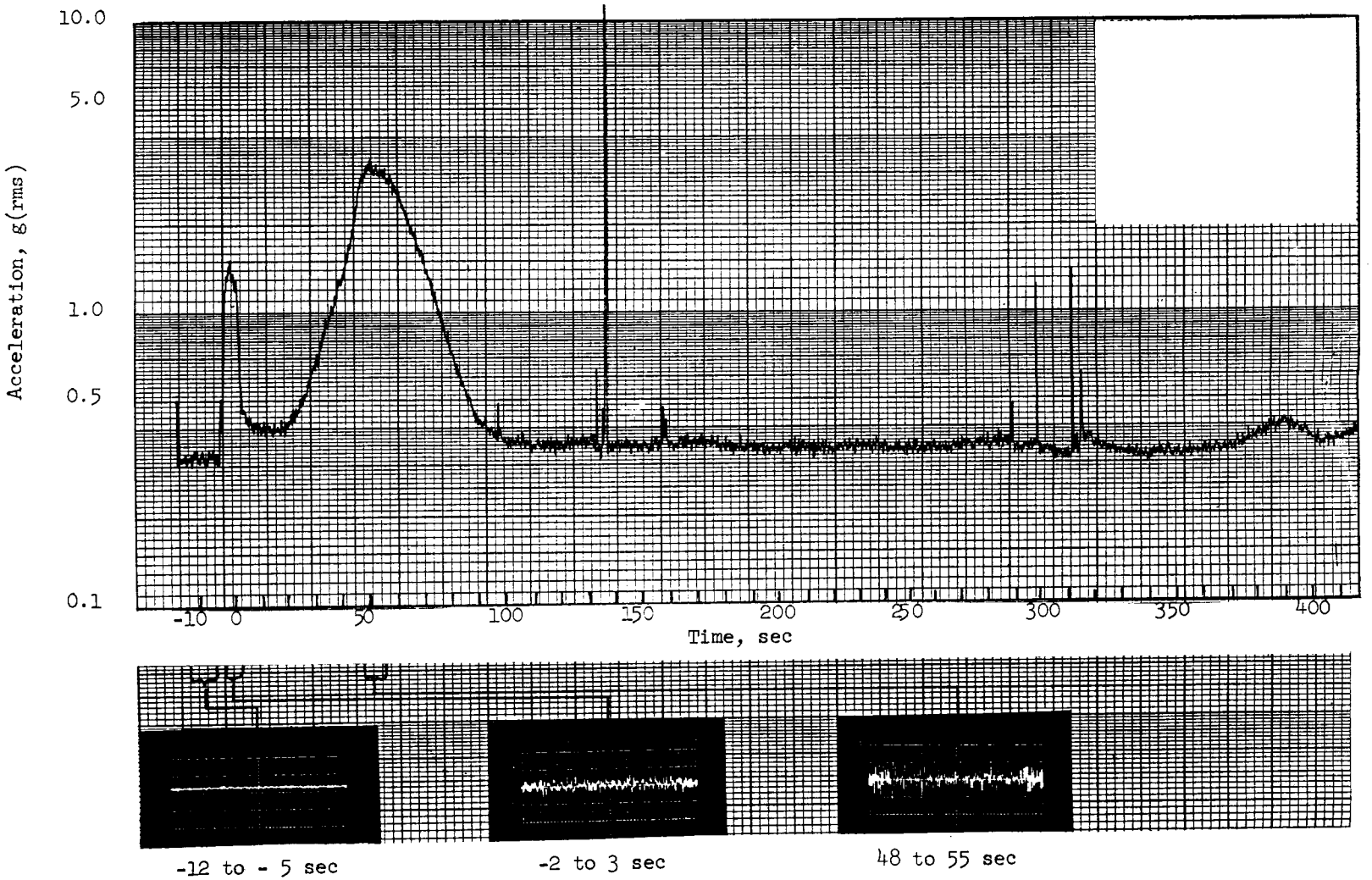

Figure 13.- Variation of vibration level with time. 40 kcps channel; 100 to 2000 cps band-pass filter.

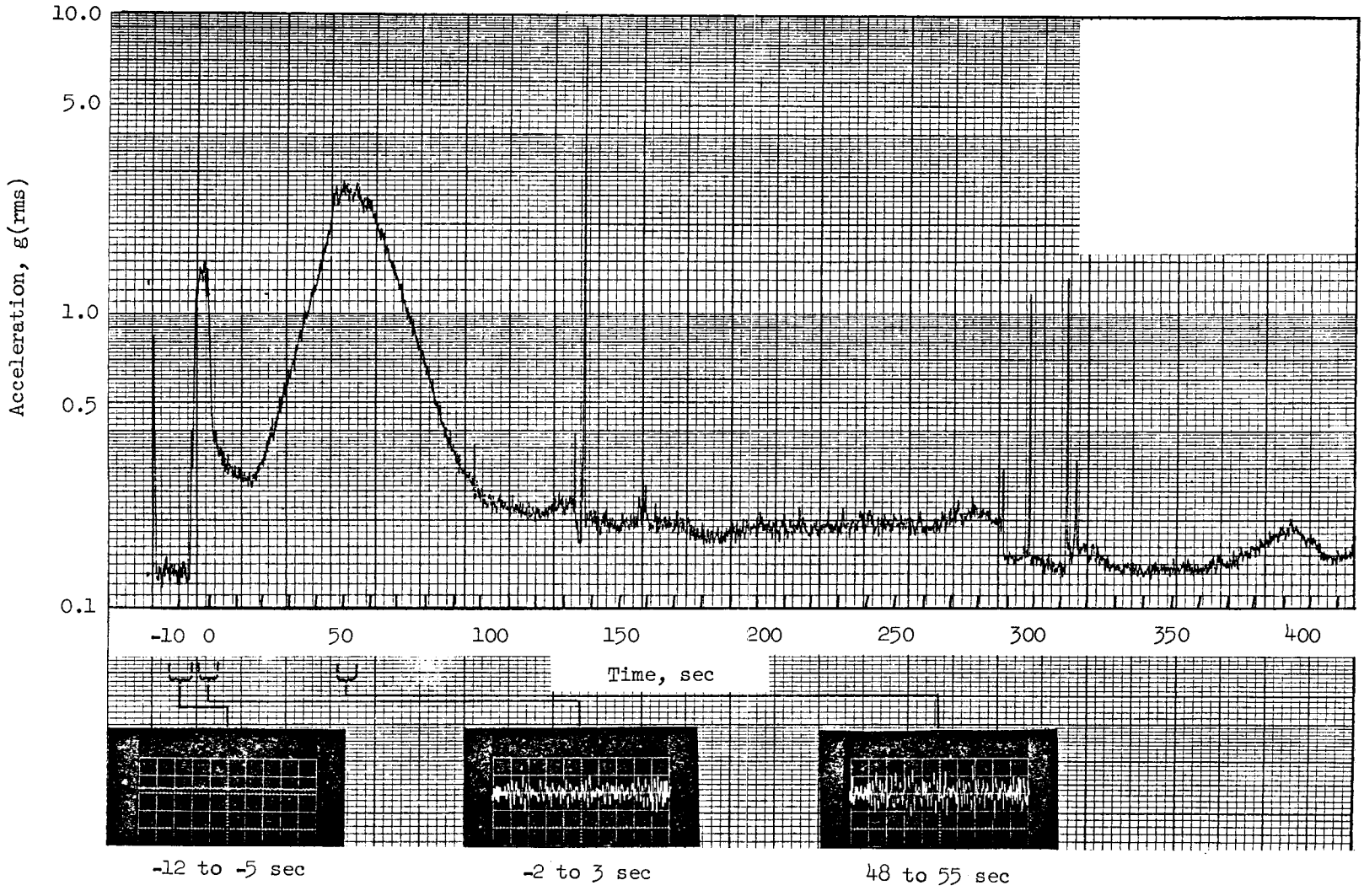

Figure 14.- Variation of vibration level with time. 52.5 kcps channel; 100 to 2000 cps band-pass filter.

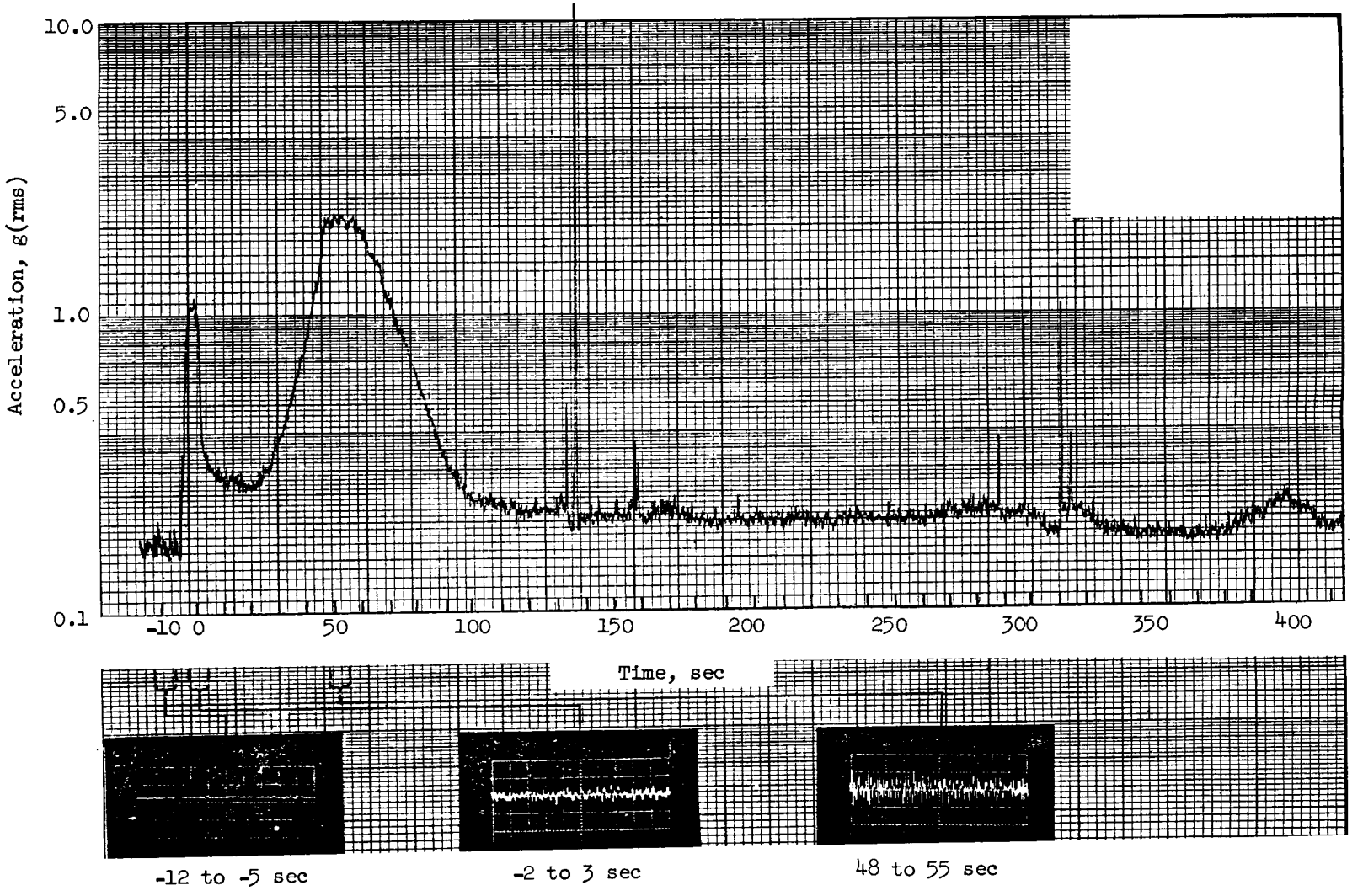

Figure 15.- Variation of vibration level with time. 70.0 kcps channel; 100 to 2000 cps band-pass filter.

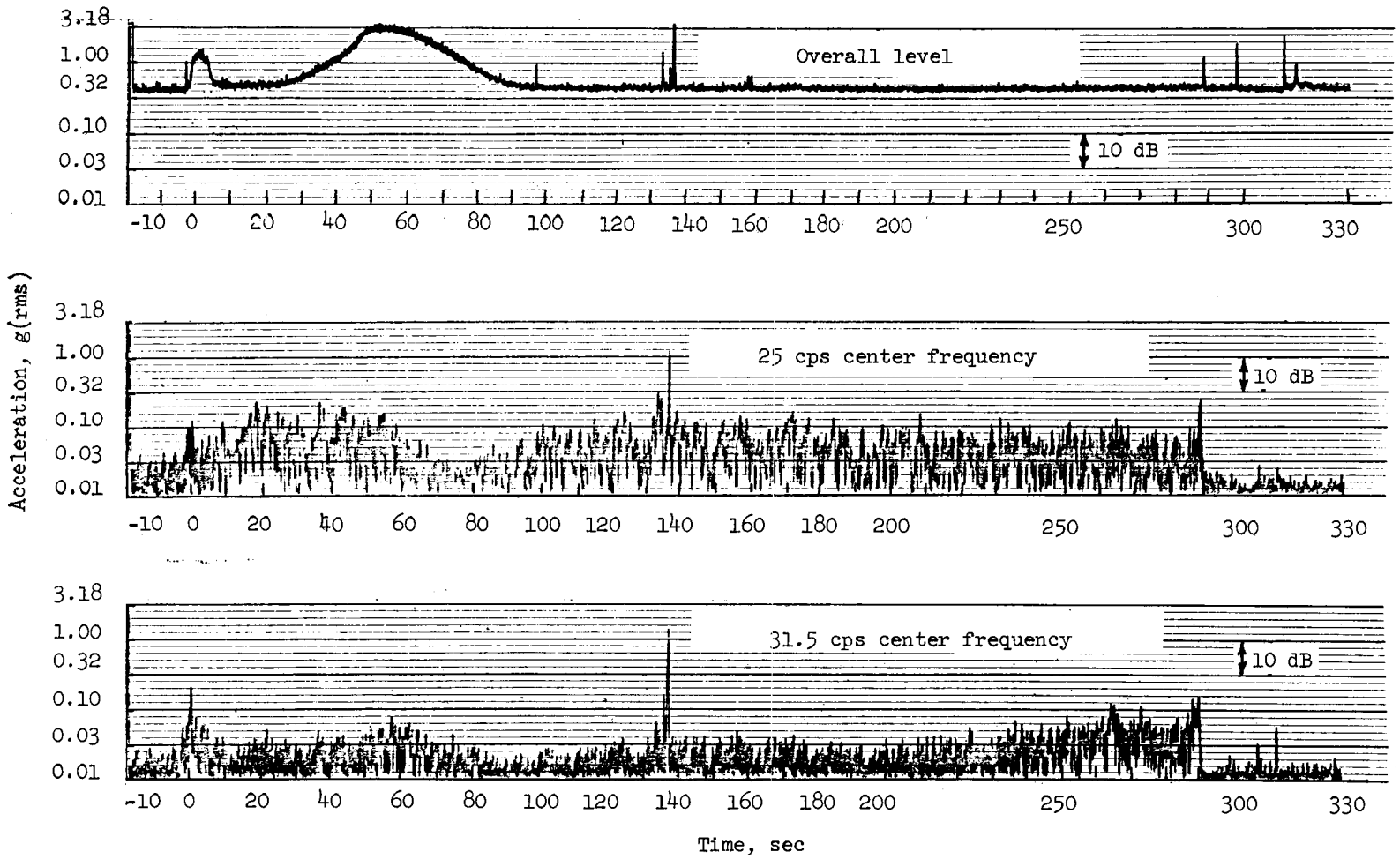

(a) 25 and 31.5 cps center frequencies.

Figure 16.- Overall level and one-third-octave band analysis. 40 kcps channel.

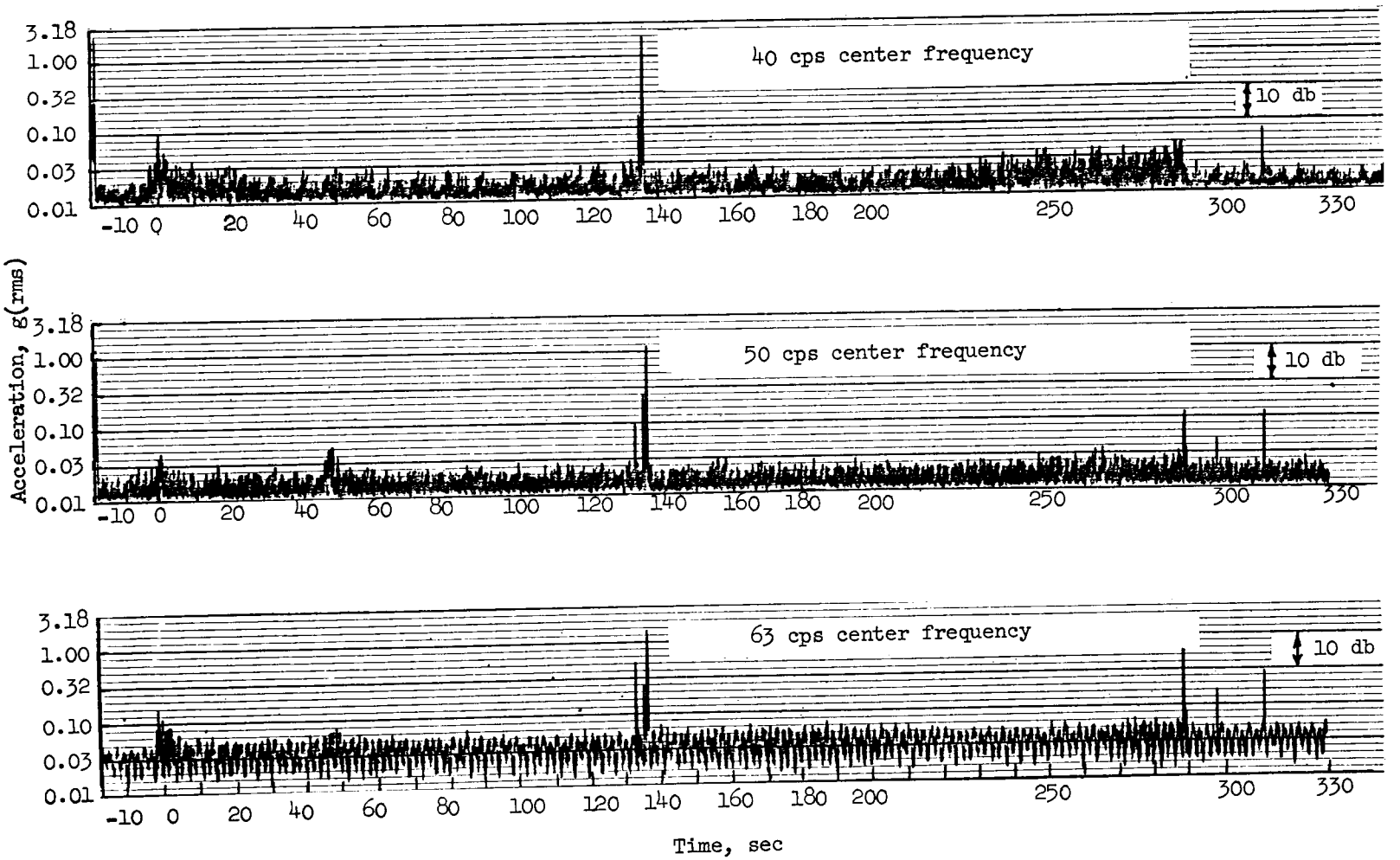

(b) 40, 50, and 63 cps center frequencies.

Figure 16.- Continued.

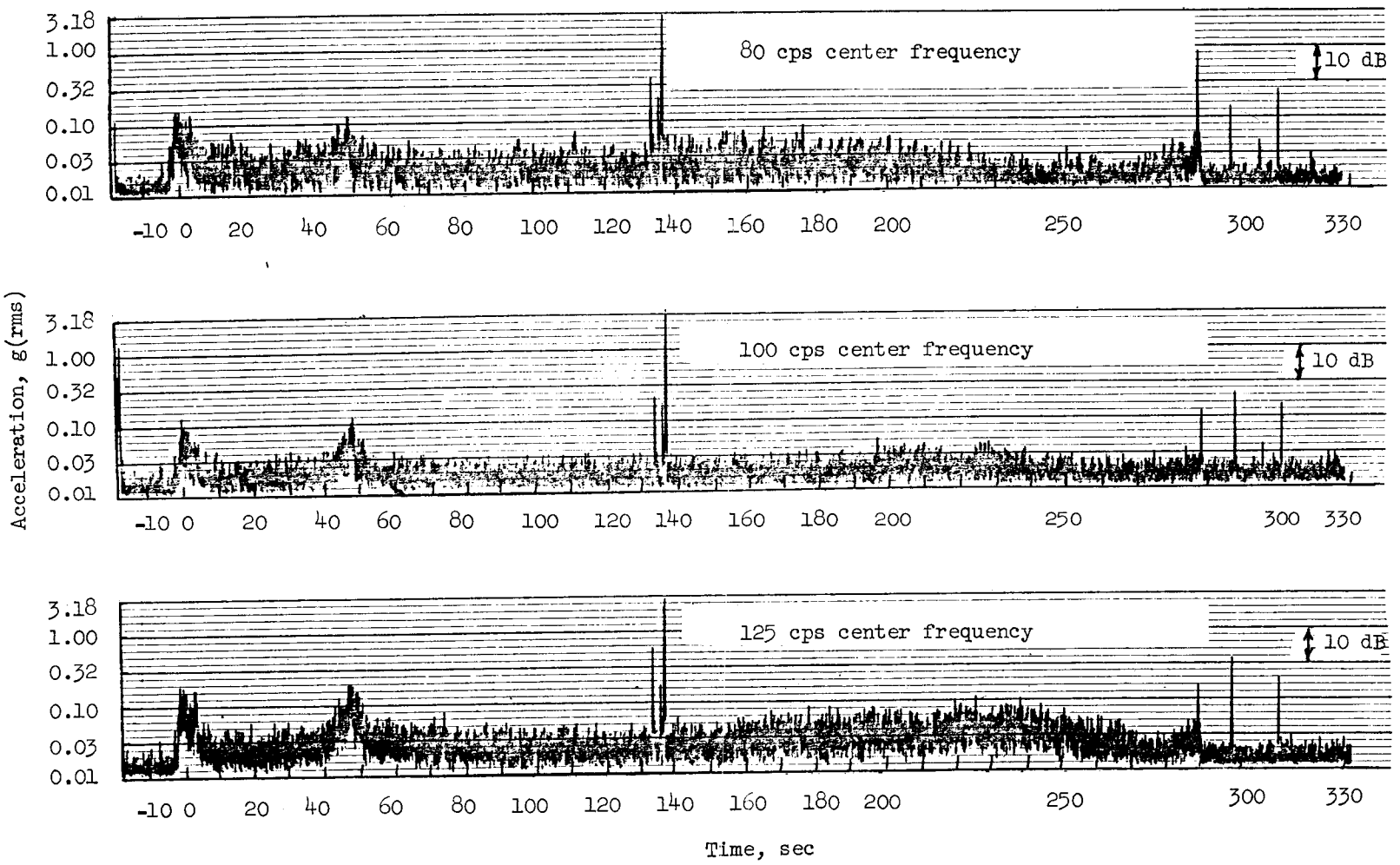

(c) 80, 100, and 125 cps center frequencies.

Figure 16.- Continued.

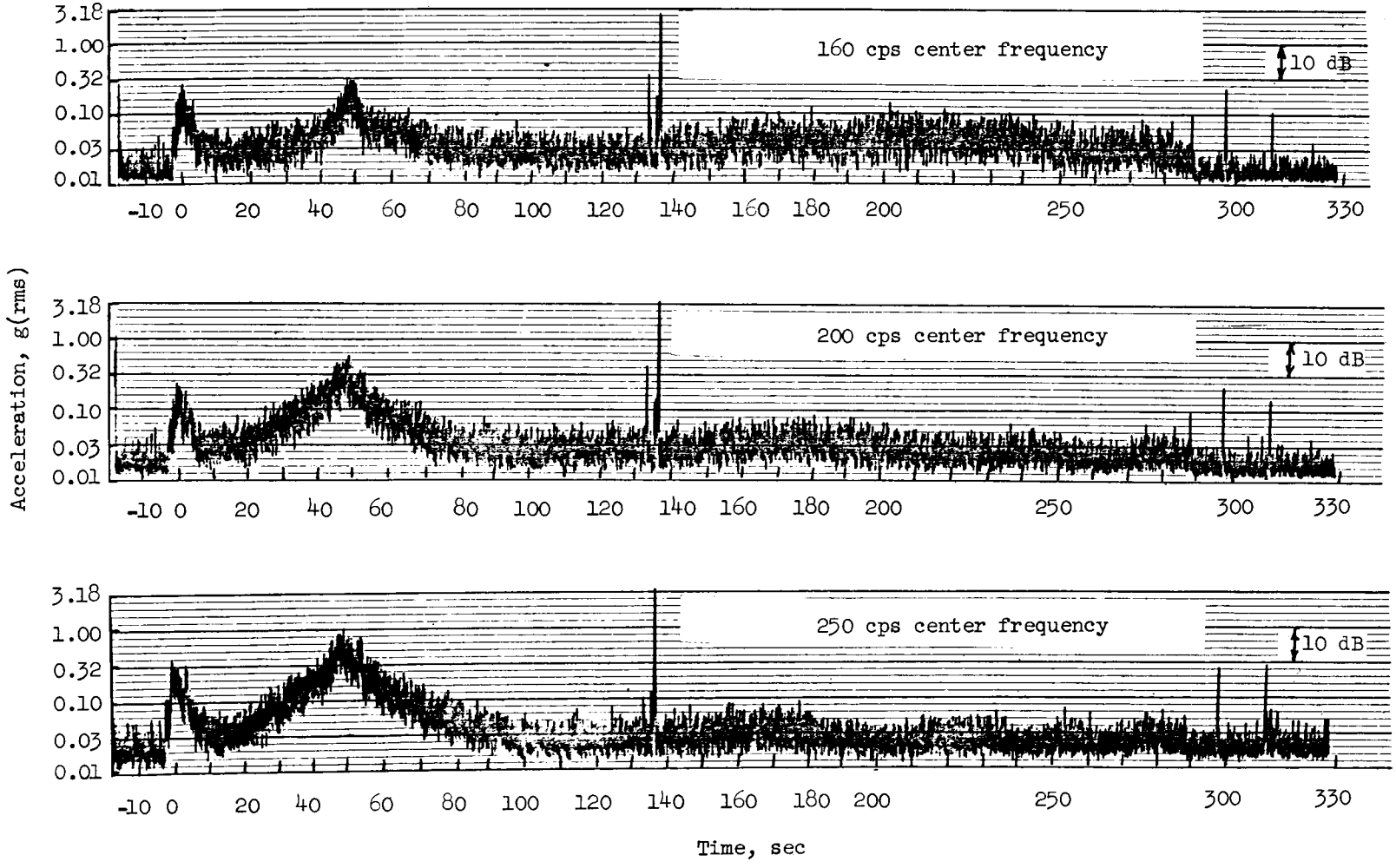

(d) 160, 200, and 250 cps center frequencies.

Figure 16.- Continued.

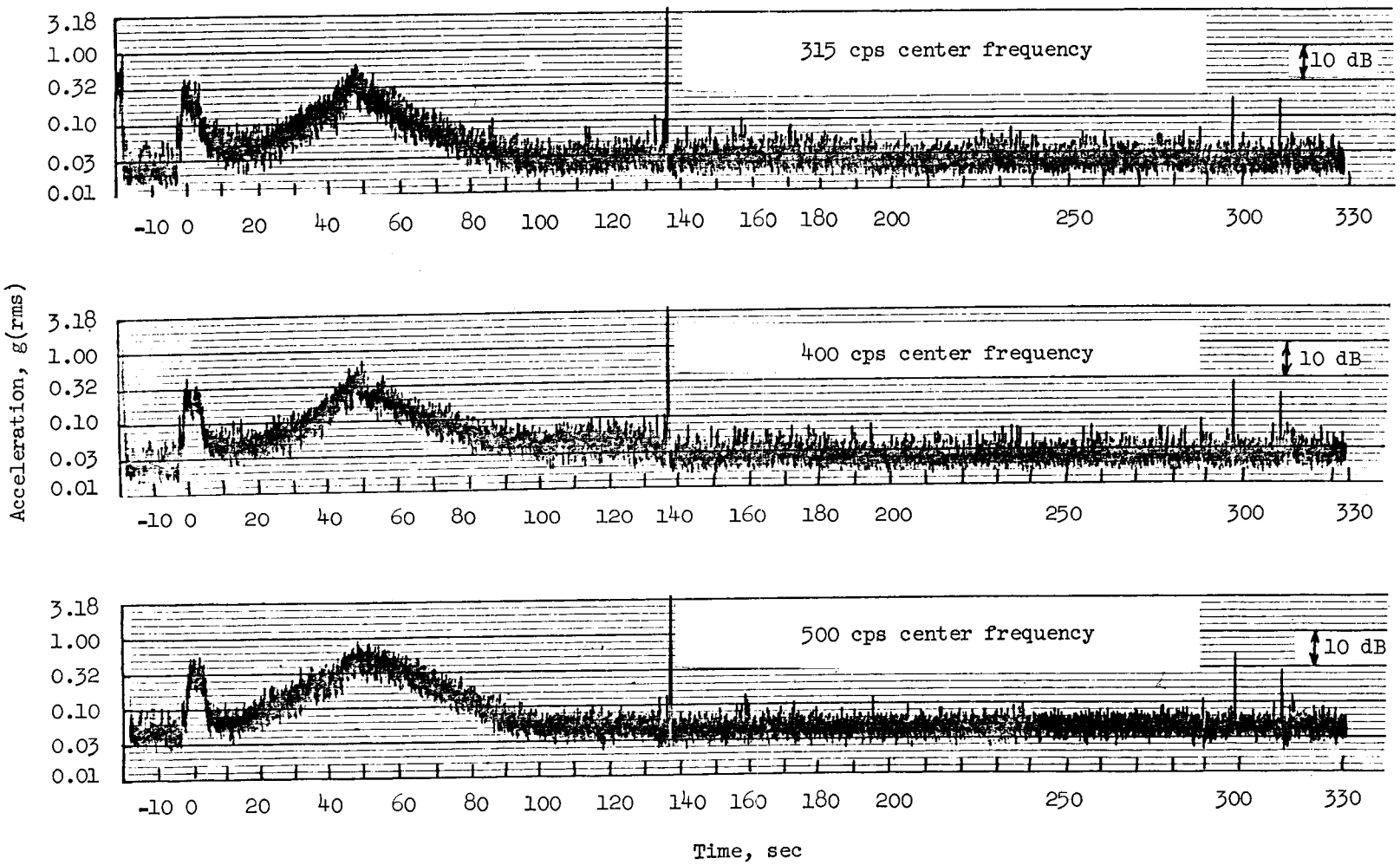

(e) 315, 400, and 500 cps center frequencies.

Figure 16.- Continued.

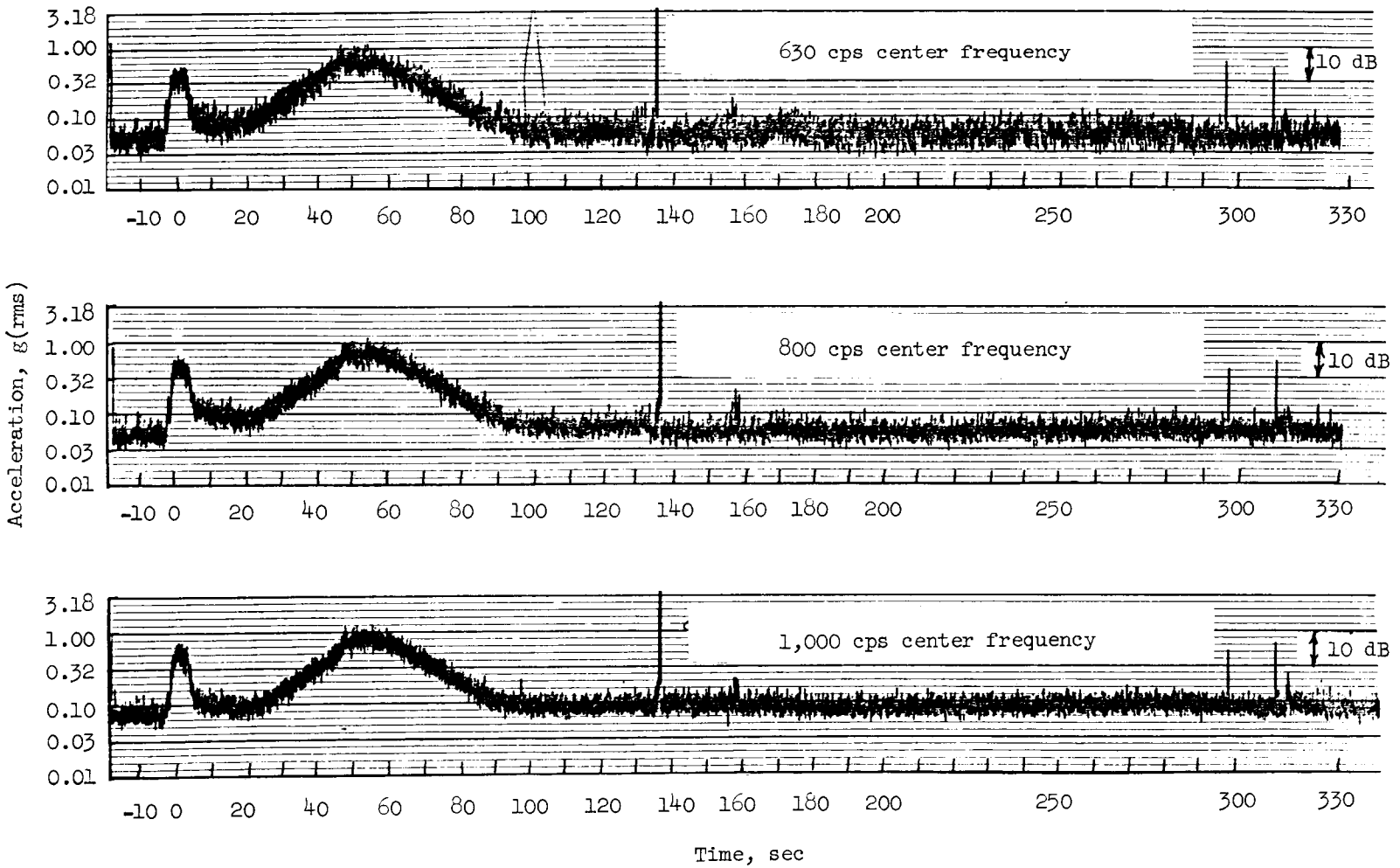

(f) 630, 800, and 1000 cps center frequencies.

Figure 16.- Continued.

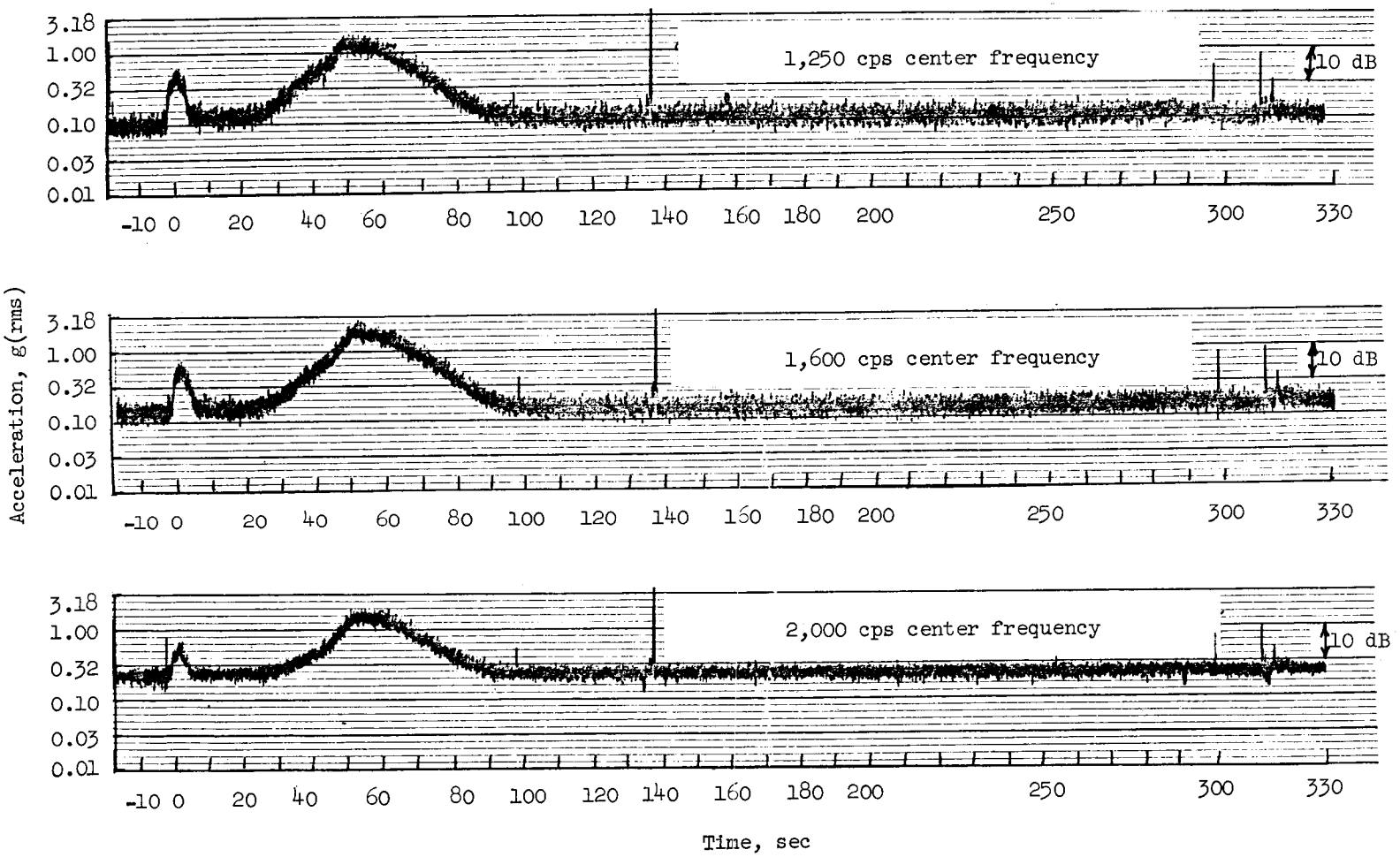

(g) 1250, 1600, and 2000 cps center frequencies.

Figure 16.- Continued.

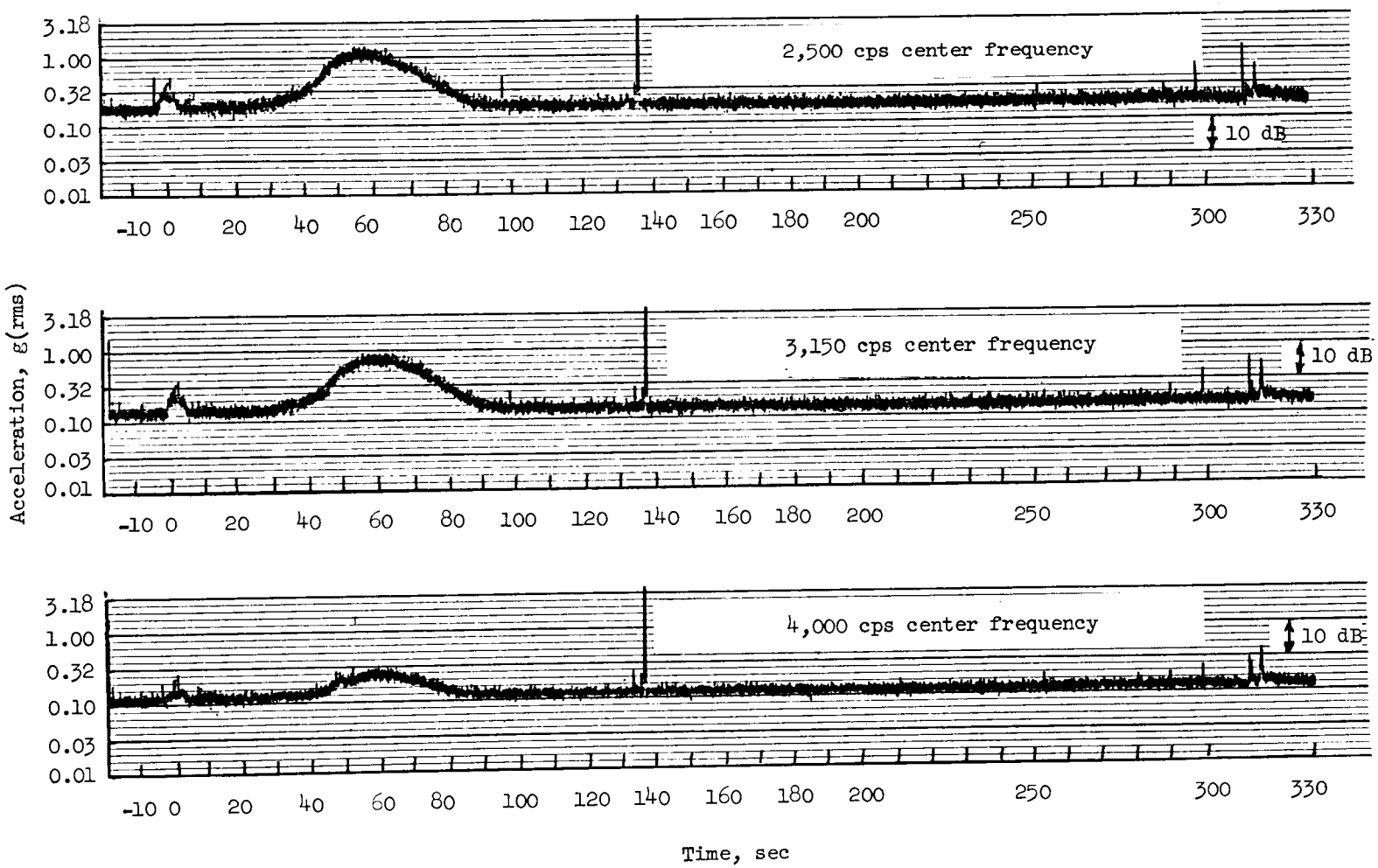

(h) 2500, 3150, and 4000 cps center frequencies.

Figure 16.- Continued.

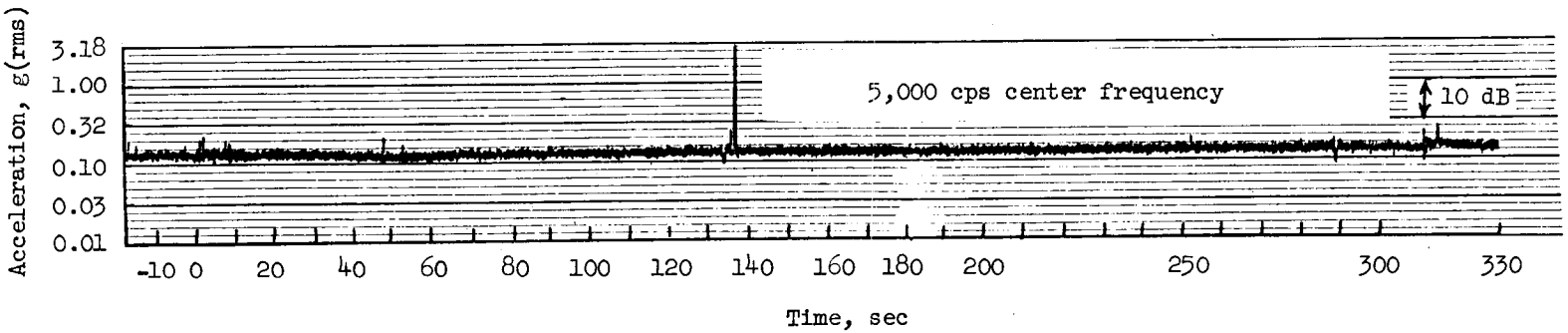

(i) 5000 cps center frequencies.

Figure 16.- Concluded.

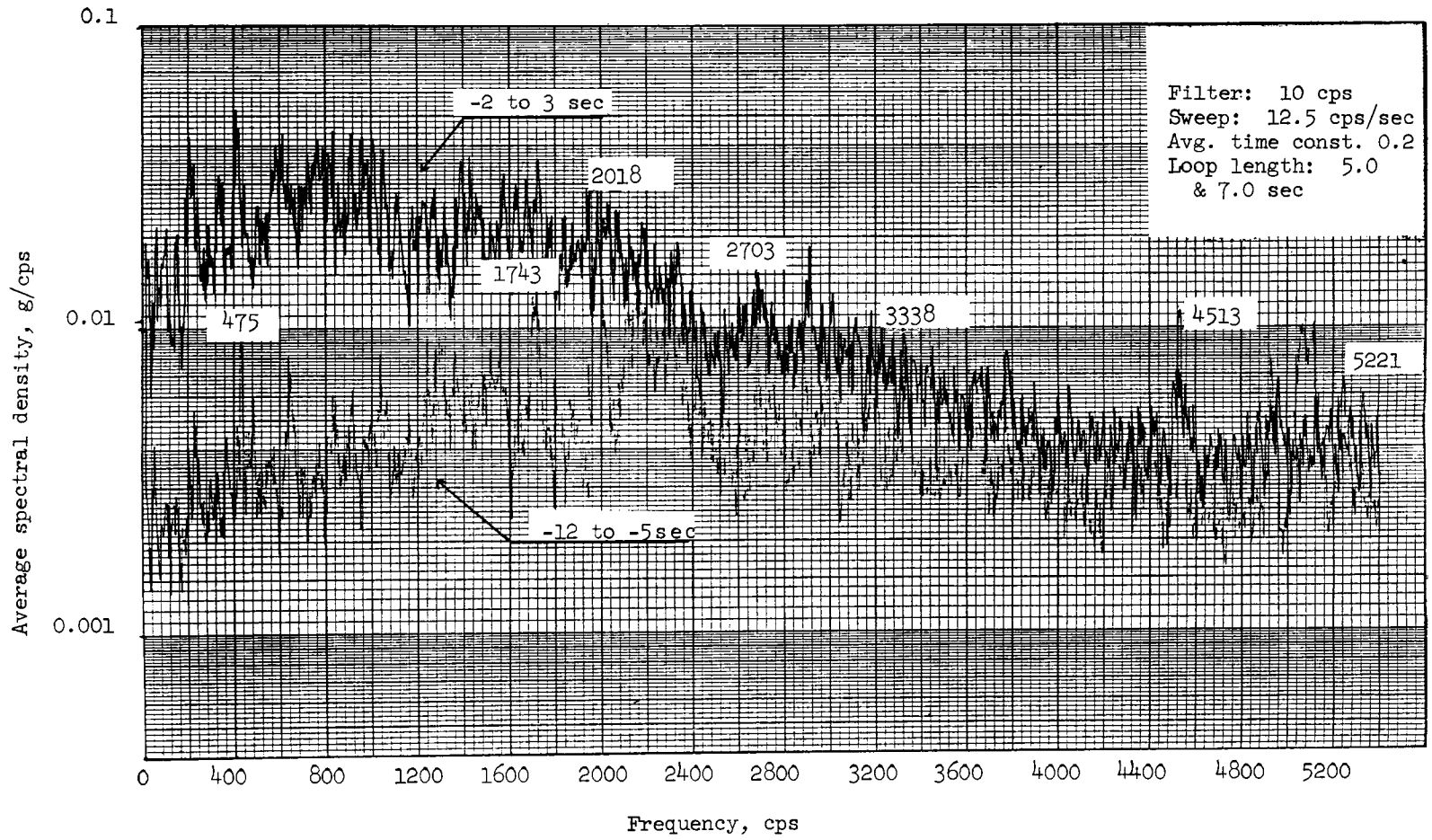

Figure 17.- Spectral density analysis. 10 cps filter; -2 to 3 seconds and -12 to -5 seconds.

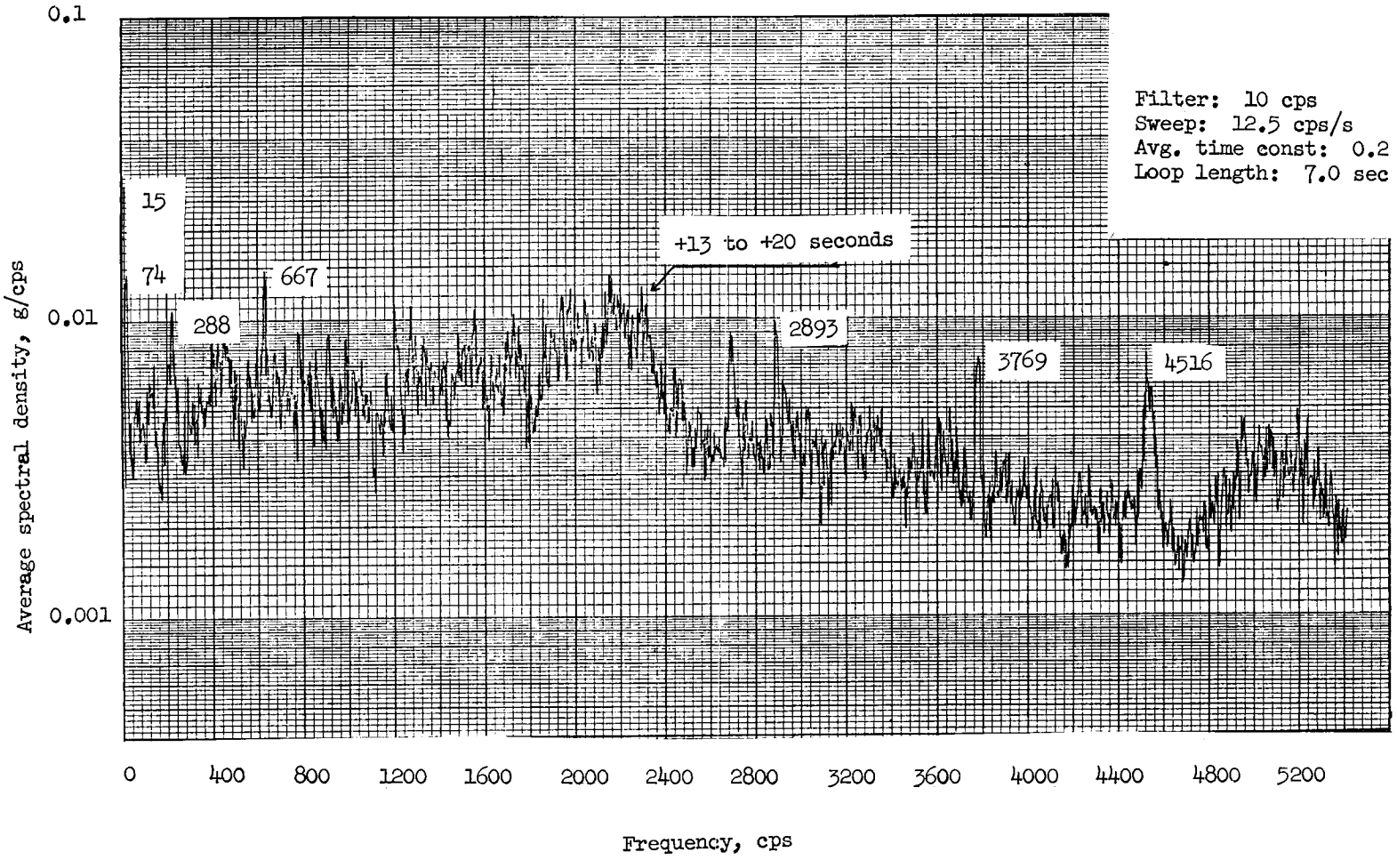

Figure 18.- Spectral density analysis. 10 cps filter; 13 to 20 seconds; 40 kcps channel.

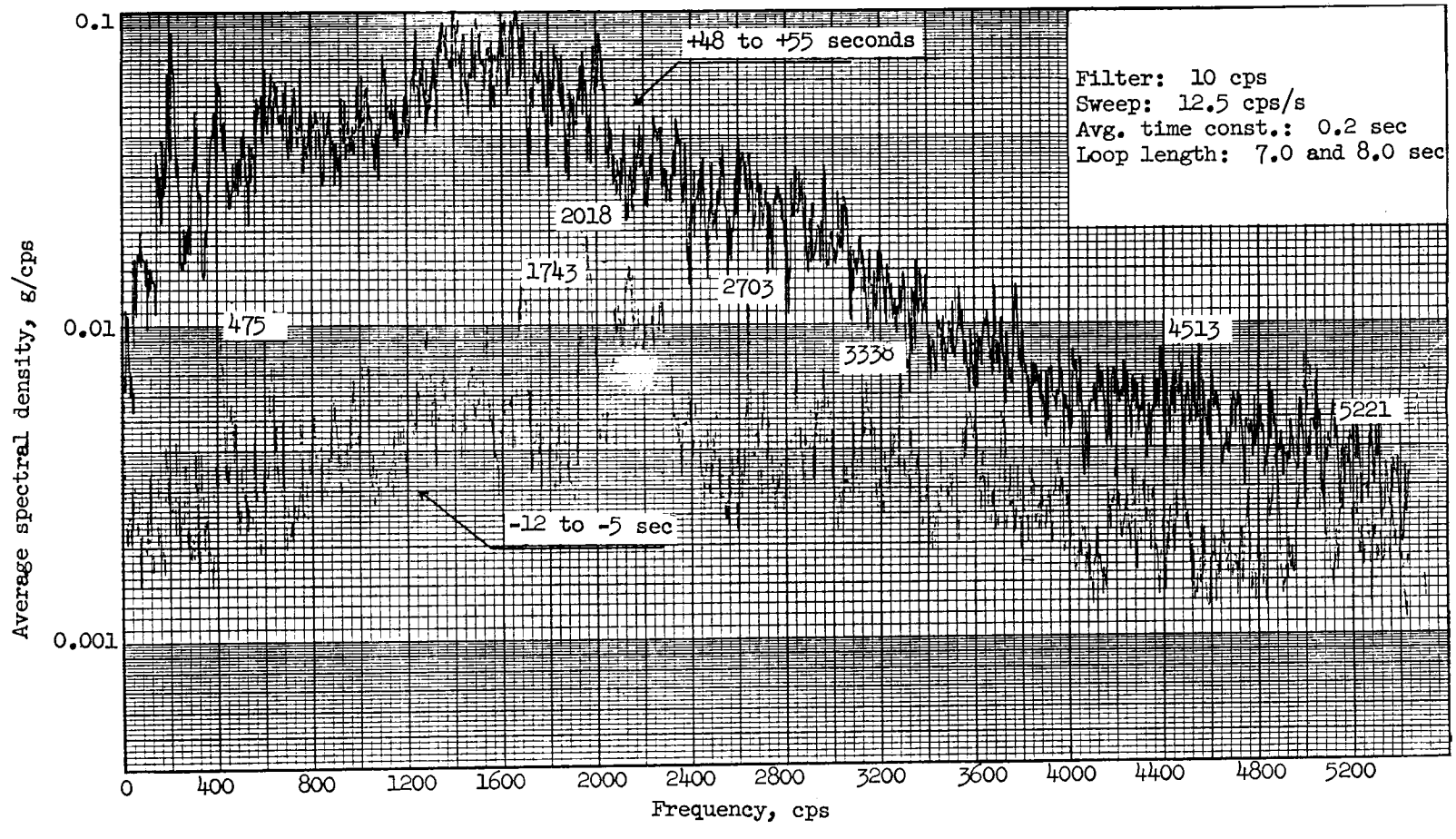

Figure 19.- Spectral density analysis. 10 cps filter; 48 to 55 seconds and -12 to -5 seconds; 40 kcps channel.

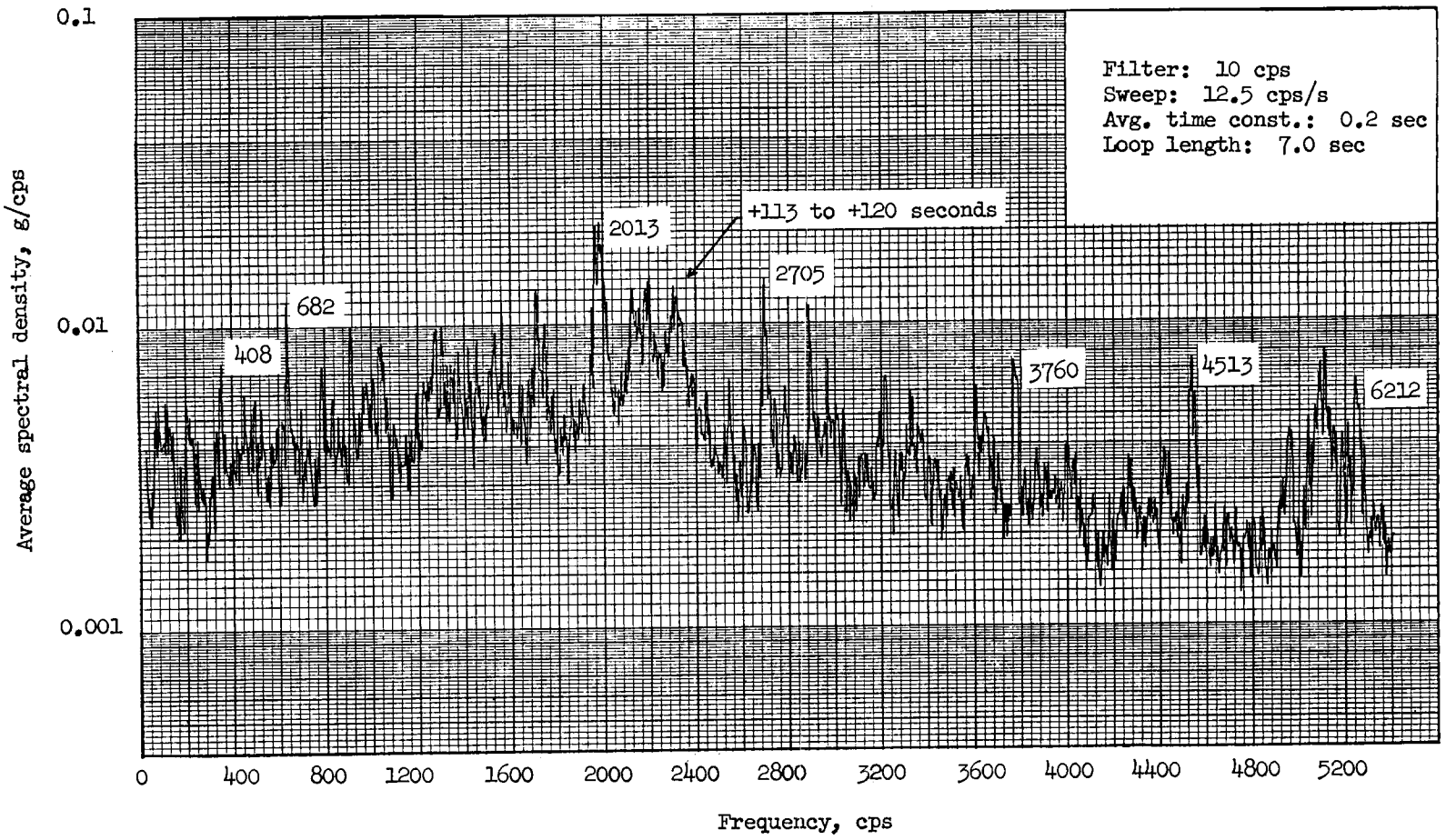

Figure 20.- Spectral density analysis. 10 cps filter; 113 to 120 seconds; 40 kcps channel.

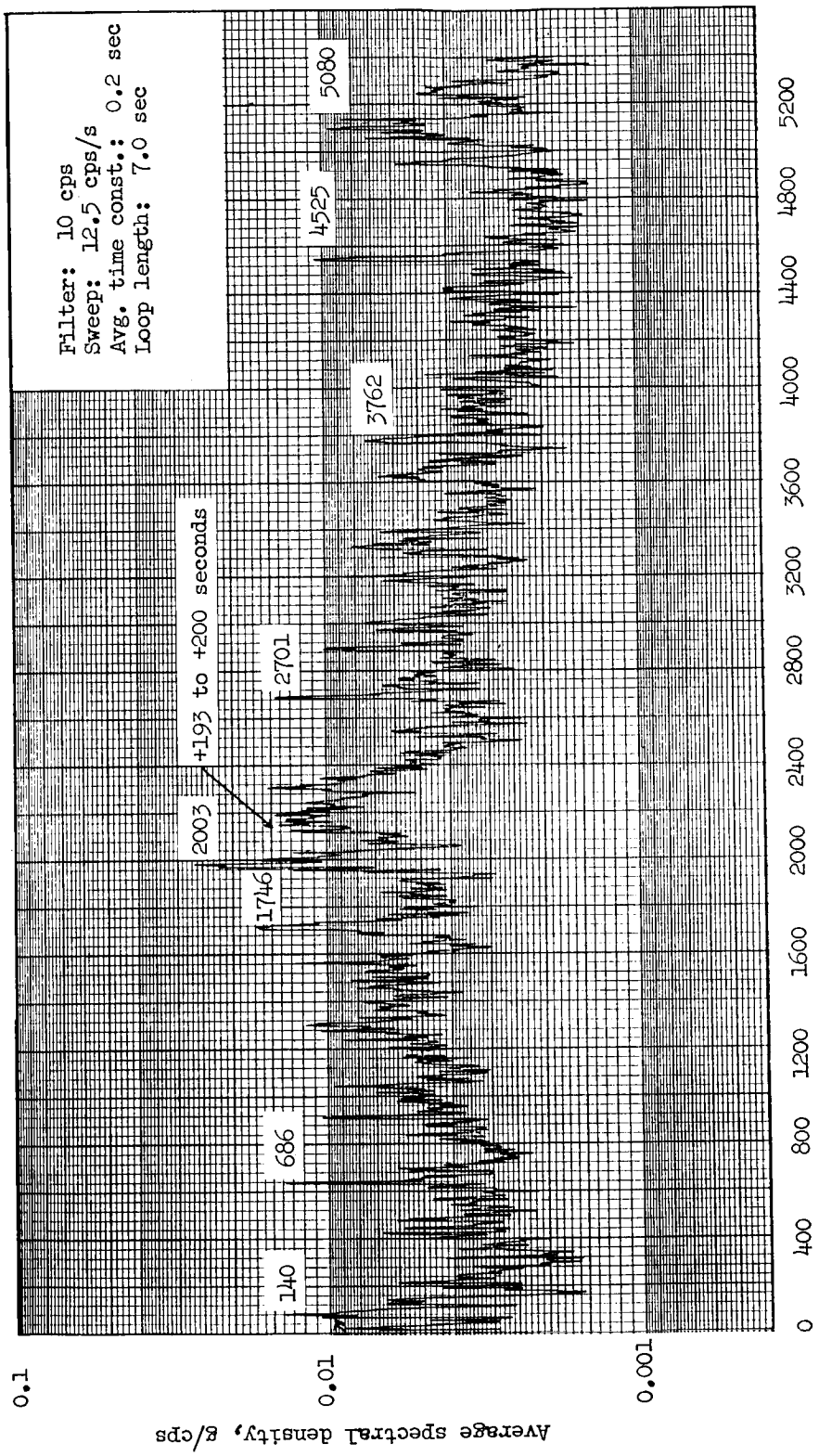

Figure 21.- Spectral density analysis. 10 cps filter; 193 to 200 seconds; 40 kcps channel.

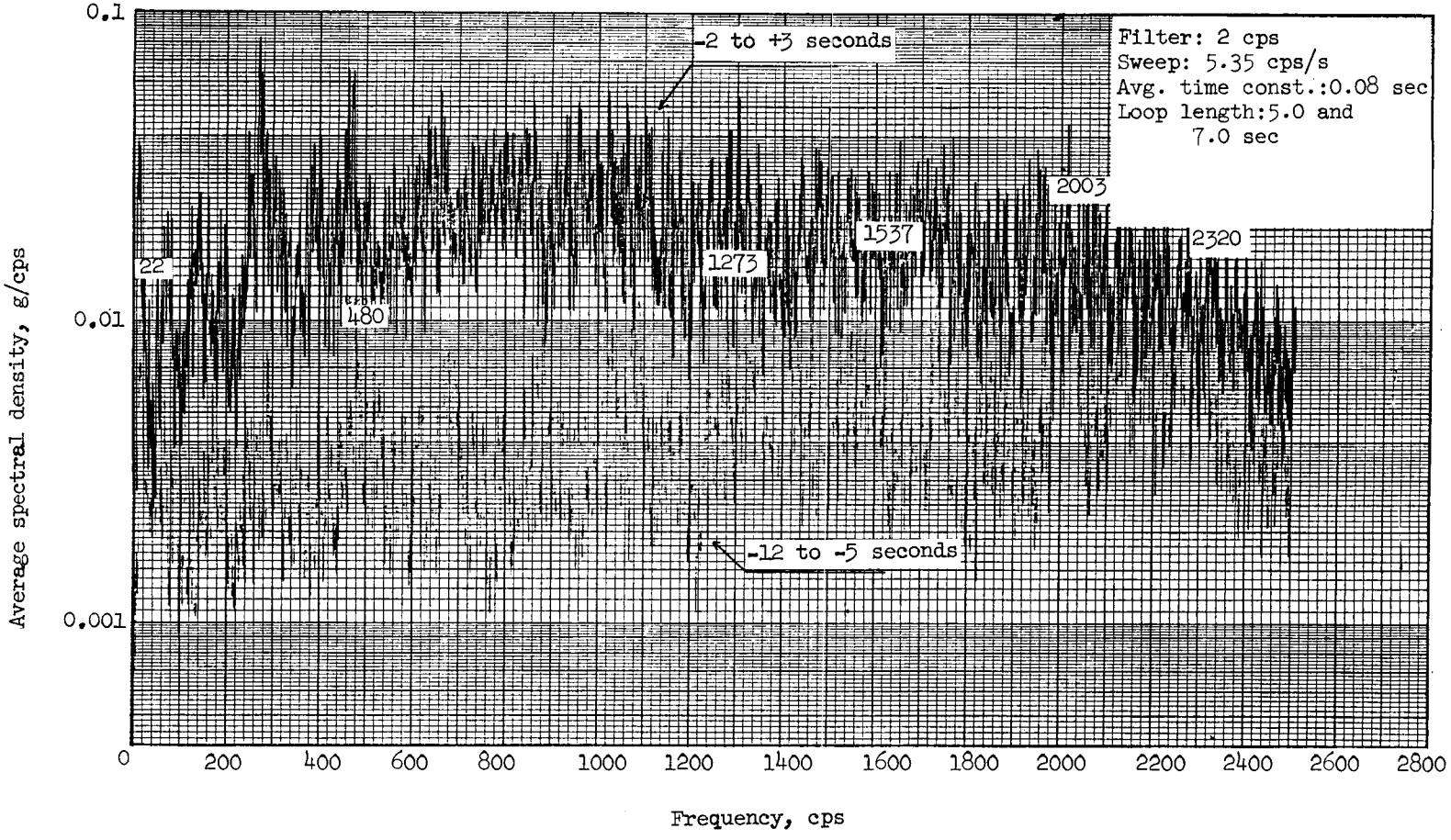

Figure 22.- Spectral density analysis. 2 cps filter; -2 to 3 seconds and -12 to -5 seconds; 40 kcps channel.

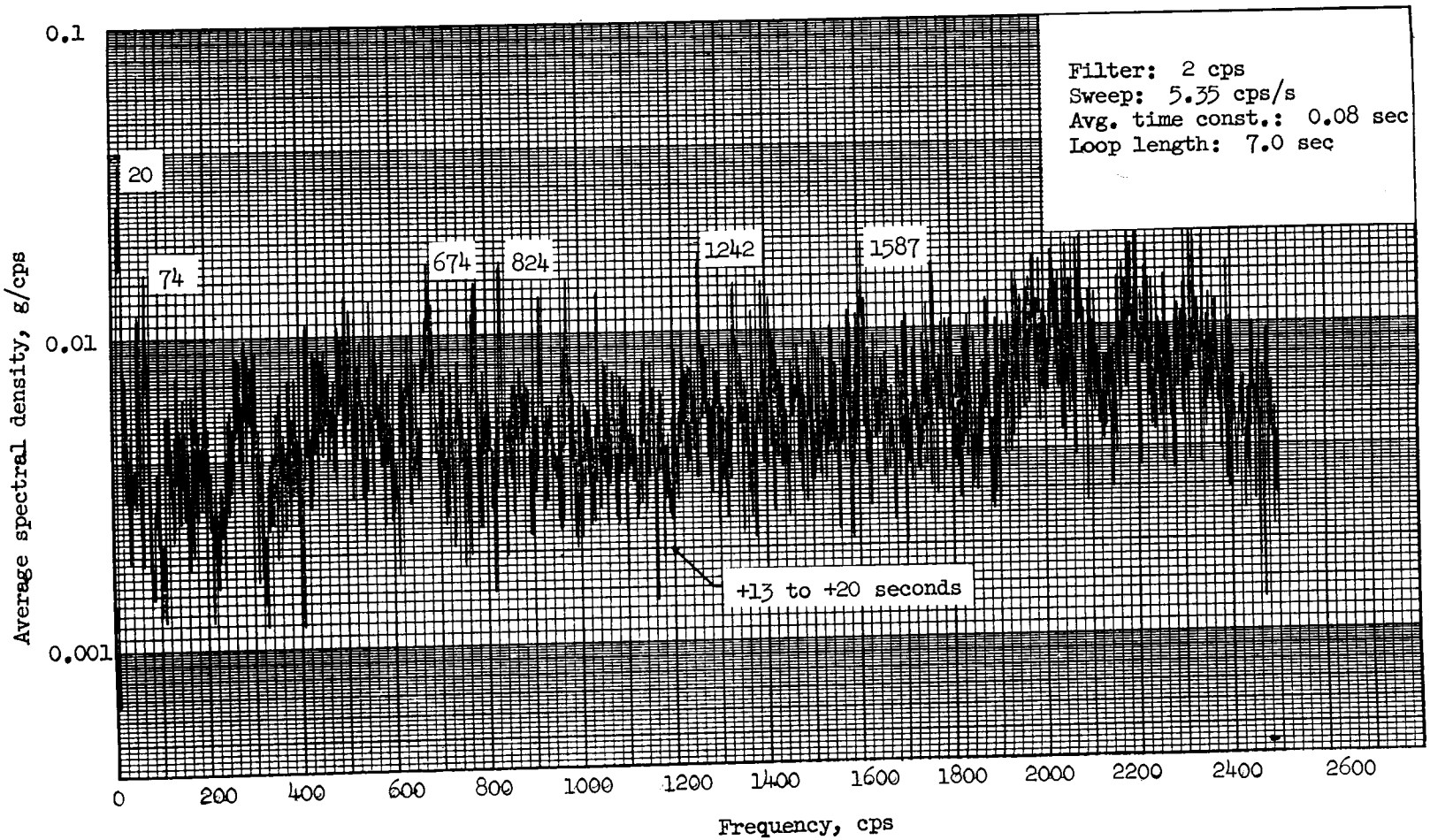

Figure 23.- Spectral density analysis. 2 cps filter; 13 to 20 seconds; 40 kcps channel.

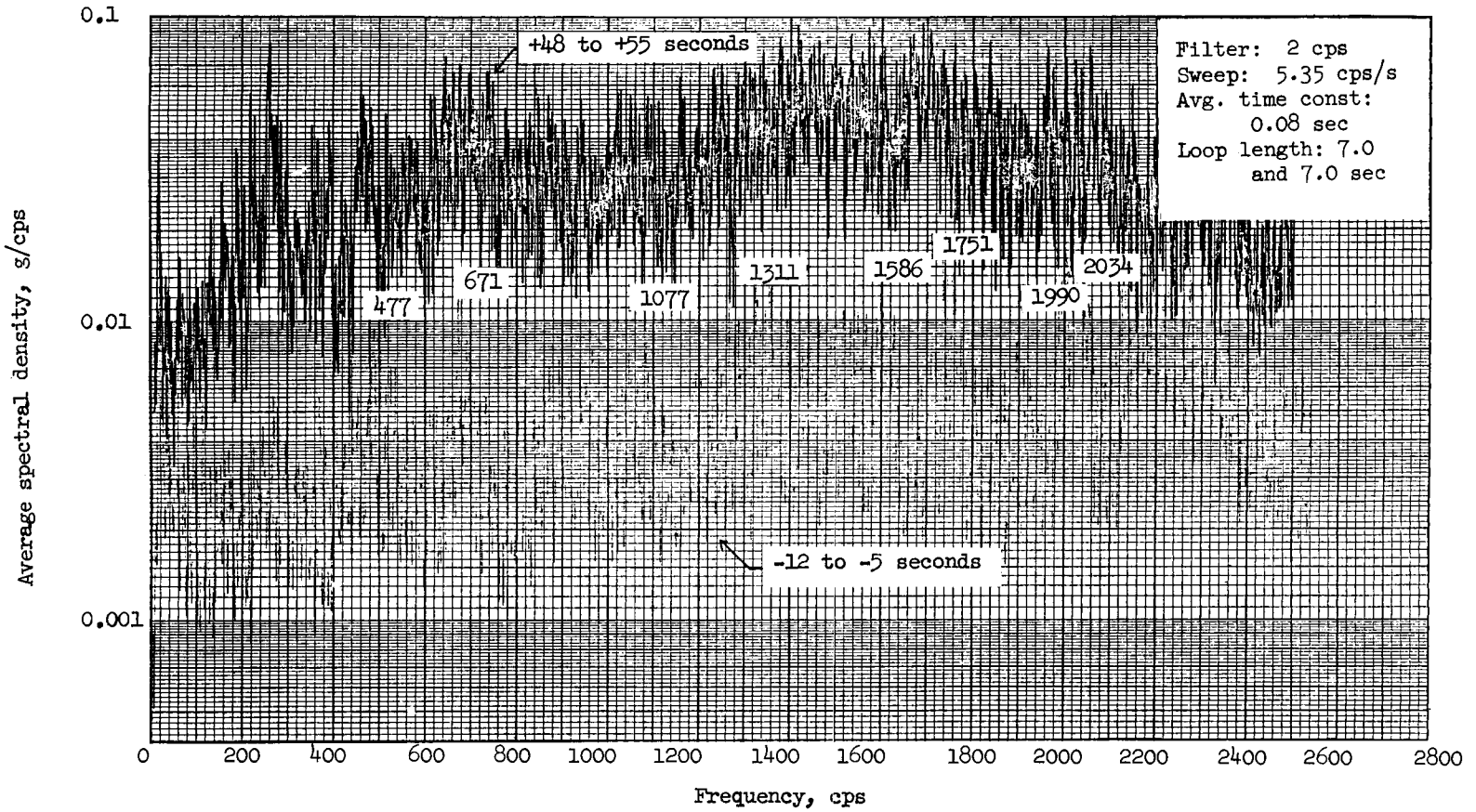

Figure 24.- Spectral density analysis. 2 cps filter; 48 to 55 seconds and -12 to -5 seconds; 40 kcps channel.

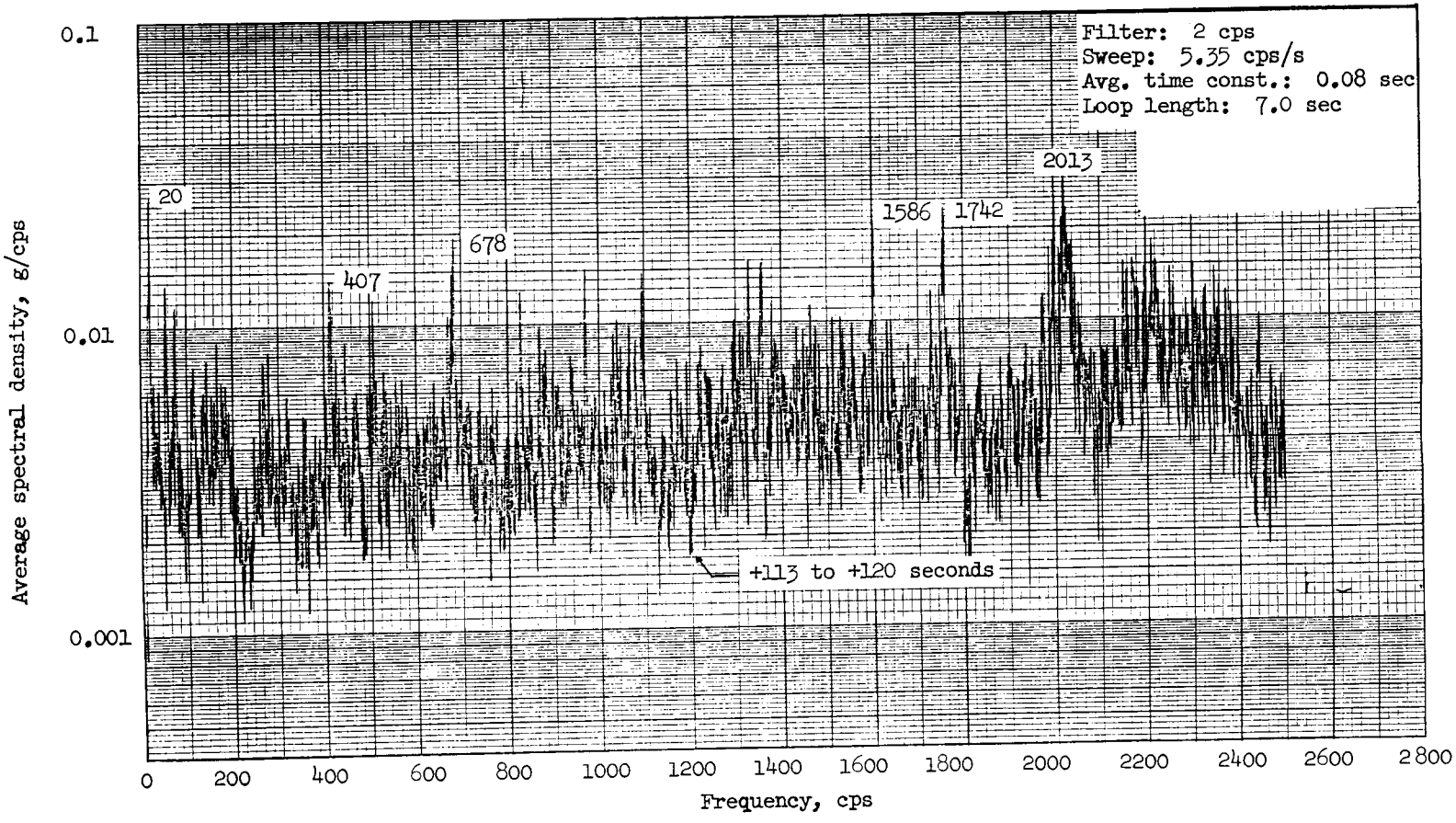

Figure 25.- Spectral density analysis. 2 cps filter; 113 to 120 seconds; 40 kcps channel.

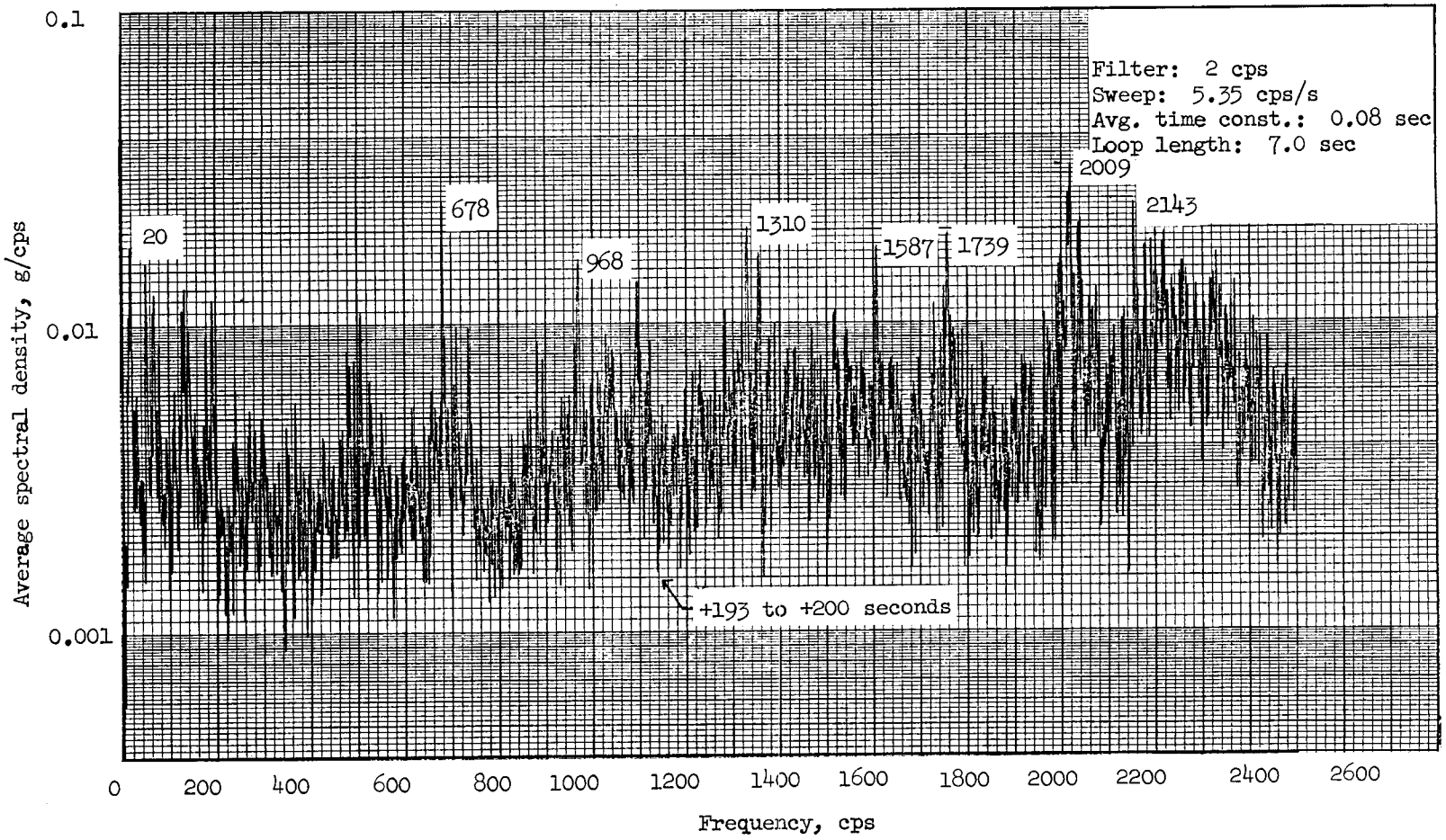

Figure 26.- Spectral density analysis. 2 cps filter; 193 to 200 seconds; 40 kcps channel.

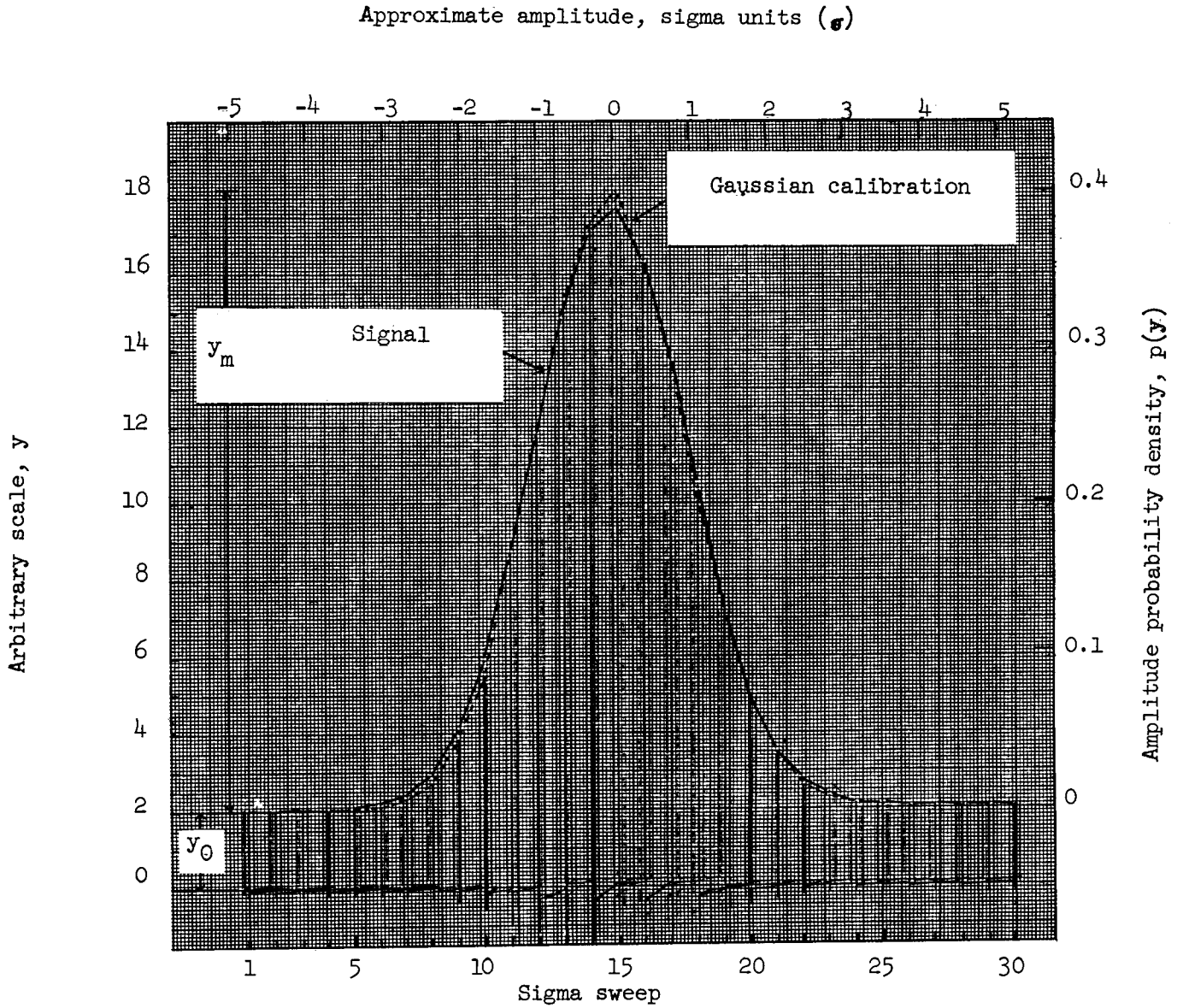

Figure 27.- Probability density analysis. -12 to -5 seconds; 40 kcps channel; Scale factor, S.F.; S.F. $= \frac{0.4}{y_m}$; $p(y) = (S.F.)(y - y_0)$.

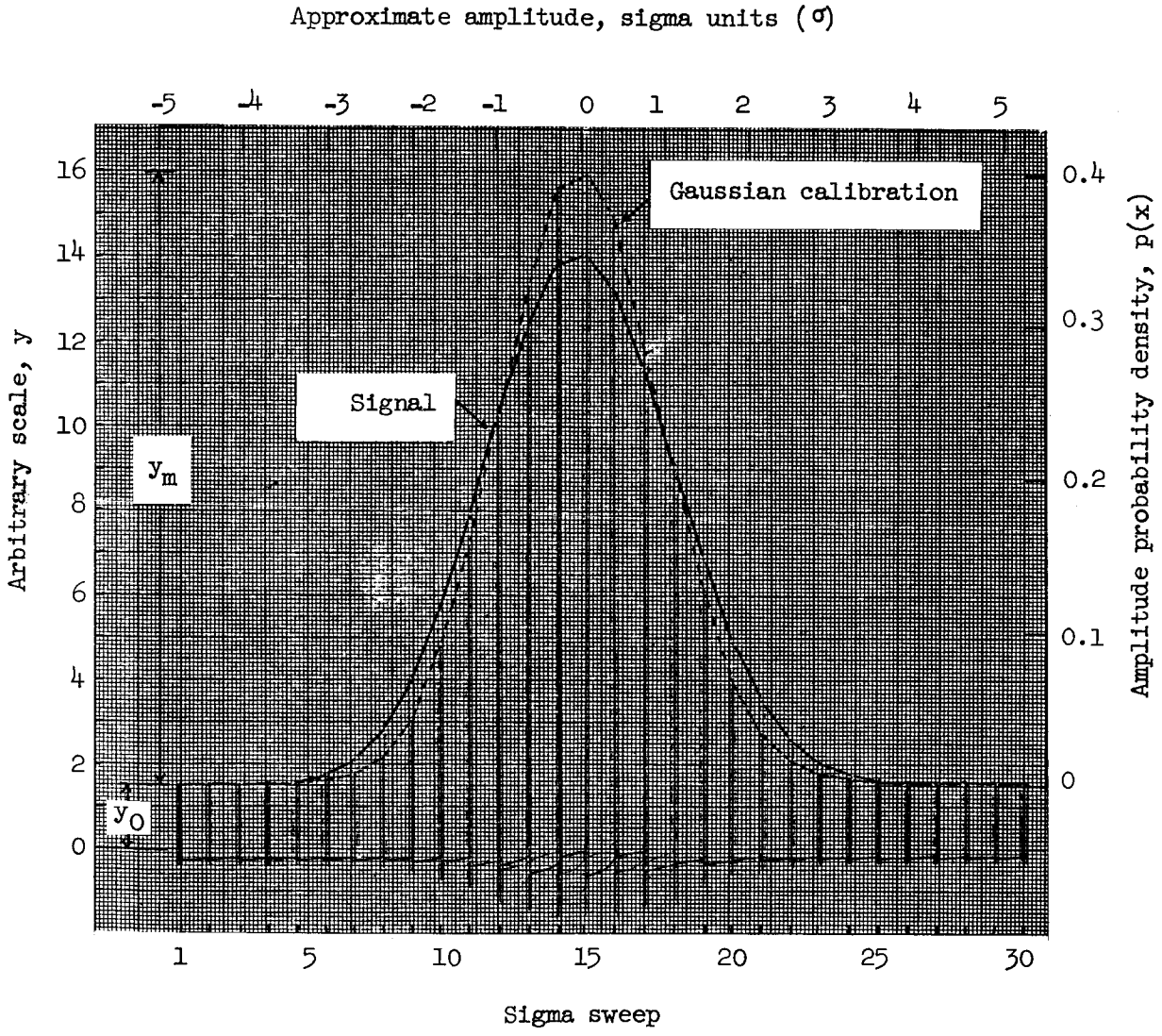

Figure 29.- Probability density analysis. 48 to 55 seconds; 40 kcps channel; Scale factor (S.F.) = $\frac{0.4}{y_m}$; $p(x) = (S.F.)(y - y_0)$.

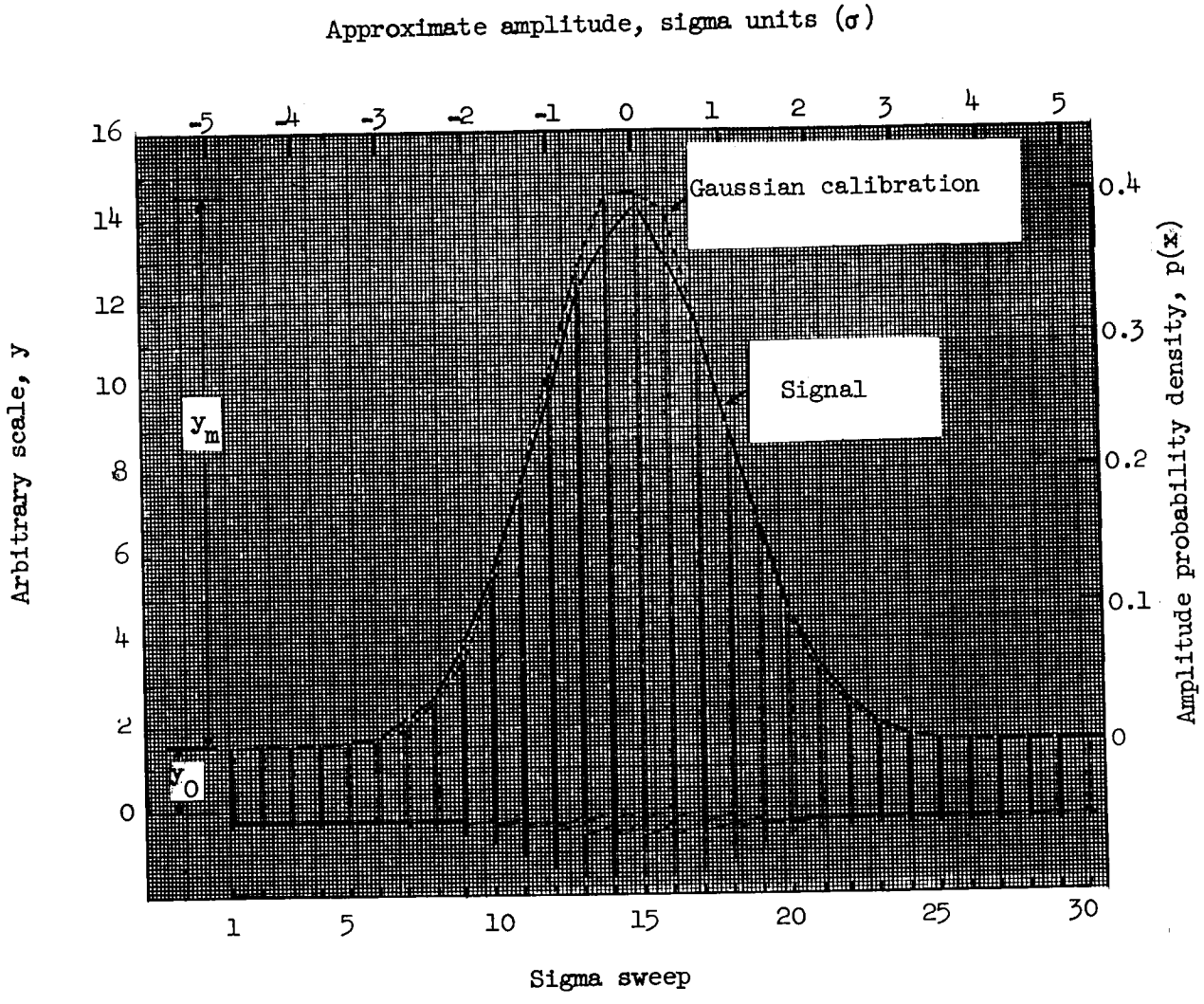

Figure 28.- Probability density analysis. -3 to 4 seconds; 40 kcps channel; Scale factor (S.F.) $= \frac{0.4}{y_m}$; $p(x) = (S.F.)(y - y_0)$.

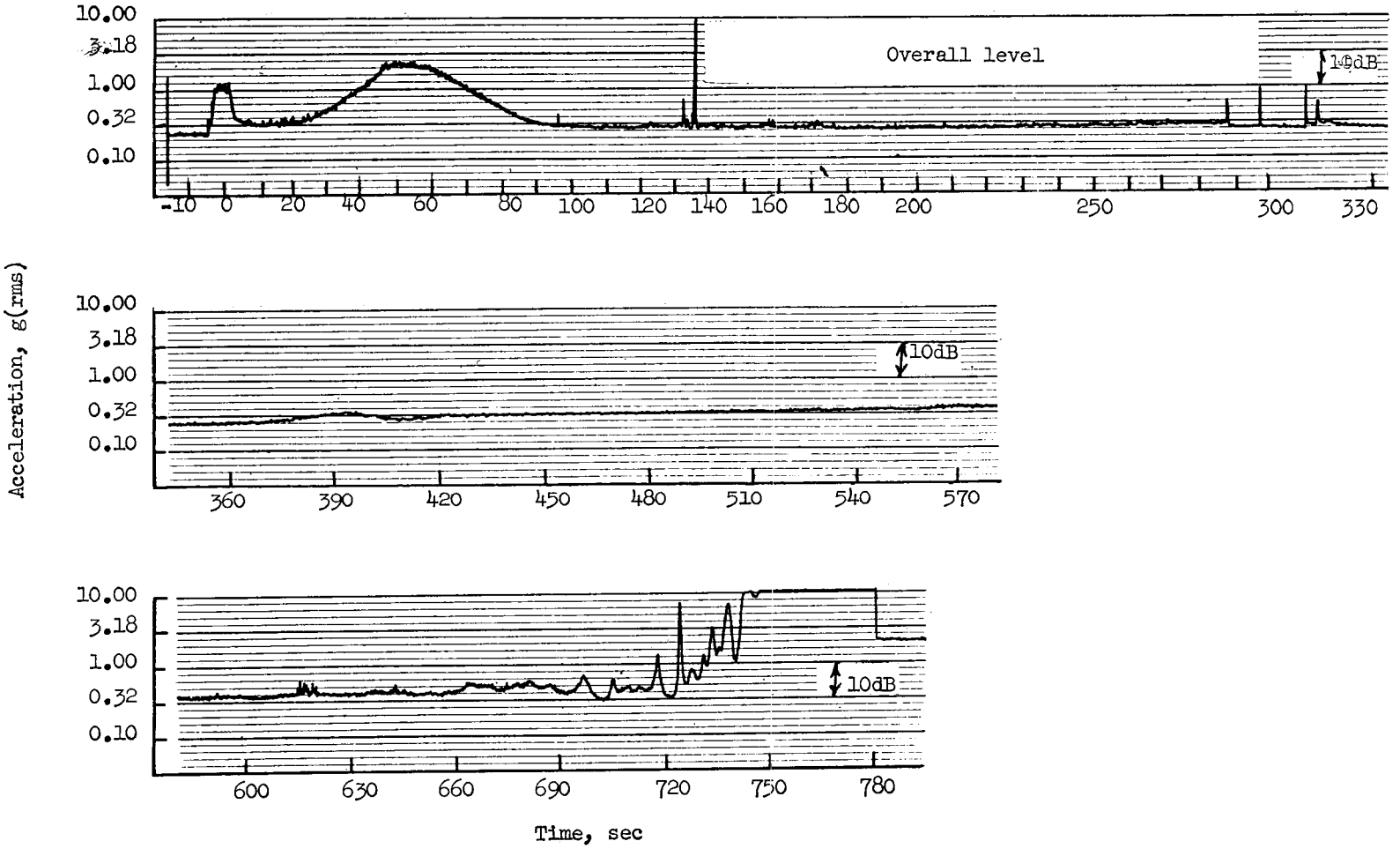

(a) Overall level; 52.5 kcps channel, 5 kcps output filter.

Figure 30.- Overall level and one-third band-pass analyses.

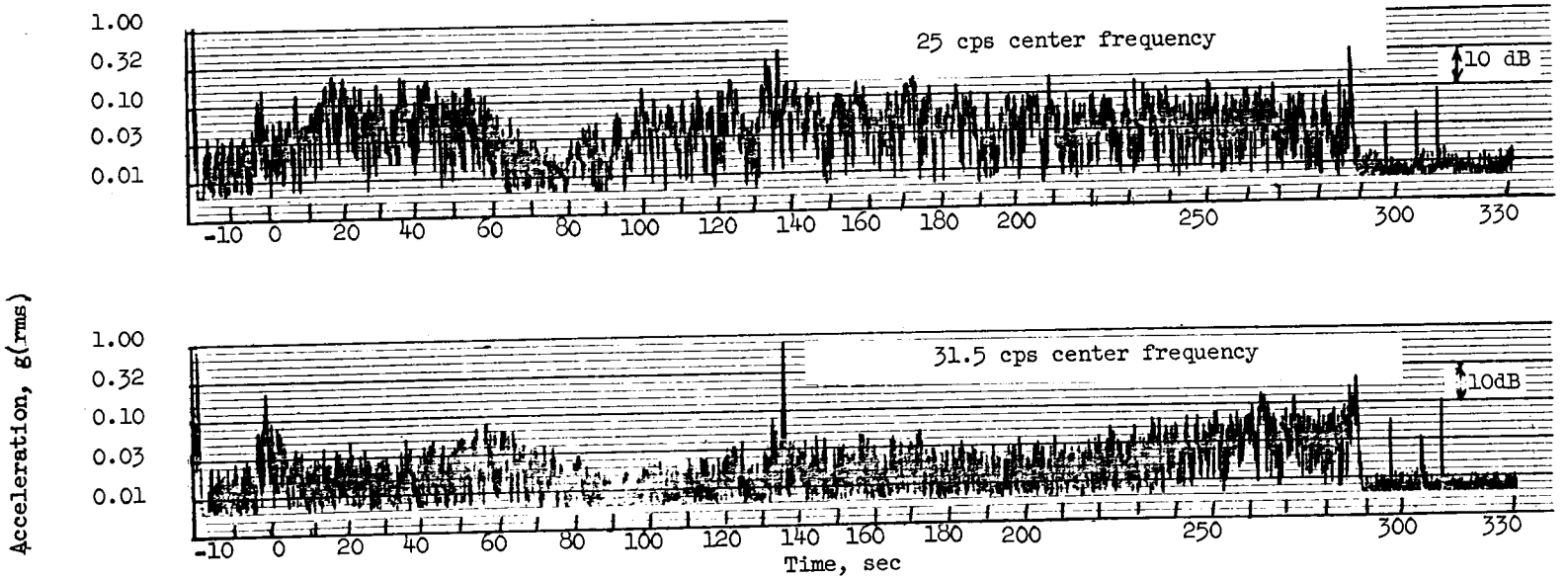

(b) 25 and 31.5 cps center frequency.

Figure 30.- Continued.

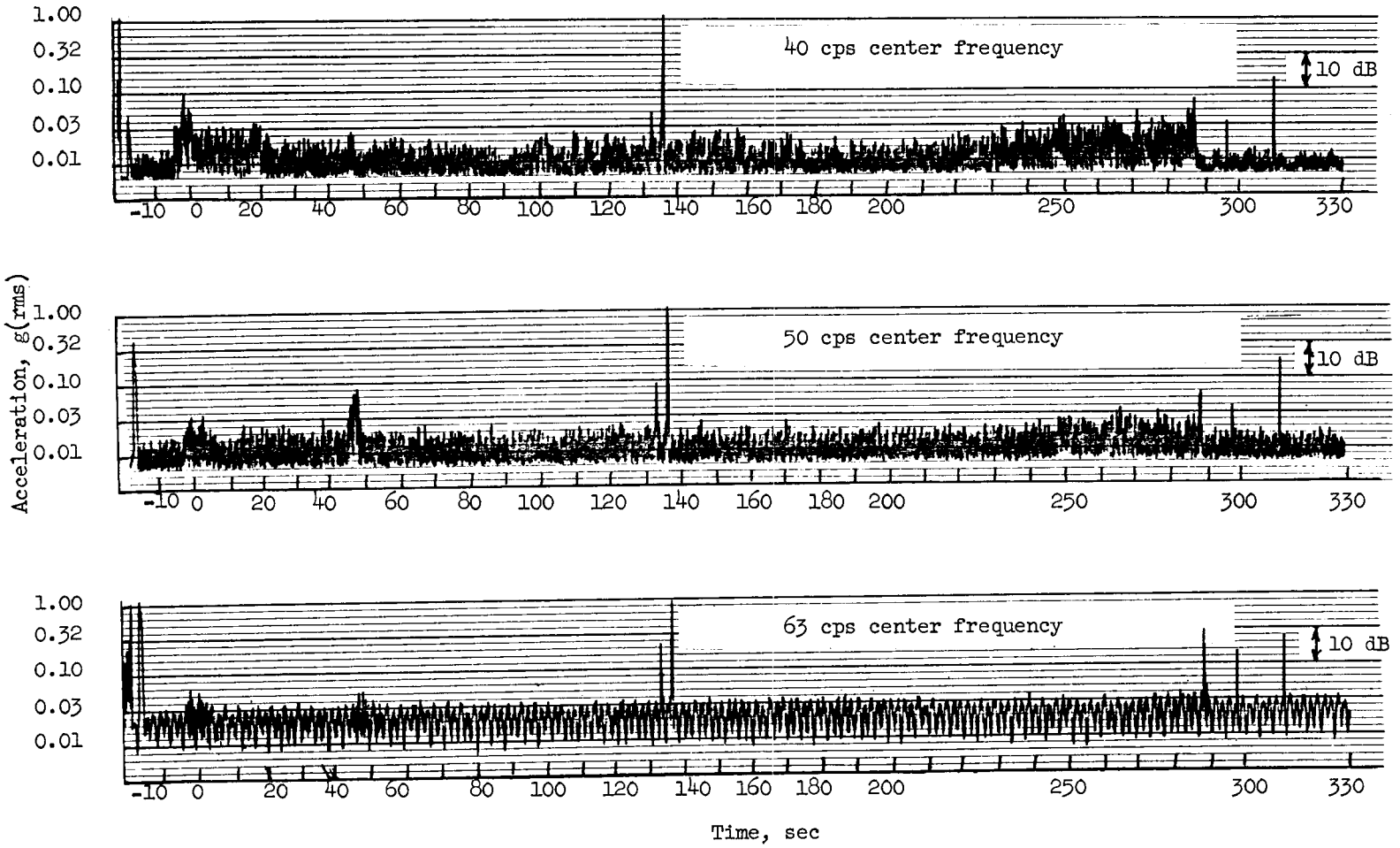

(c) 40, 50, and 63 cps center frequency.

Figure 30.- Continued.

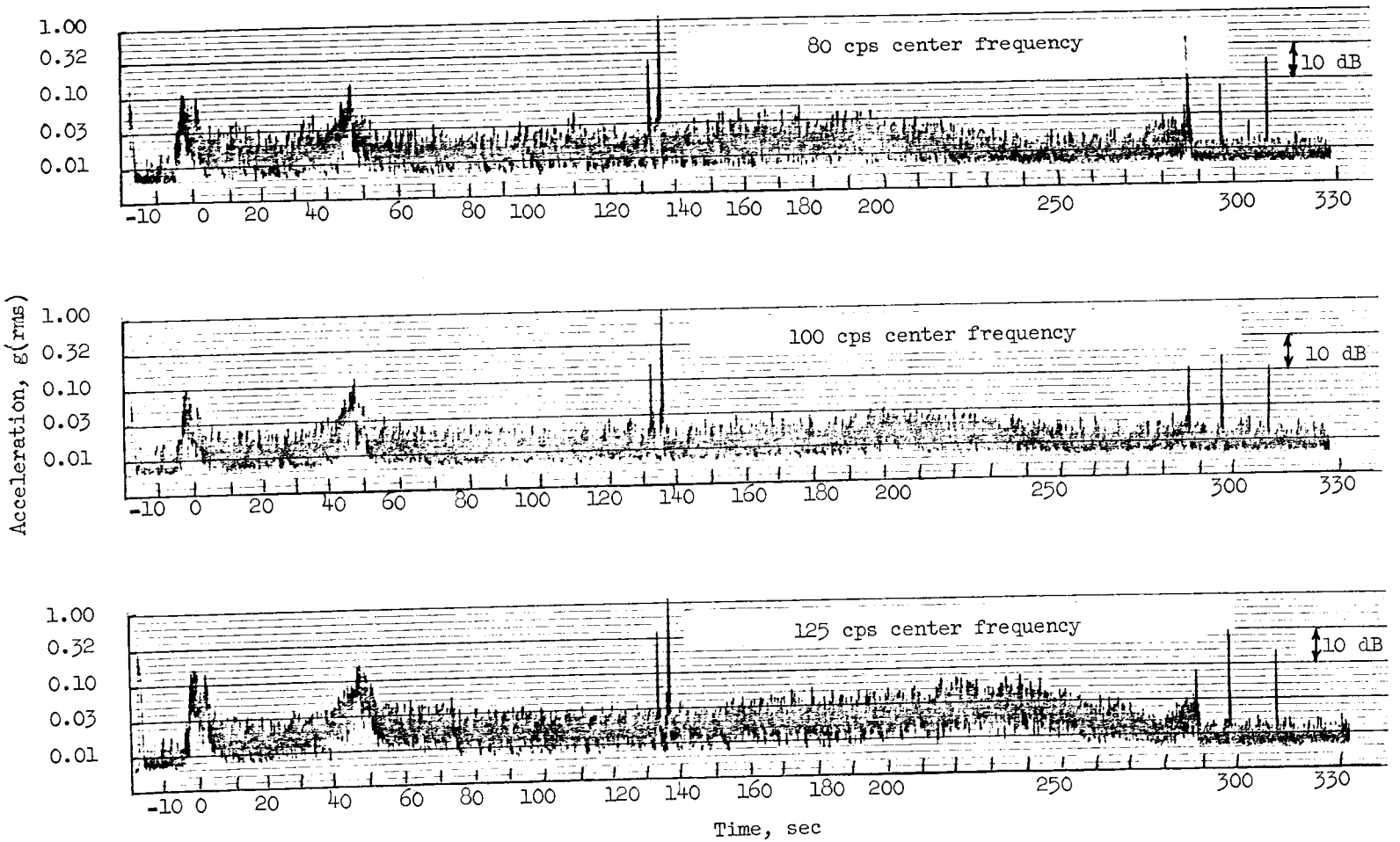

(d) 80, 100, and 125 cps center frequency.

Figure 30.- Continued.

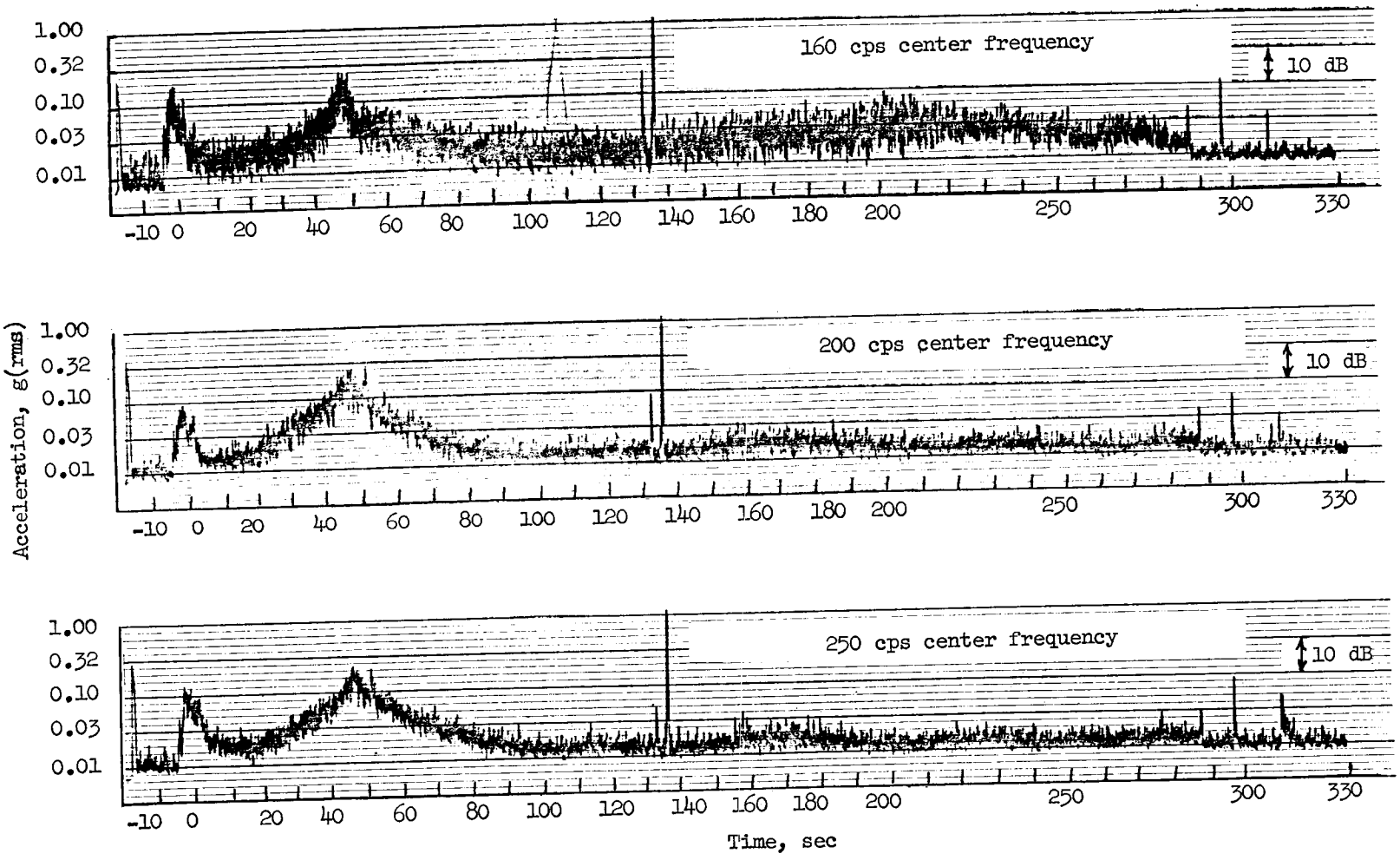

(e) 160, 200, and 250 cps center frequency.

Figure 30.- Continued.

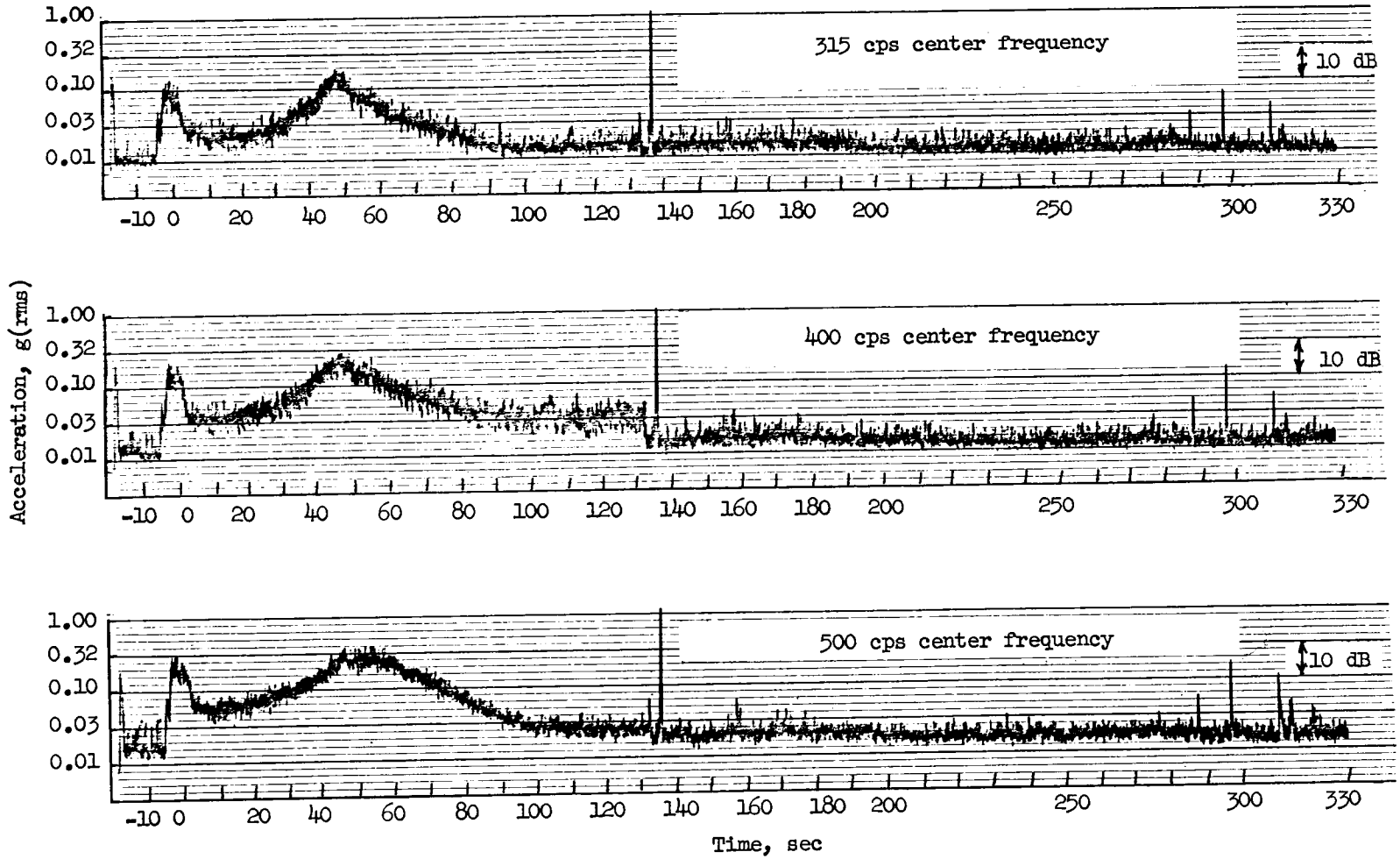

(f) 315, 400, and 500 cps center frequency.

Figure 30.- Continued.

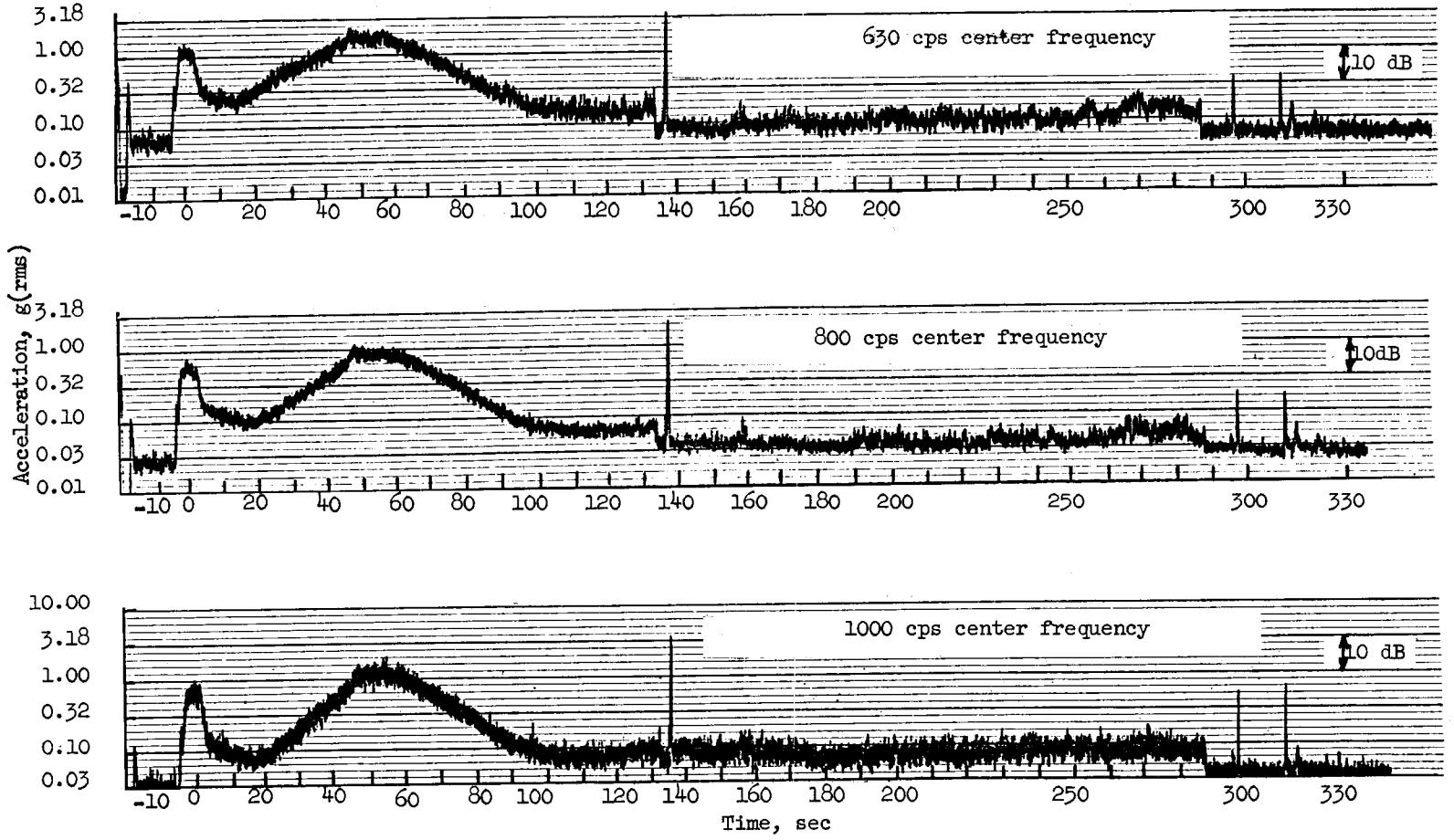

(g) 630, 800, and 1000 cps center frequency.

Figure 30.- Continued.

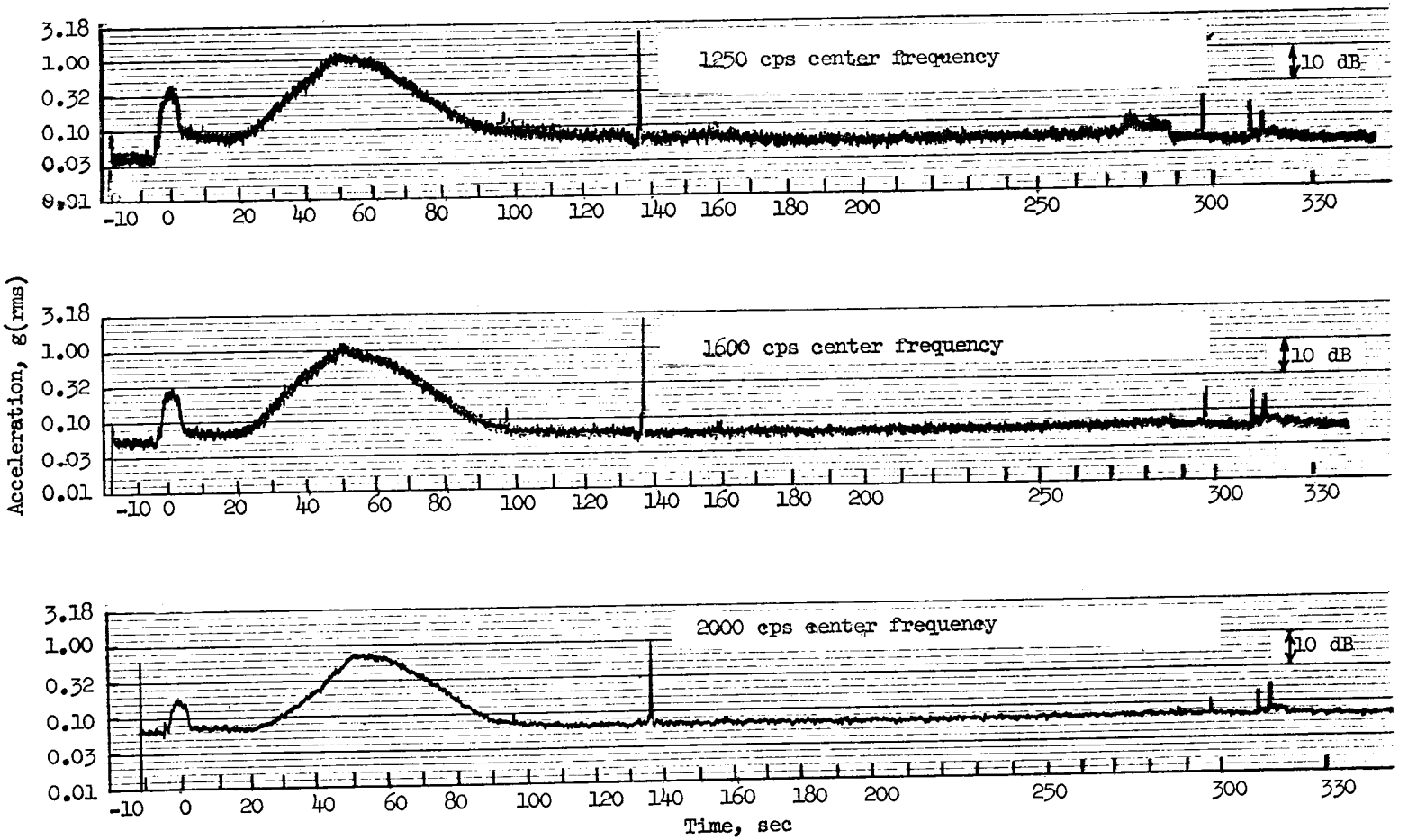

(h) 1250, 1600, and 2000 cps center frequency.

Figure 30.- Continued.

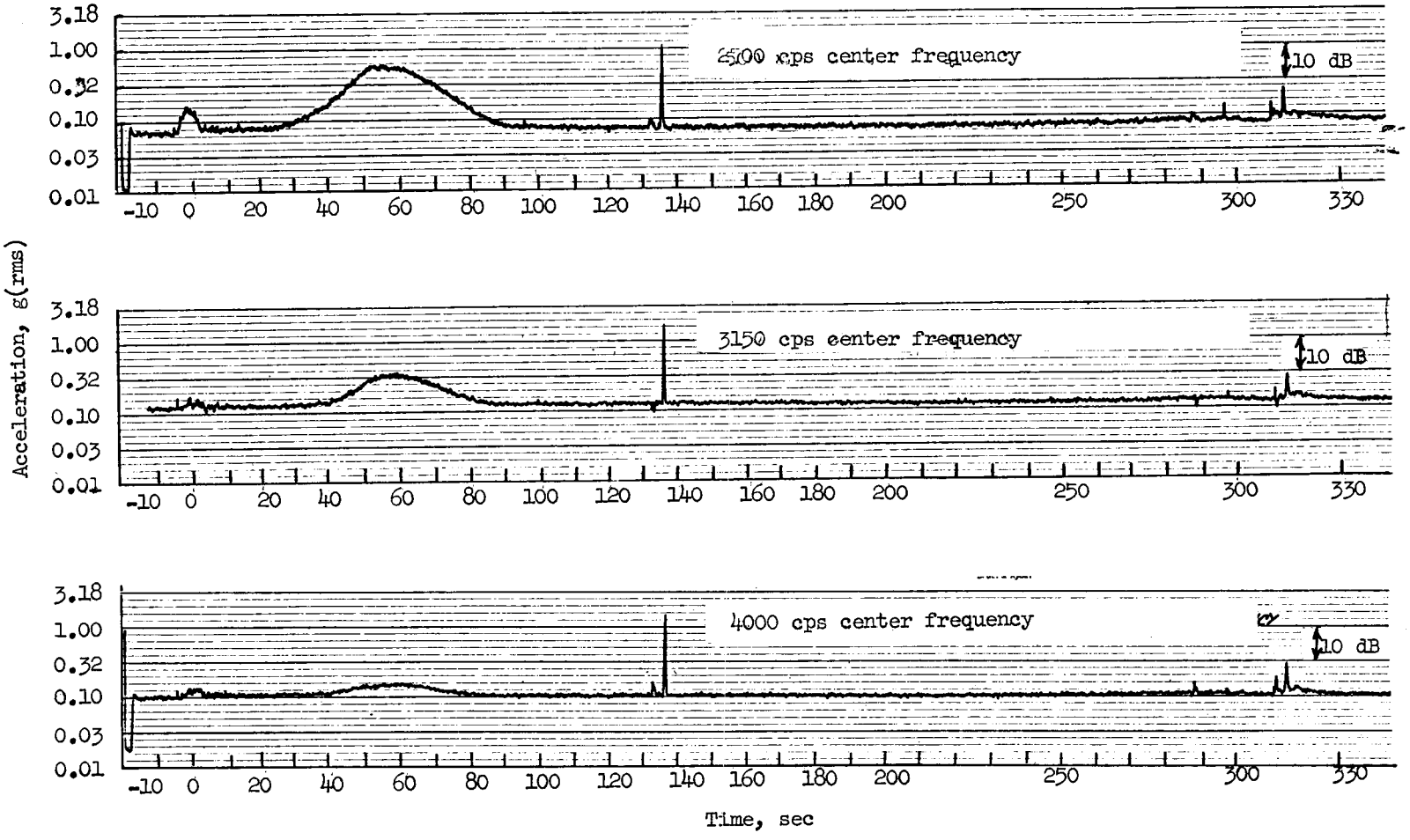

(i) 2500, 3150, and 4000 cps center frequency.

Figure 30.- Continued.

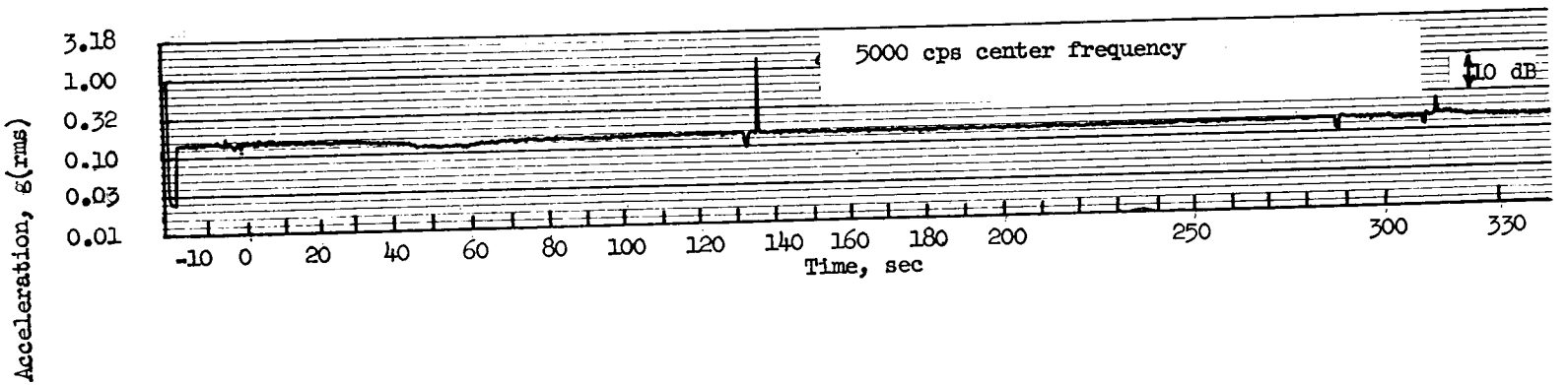

(j) 5000 cps center frequency.

Figure 30.- Concluded.

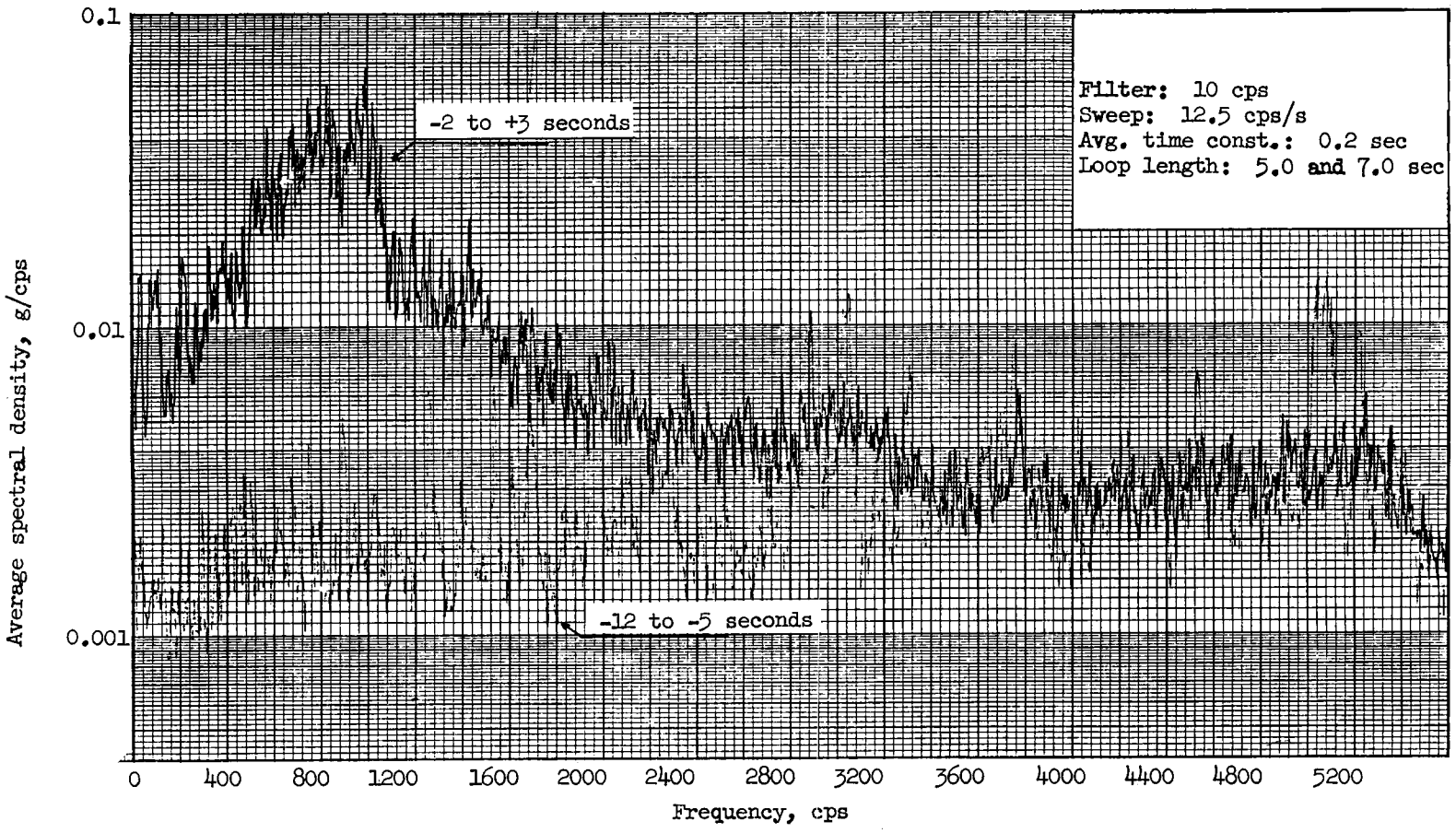

Figure 31.- Spectral density analysis. 10 cps filter; -2 to 3 seconds; -12 to -5 seconds; 52.5 kcps channel.

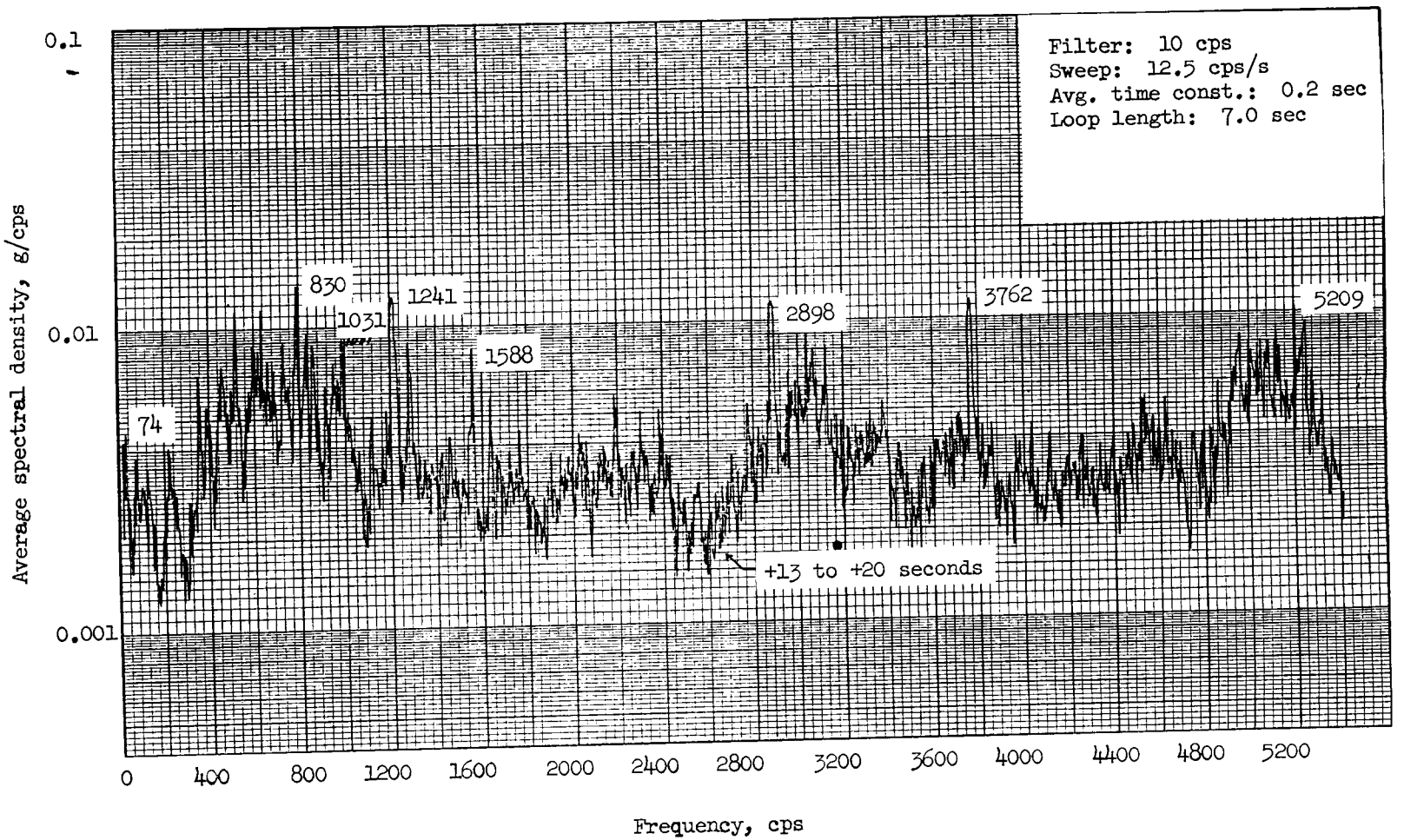

Figure 32.- Spectral density analysis. 10 cps filter; 13 to 20 seconds; 52.5 kcps channel.

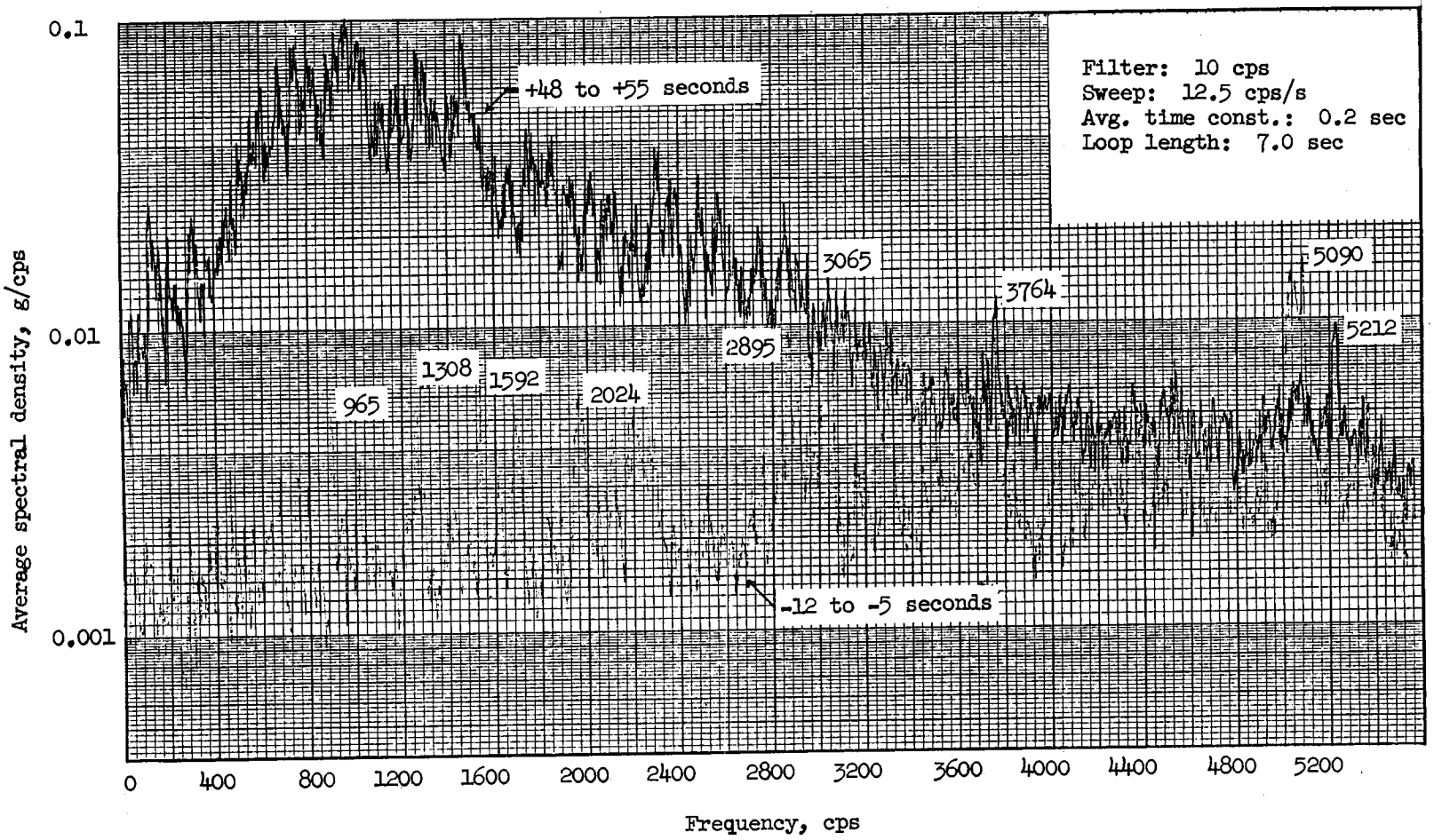

Figure 33.- Spectral density analysis. 10 cps filter; 48 to 55 seconds; -12 to -5 seconds; 52.5 kcps channel.

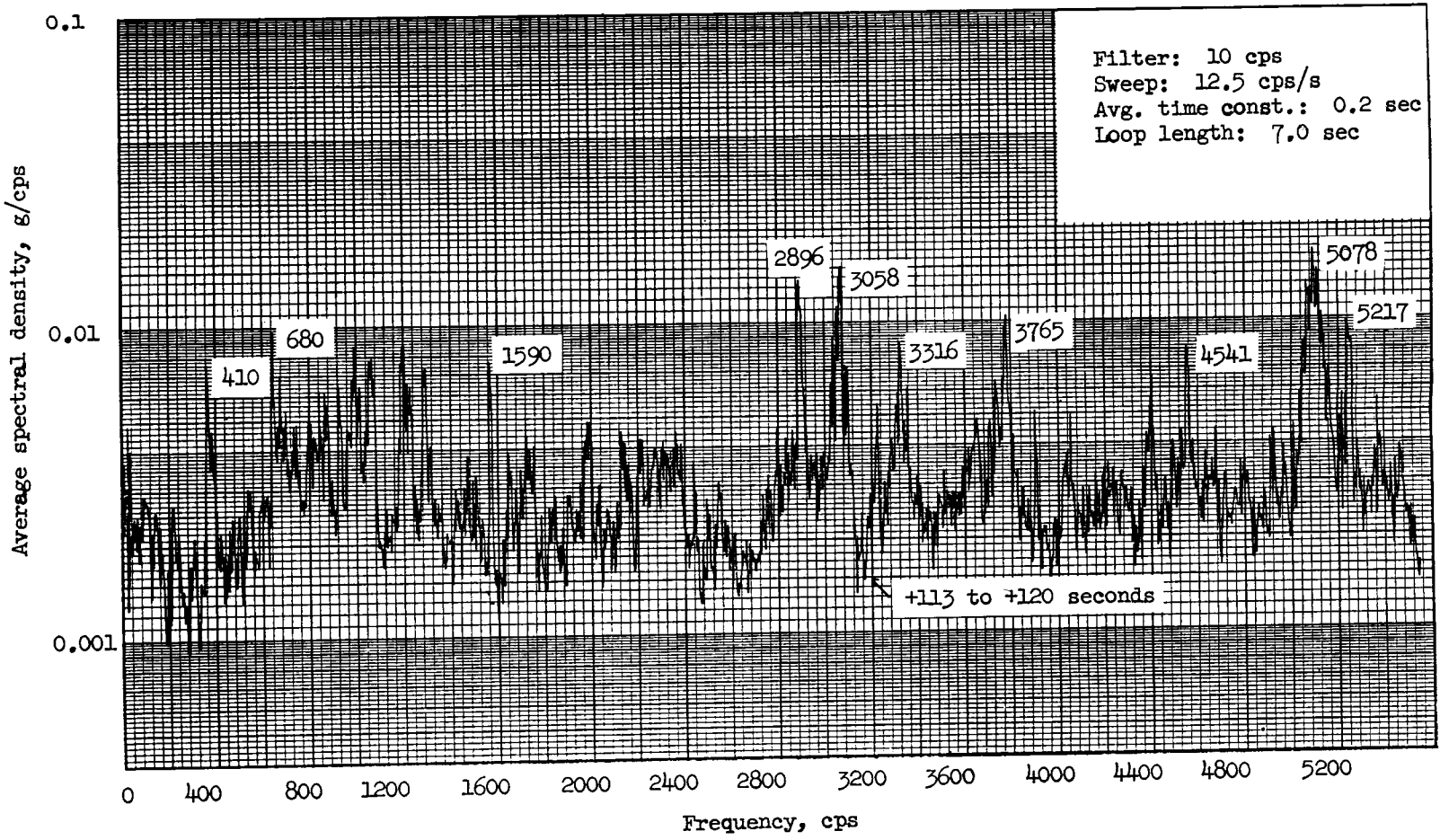

Figure 34.- Spectral density analysis. 10 cps filter; 113 to 120 seconds; 52.5 kcps channel.

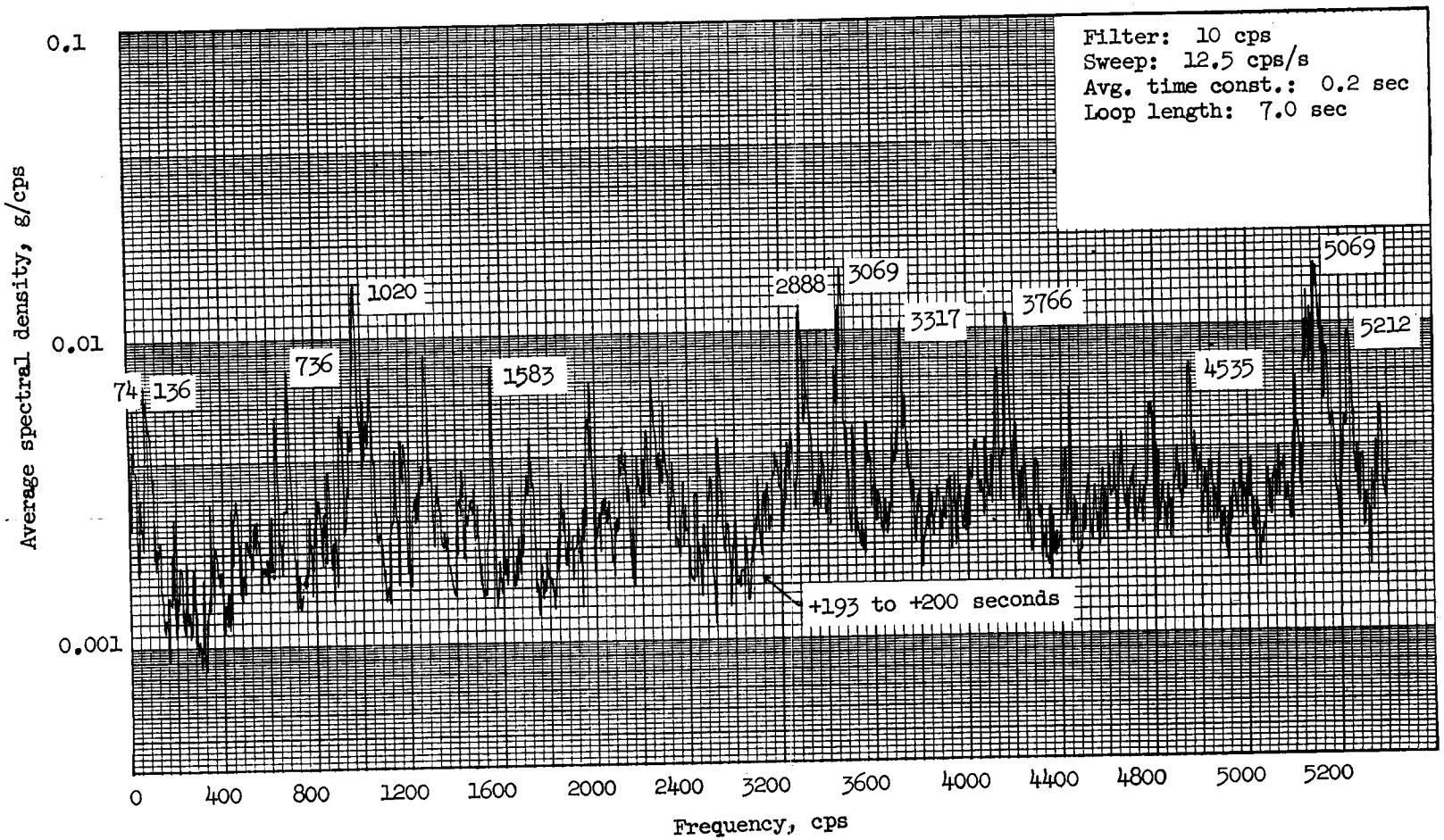

Figure 35.- Spectral density analysis. 10 cps filter; 193 to 200 seconds; 52.5 kcps channel.

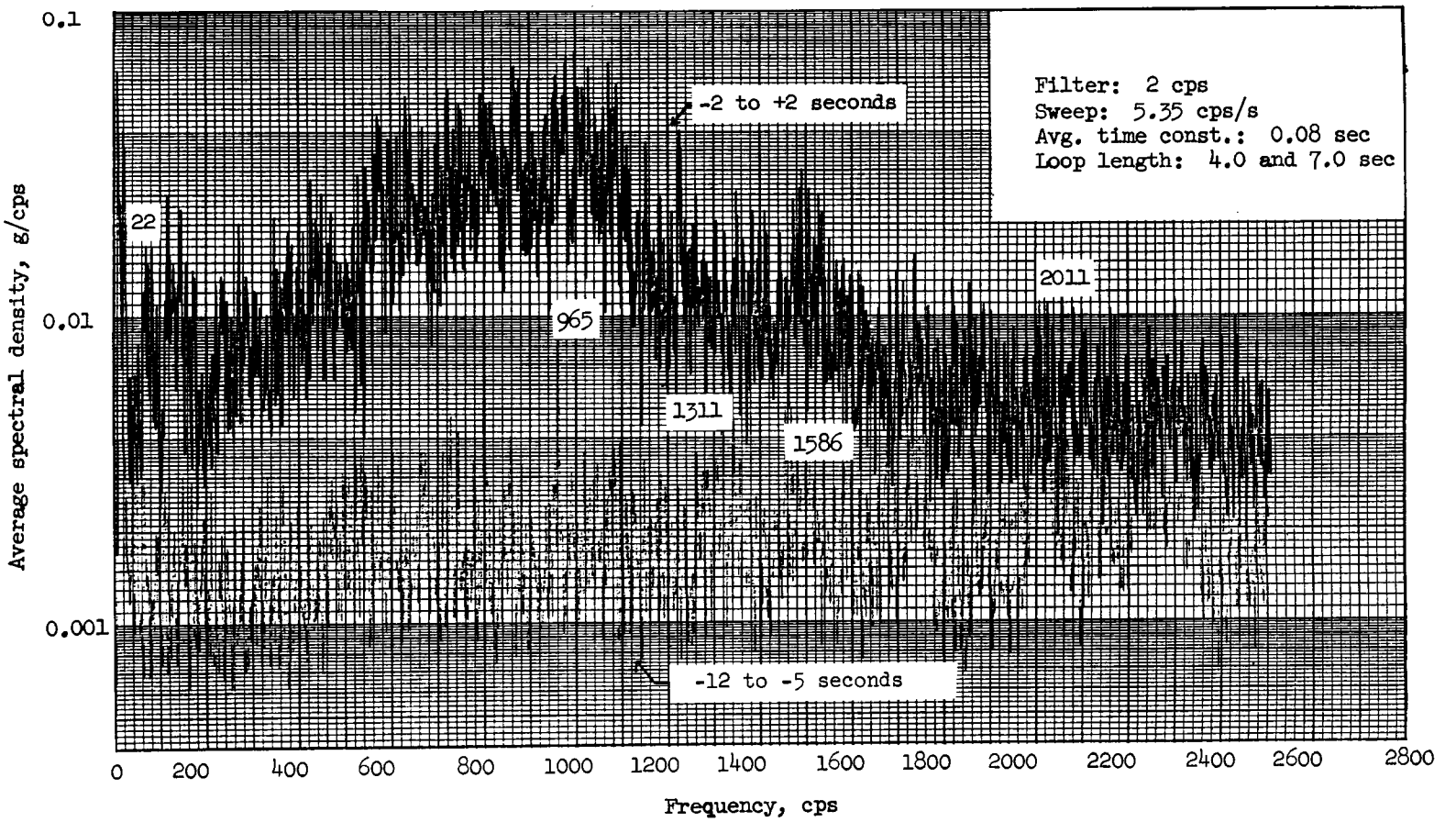

Figure 36.- Spectral density analysis. 2 cps filter; -2 to 2 seconds; -12 to -5 seconds; 52.5 kcps channel.

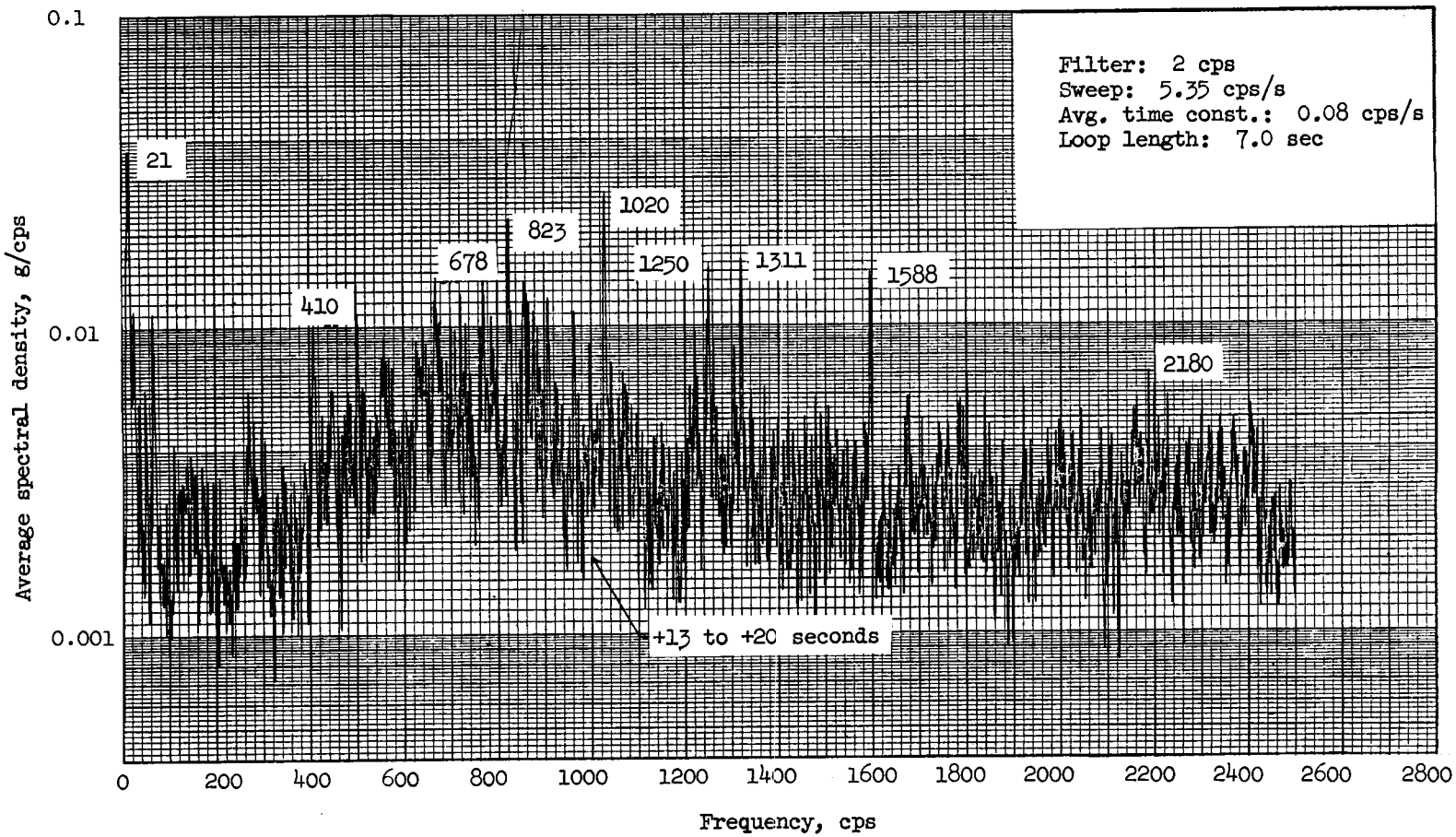

Figure 37.- Spectral density analysis. 2 cps filter; 13 to 20 seconds; 52.5 kcps channel.

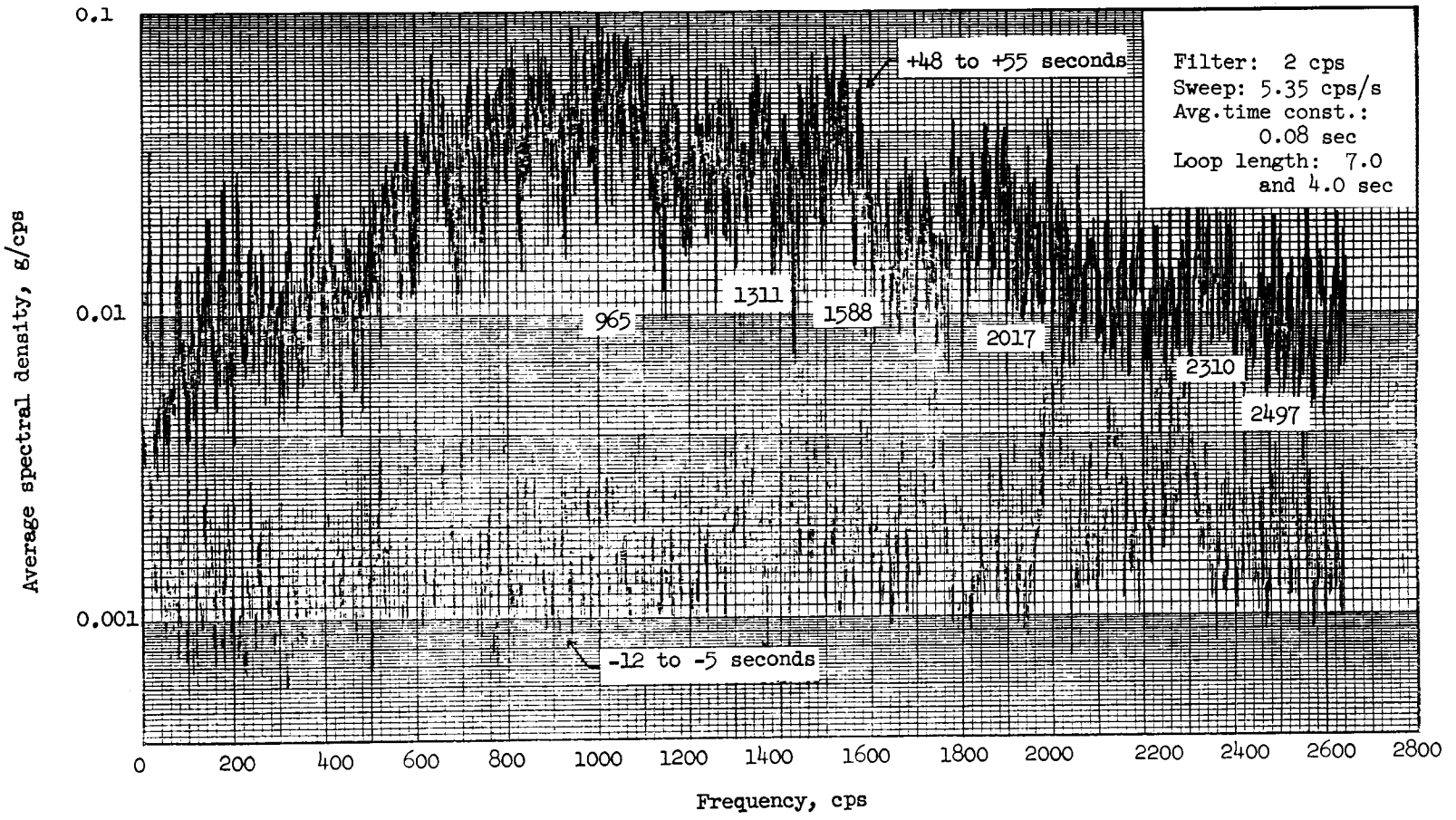

Figure 38.- Spectral density analysis. 2 cps filter; 48 to 55 seconds; -12 to -5 seconds; 52.5 kcps channel.

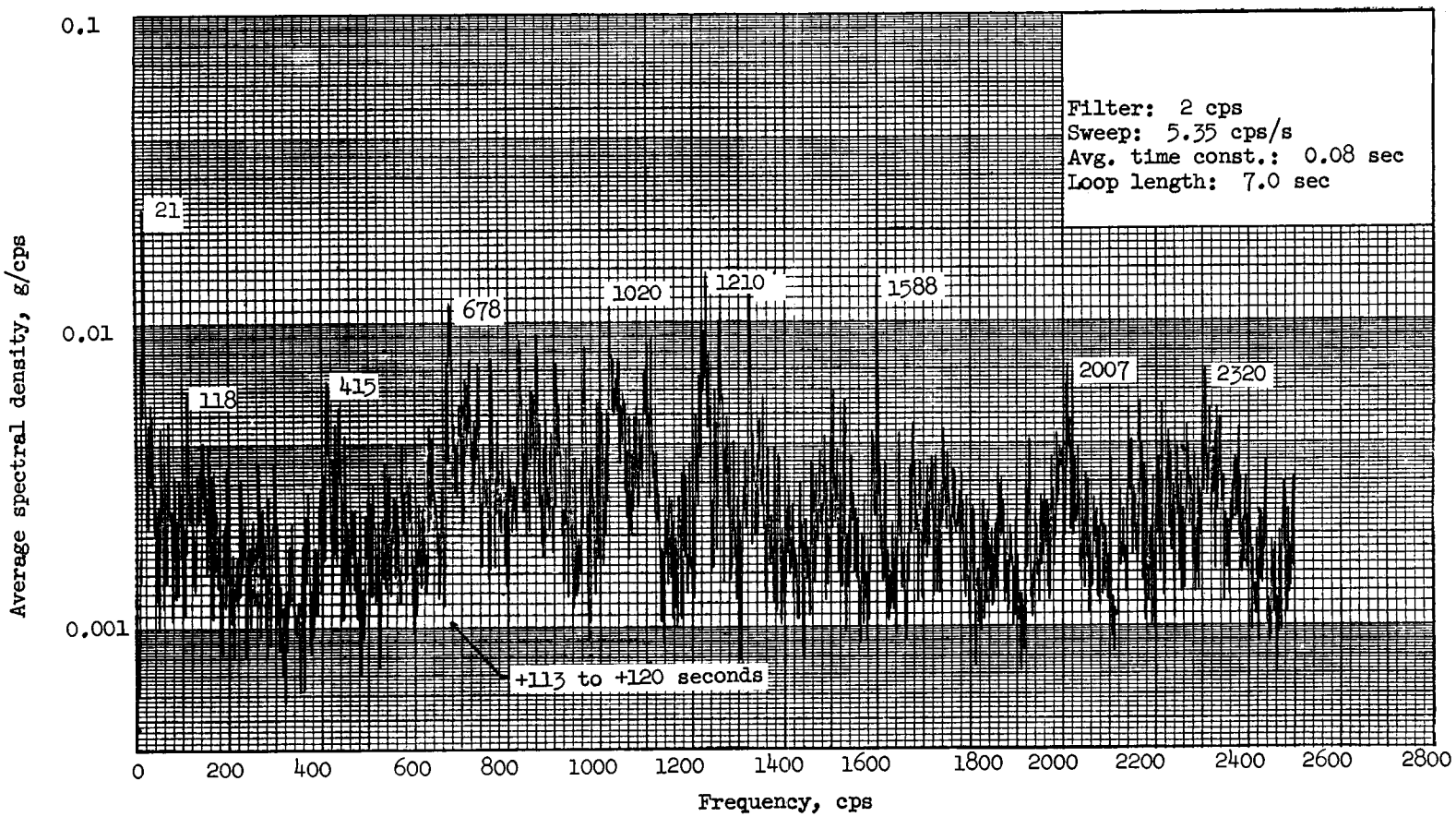

Figure 39.- Spectral density analysis. 2 cps filter; 113 to 120 seconds; 52.5 kcps channel.

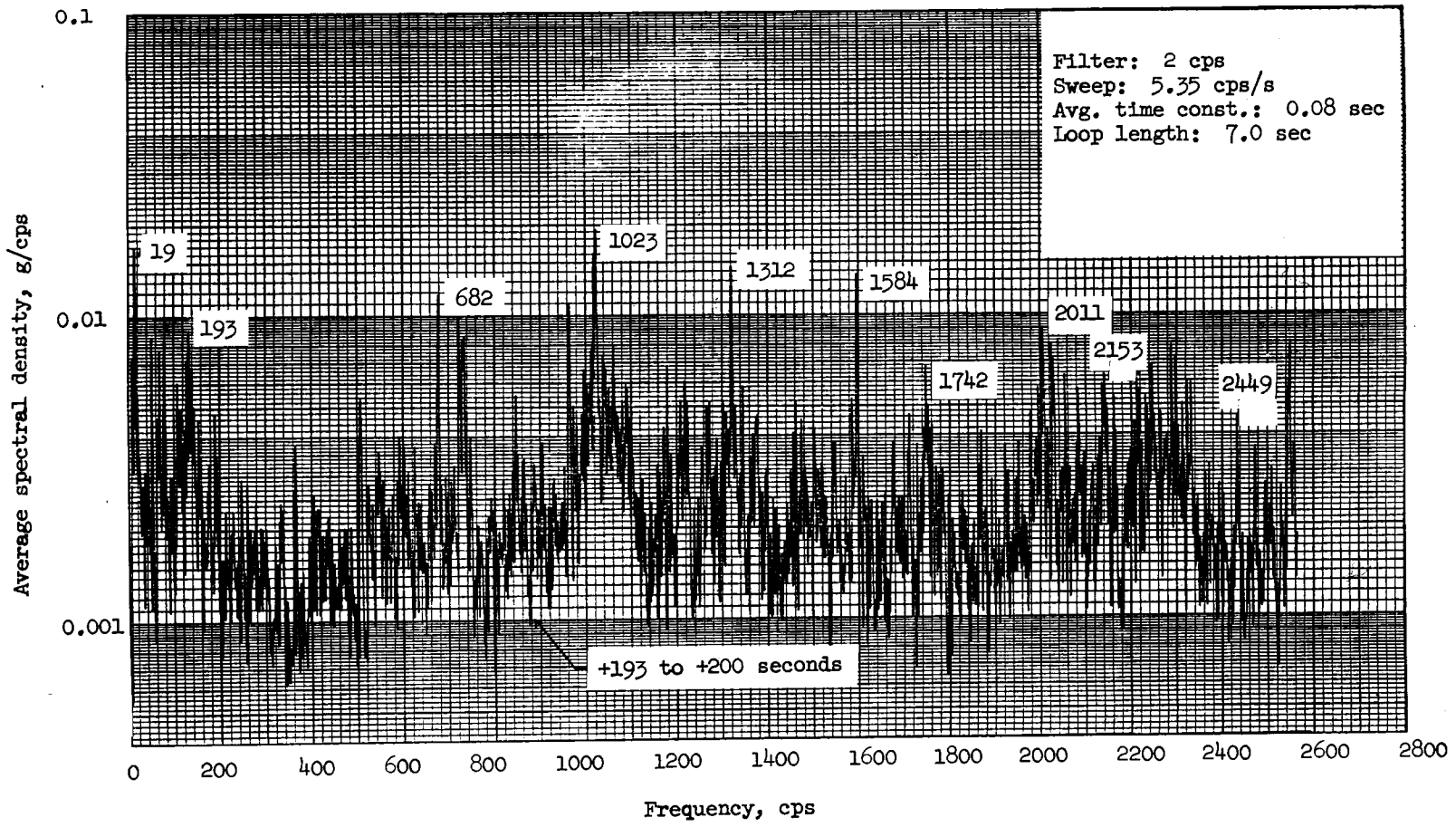

Figure 40.- Spectral density analysis. 2 cps filter; 193 to 200 seconds; 52.5 kcps channel.

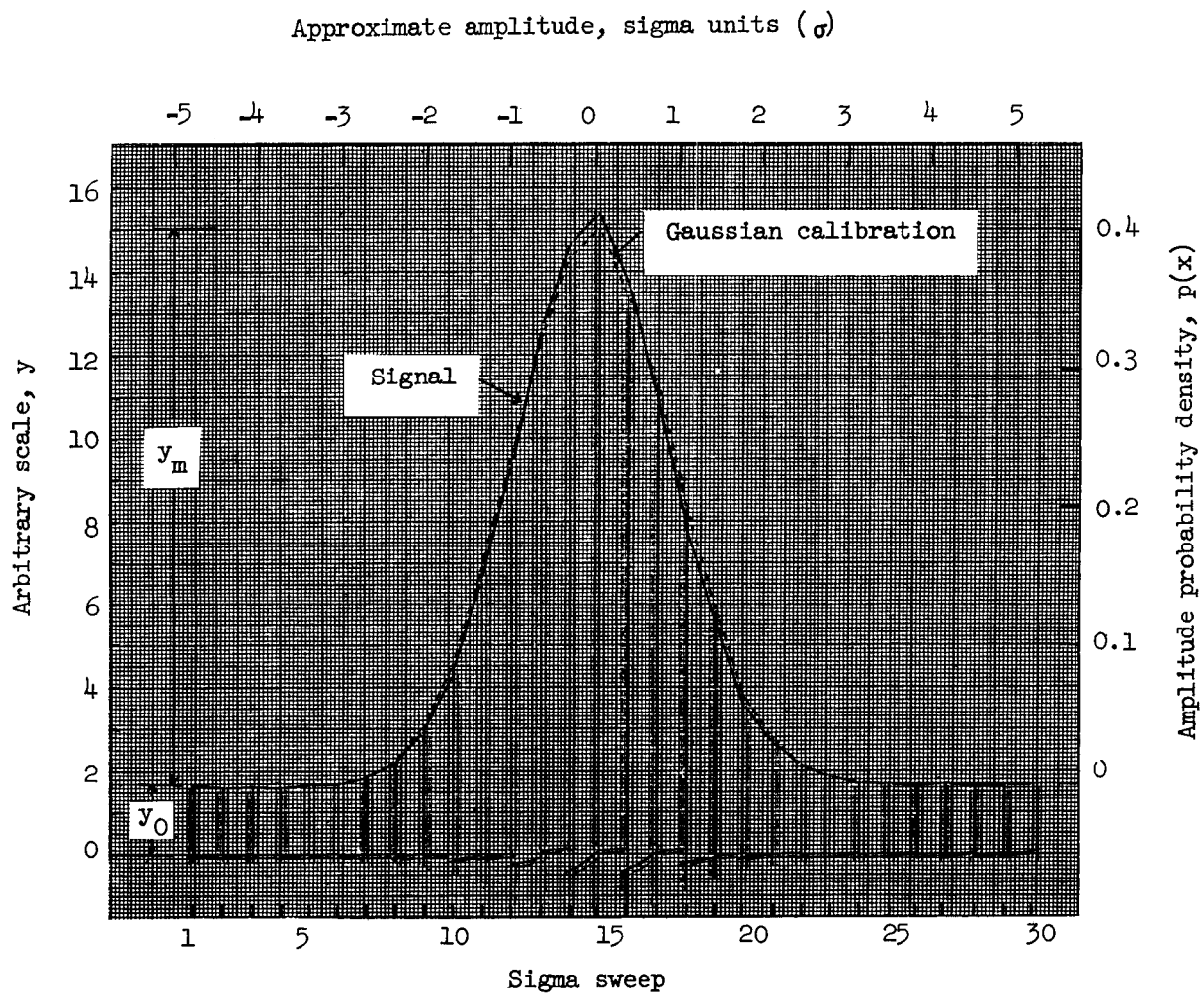

Figure 41.- Probability density analysis. -12 to -5 seconds; 52.5 kcps channel; Scale factor (S.F.) = $\frac{0.4}{y_m}$; p(x) = (S.F.)(y - y_0).

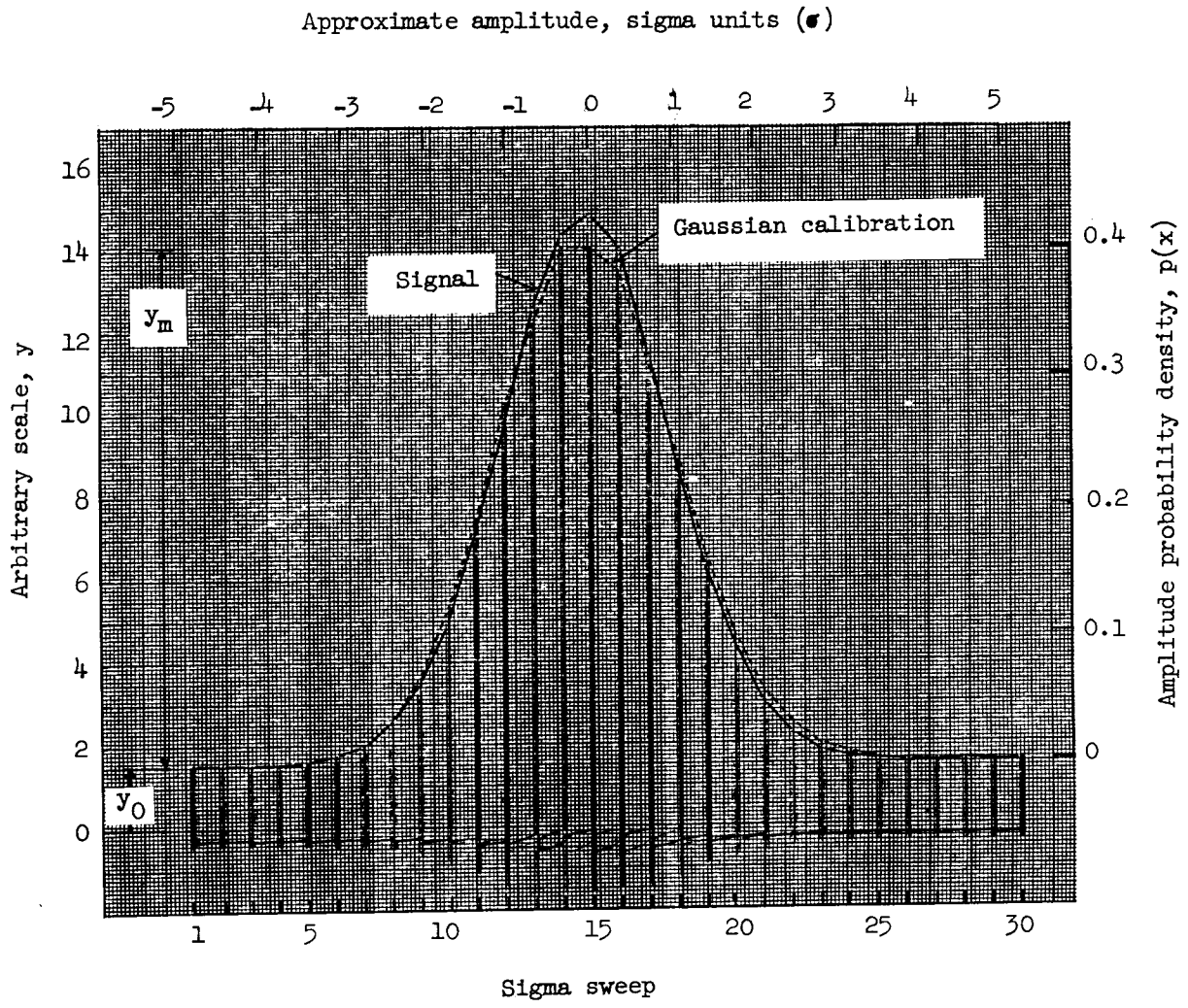

Figure 42.- Probability density analysis. -2 to 4 seconds; 52.5 kcps channel; Scale factor (S.F.) = $\frac{0.4}{y_m}$; $p(x) = (S.F.)(y - y_0)$.

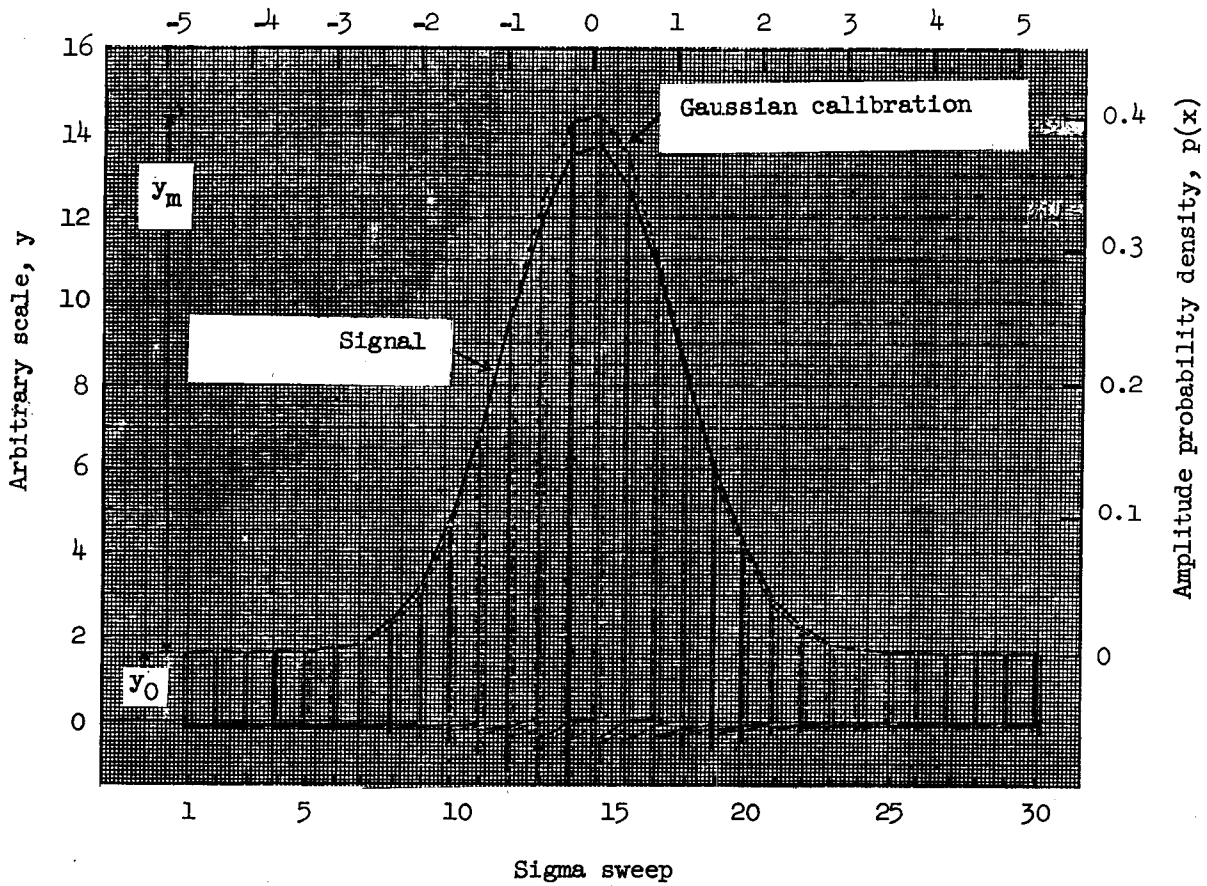

Figure 43.- Probability density analysis. 48 to 55 seconds; 52.5 kcps channel; Scale factor (S.F.) $= \frac{0.4}{y_m}$; $p(x) = (S.F.)(y - y_0)$.

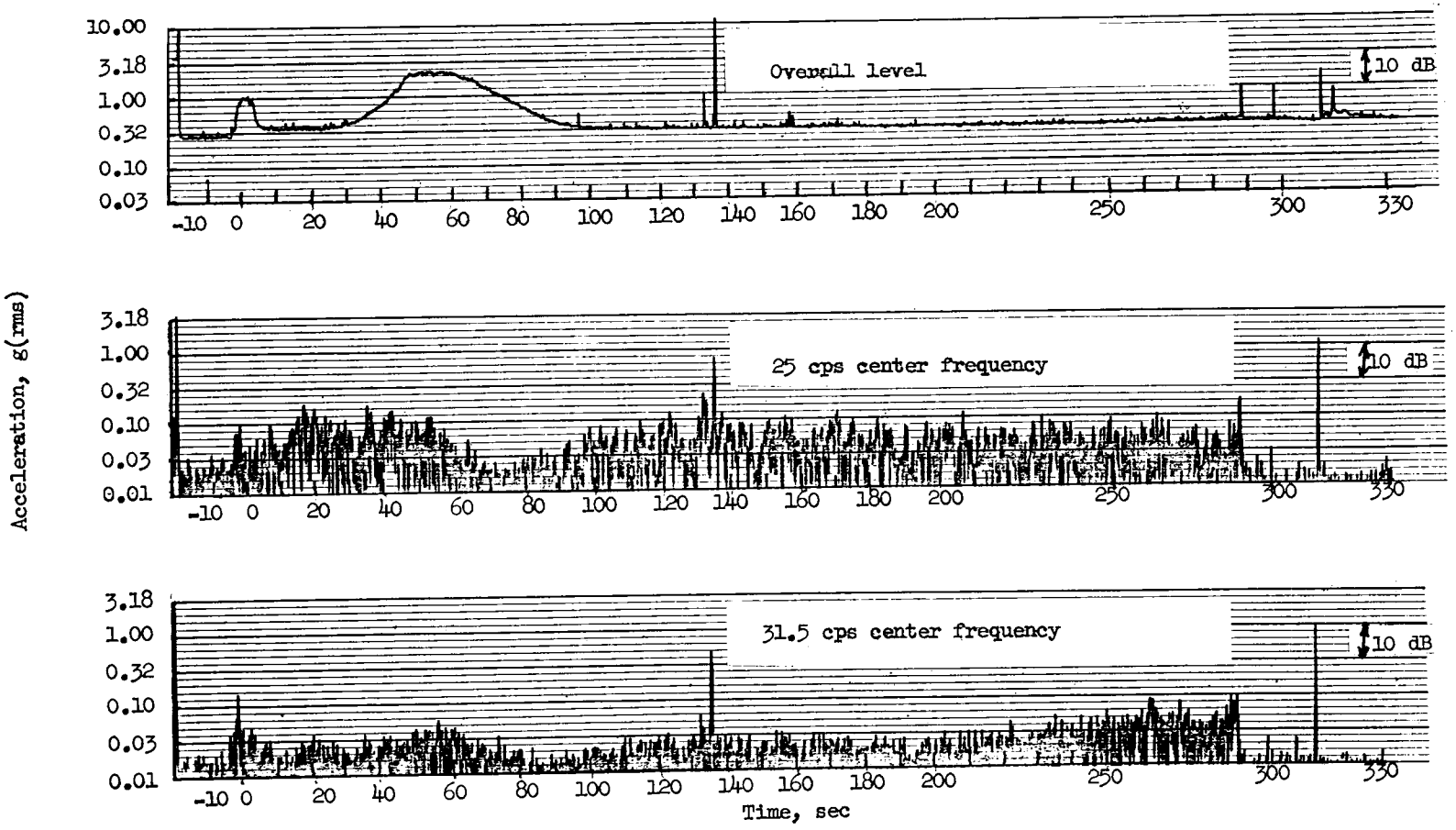

(a) 25 and 31.5 cps center frequency; 70 kcps channel; 5 kcps output filter.

Figure 44.- Overall level and one-third-octave band analyses.

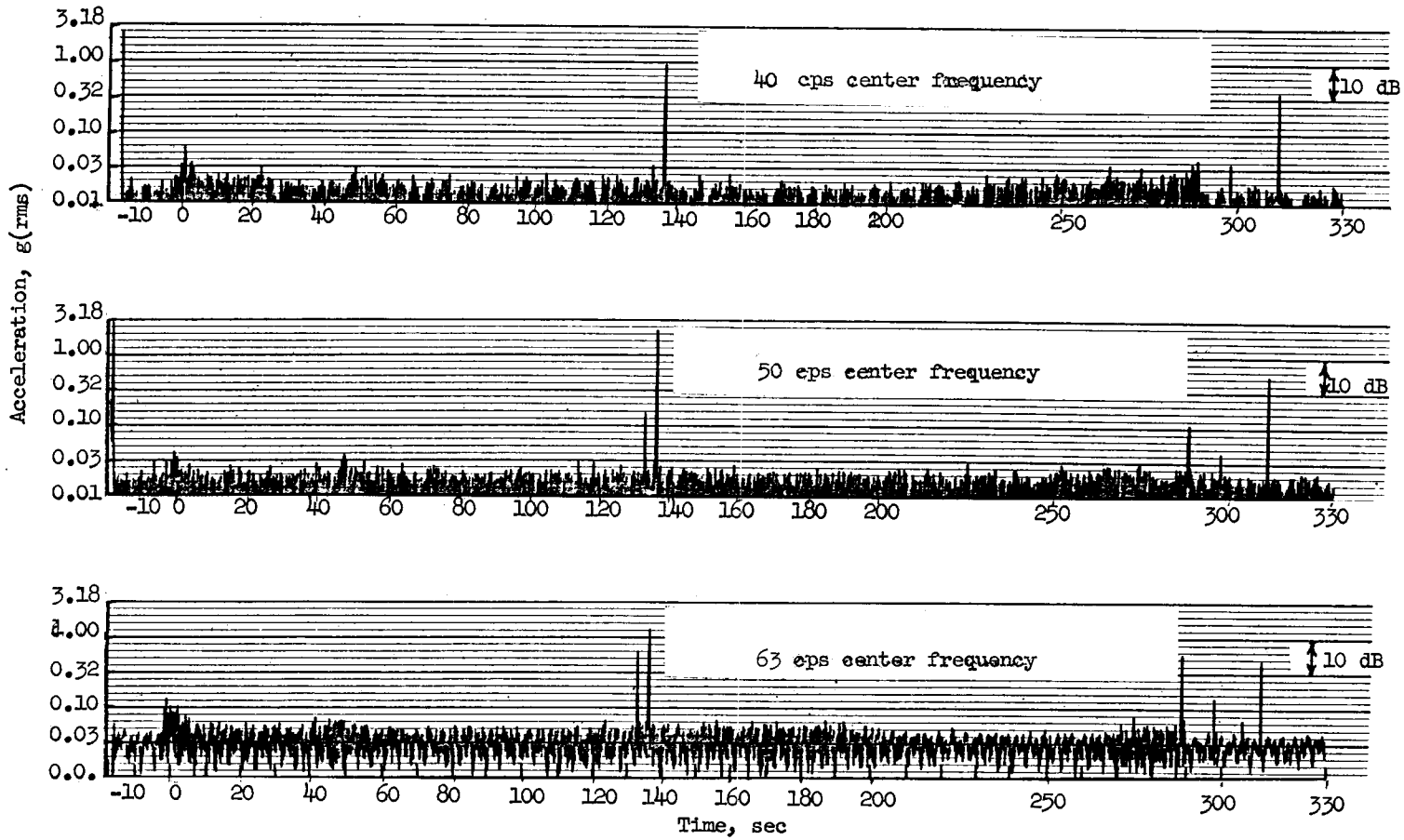

(b) 40, 50, and 63 cps center frequency.

Figure 44.- Continued.

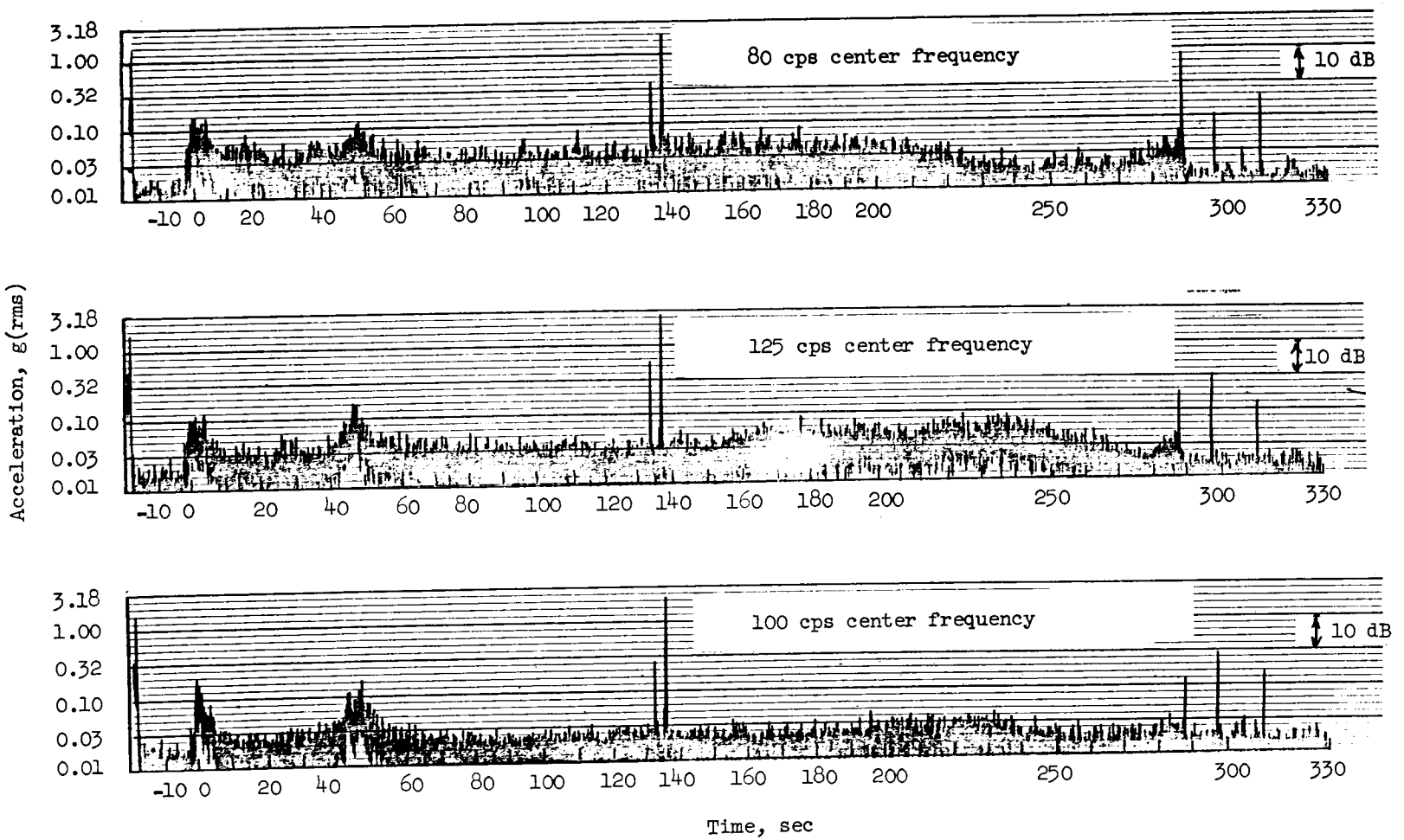

(c) 80, 125, and 100 cps center frequency.

Figure 44.- Continued.

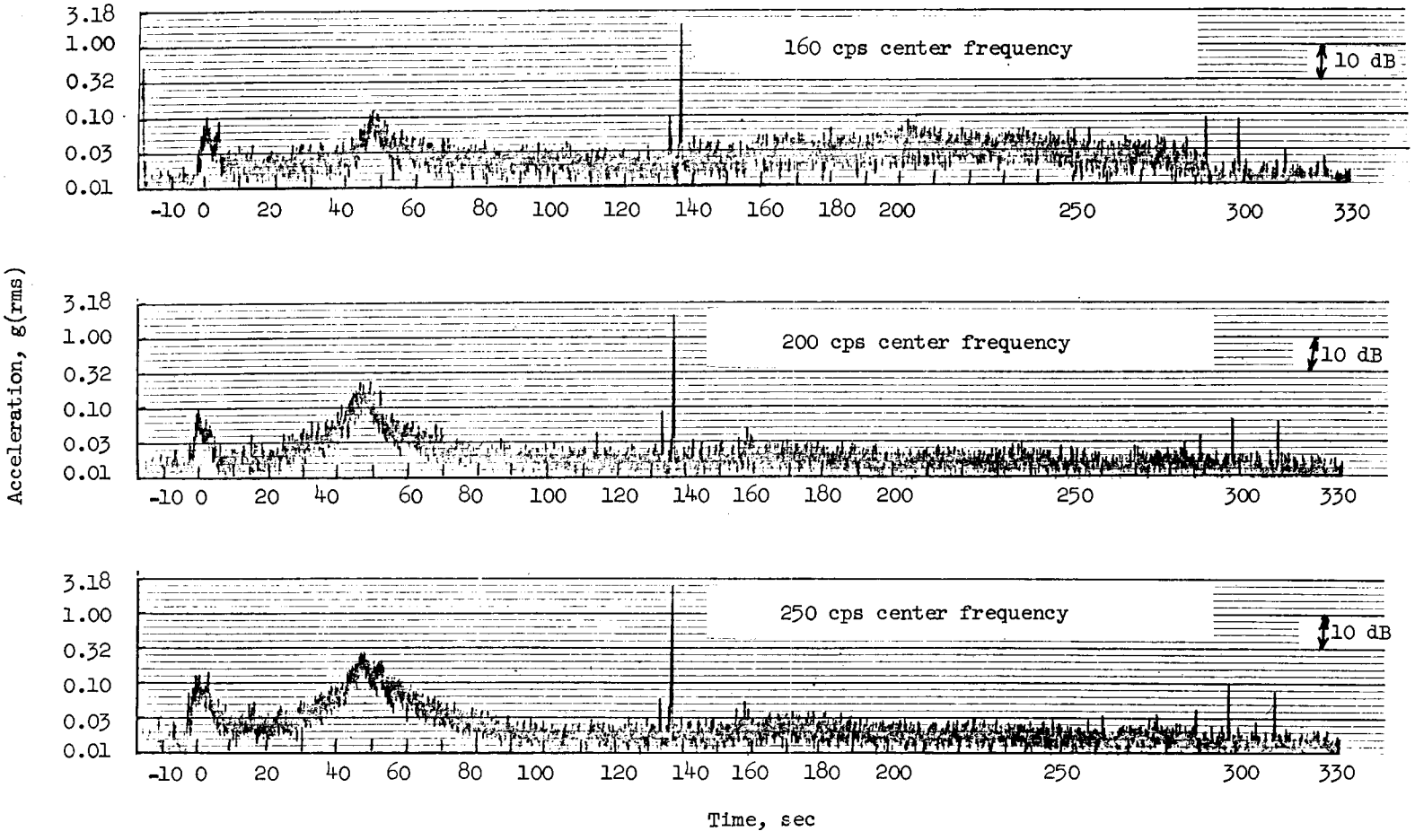

(d) 160, 200, and 250 cps center frequency.

Figure 44.- Continued.

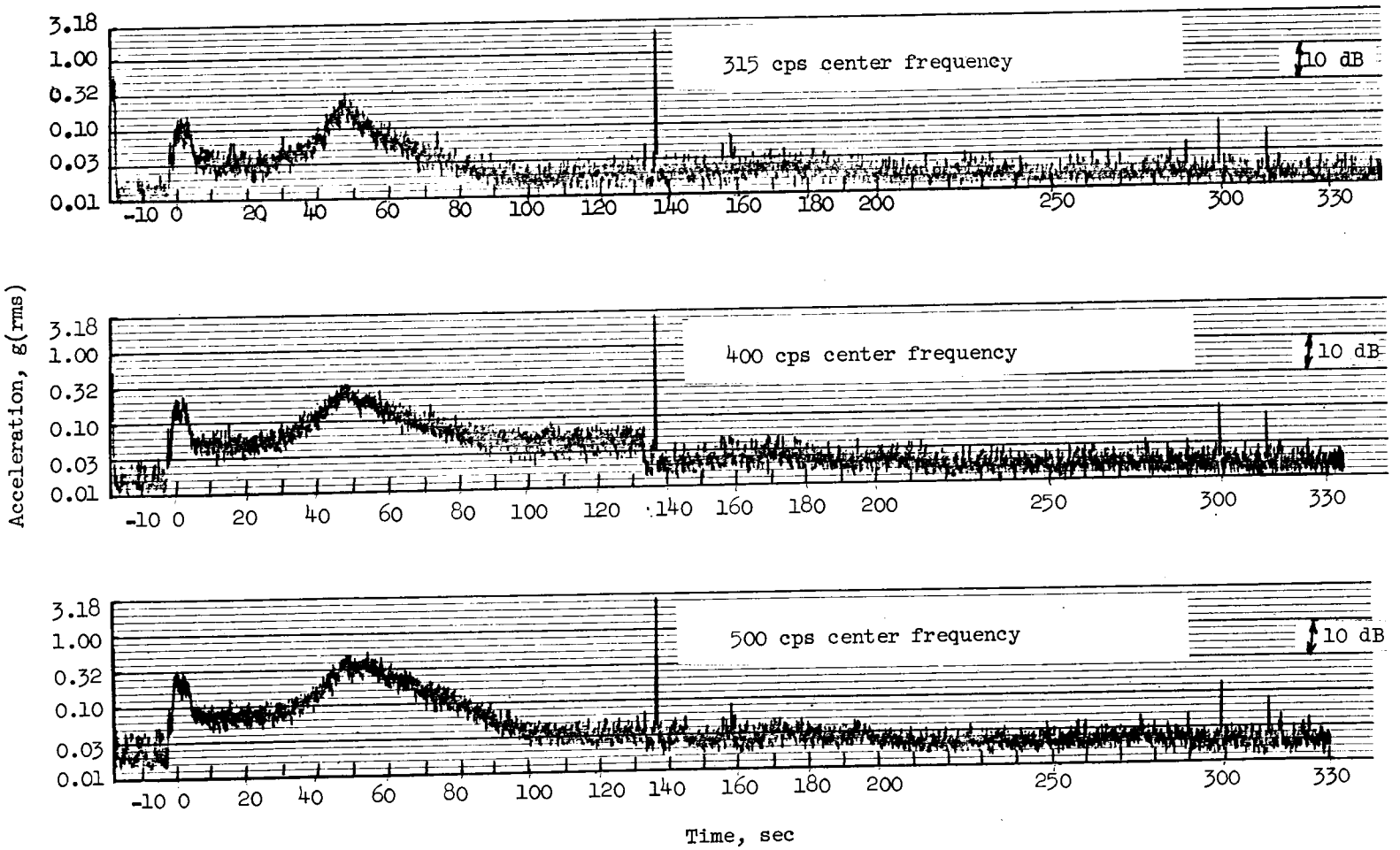

(e) 315, 400, and 500 cps center frequency.

Figure 44.- Continued.

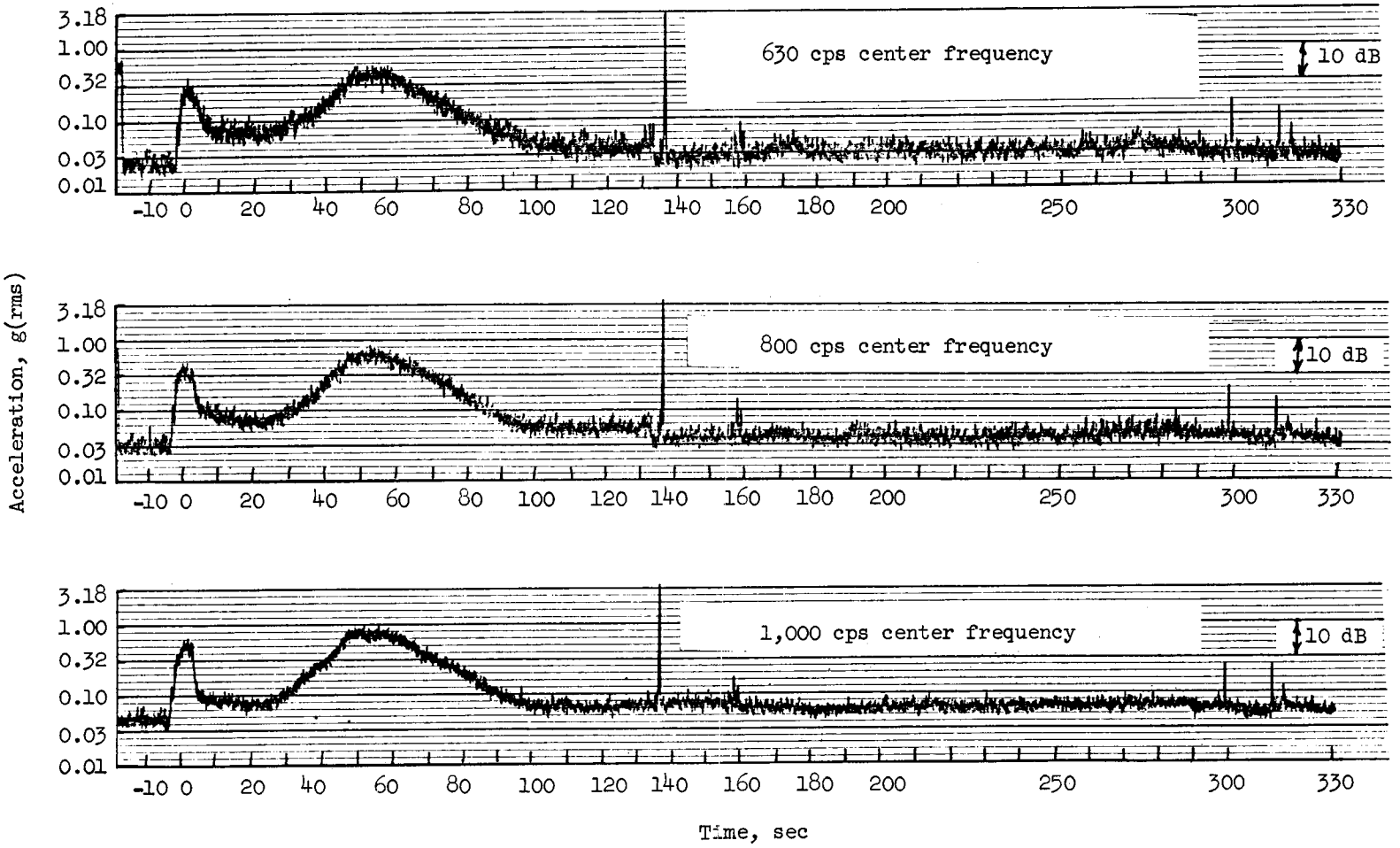

(f) 630, 800, and 1000 cps center frequency.

Figure 44.- Continued.

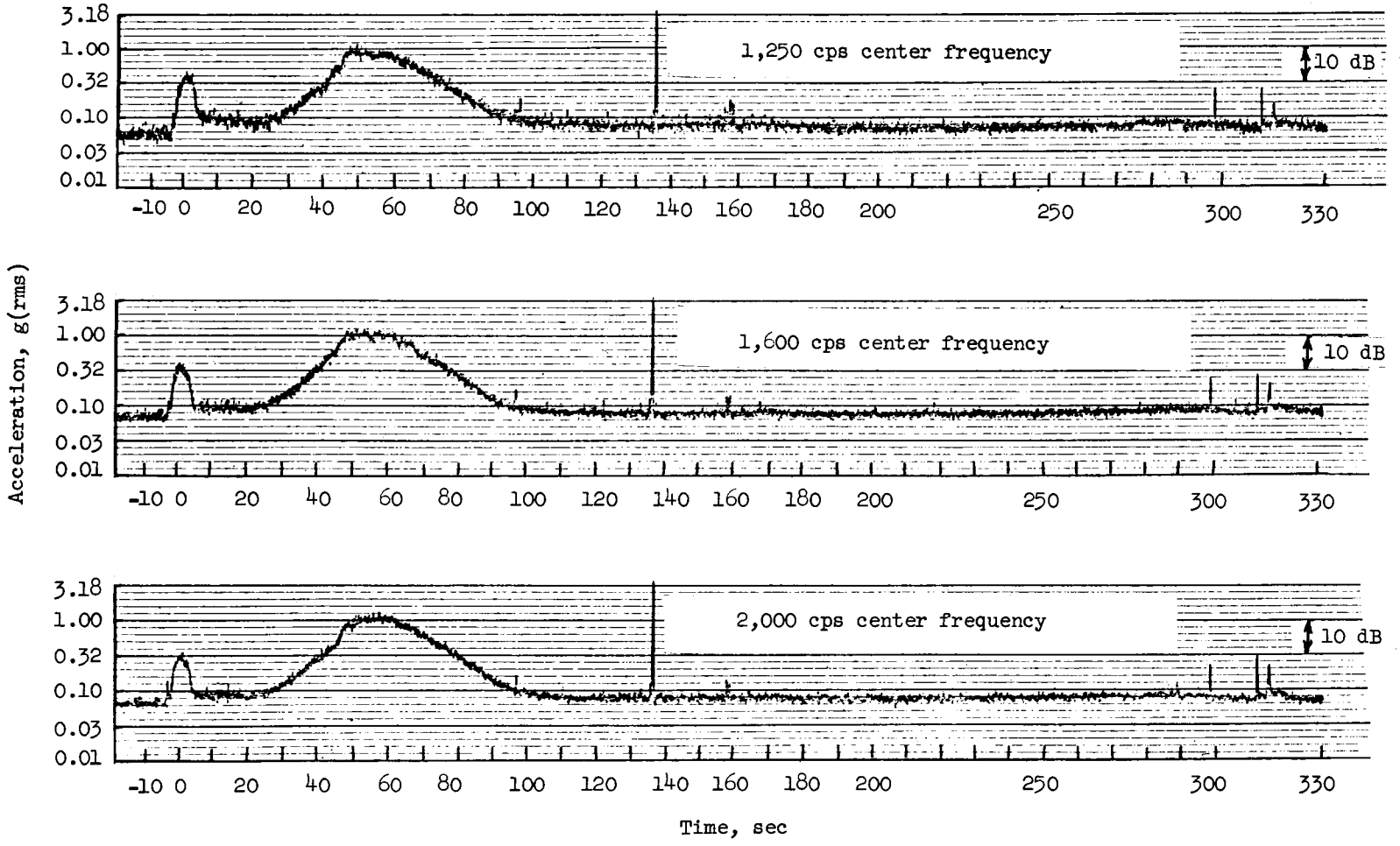

(g) 1250, 1600, and 2000 cps center frequency.

Figure 44.- Continued.

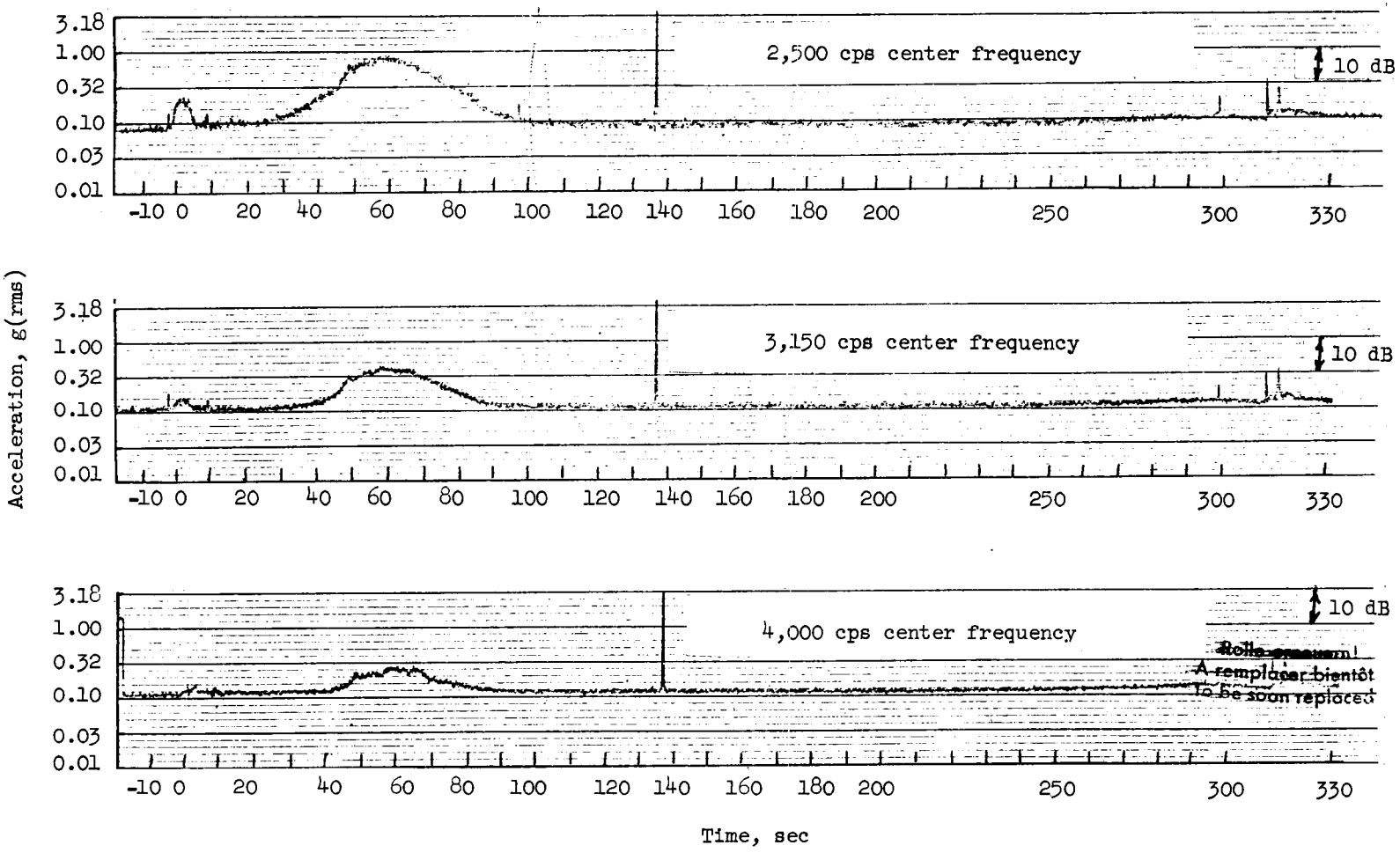

(h) 2500, 3150, and 4000 cps center frequency.

Figure 44.- Continued.

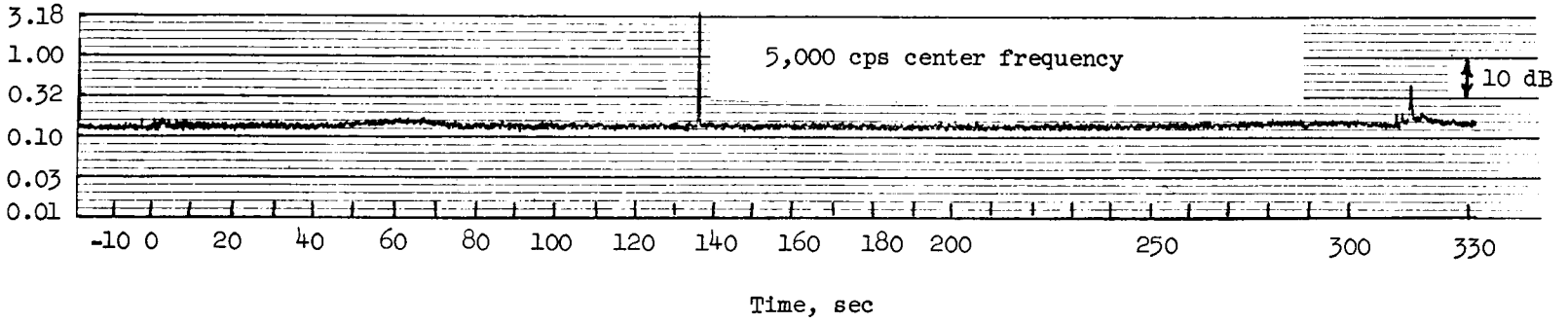

(i) 5000 cps center frequency.

Figure 44.- Concluded.

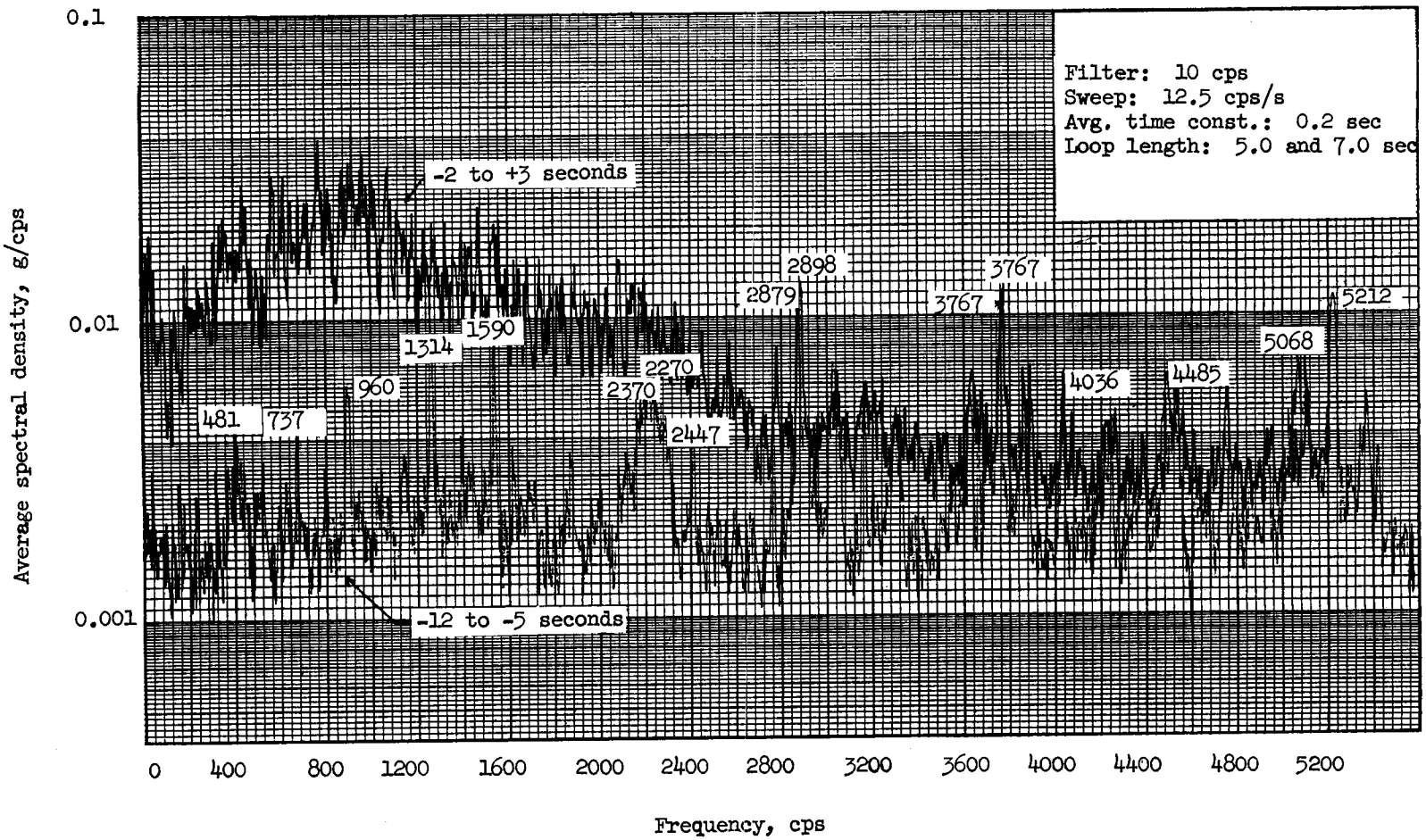

Figure 45.- Spectral density analysis. 10 cps filter; -2 to 3 seconds; -12 to -5 seconds; 70 kcps channel.

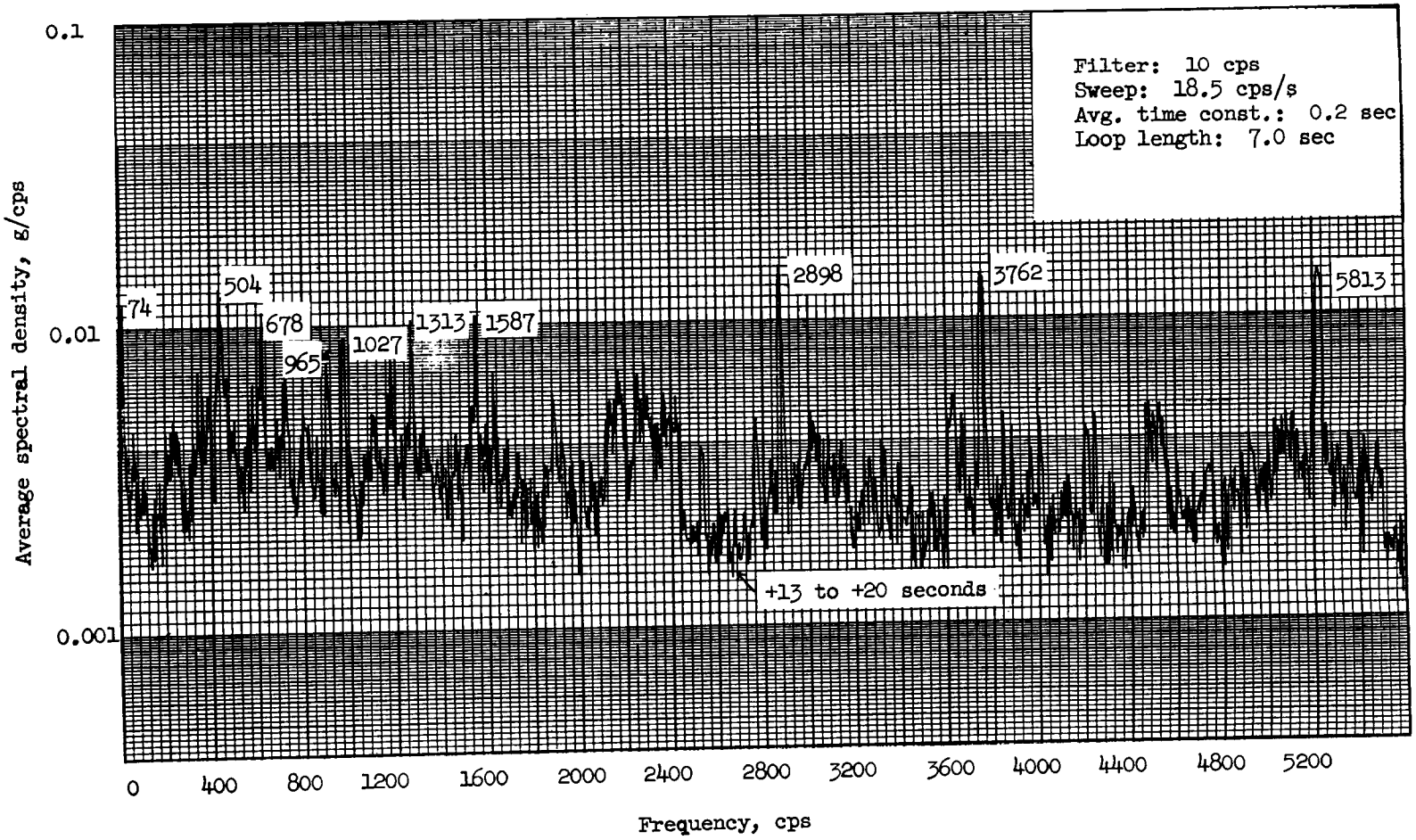

Figure 46.- Spectral density analysis. 10 cps filter; 13 to 20 seconds; 70 kcps channel.

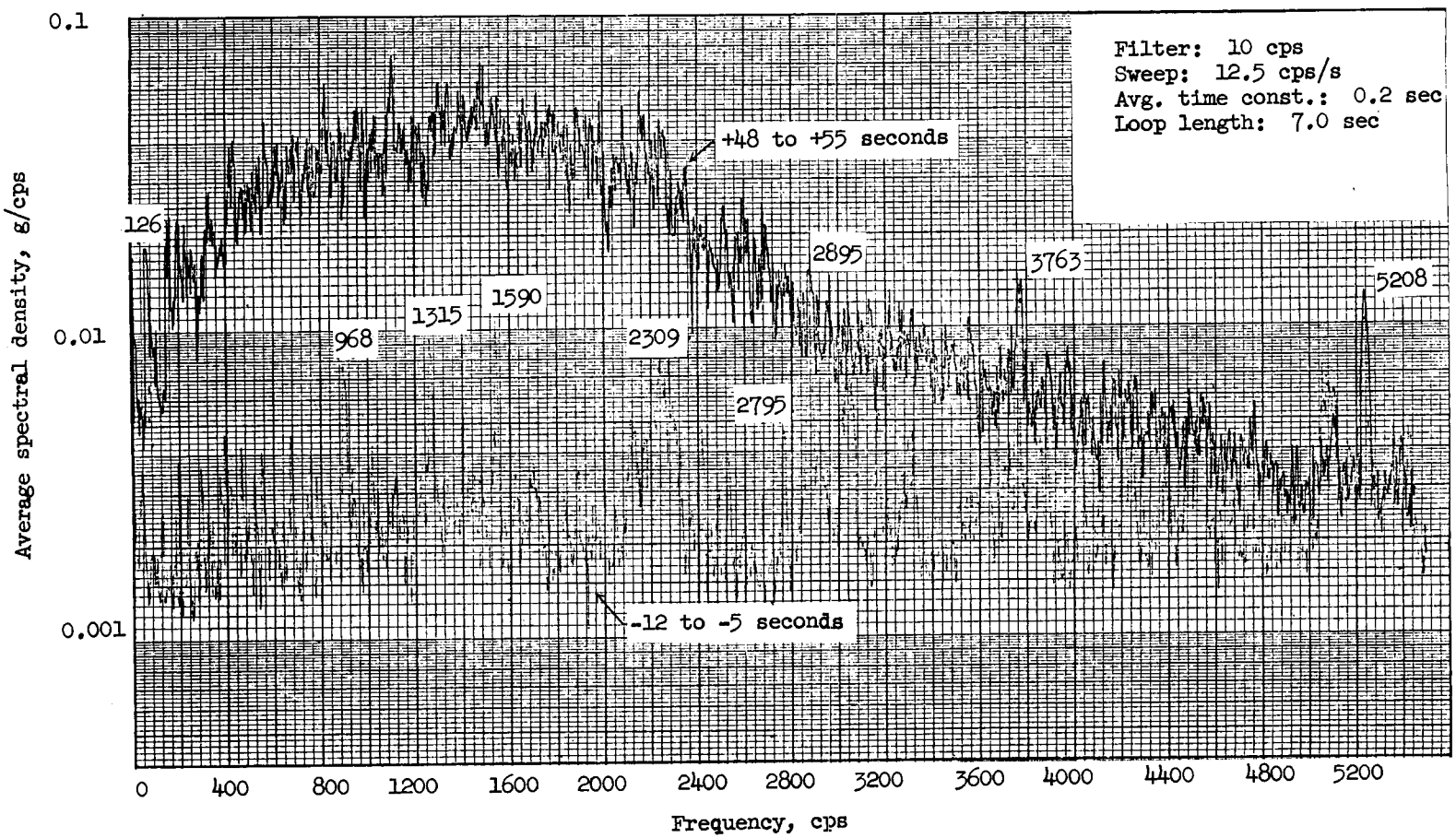

Figure 47.- Spectral density analysis. 10 cps filter; 48 to 55 seconds; -12 to -5 seconds; 70 kcps channel.

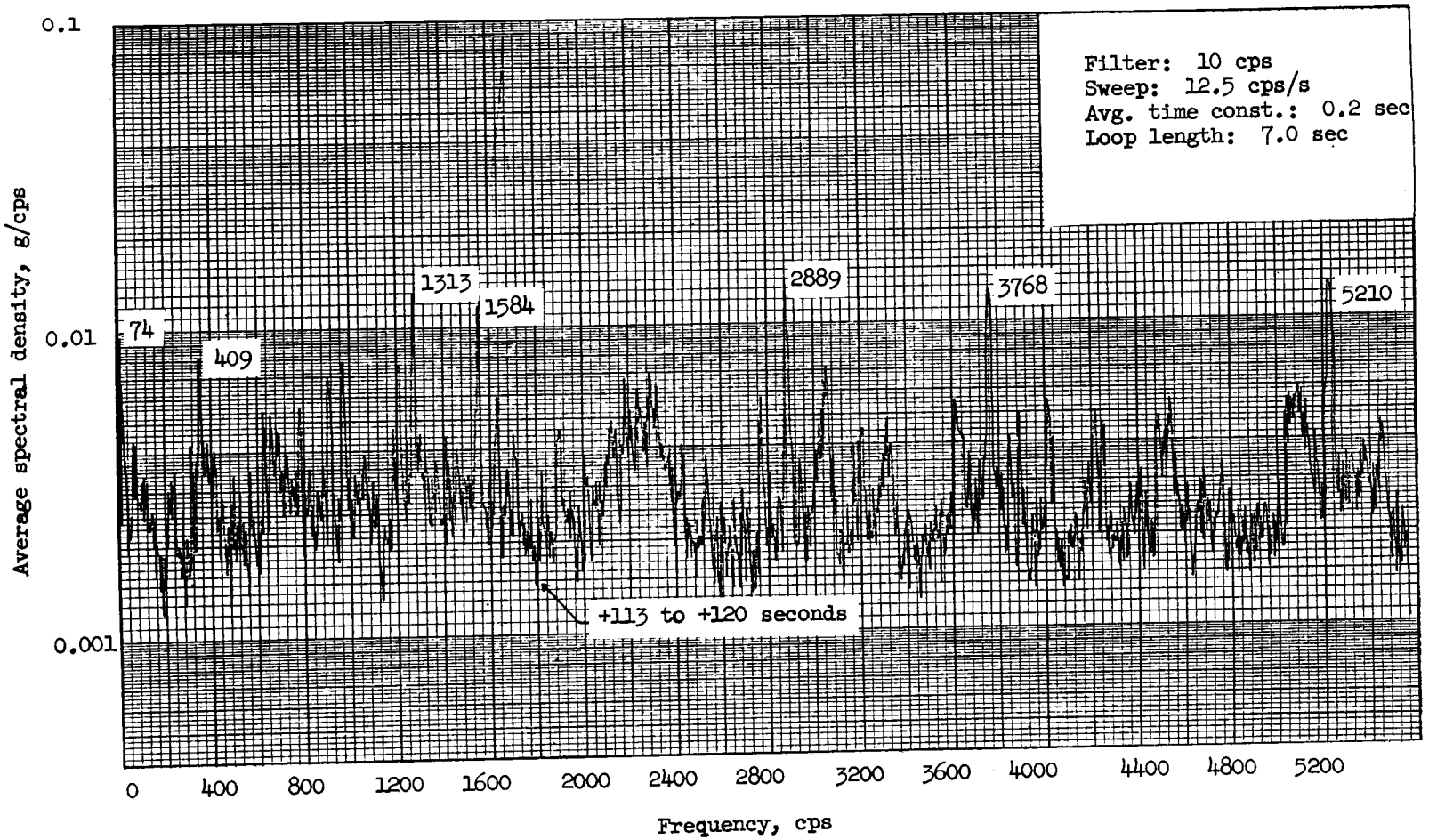

Figure 48.- Spectral density analysis. 10 cps filter; 113 to 120 seconds; 70 kcps channel.

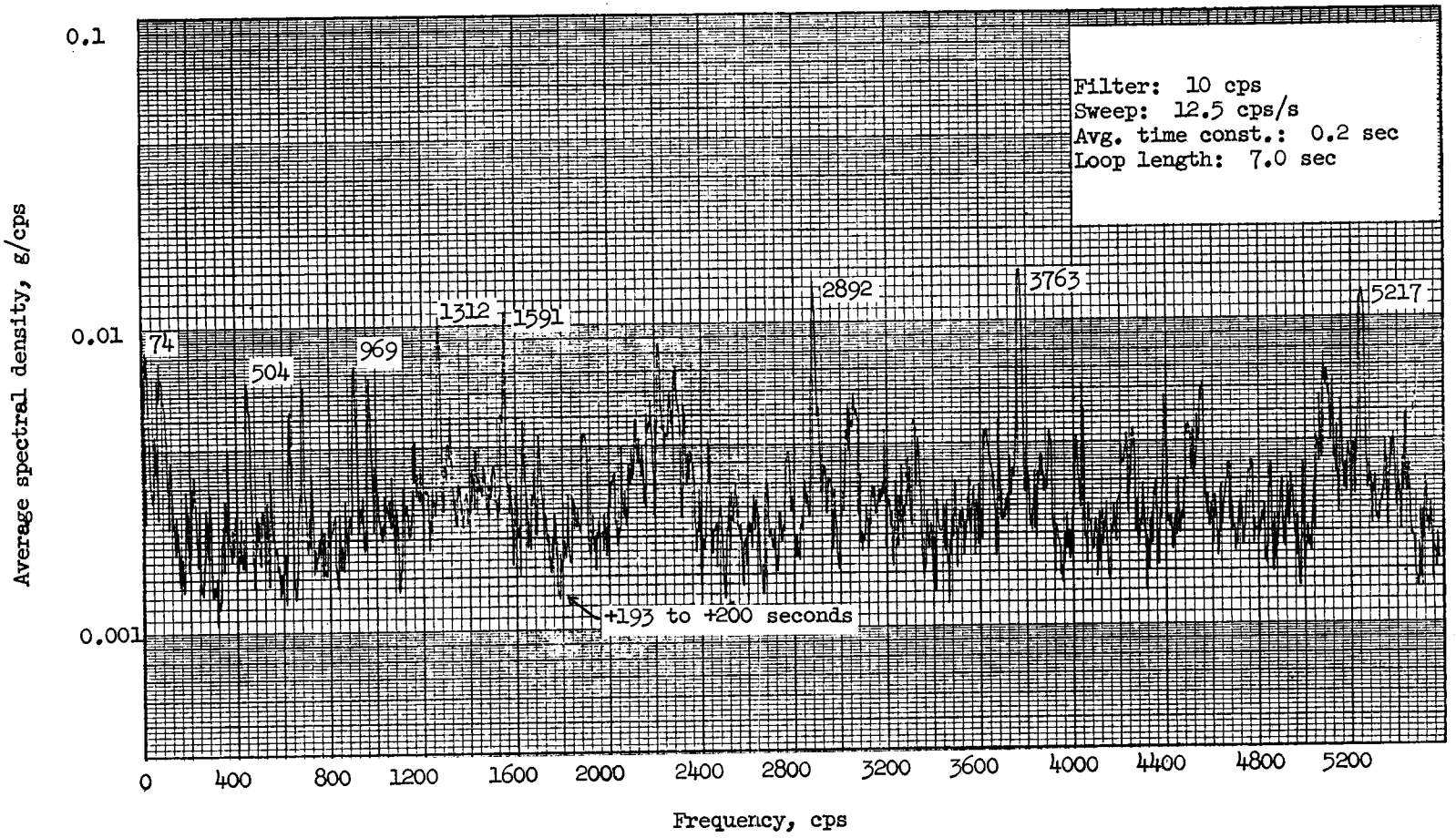

Figure 49.- Spectral density analysis. 10 cps filter; 193 to 200 seconds; 70 kcps channel.

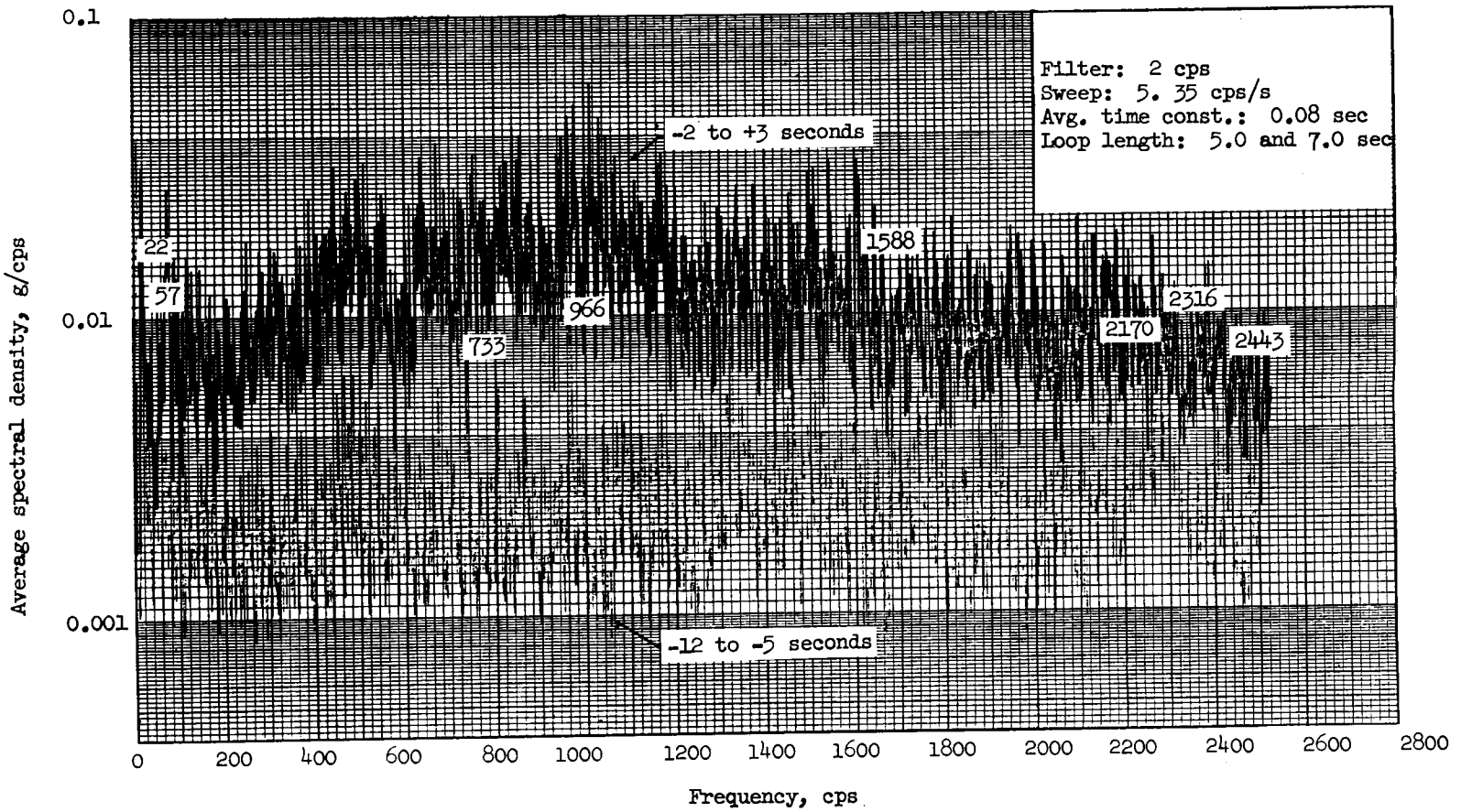

Figure 50.- Spectral density analysis. 2 cps filter; -2 to 3 seconds; -12 to -5 seconds; 70 kcps channel.

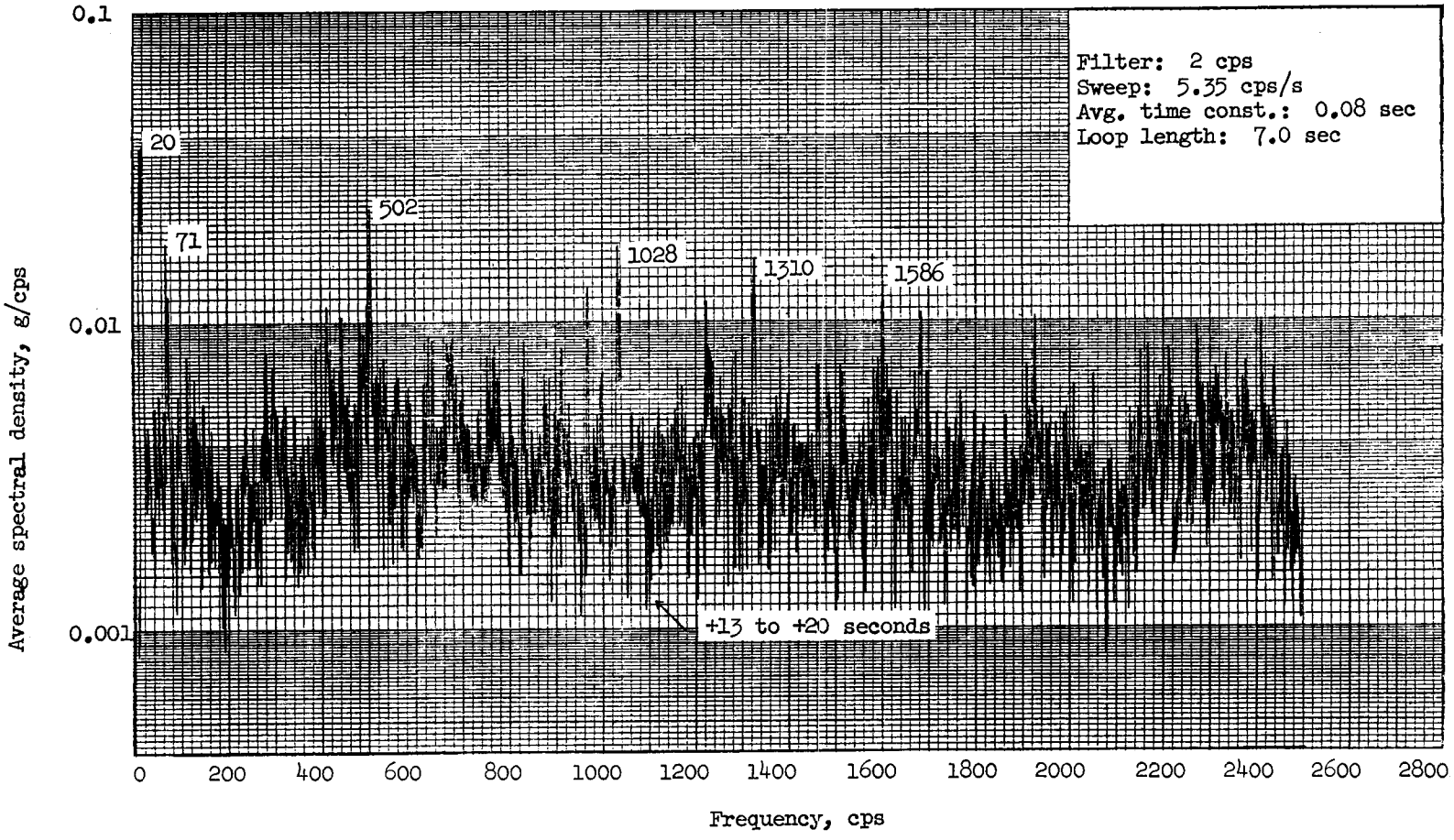

Figure 51.- Spectral density analysis. 2 cps filter; 13 to 20 seconds; 70 kcps channel.

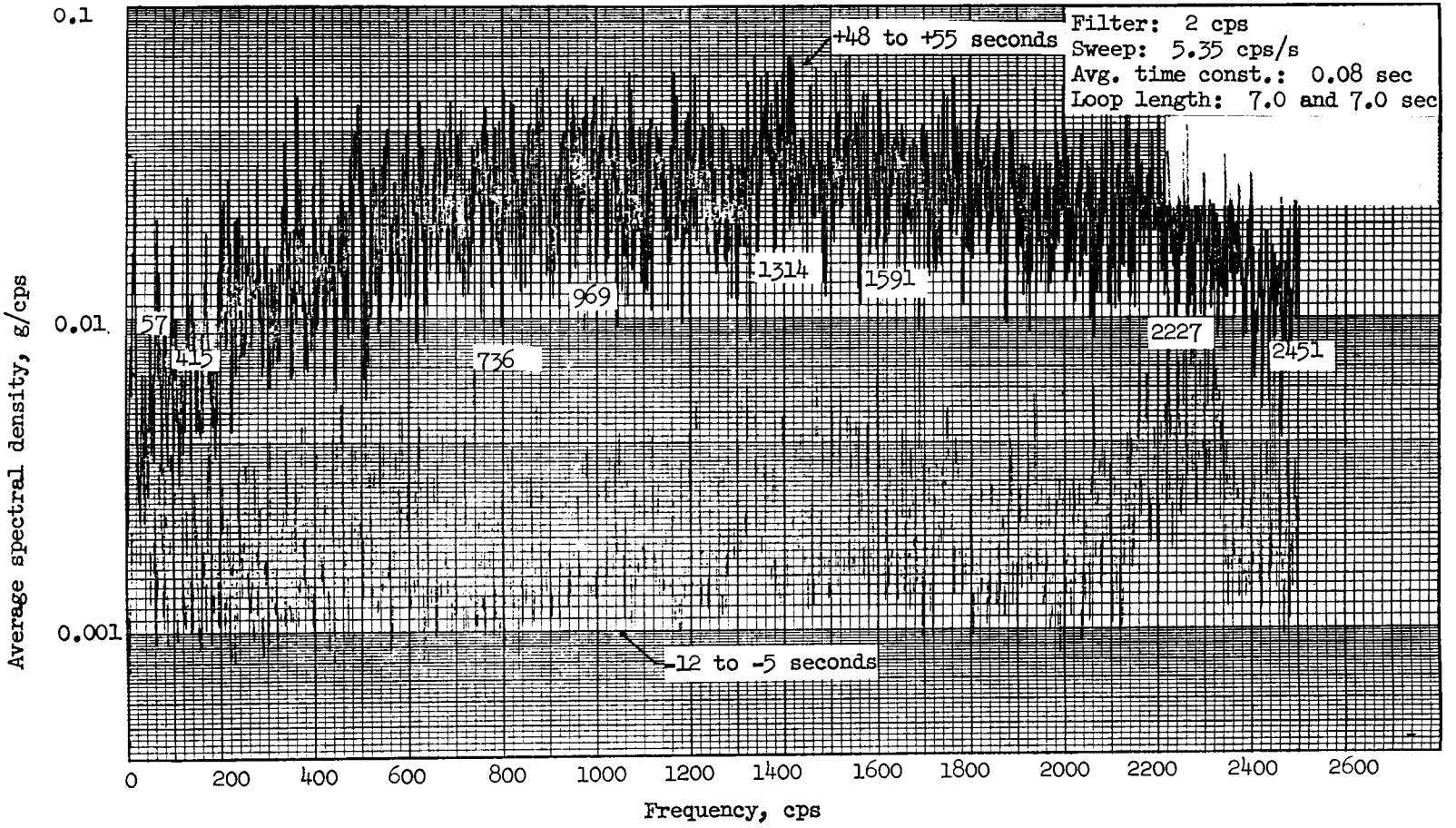

Figure 52.- Spectral density analysis. 2 cps filter; 48 to 55 seconds; -12 to -5 seconds; 70 kcps channel.

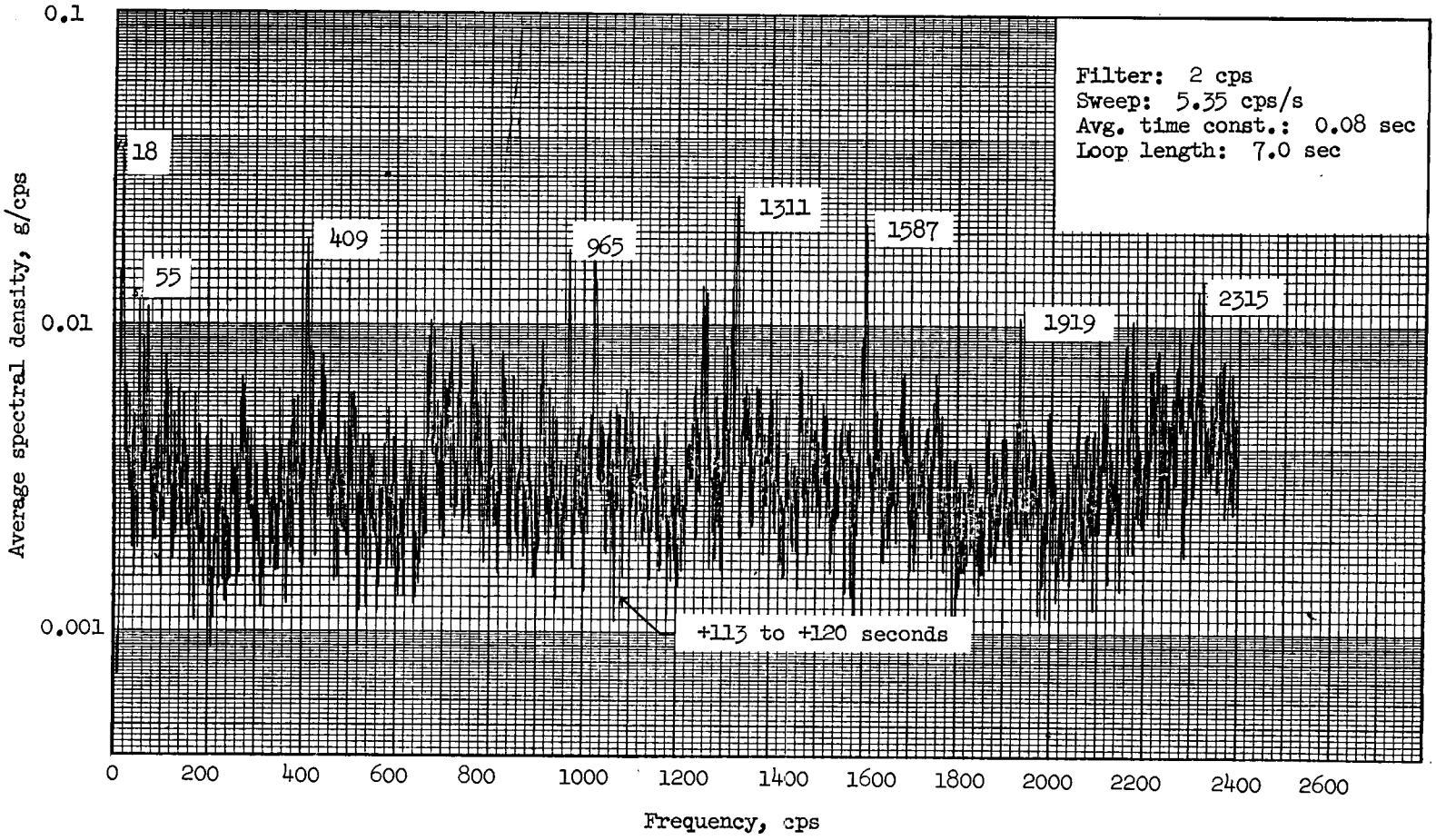

Figure 53.- Spectral density analysis. 2 cps filter; 113 to 120 seconds; 74 kcps channel.

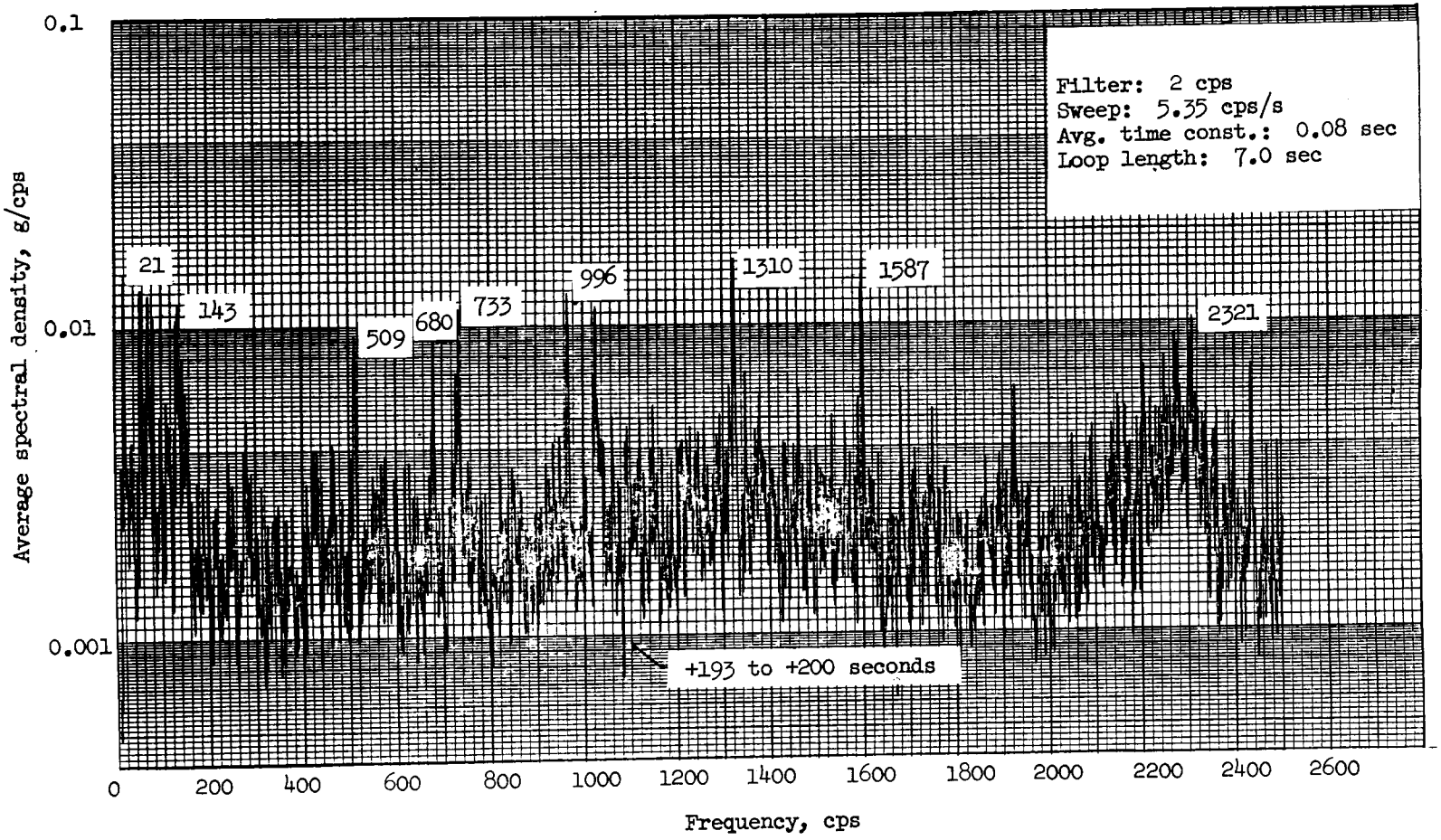

Figure 54.- Spectral density analysis. 2 cps filter; 193 to 200 seconds; 70 kcps channel.

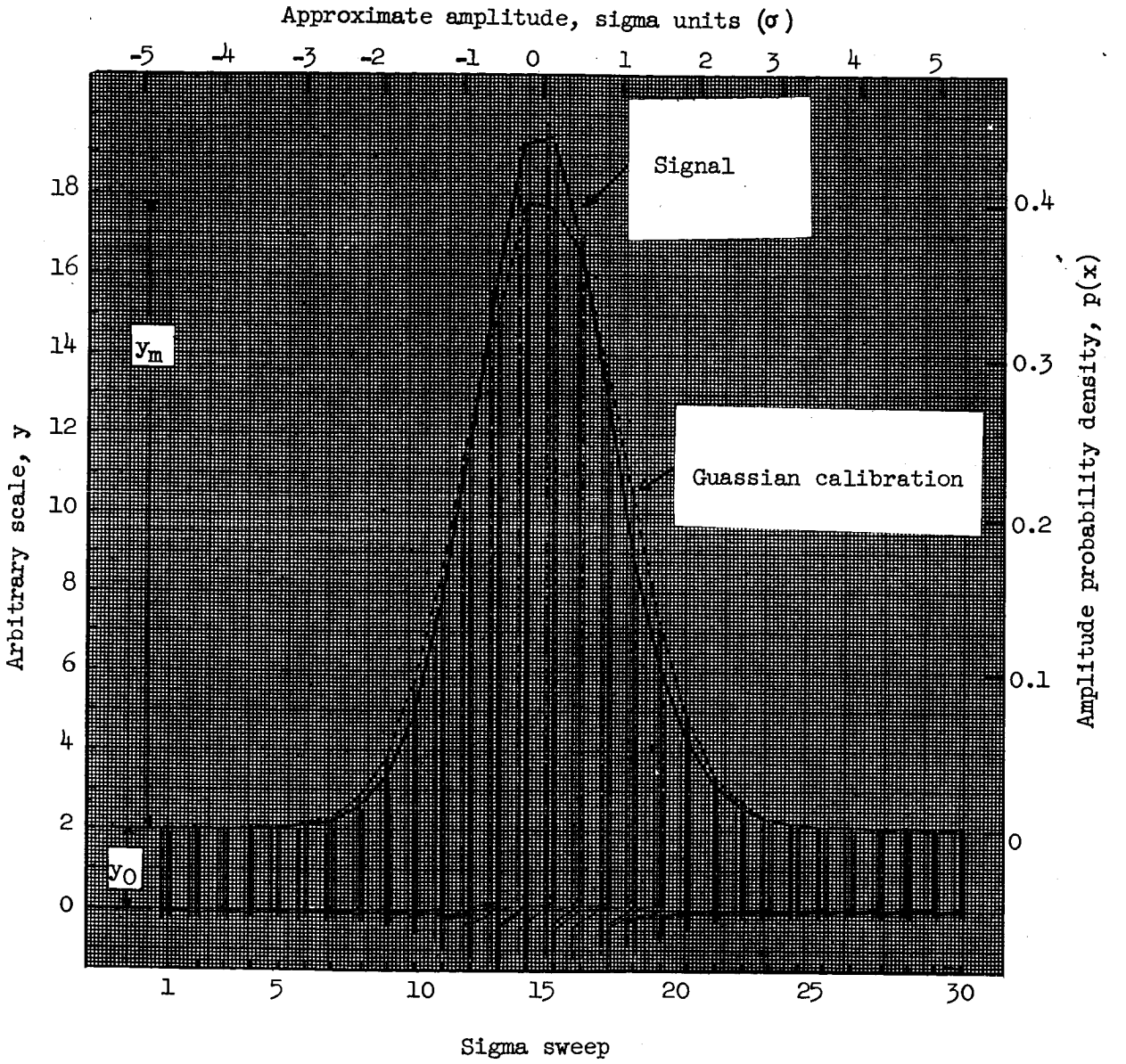

Figure 55.- Probability density analysis. -12 to -5 seconds; 70 kcps channel; Scale factor (S.F.) = $\frac{0.4}{y_m}$; p(x) = (S.F.)(y - y_0).

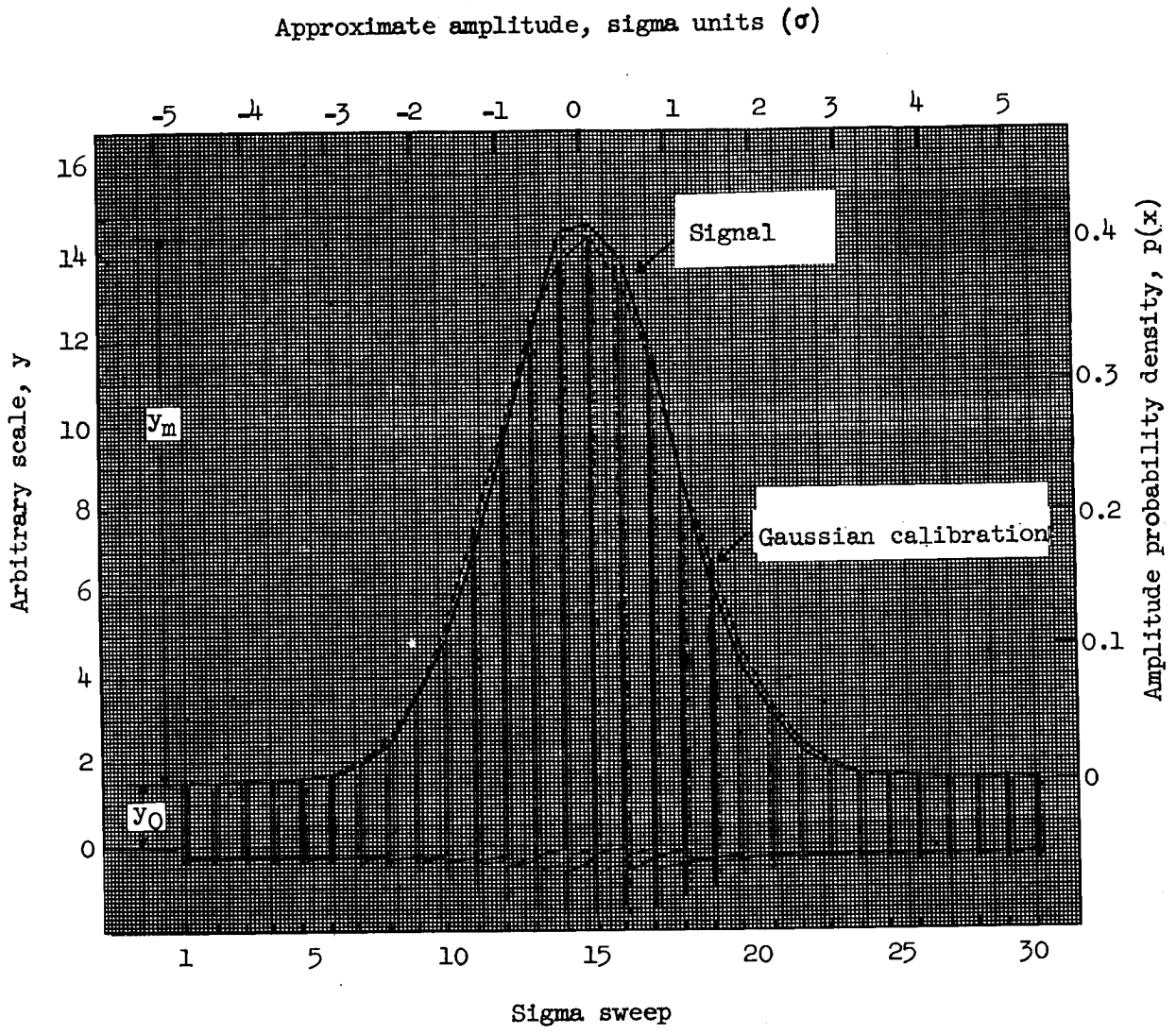

Figure 56.- Probability density analysis. -2 to 3 seconds; 70 kcps channel; Scale factor (S.F.) $= \frac{0.4}{y_m}$; $p(x) = (S.F.)(y - y_0)$.

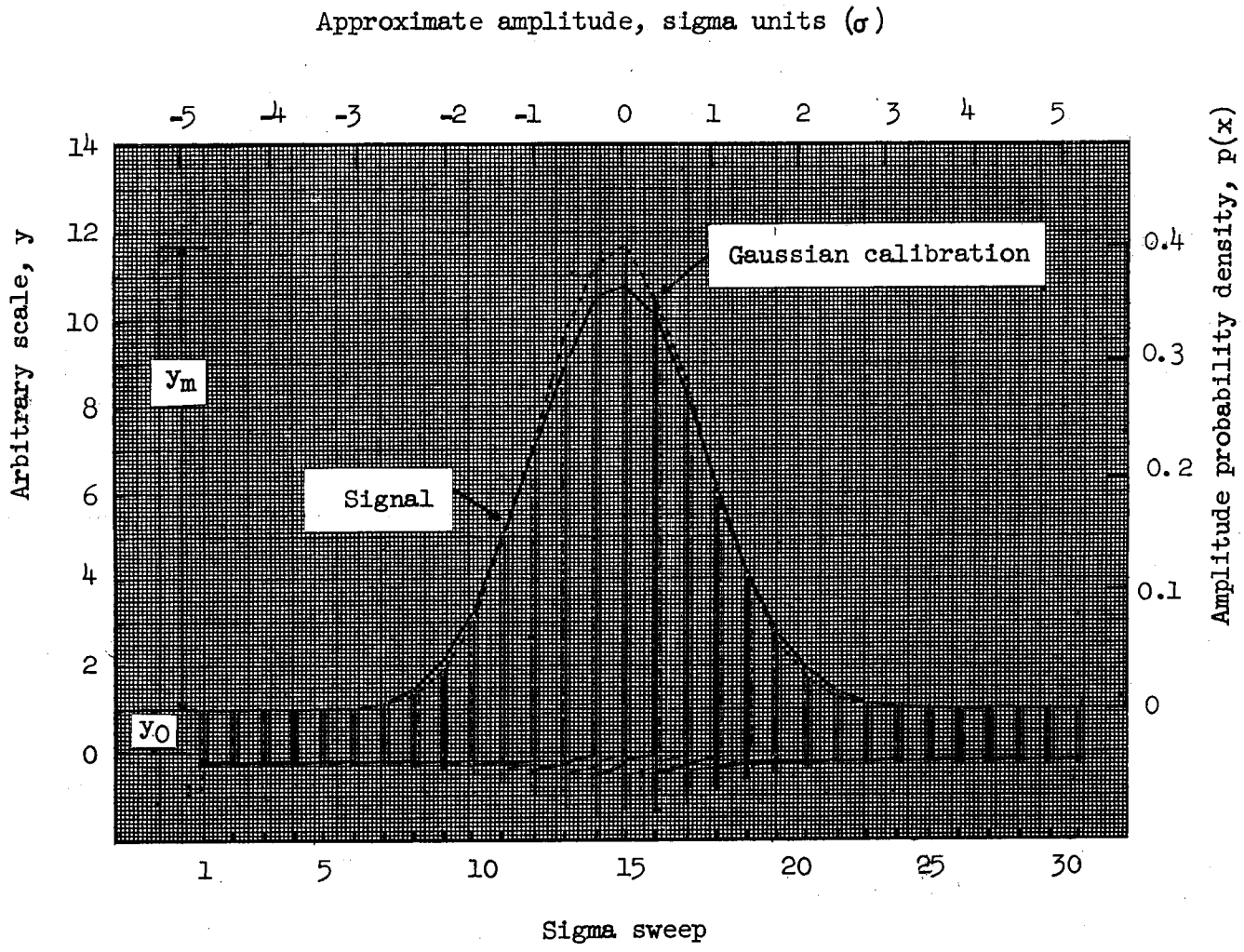

Figure 57.- Probability density analysis. 48 to 55 seconds; 70 kcps channel; Scale factor (S.F.) = $\frac{0.4}{y_m}$; p(x) 2 (S.F.)(y - y_0).

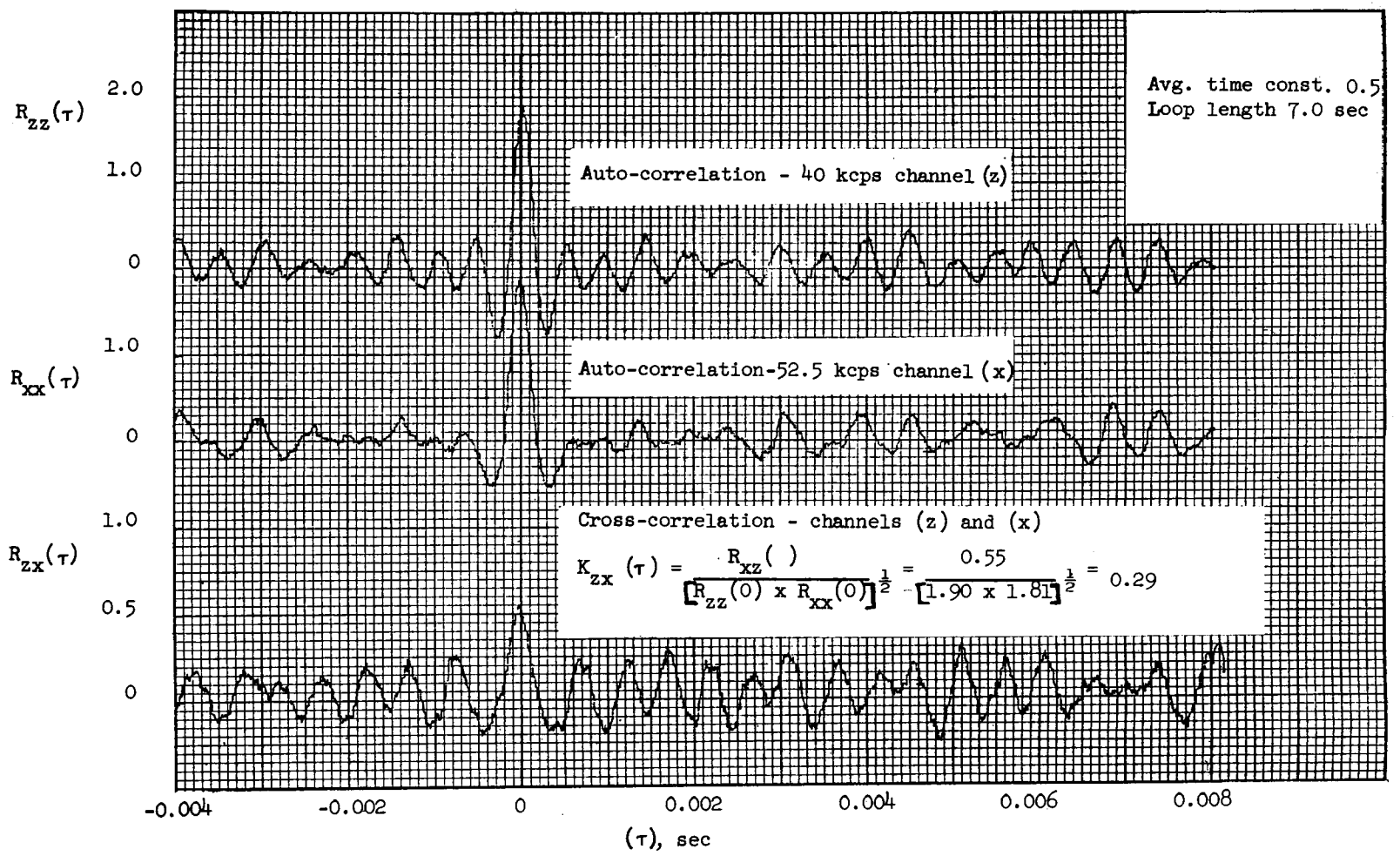

Figure 58.- Auto and cross correlation. -12 to -5 seconds.

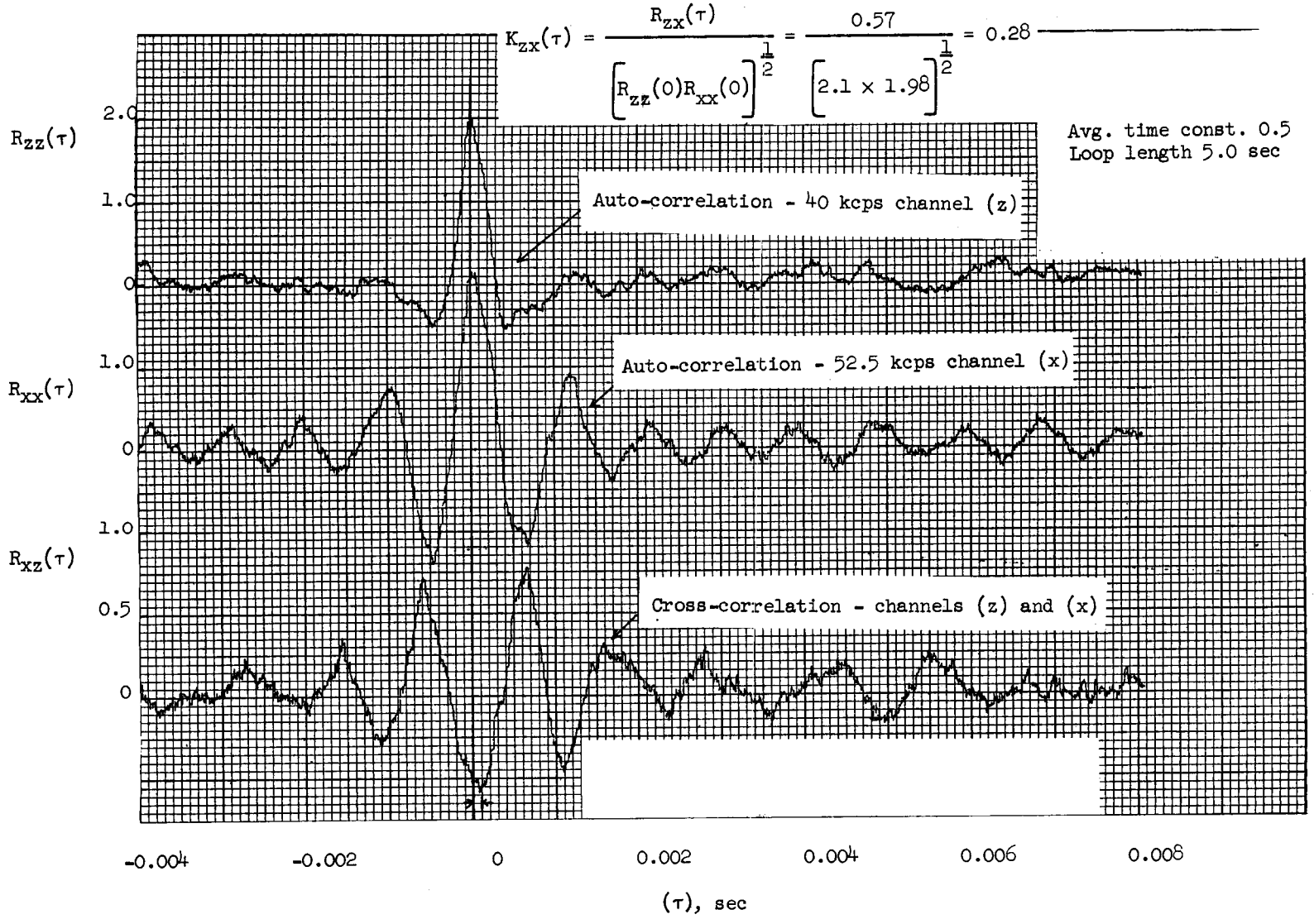

Figure 59.- Auto and cross correlation. -2 to 3 seconds.

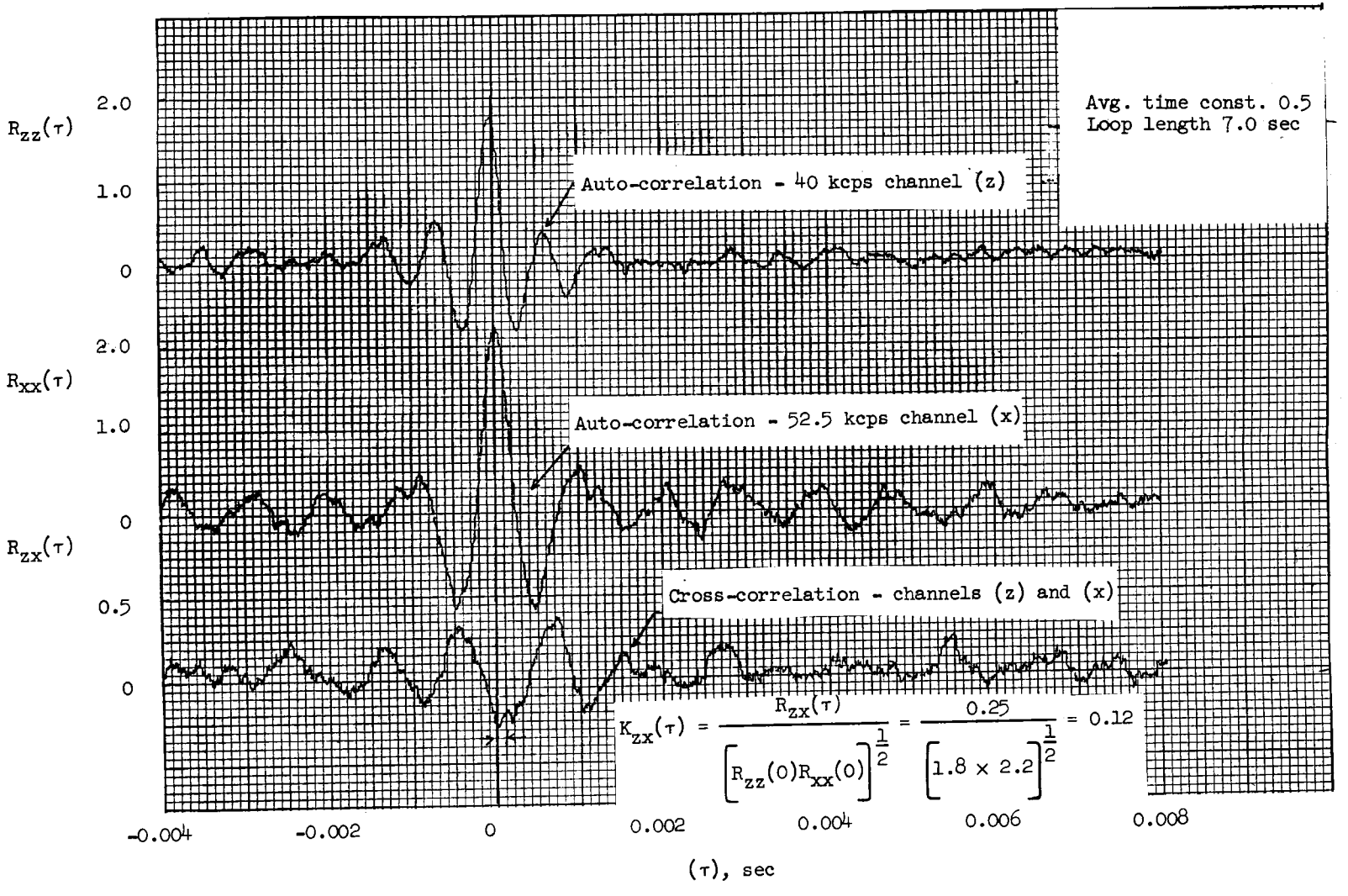

Figure 60.- Auto and cross correlation. 48 to 55 seconds.

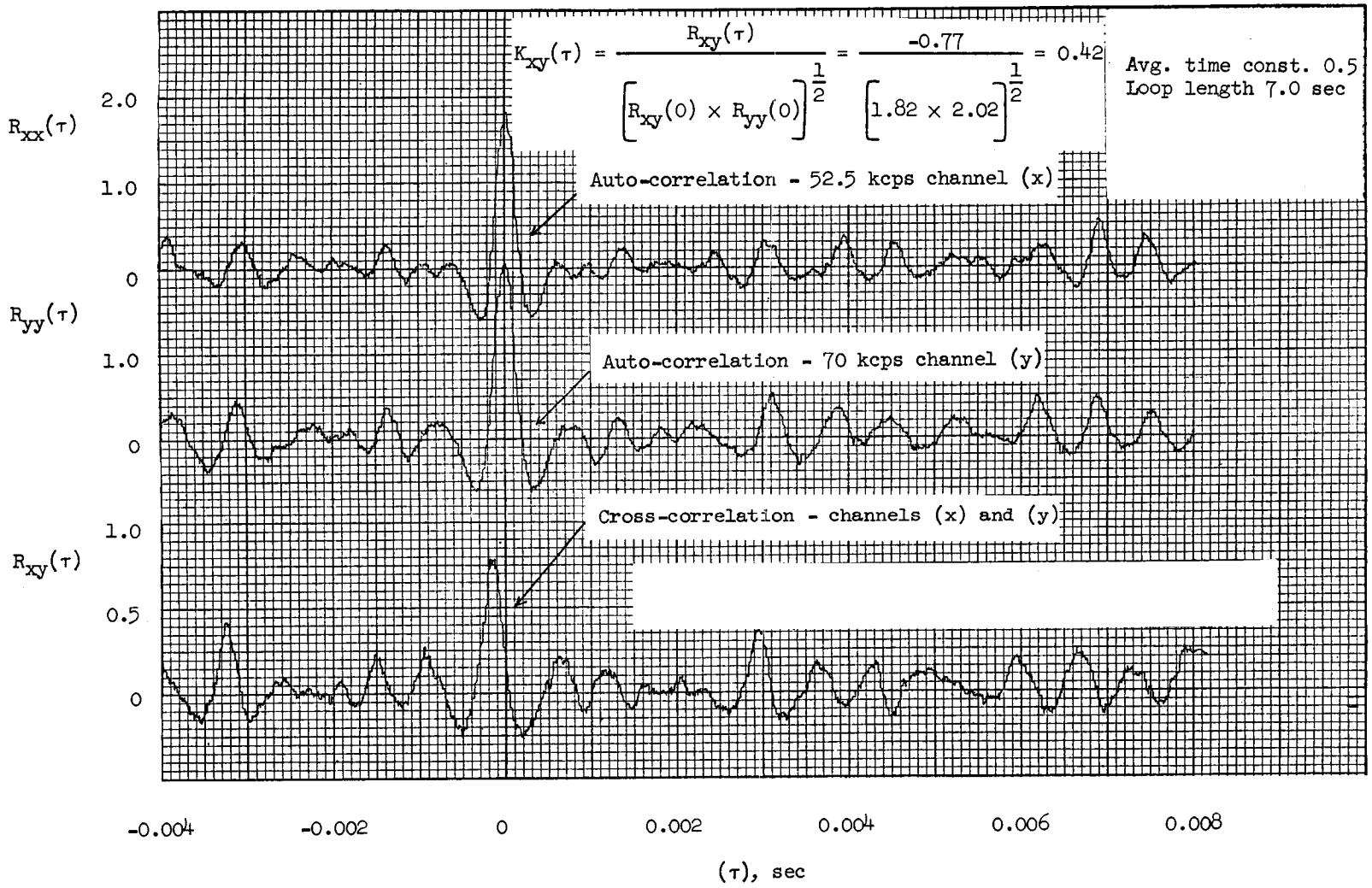

Figure 61.- Auto and cross correlation. -12 to -5 seconds.

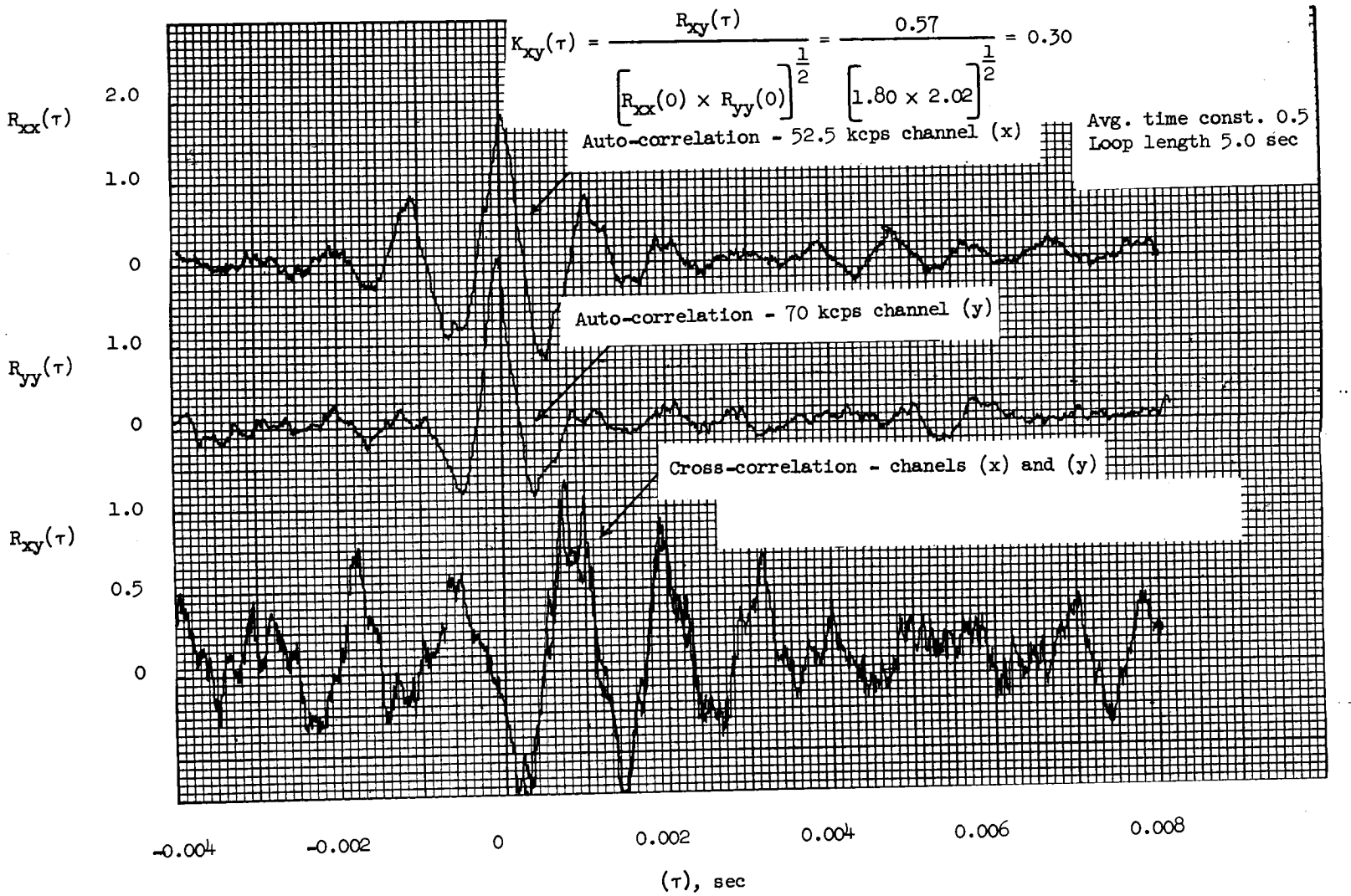

Figure 62. Auto and cross correlation. -2 to 3 seconds.

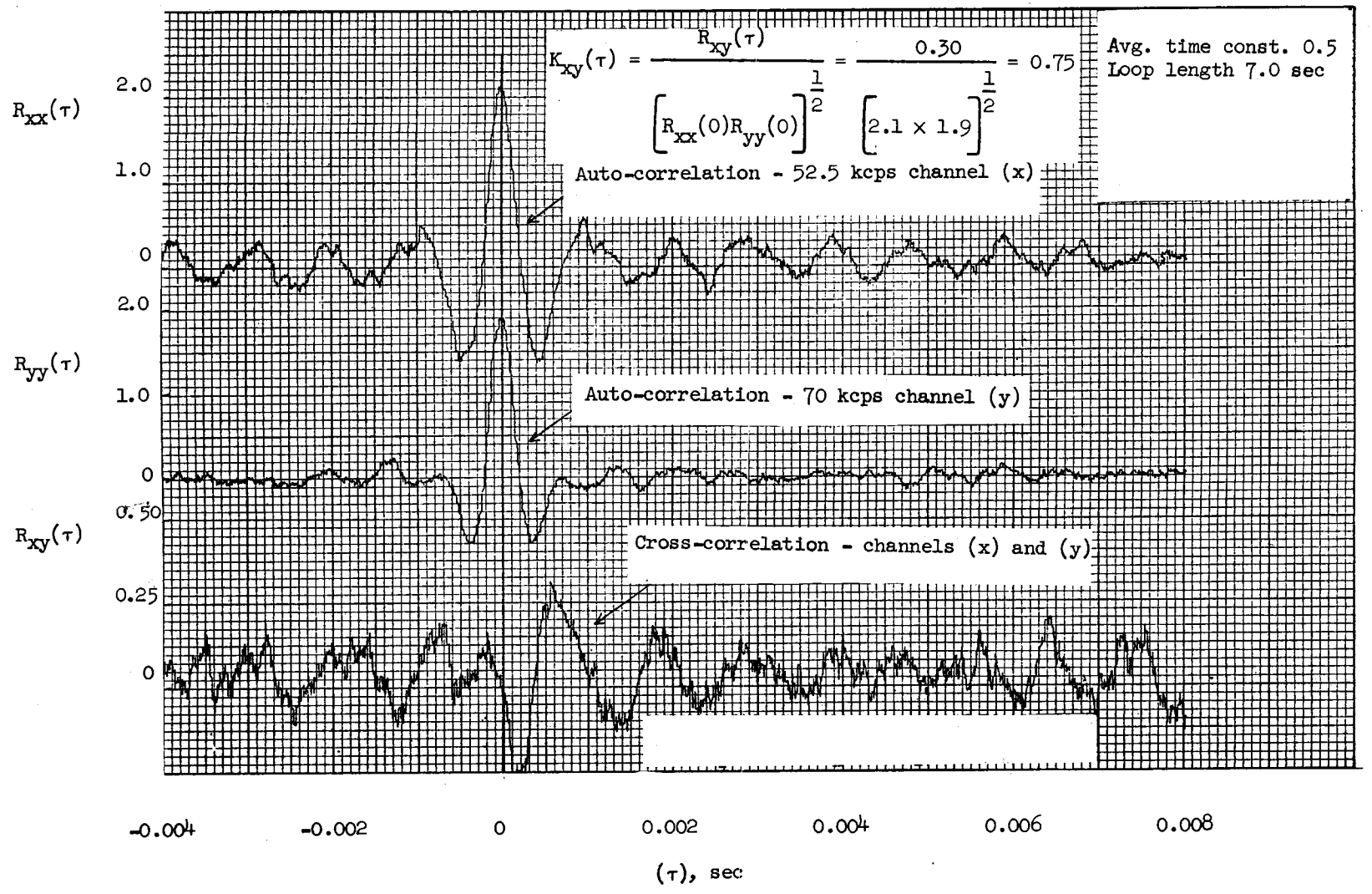

Figure 63.- Auto and cross correlation. 48 to 55 seconds.

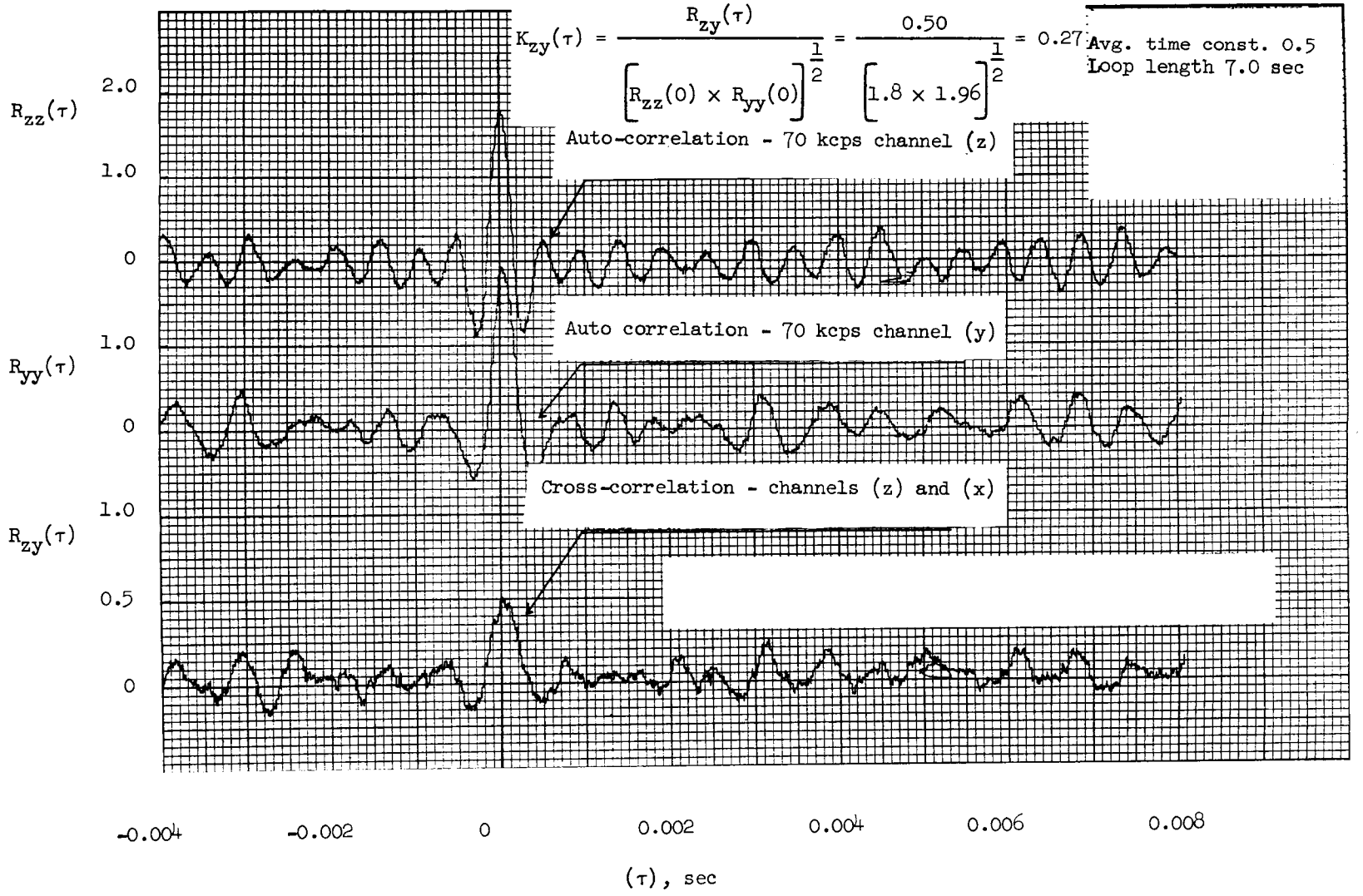

Figure 64.- Auto and cross correlation. -12 to -5 seconds.

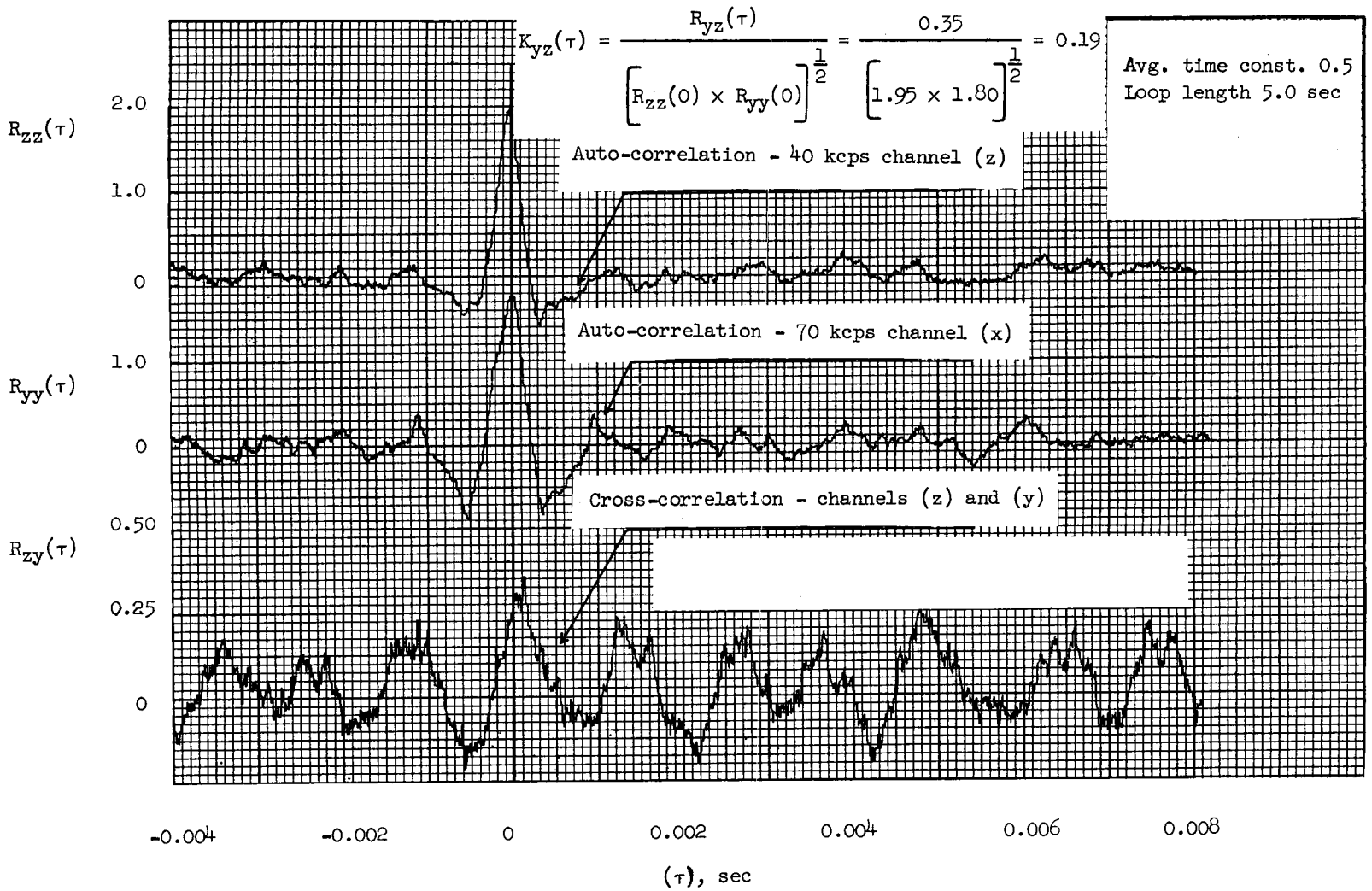

Figure 65.- Auto and cross correlation. -2 to 3 seconds.

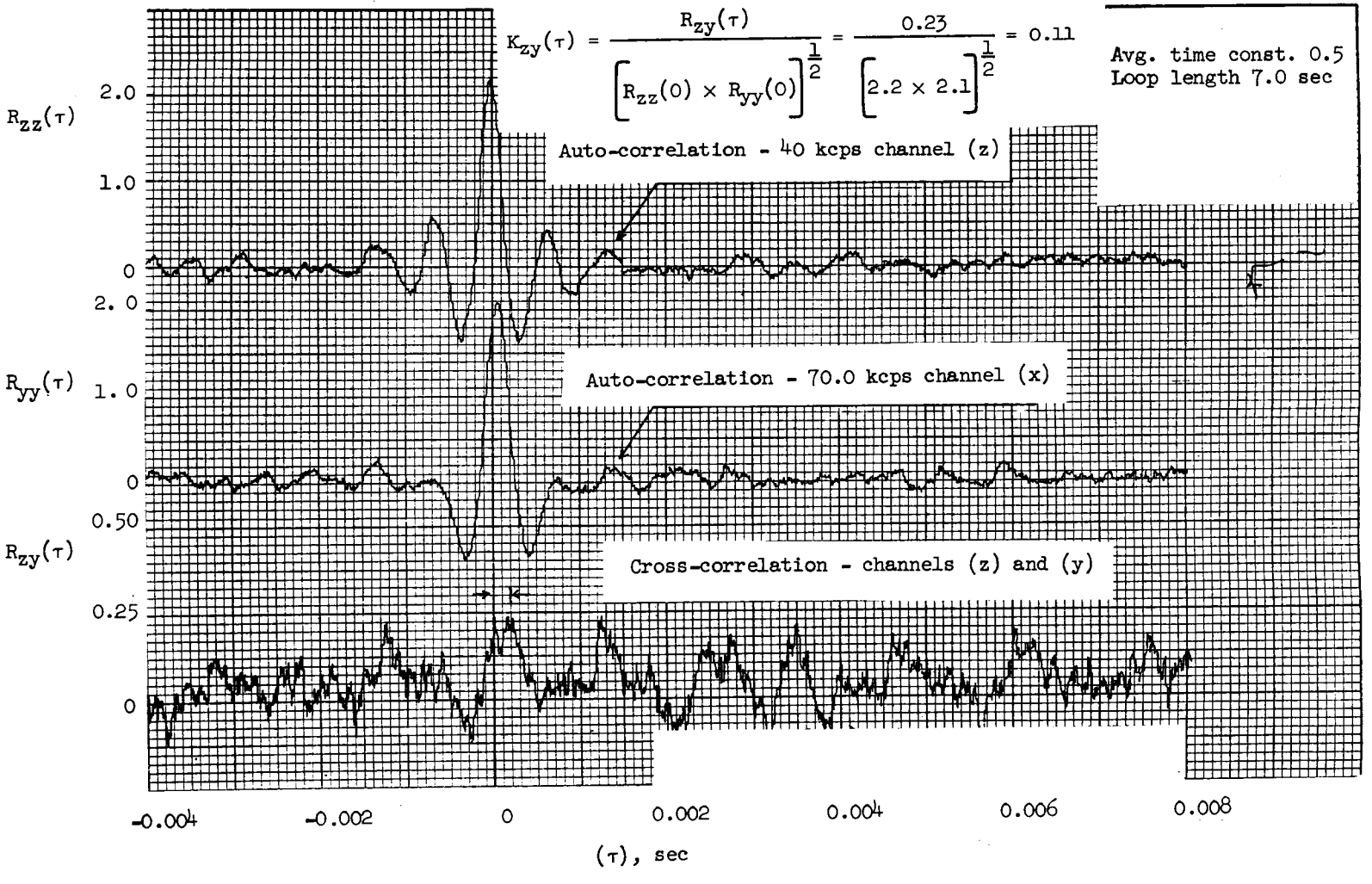

Figure 66.- Auto and cross correlation. 48 to 55 seconds.

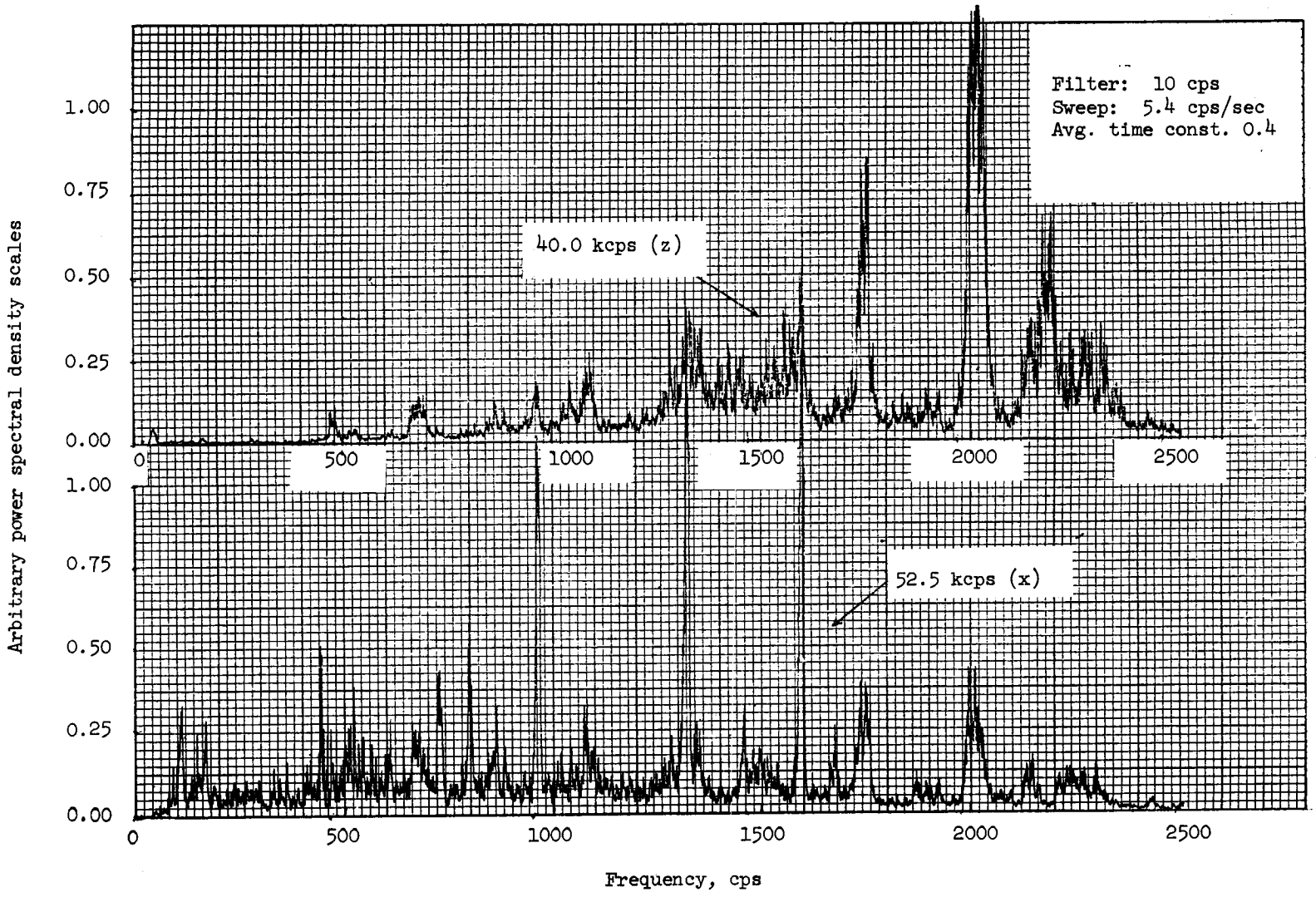

Figure 67.- Auto and cross correlation. -12 to -5 seconds.

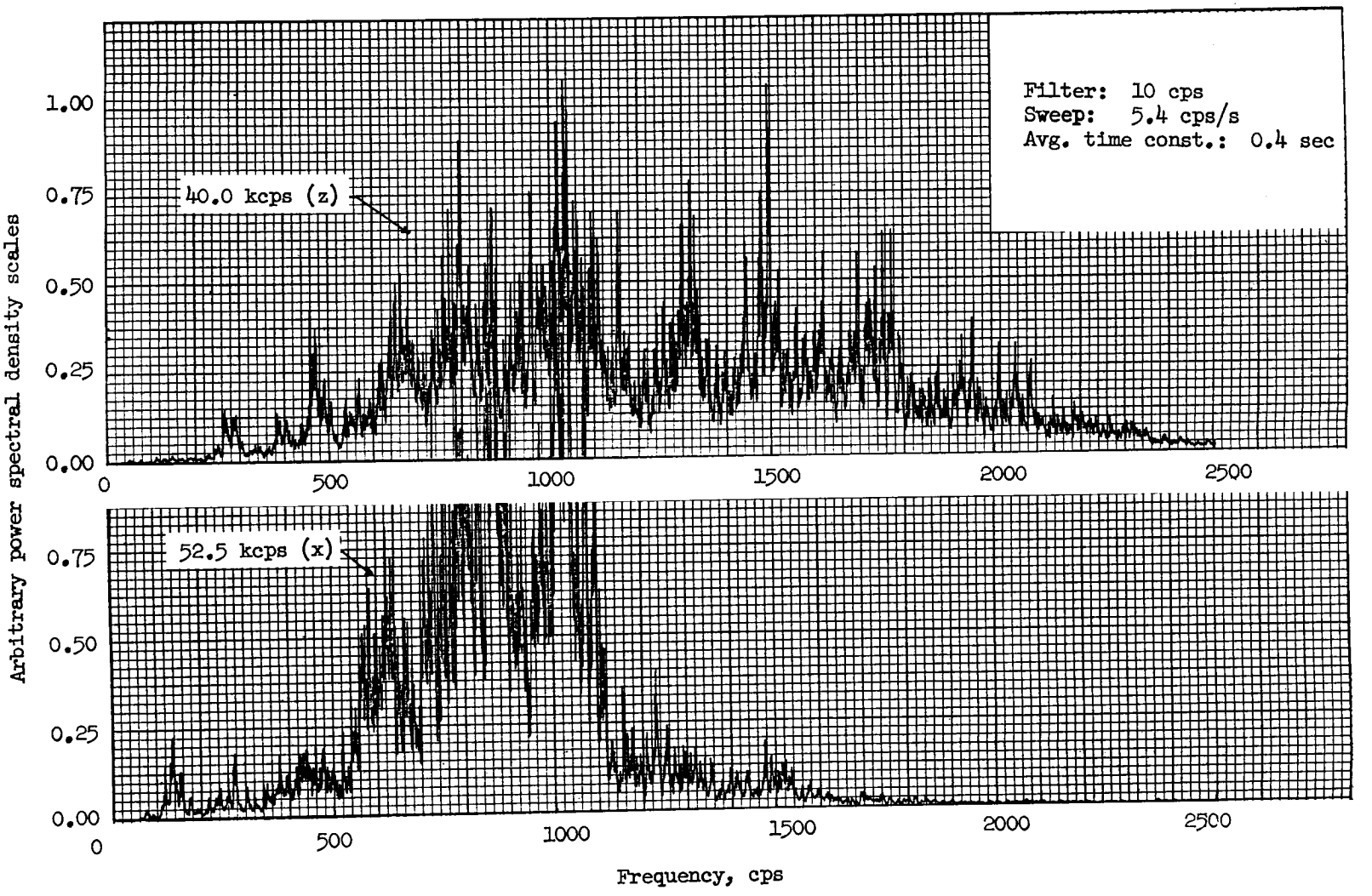

Figure 68.- Power spectral density. -2 to 3 seconds.

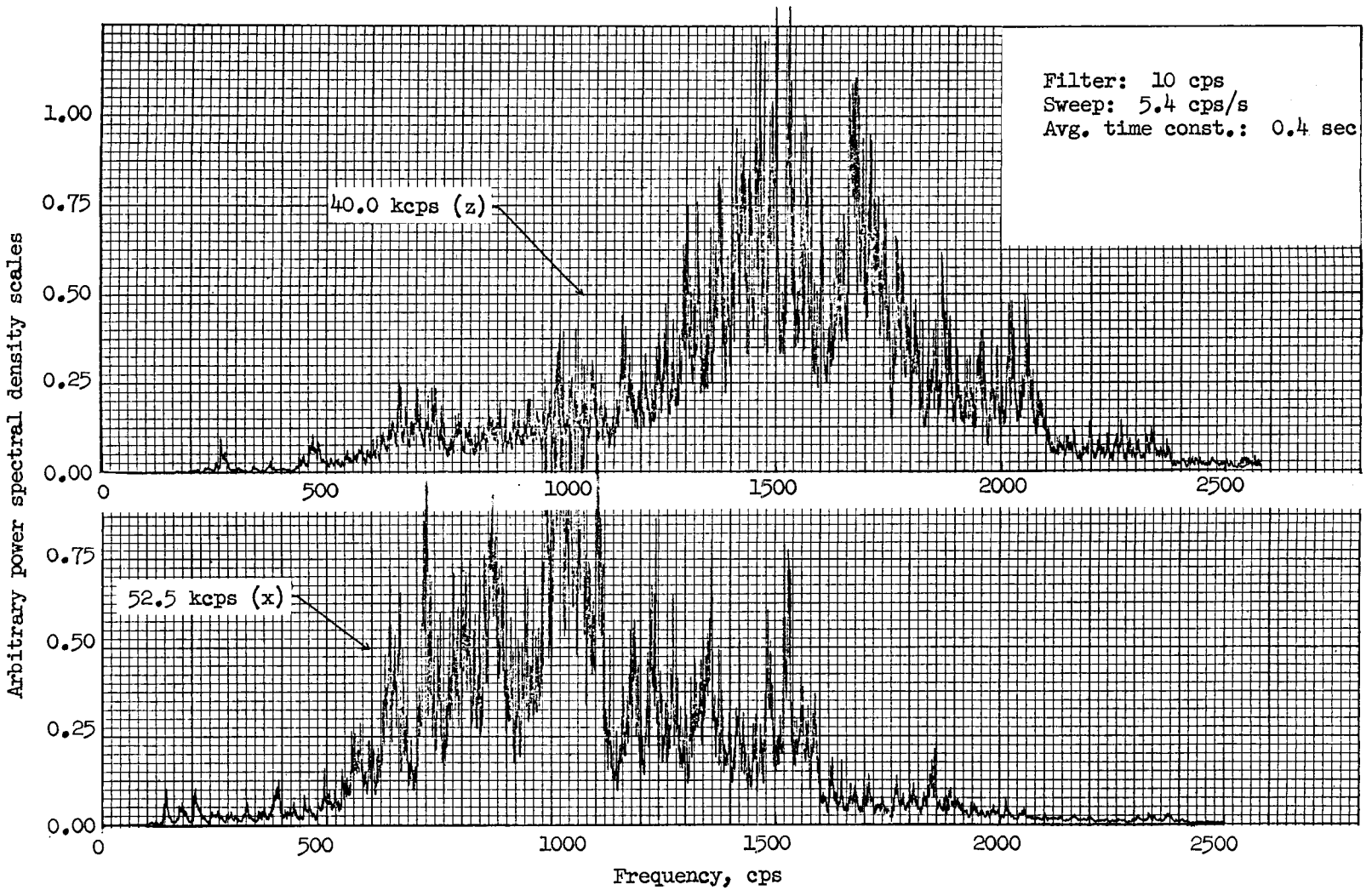

Figure 69.- Power spectral density. 48 to 55 seconds.

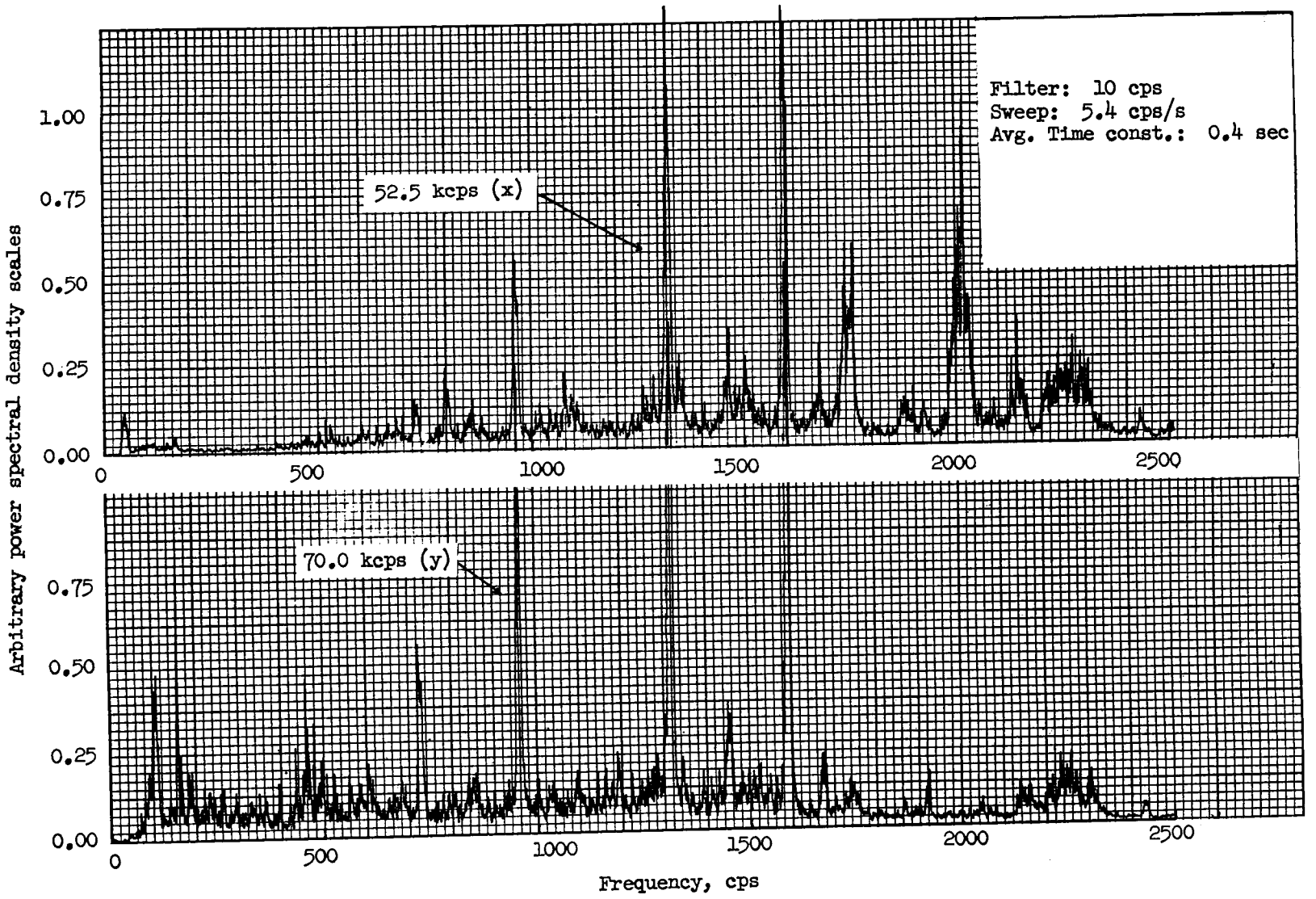

Figure 70.- Power spectral density. -12 to -5 seconds.

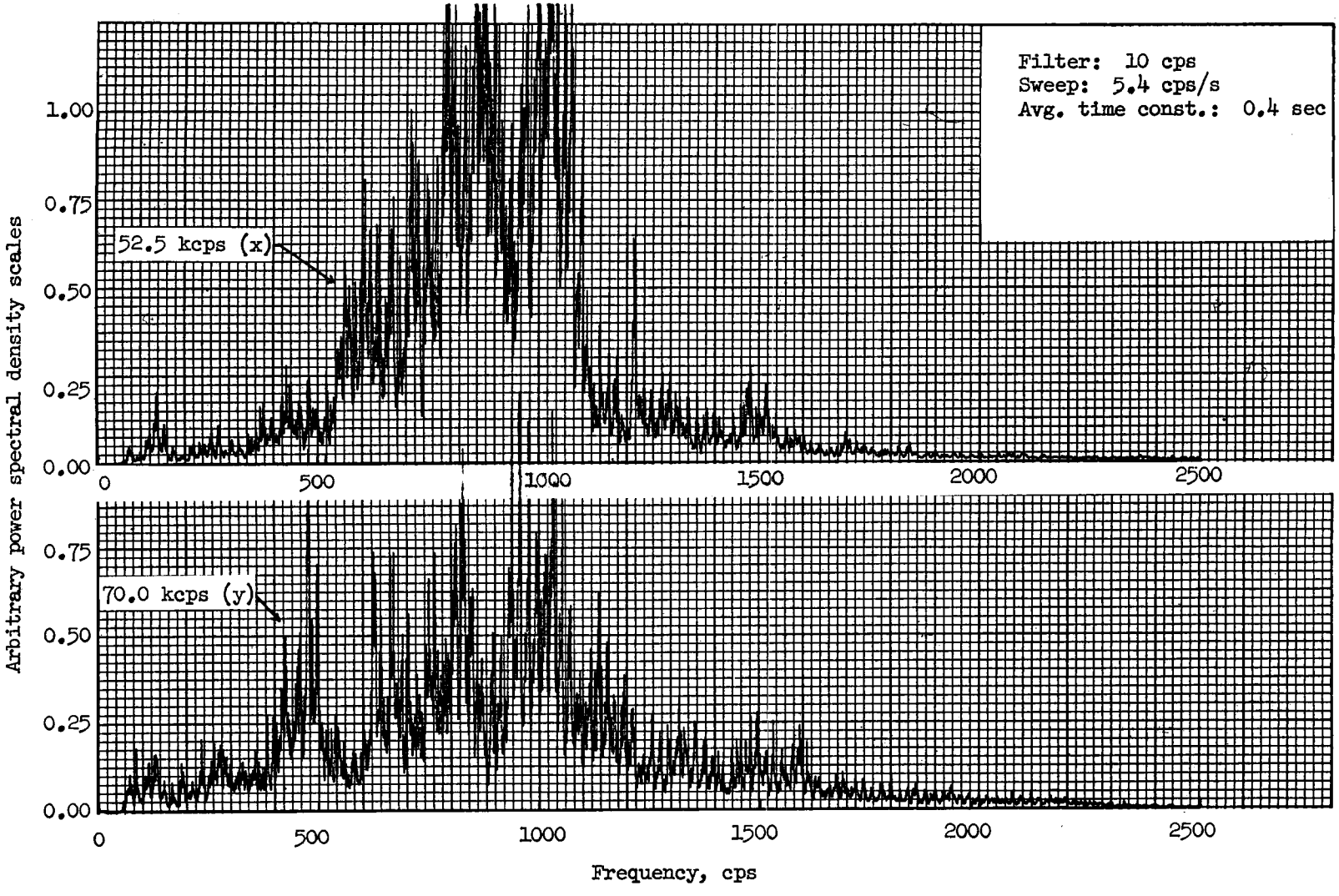

Figure 71.- Power spectral density. -2 to 3 seconds.

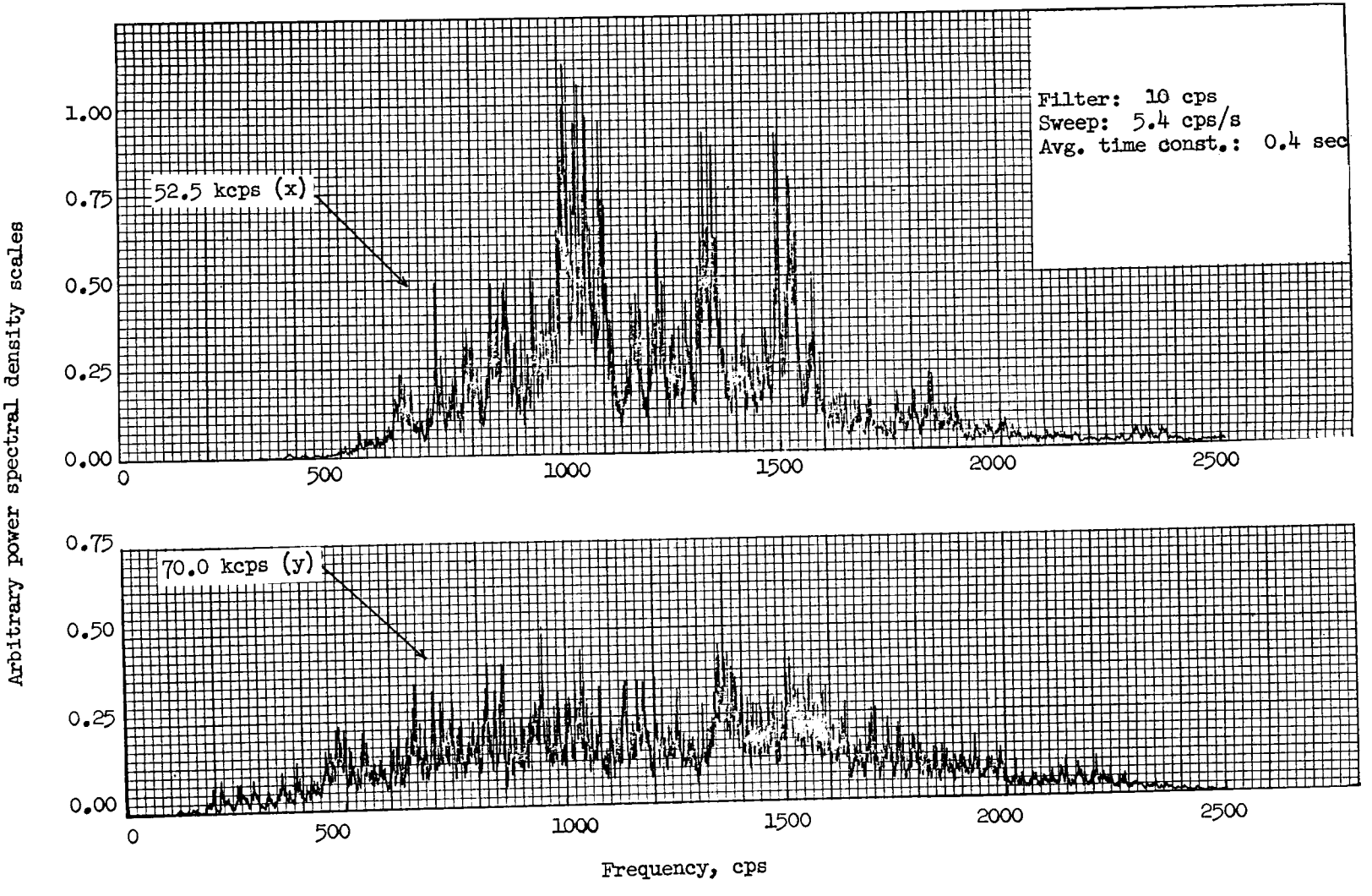

Figure 72.- Power spectral density. 48 to 55 seconds.

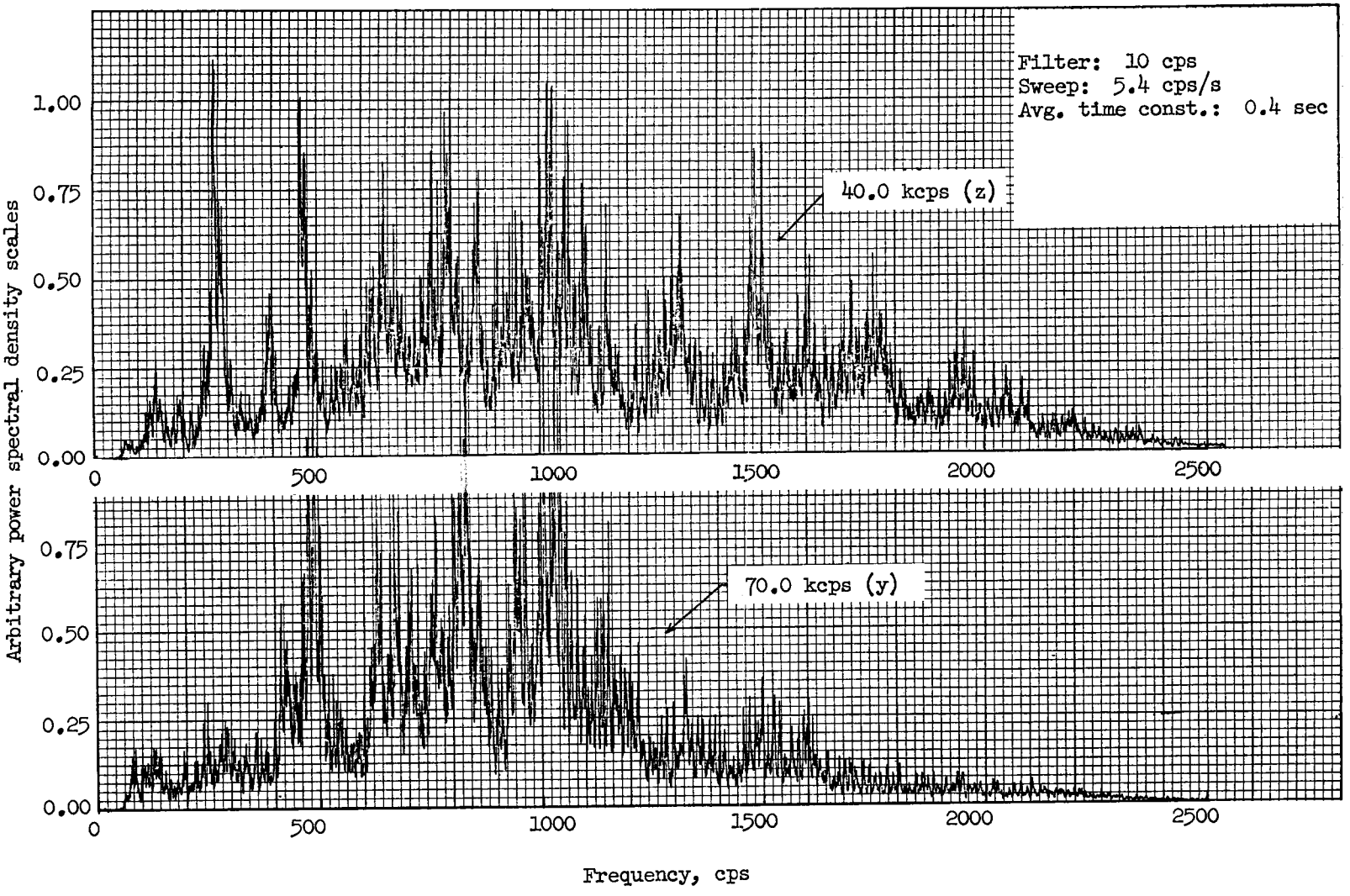

Figure 73.- Power spectral density. -2 to 3 seconds.

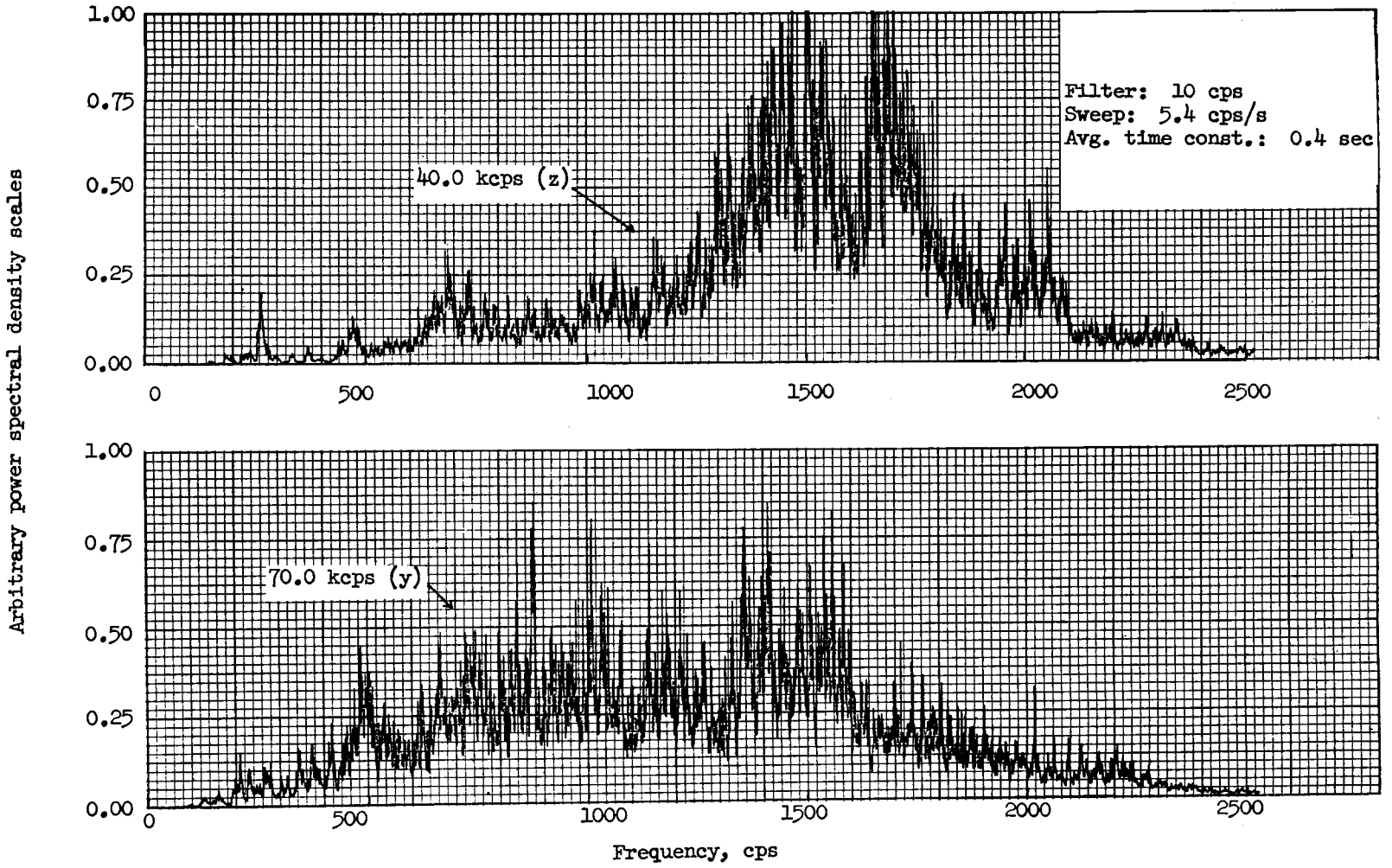

Figure 74.- Power spectral density. 48 to 55 seconds.

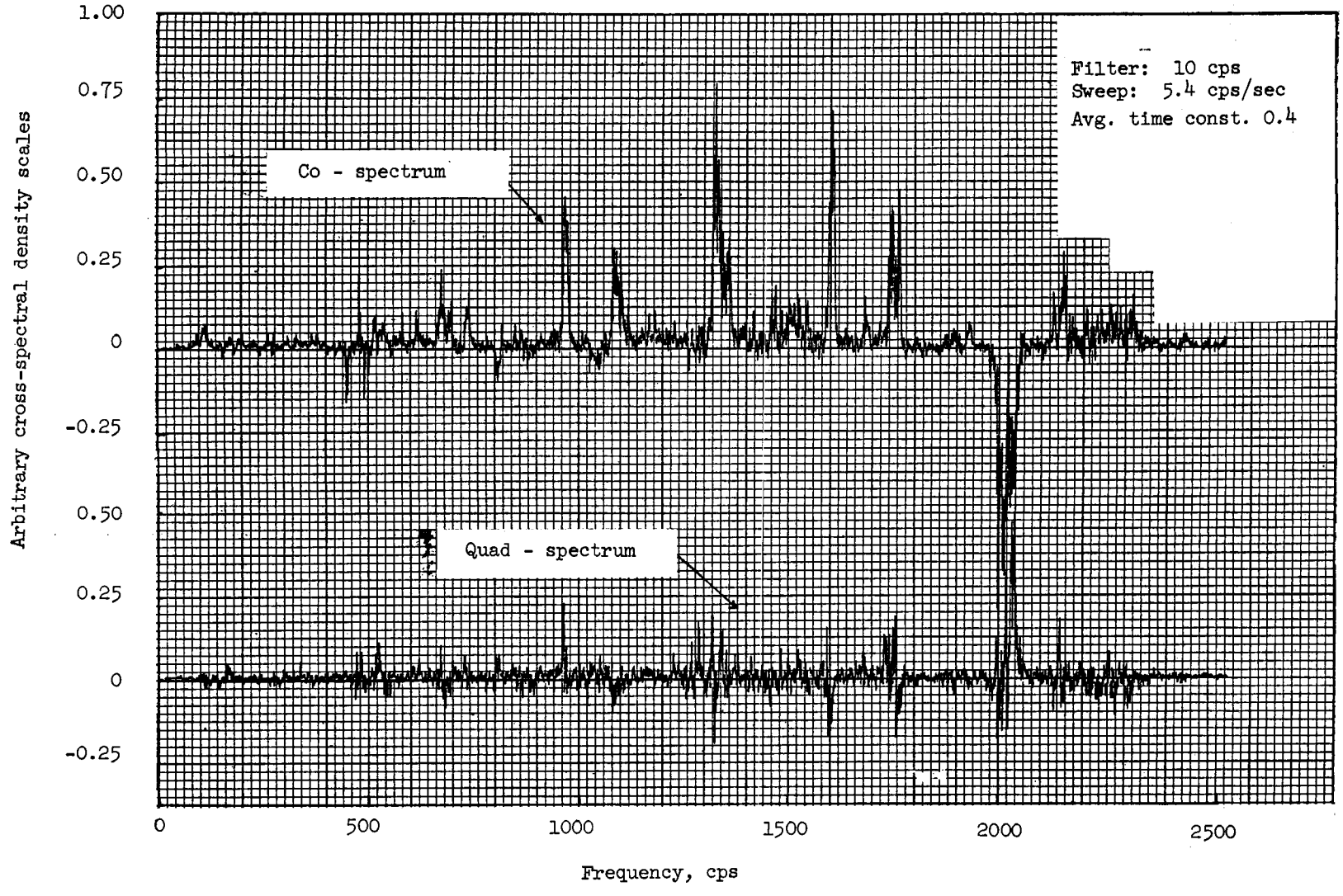

Figure 75.- Cross spectral density. -12 to -5 seconds.

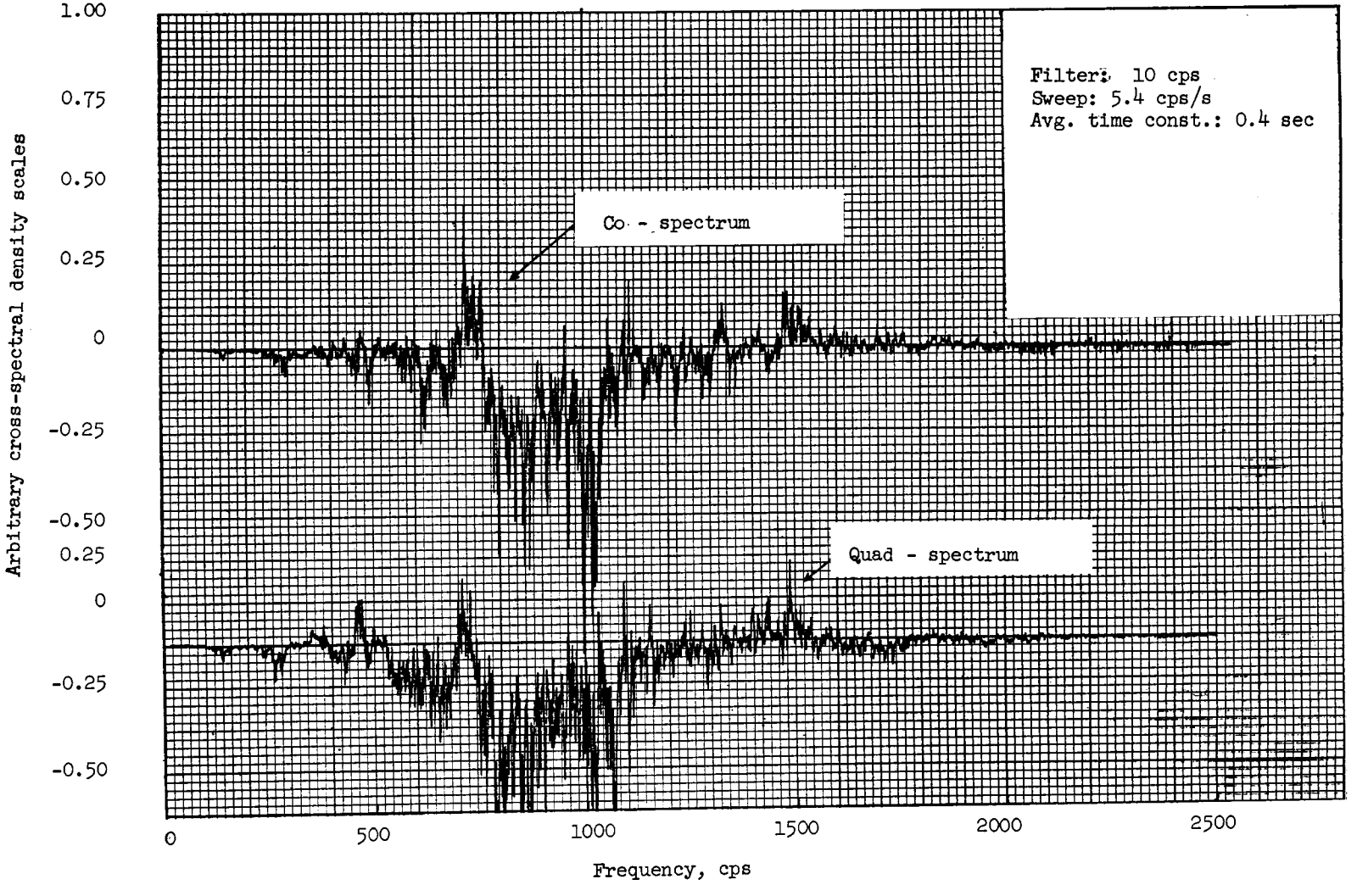

Figure 76.- Cross spectral density. -2 to 3 seconds; 40 and 52.5 kcps channels.

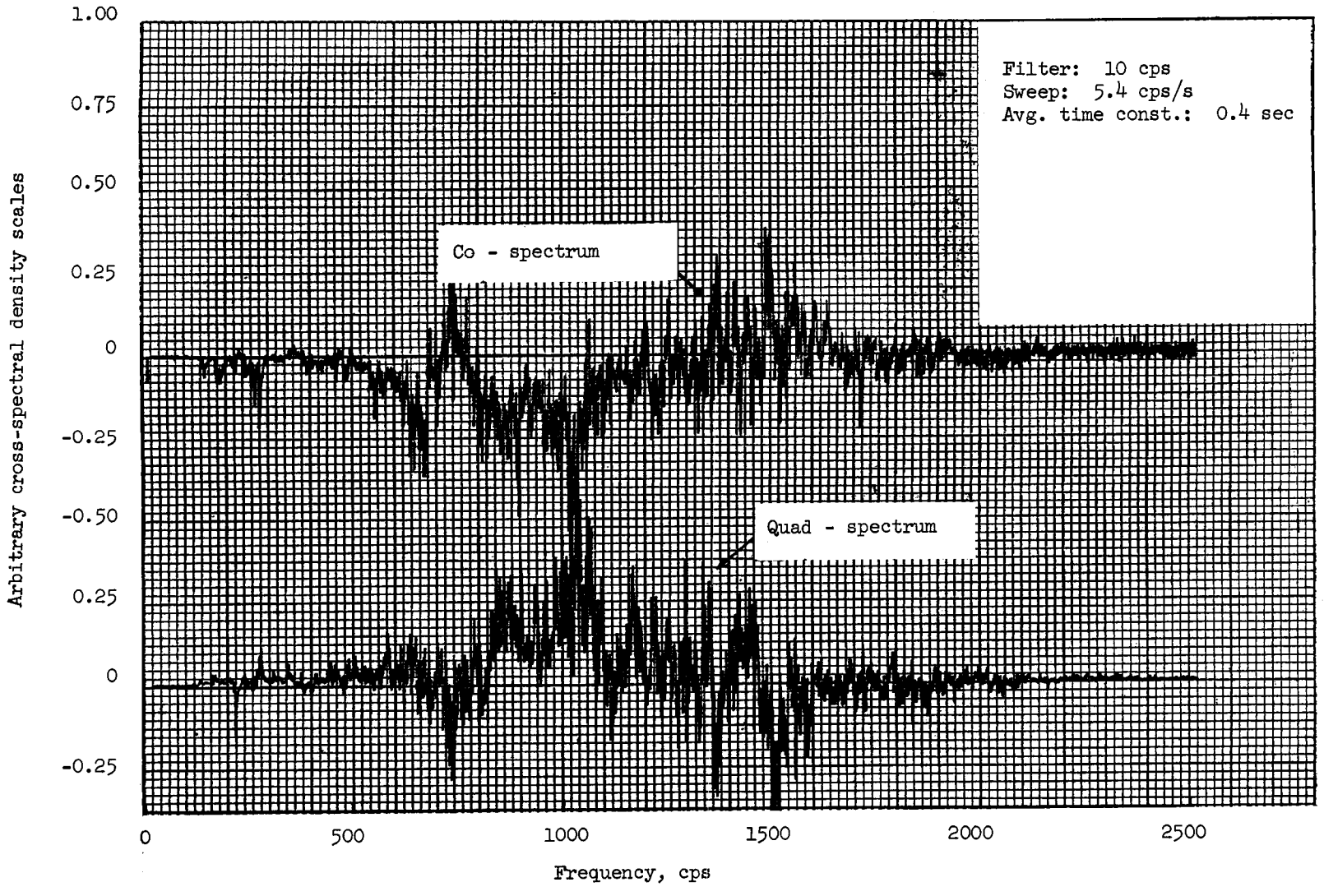

Figure 77.- Cross spectral density. 48 to 55 seconds; 40 and 52.5 kcps channels.

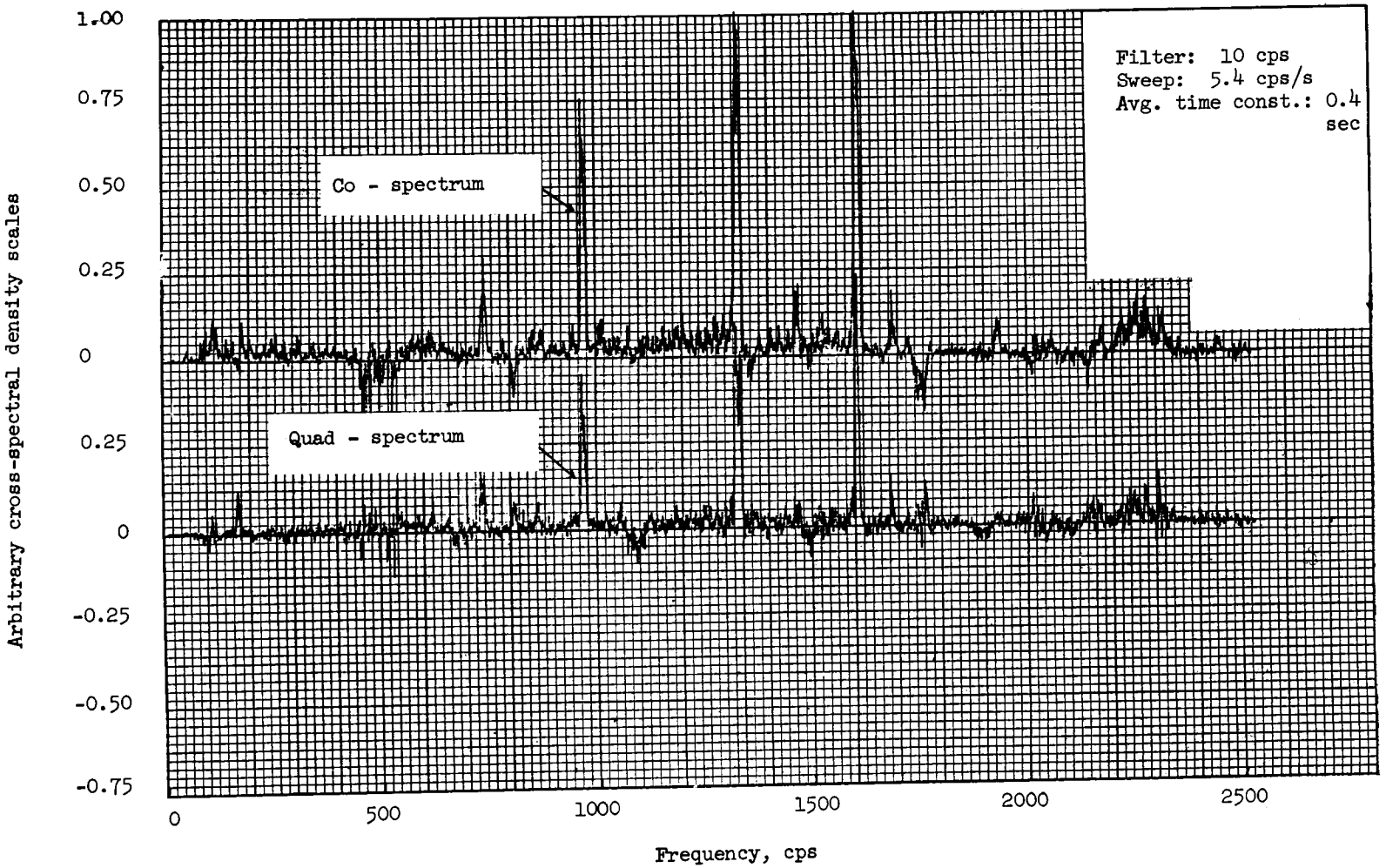

Figure 78.- Cross spectral density. -12 to -5 seconds; 52.5 and 70 kcps channels.

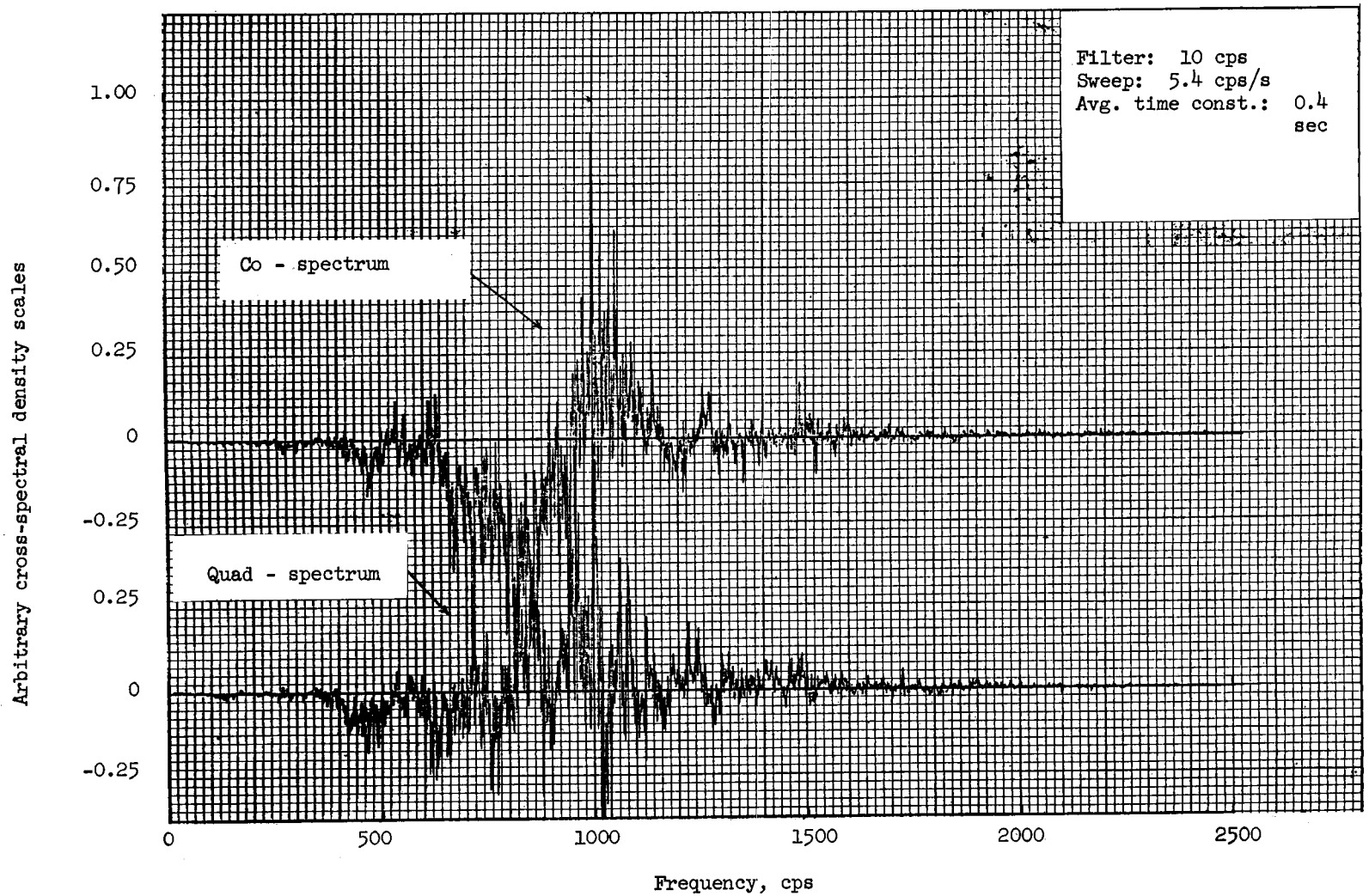

Figure 79.- Cross spectral density. -2 to 3 seconds; 52.5 and 70 kcps channels.

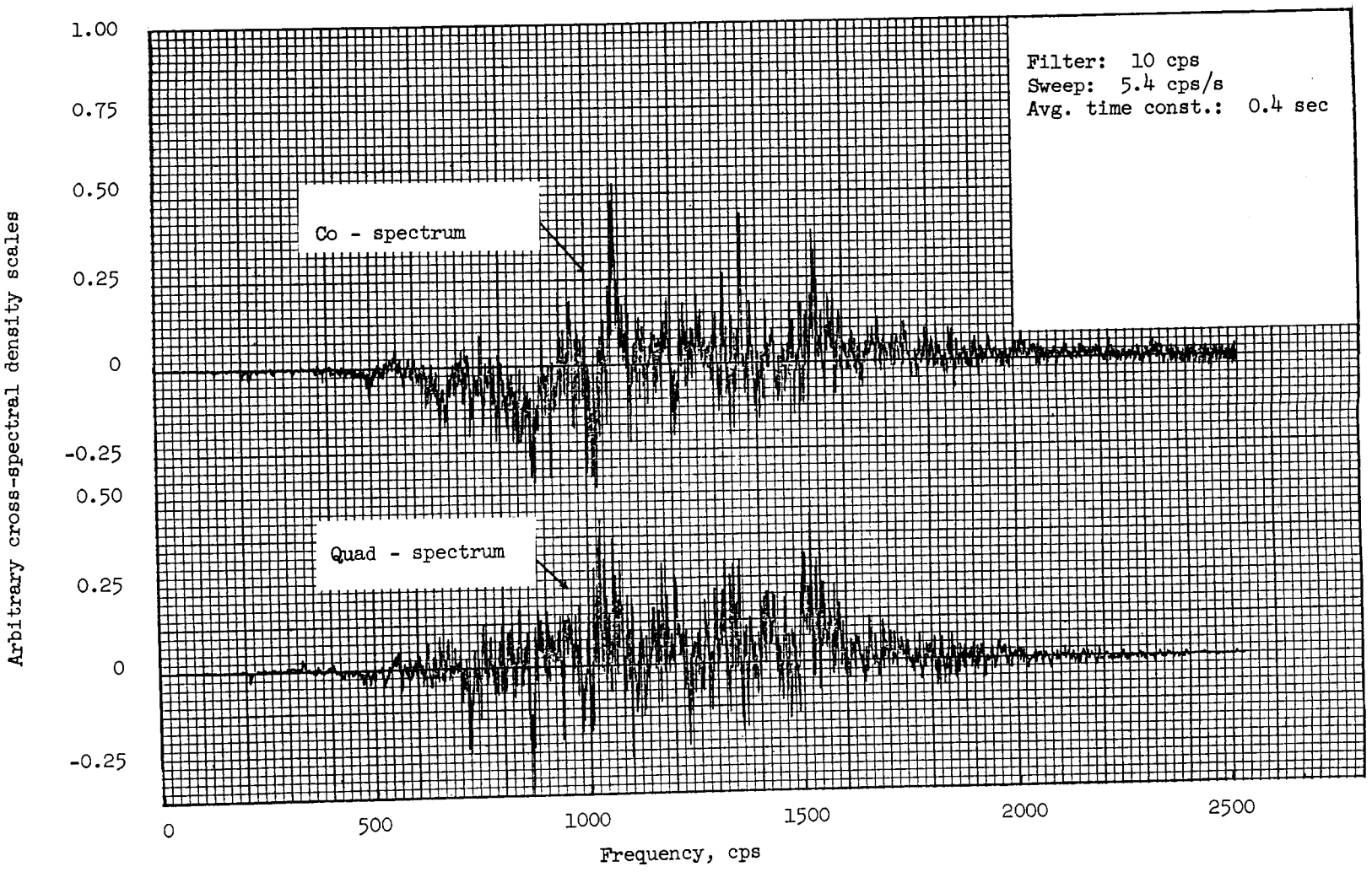

Figure 80.- Cross spectral density. 48 to 55 seconds; 52.5 and 70 kcps channels.

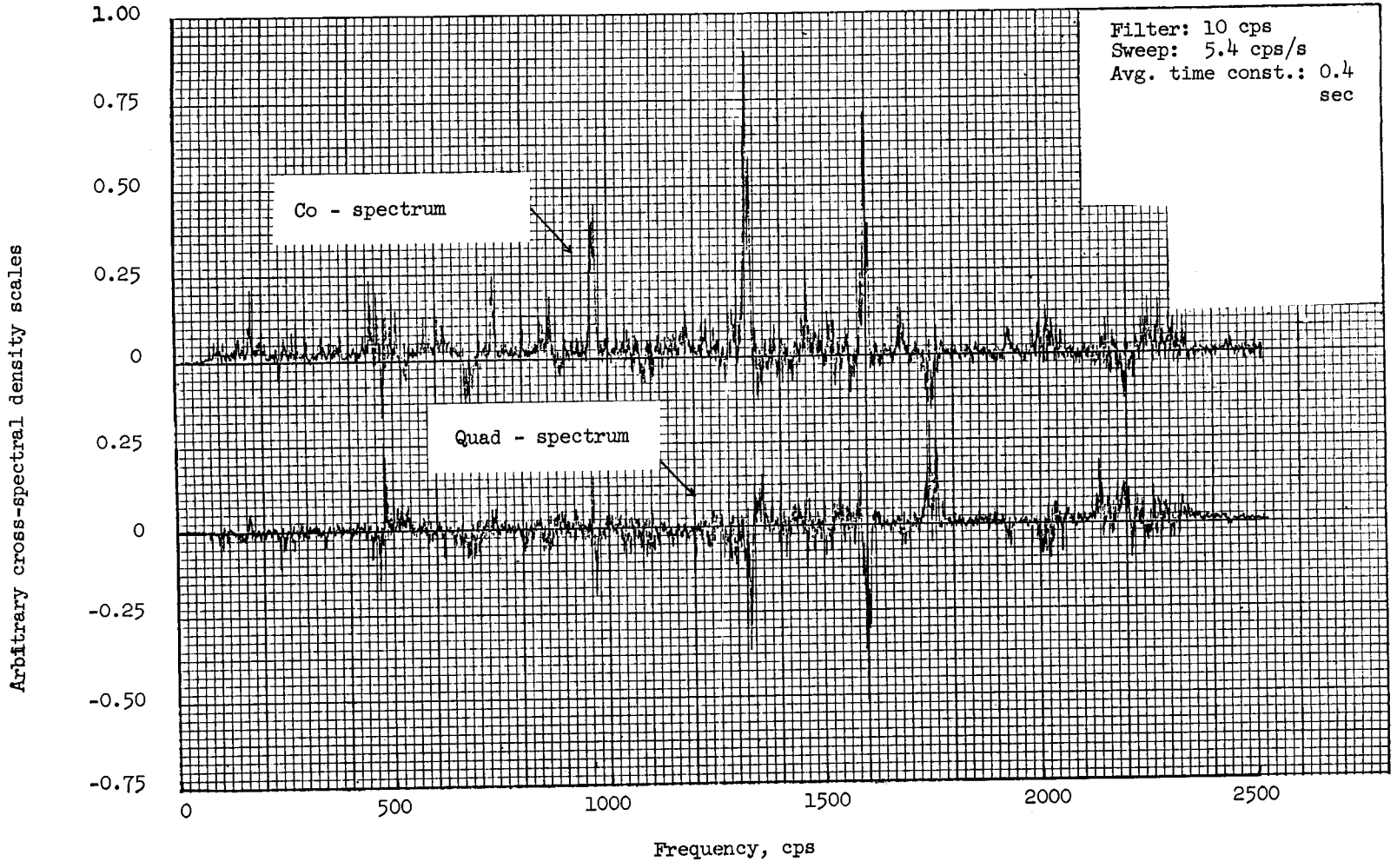

Figure 81.- Cross spectral density. -12 to -5 seconds; 40 and 70 kcps channels.

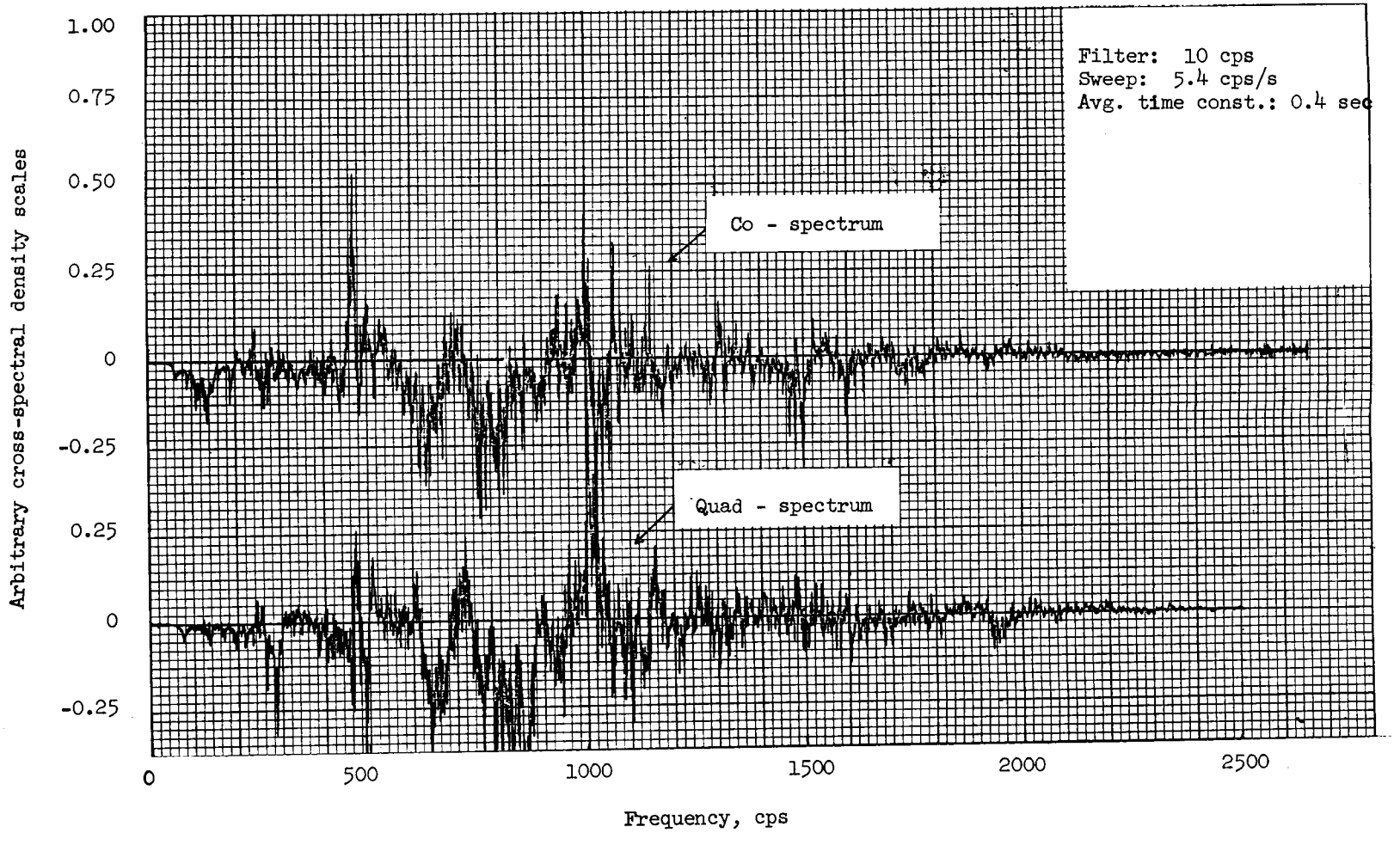

Figure 82.- Cross spectral density. -2 to 3 seconds; 40 and 70 kcps channels.

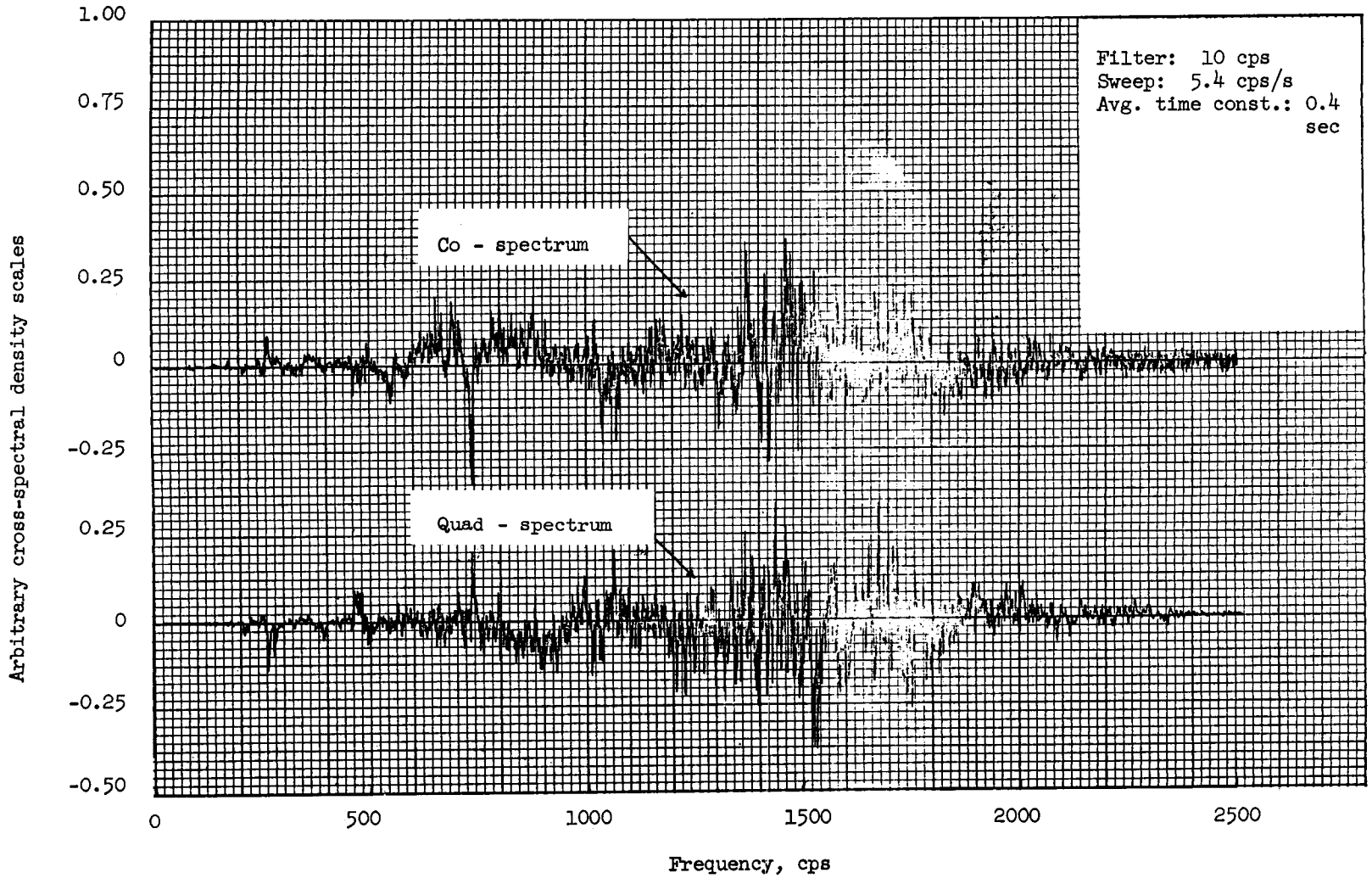

Figure 83.- Cross spectral density. 48 to 55 seconds; 40 and 70 kcps channels.

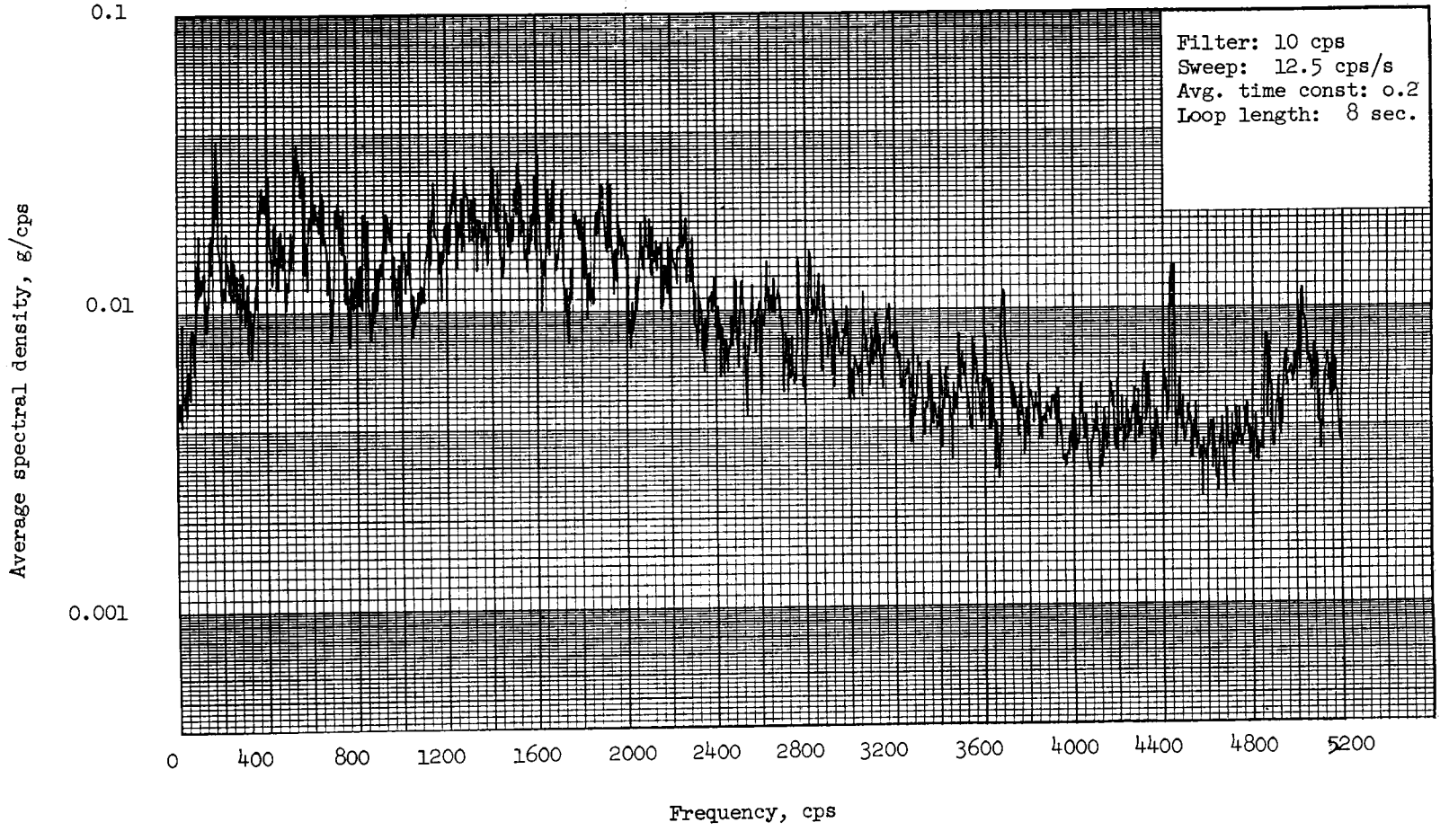

Figure 84.- Spectral density analysis. 10 cps filter; 31 to 39 seconds; 40 kcps.

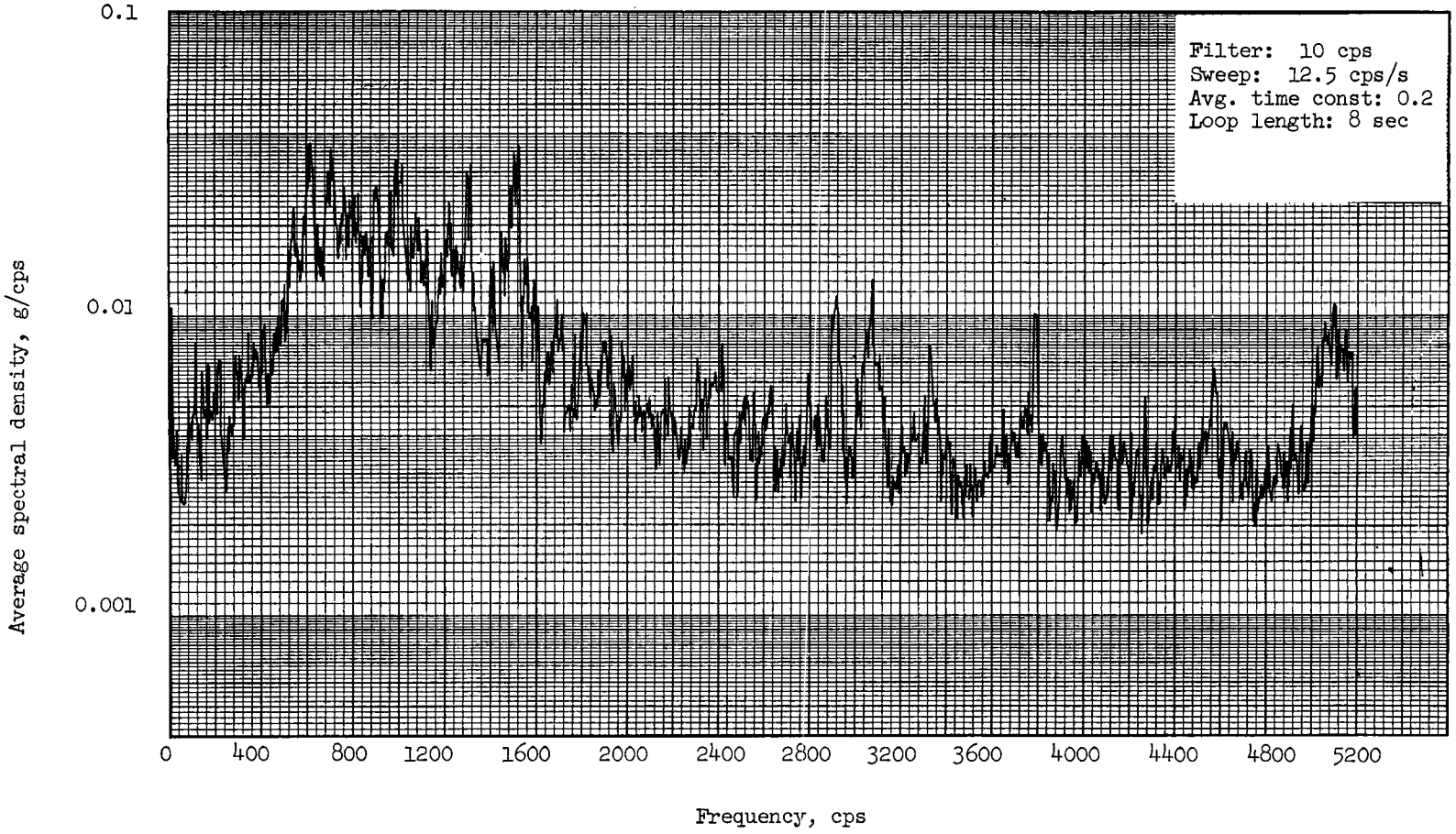

Figure 85.- Spectral density analysis. 10 cps filter; 31 to 39 seconds; 52.5 kcps.

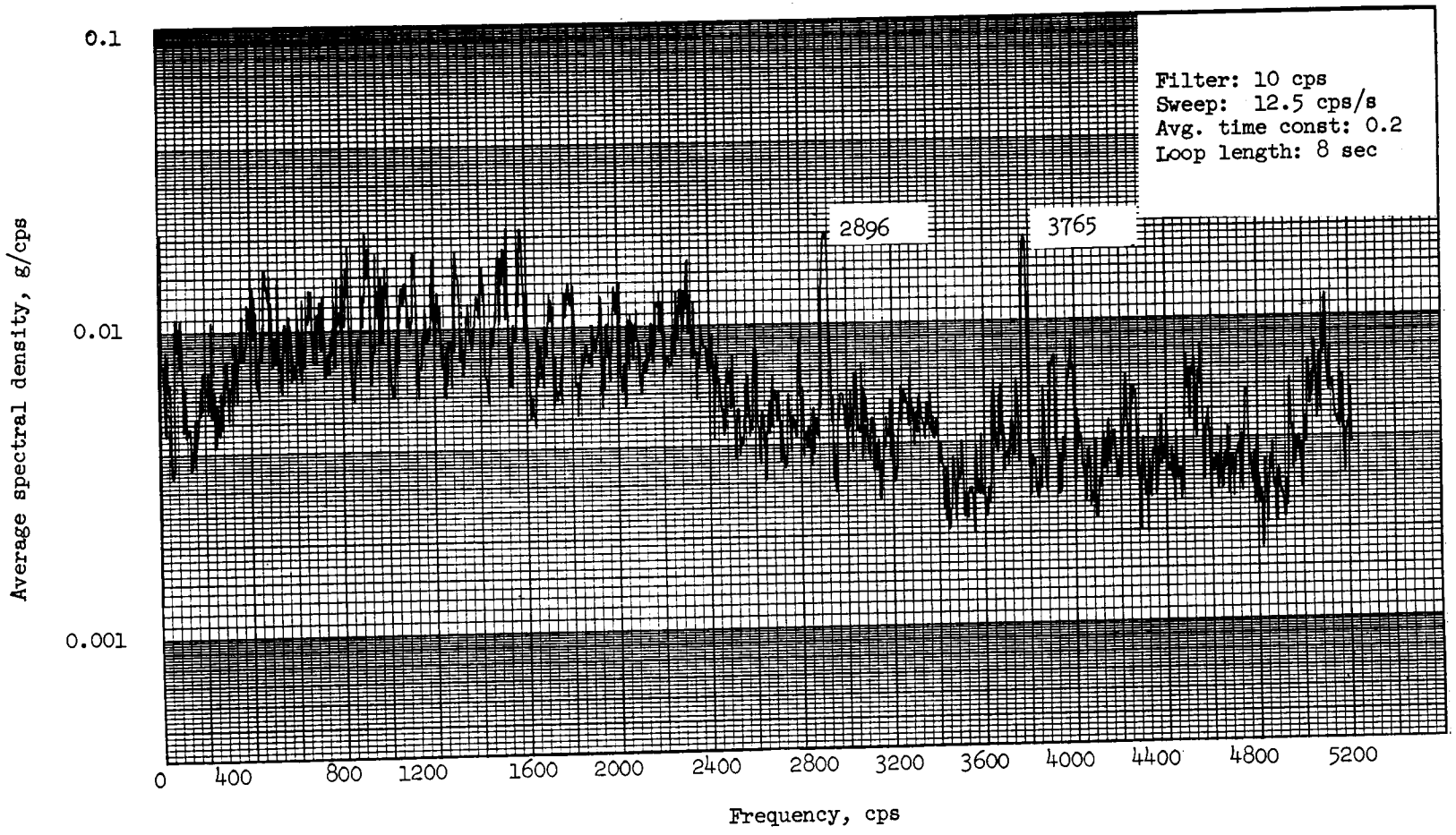

Figure 86.- Spectral density analysis. 10 cps filter; 31 to 39 seconds; 70 kcps.

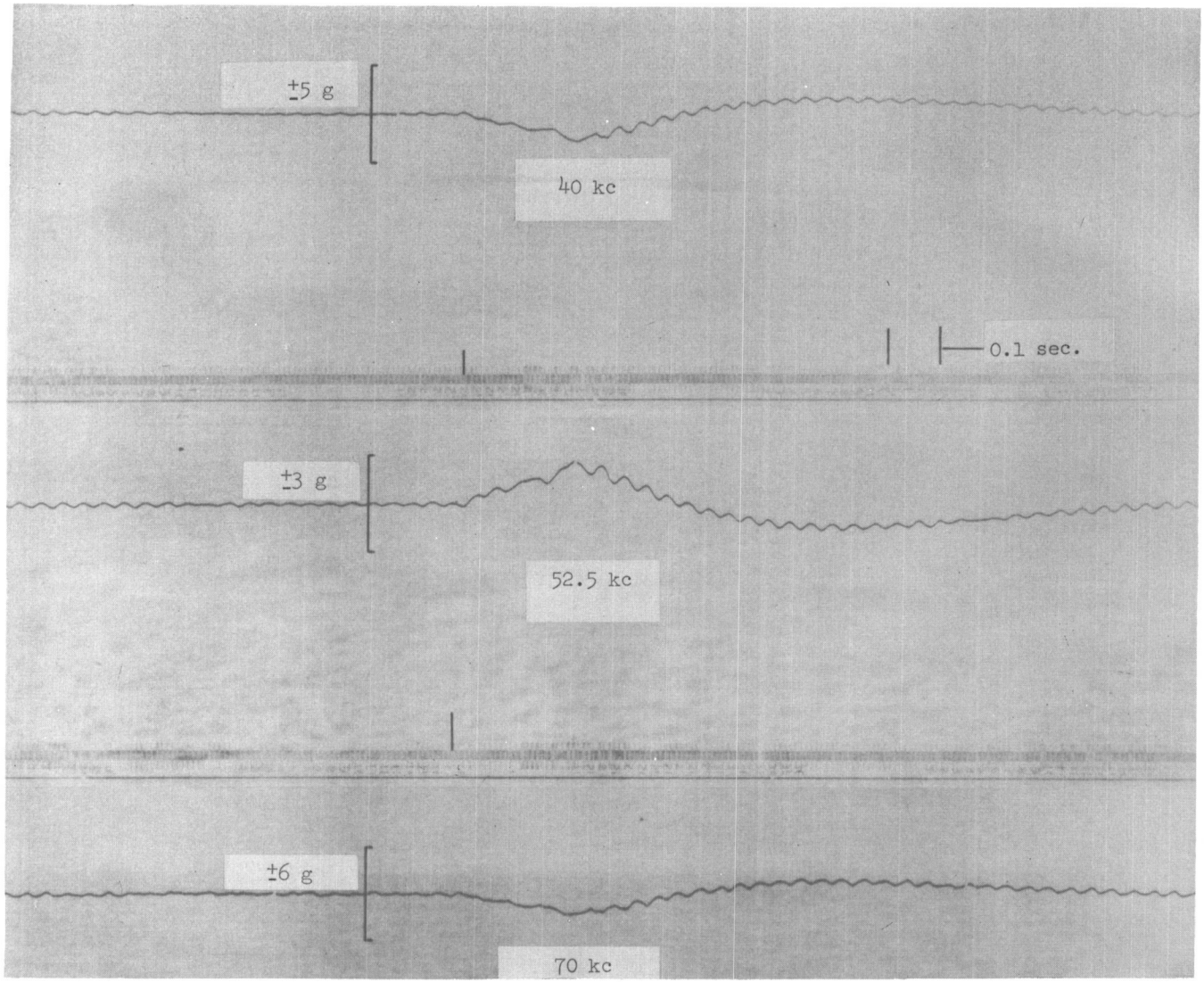

(a) 25 cps low pass filter.

Figure 87.- Booster engine cutoff.

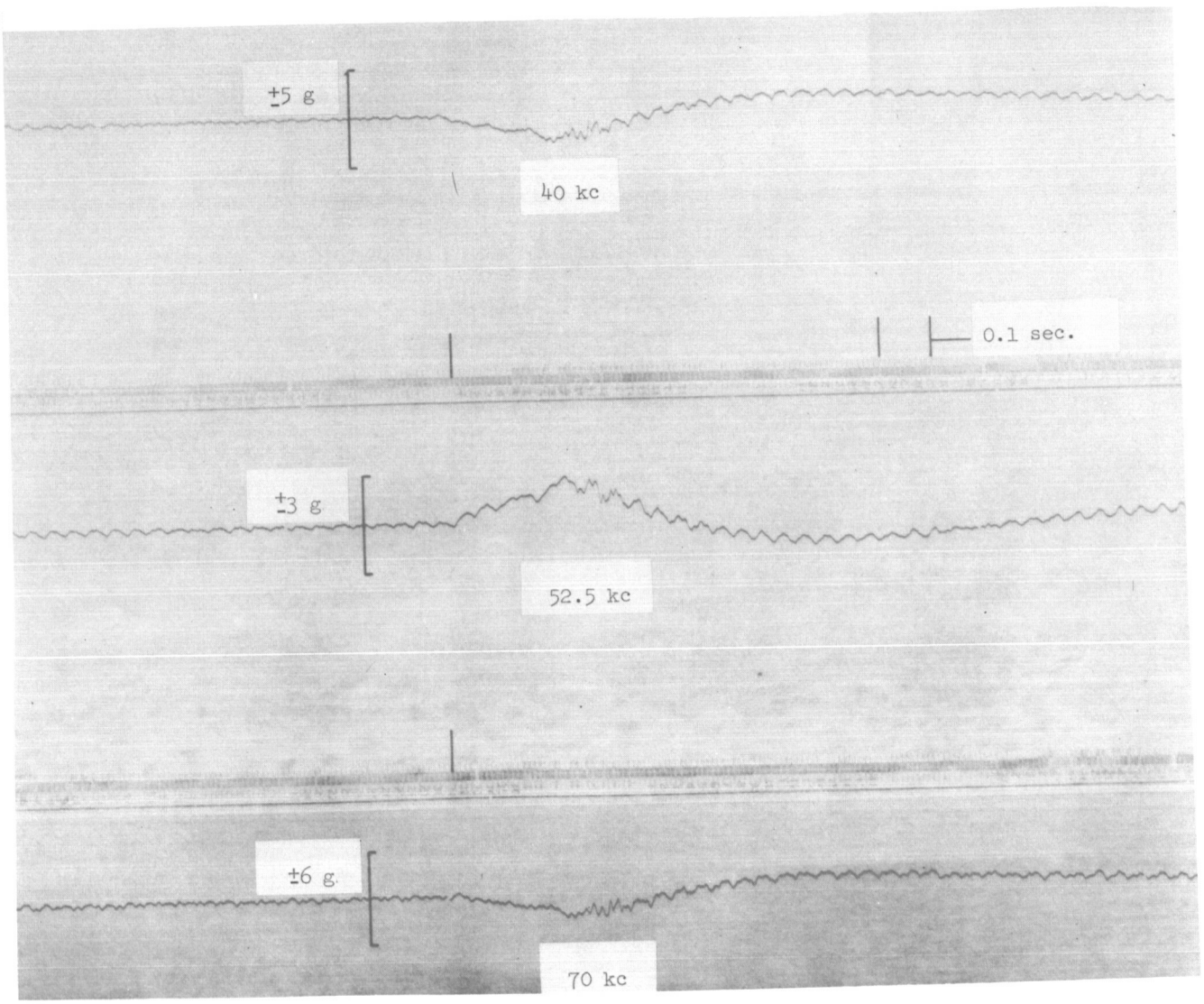

(b) 59 cps low pass filter.

Figure 87.- Continued.

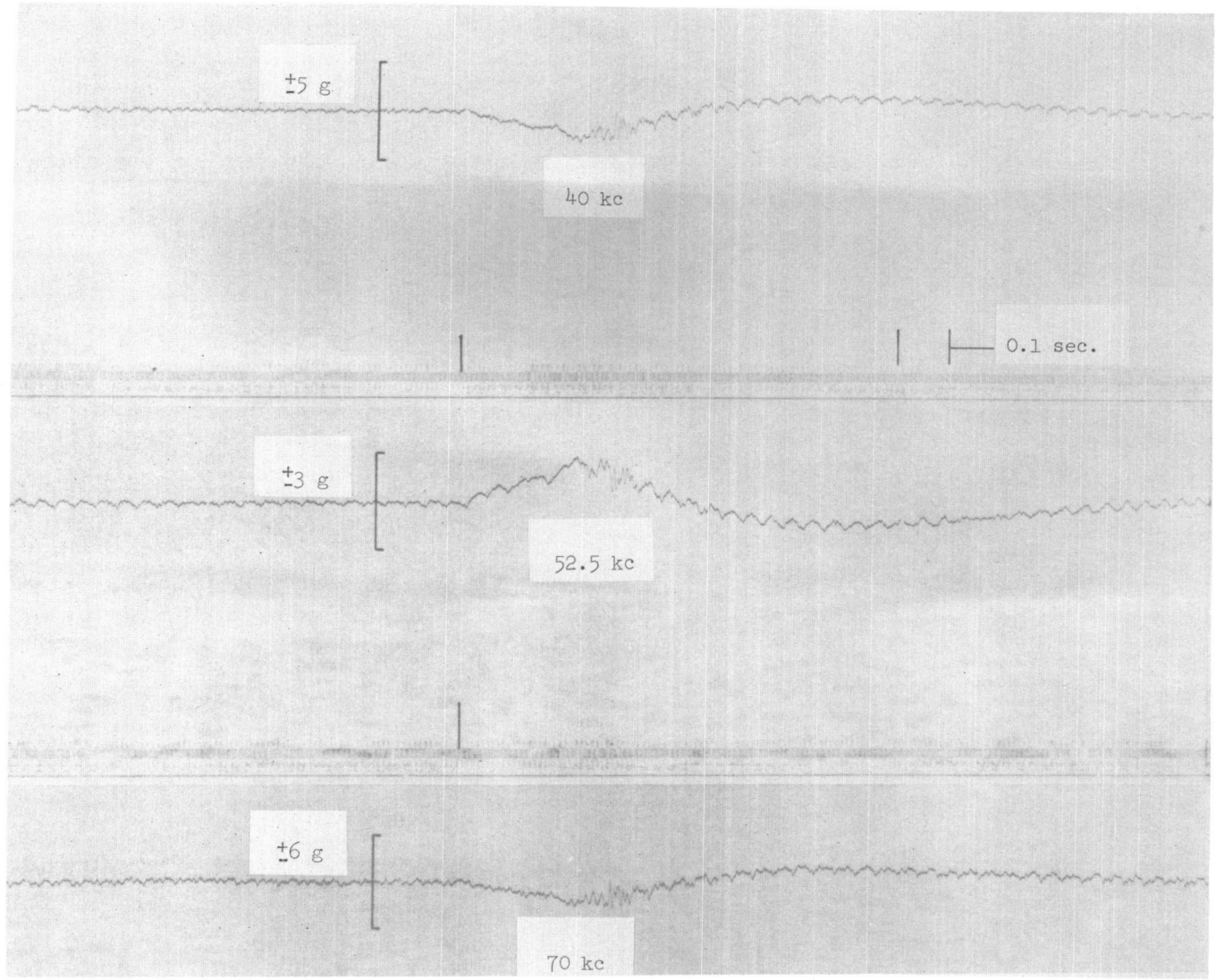

(c) 110 cps low pass filter.

Figure 87.- Continued.

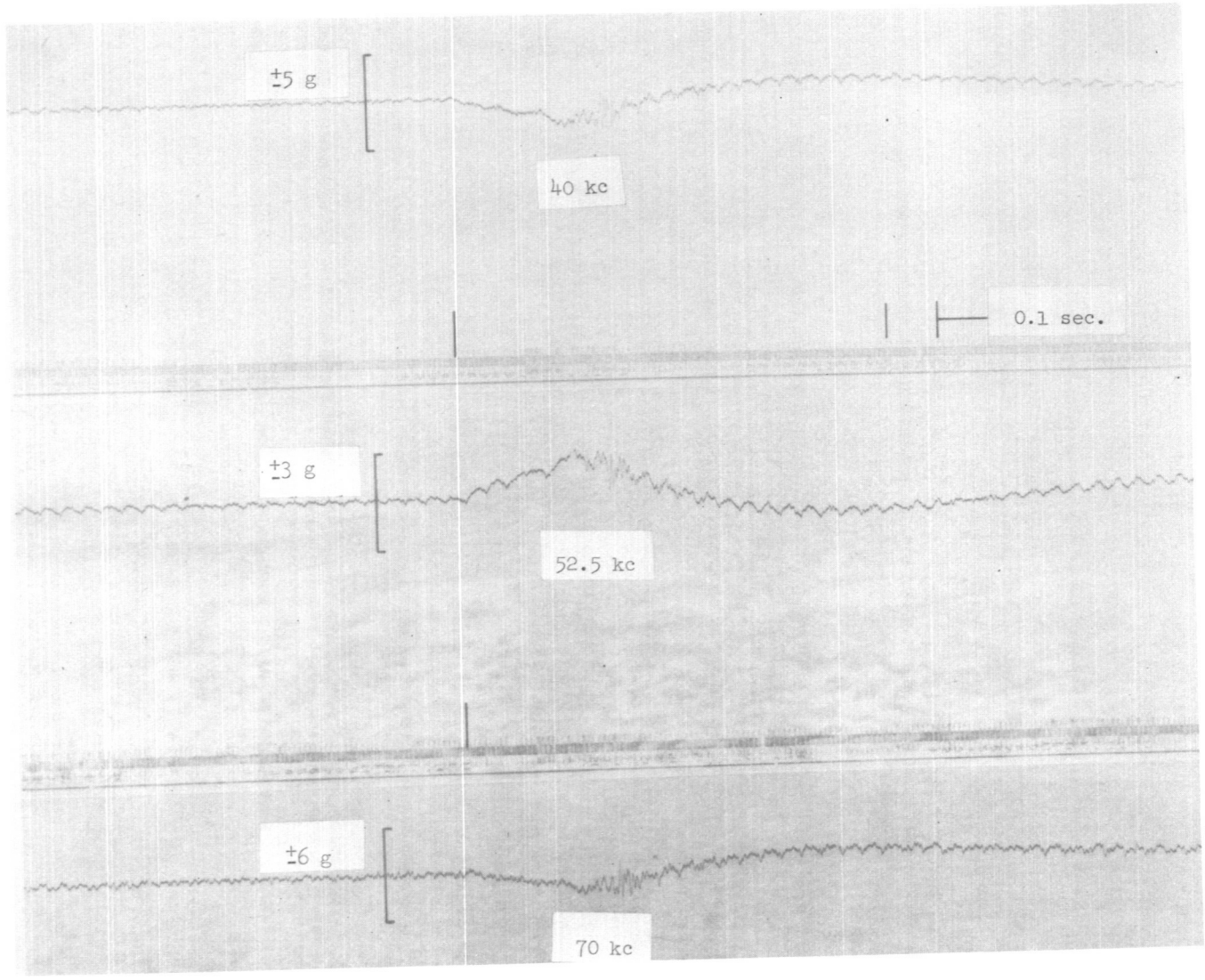

(d) 220 cps low pass filter.

Figure 87.- Concluded.

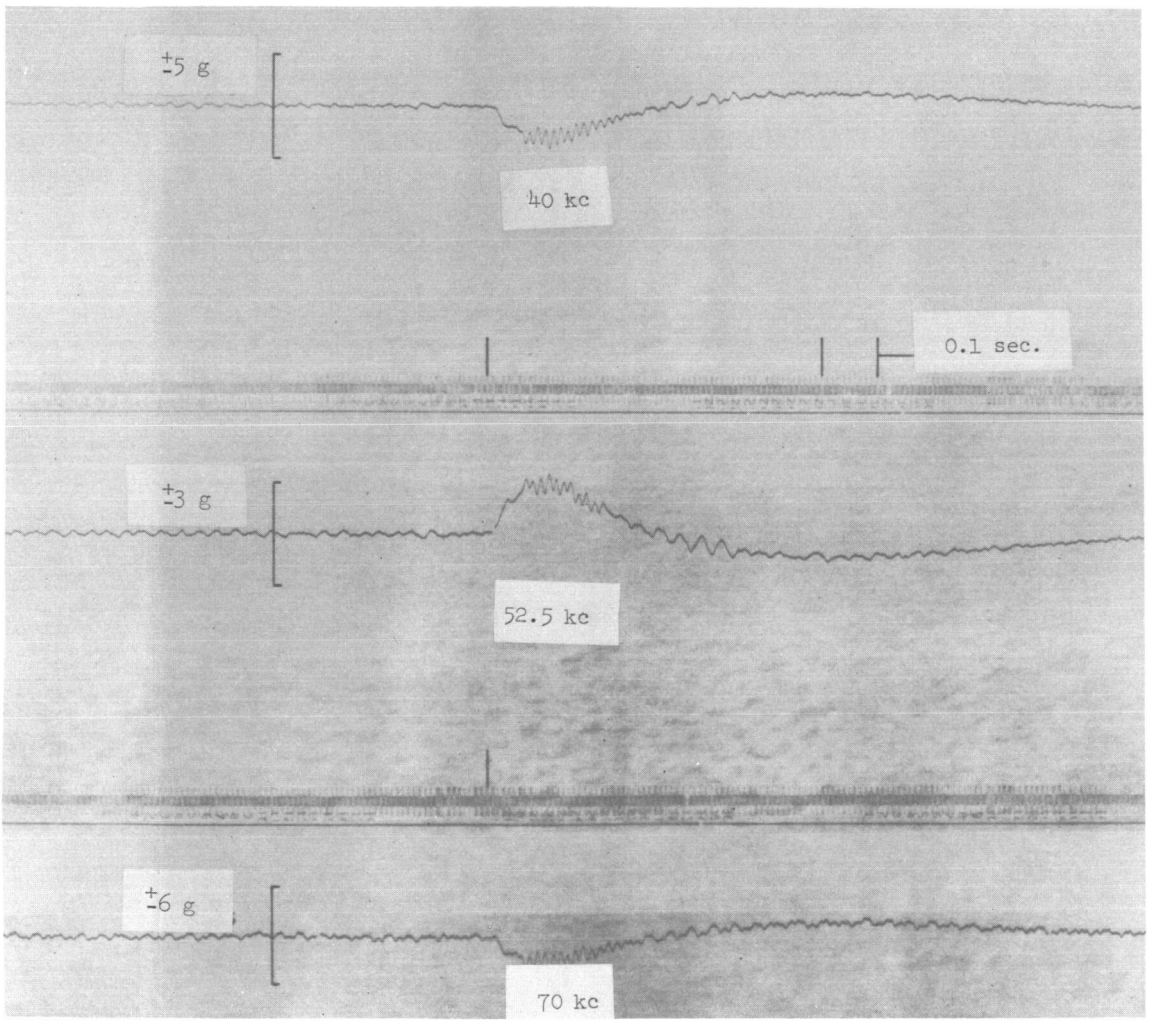

(a) 59 cps low pass filter.

Figure 88.- Sustainer engine cutoff.

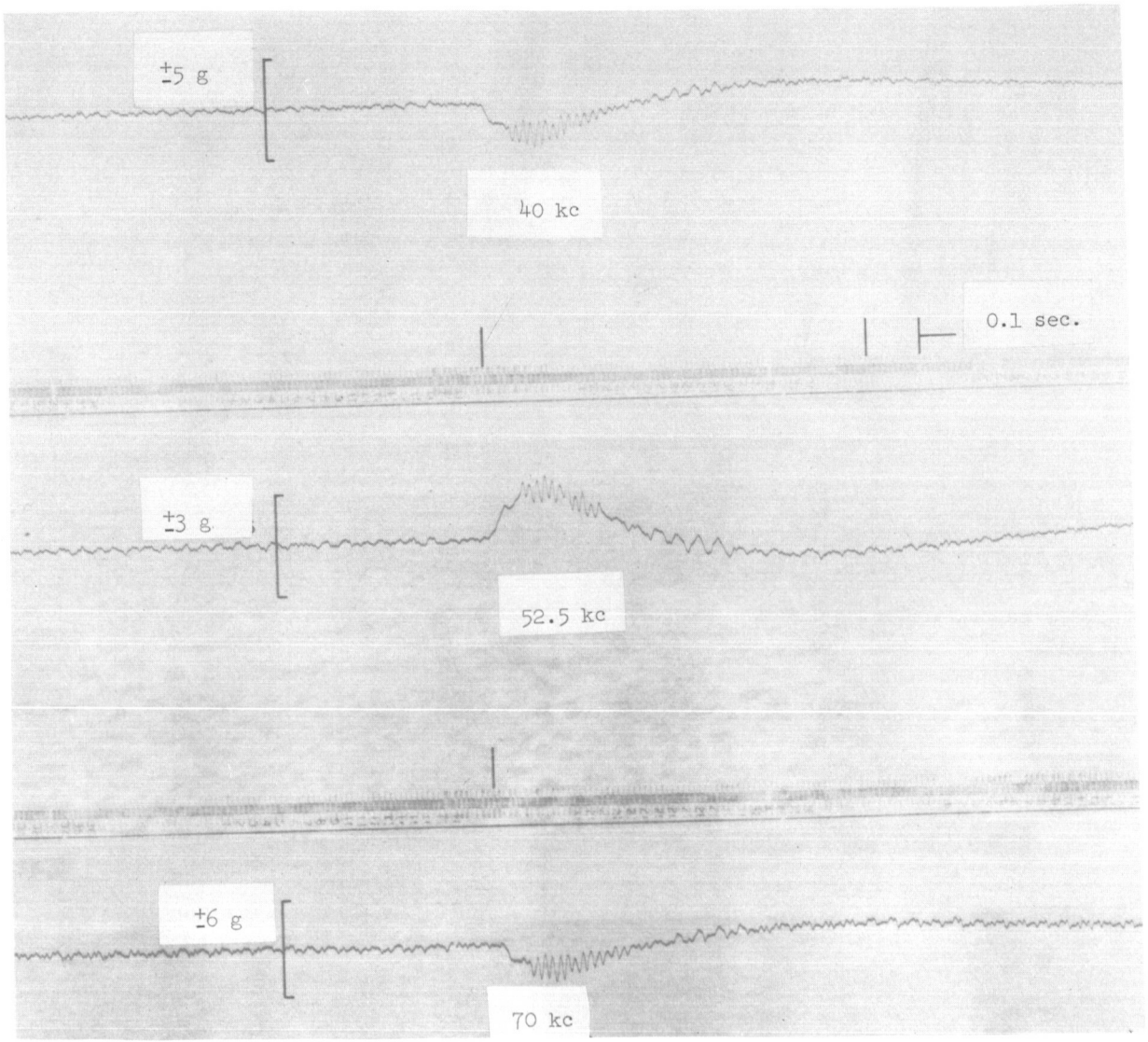

(b) 110 cps low pass filter.

Figure 88.- Continued.

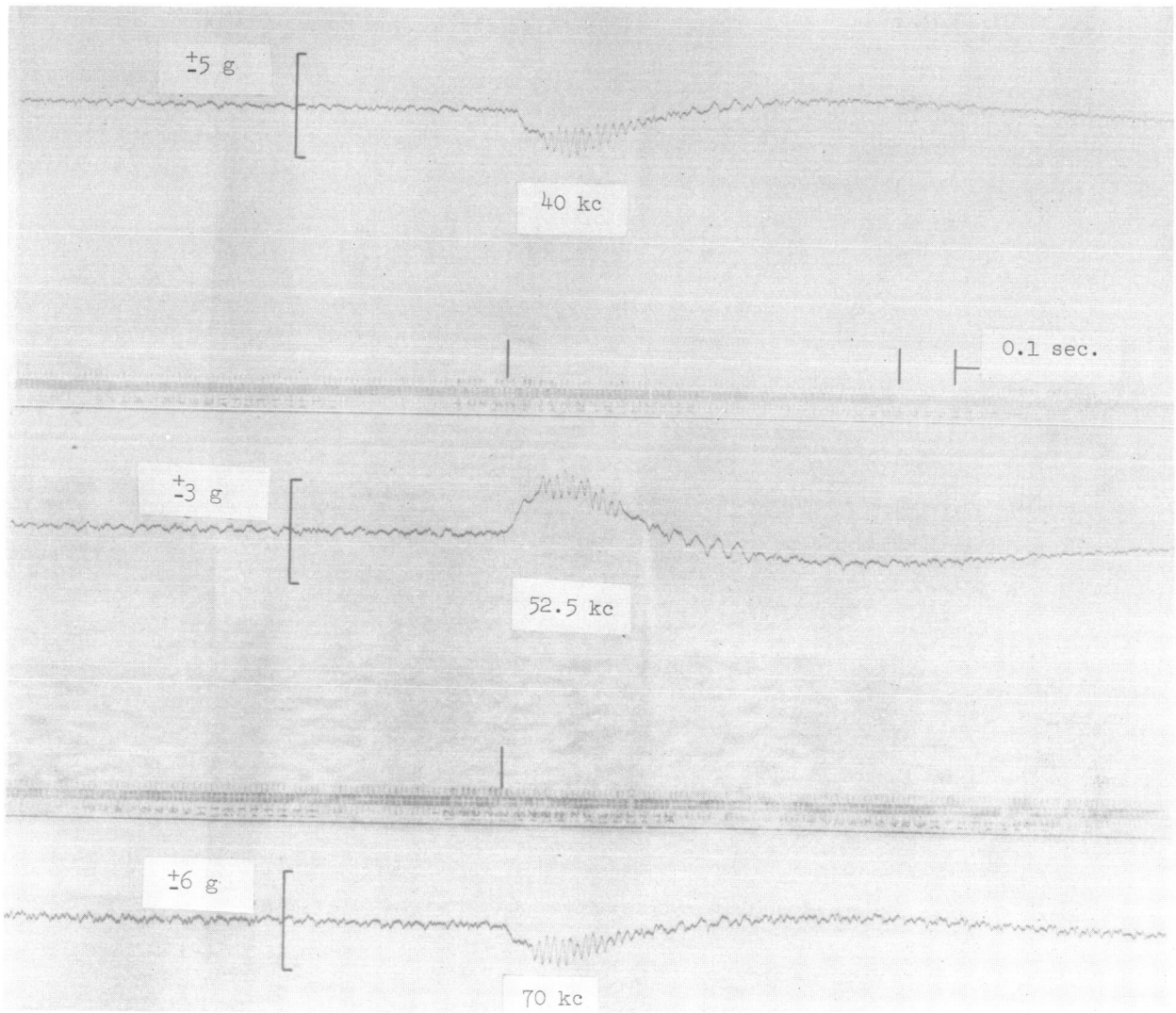

(c) 220 cps low pass filter.

Figure 88.- Continued.

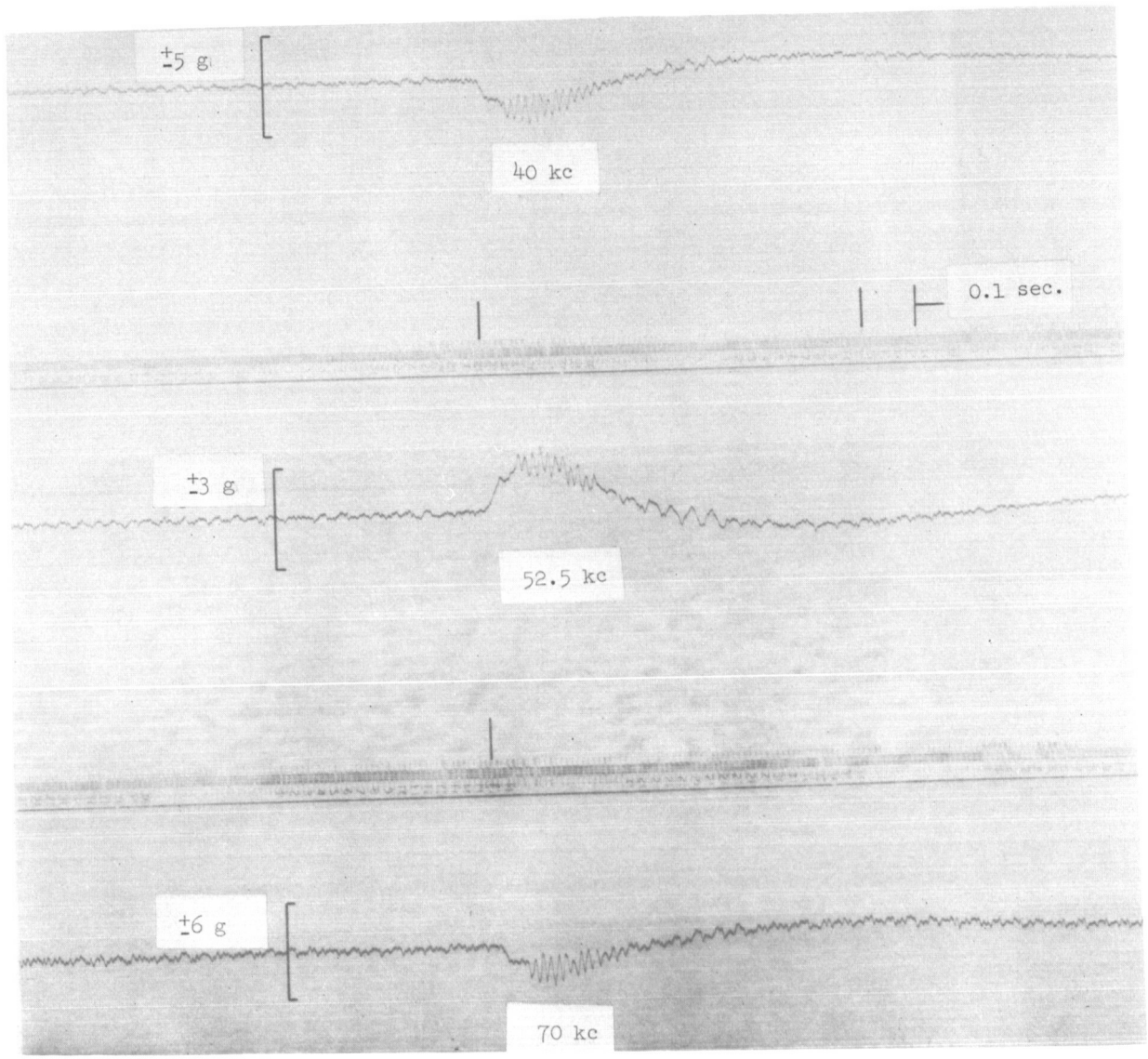

(d) 330 cps low pass filter.

Figure 88.- Continued.

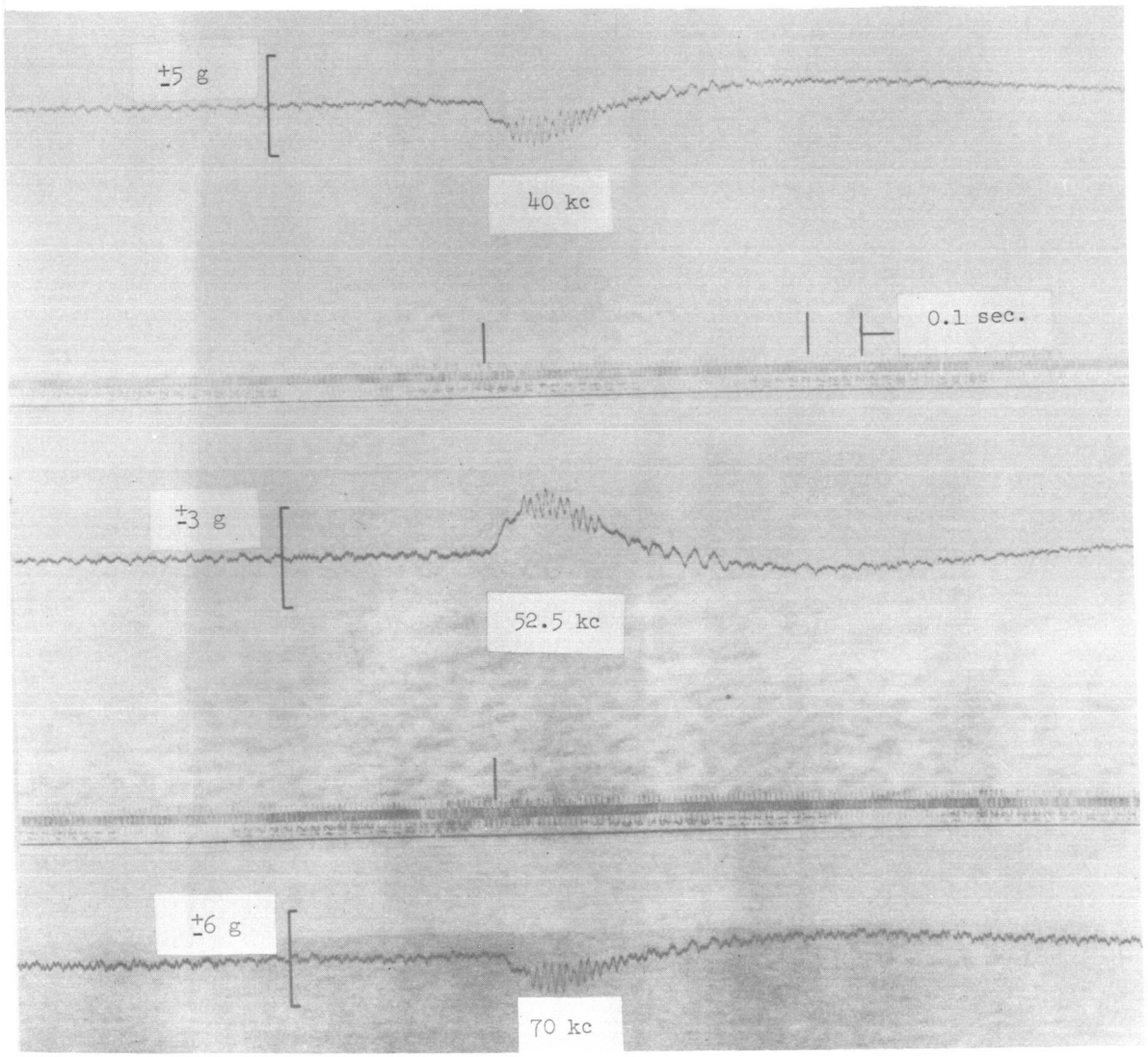

(e) 600 cps low pass filter.

Figure 88.- Concluded.

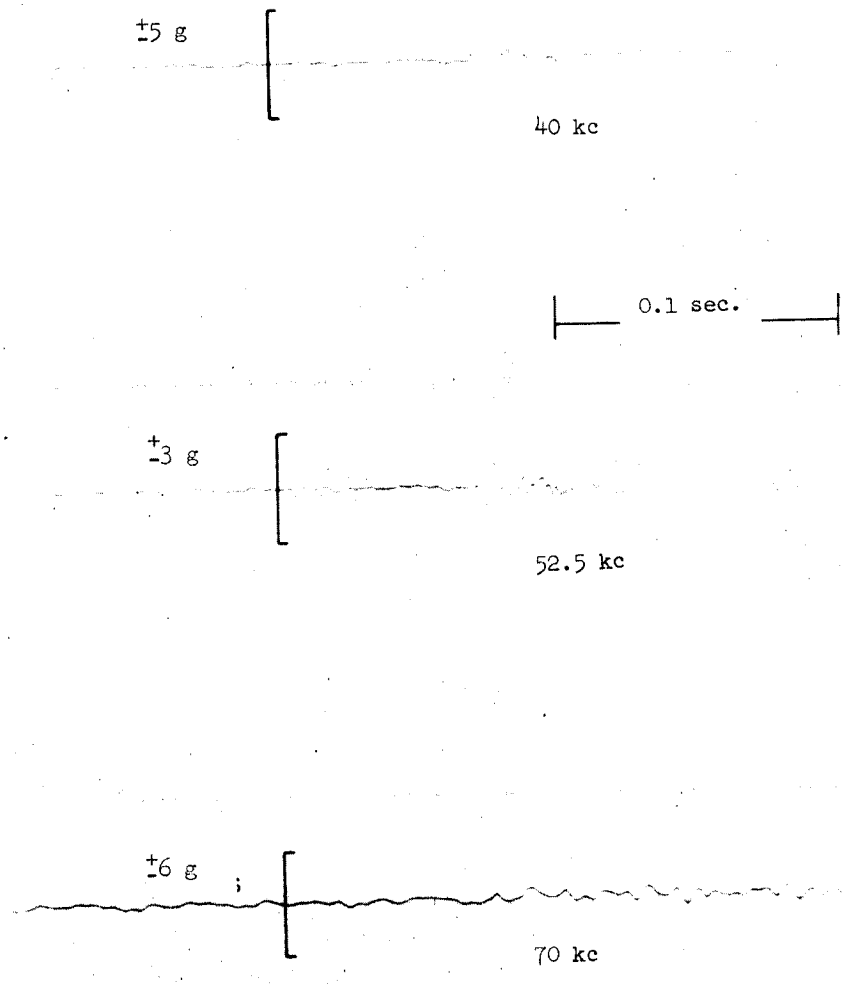

(a) 110 cps low pass filter.

Figure 89.- Shroud jettison.

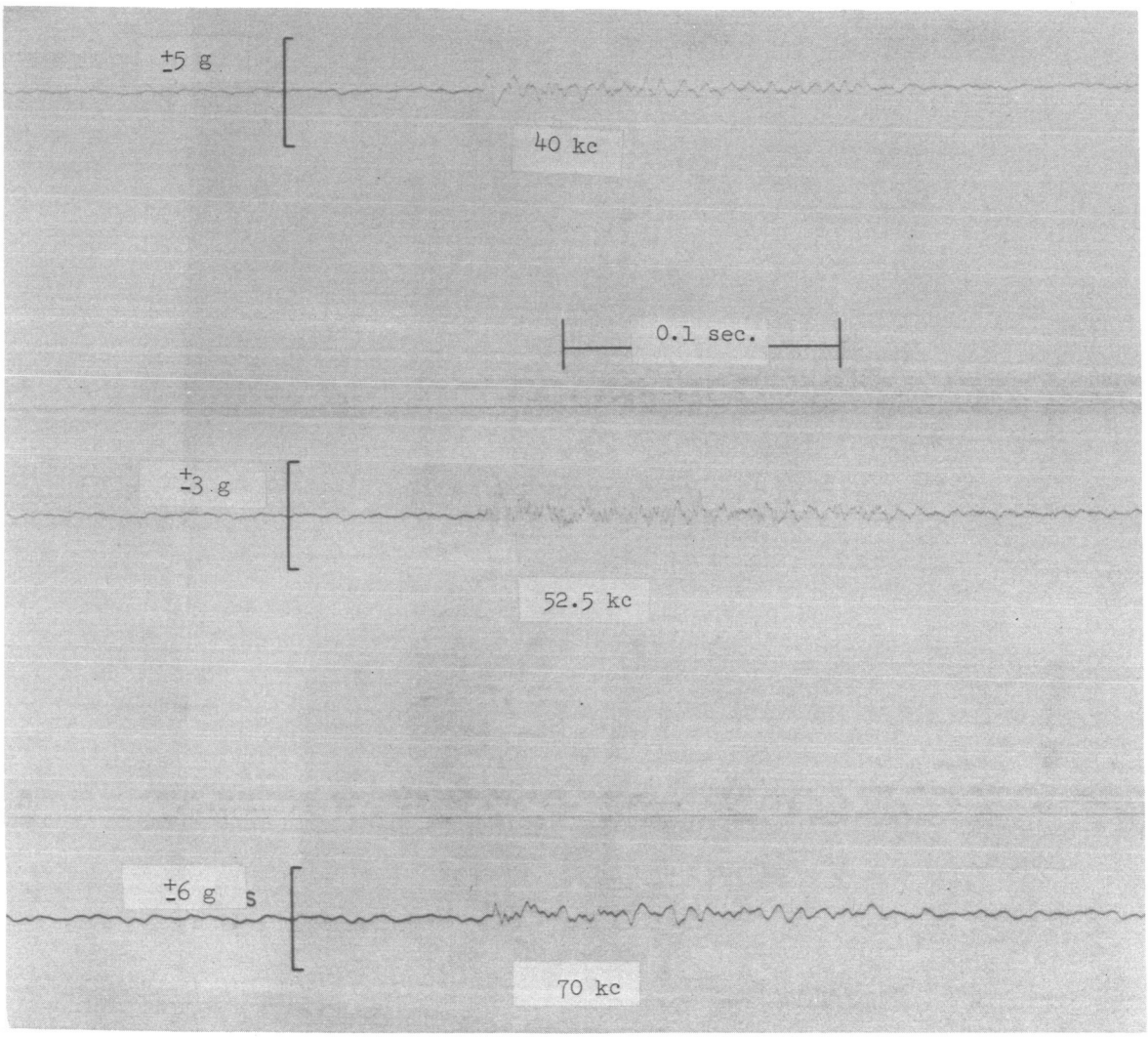

(b) 220 cps low pass filter.

Figure 89.- Continued.

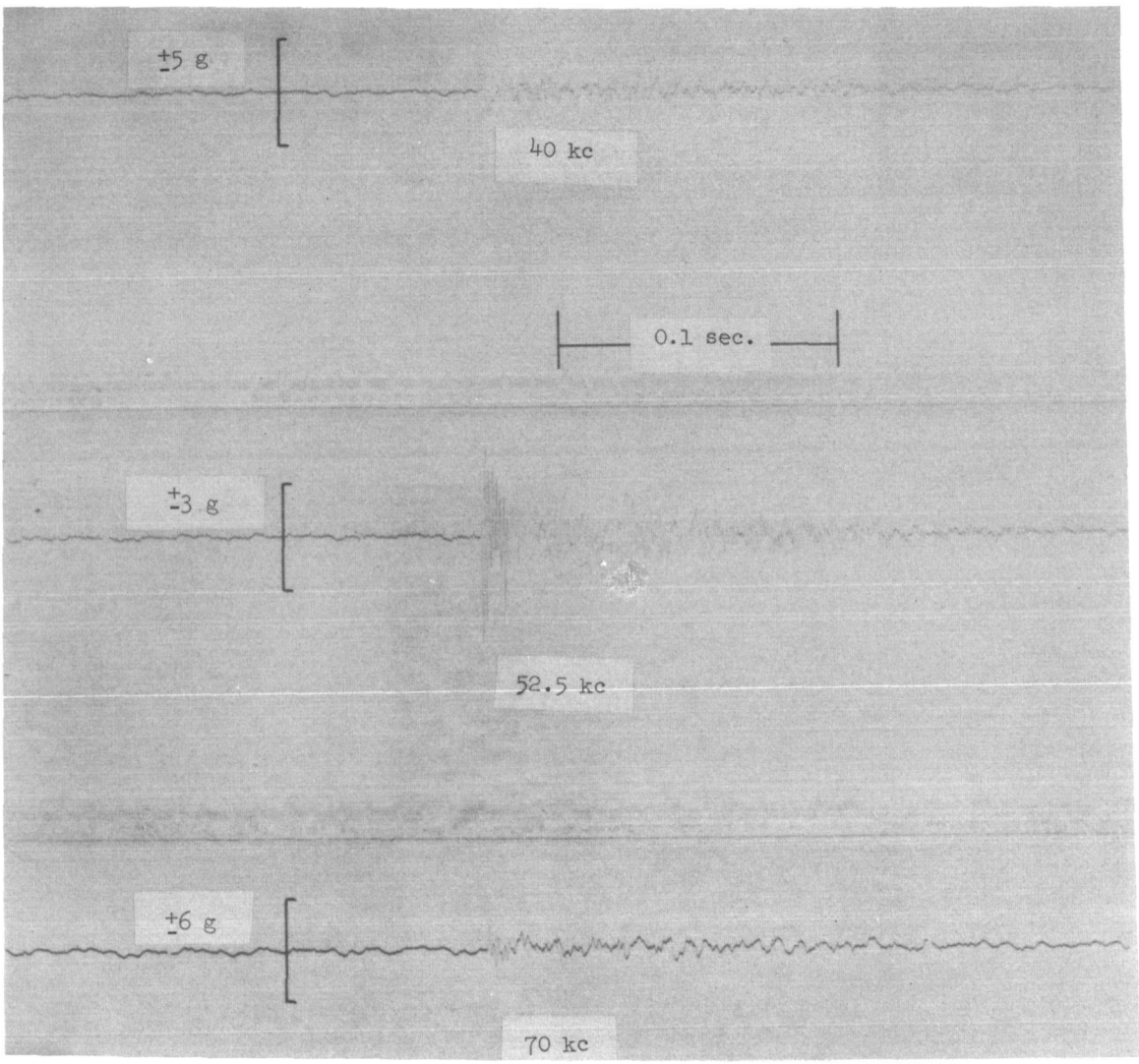

(c) 330 cps low pass filter.

Figure 89.- Concluded.

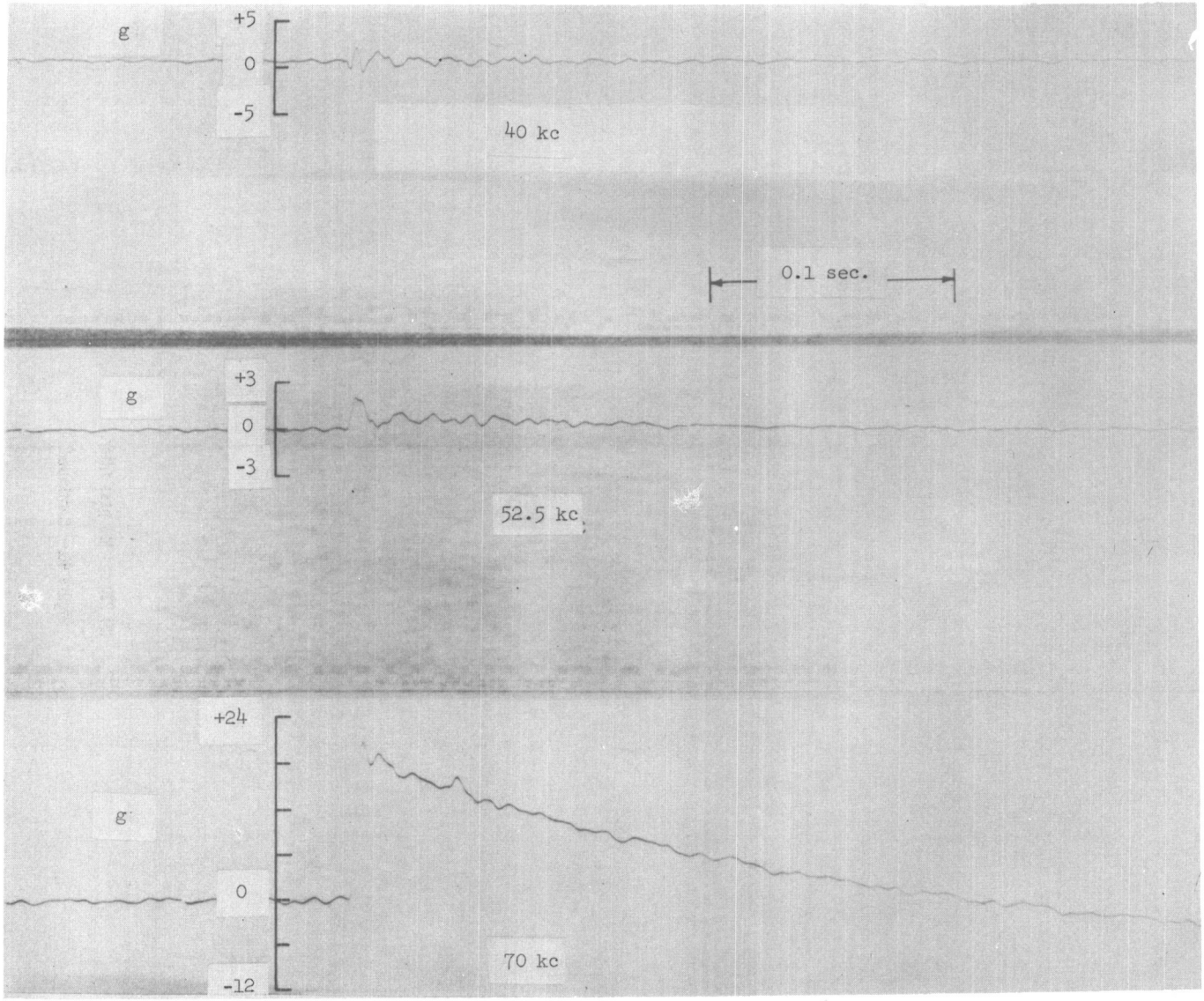

(a) 110 cps low pass filter.

Figure 90.- Spacecraft separation.

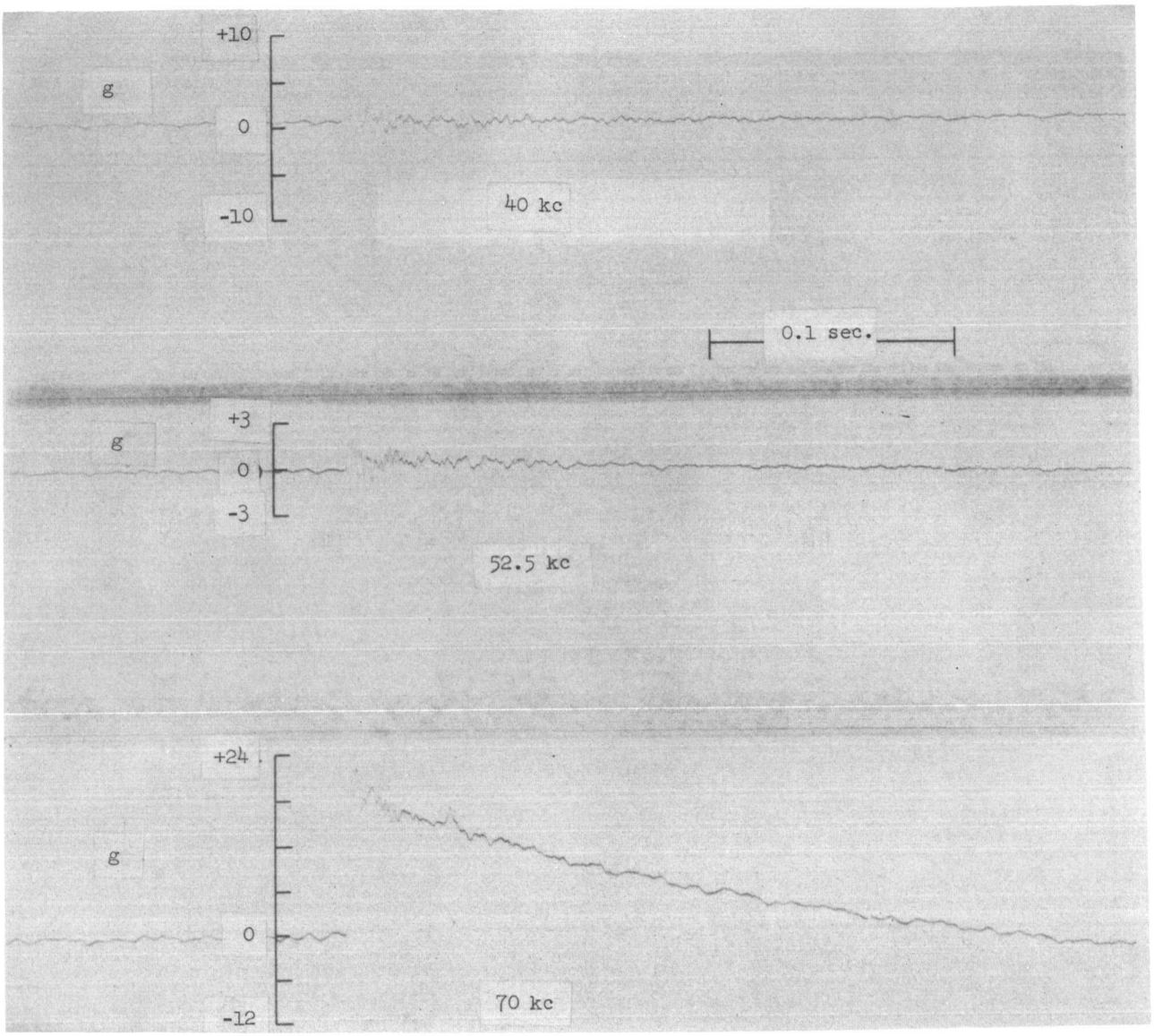

(b) 220 cps low pass filter.

Figure 90.- Continued.

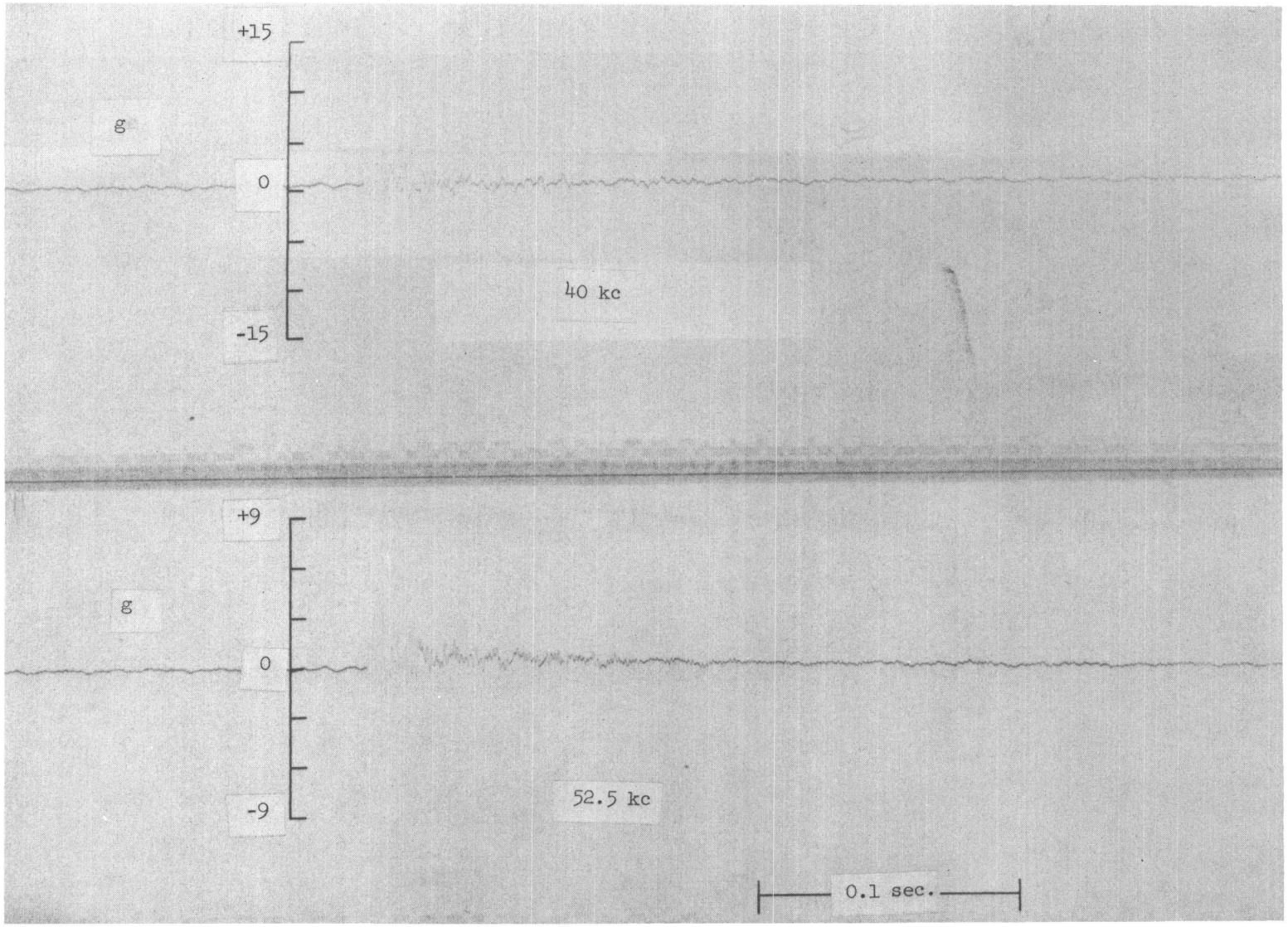

(c) 330 cps low pass filter; channels 16 and 17.

Figure 90.- Continued.

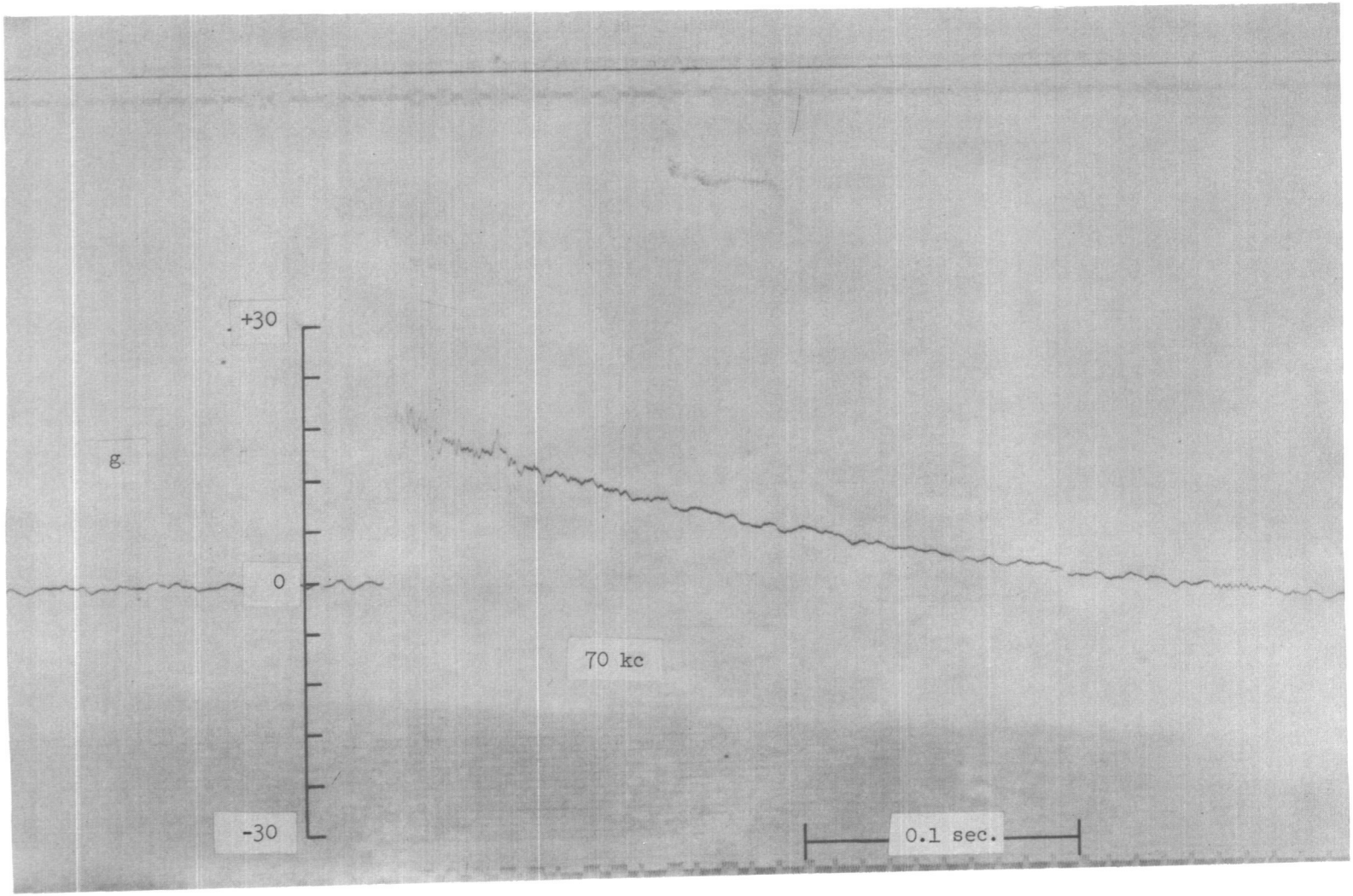

(d) 330 cps low pass filter; channel 18.

Figure 90.- Continued.

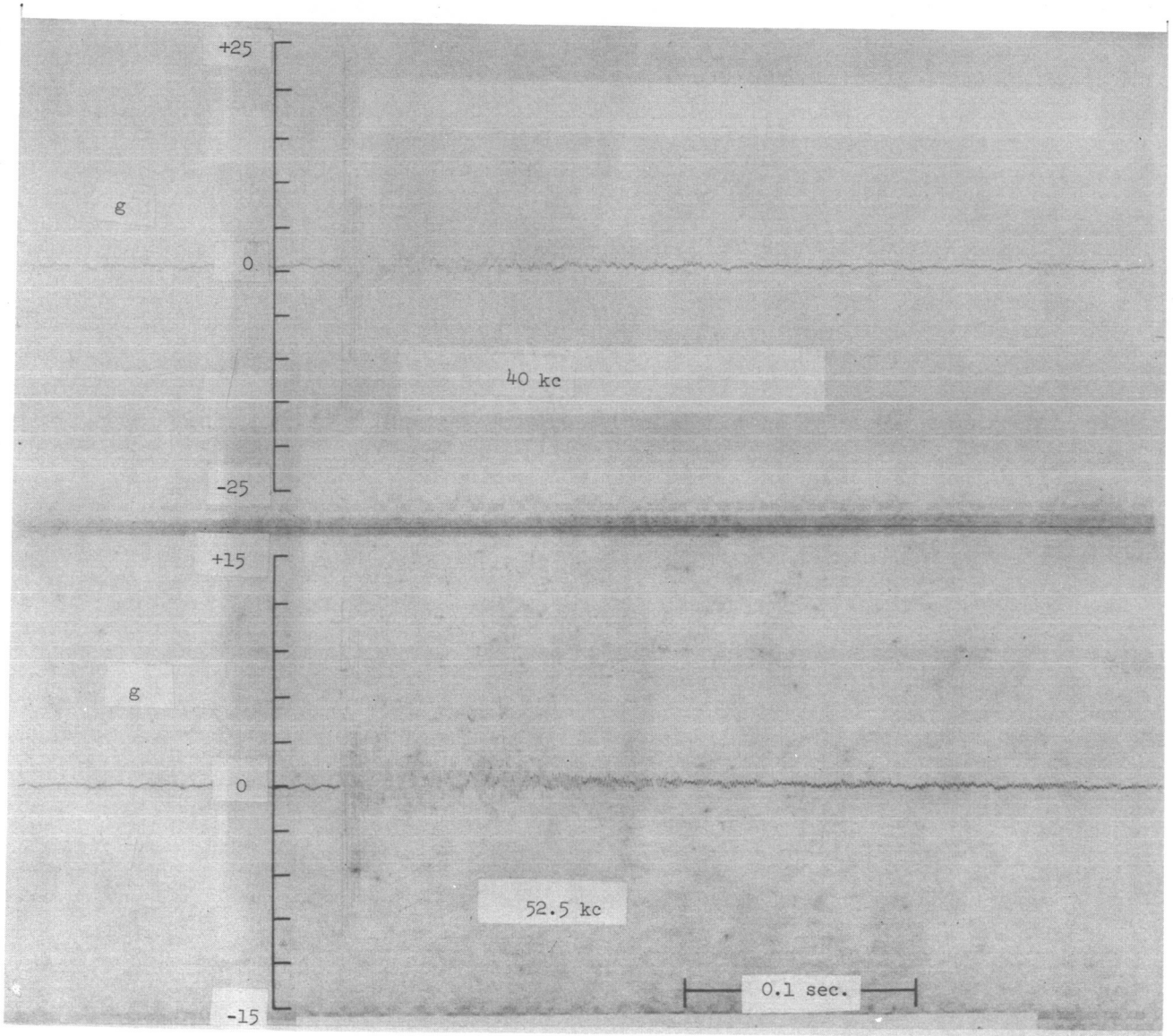

(e) 600 cps low pass filter; channels 16 and 17.

Figure 90.- Continued.

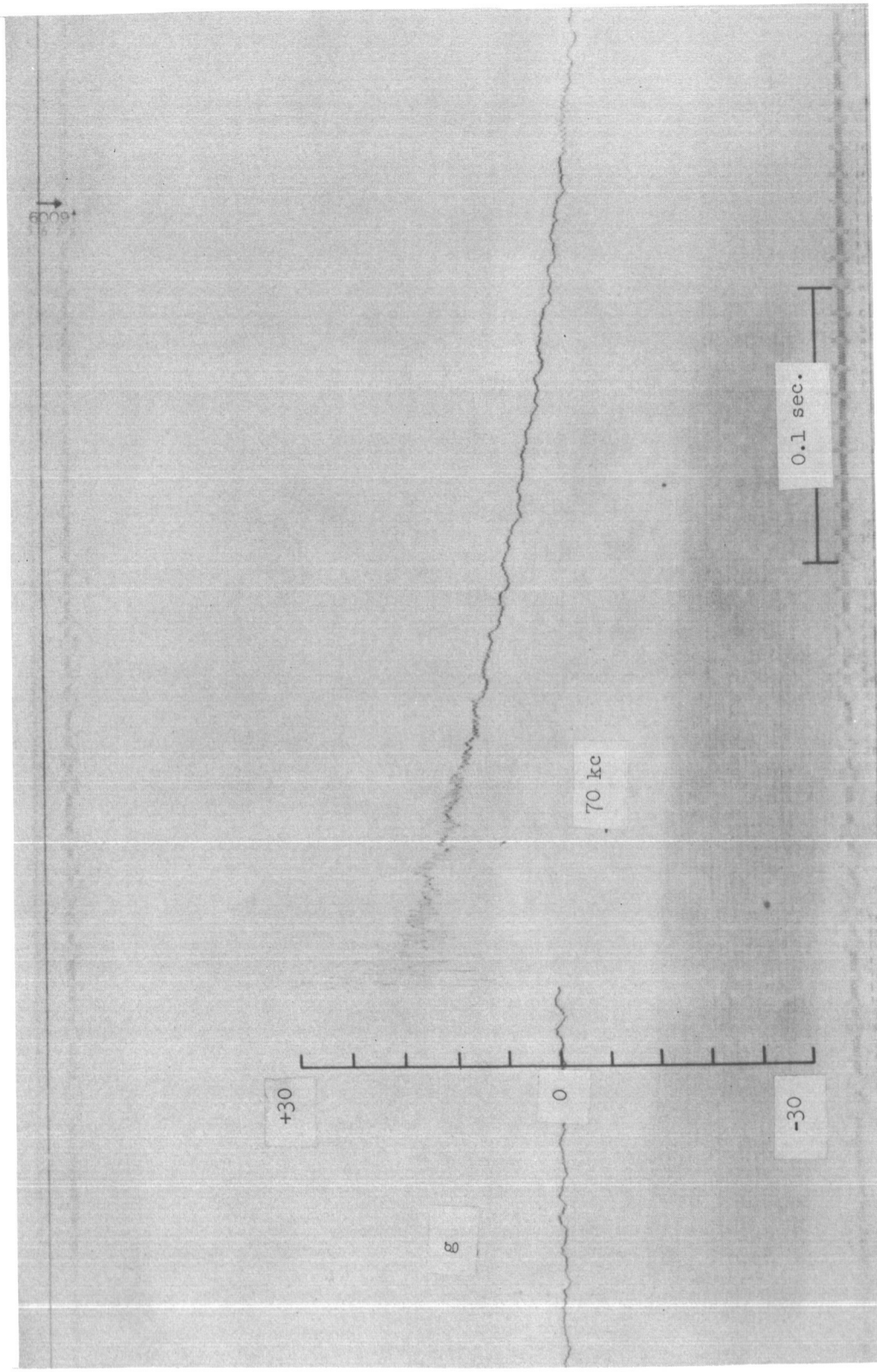

(f) 600 cps low pass filter; channel 18.

Figure 90.- Concluded.

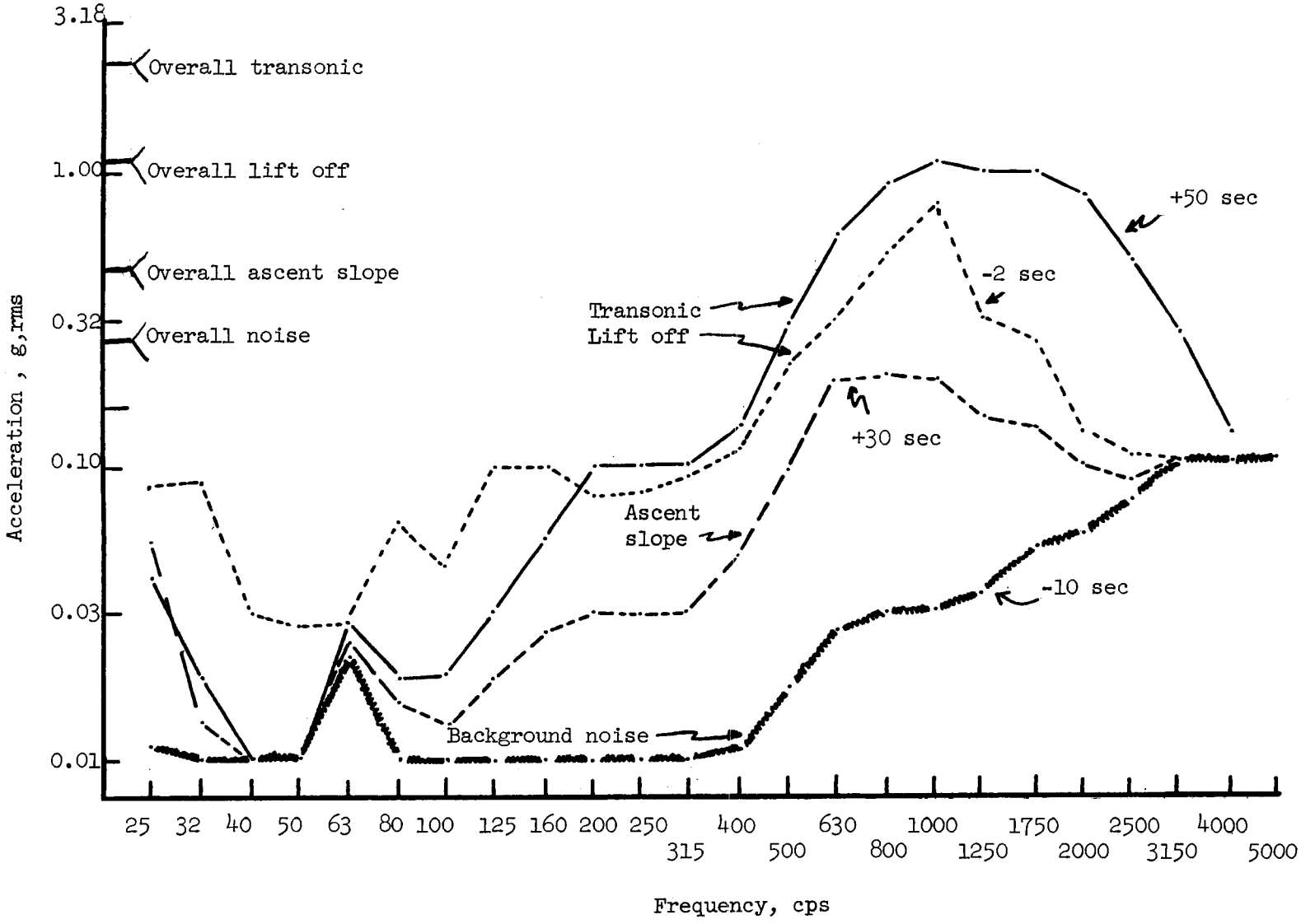

Figure 91.- One-third-octave band analyses. Selected events; 52.5 kcps channel.

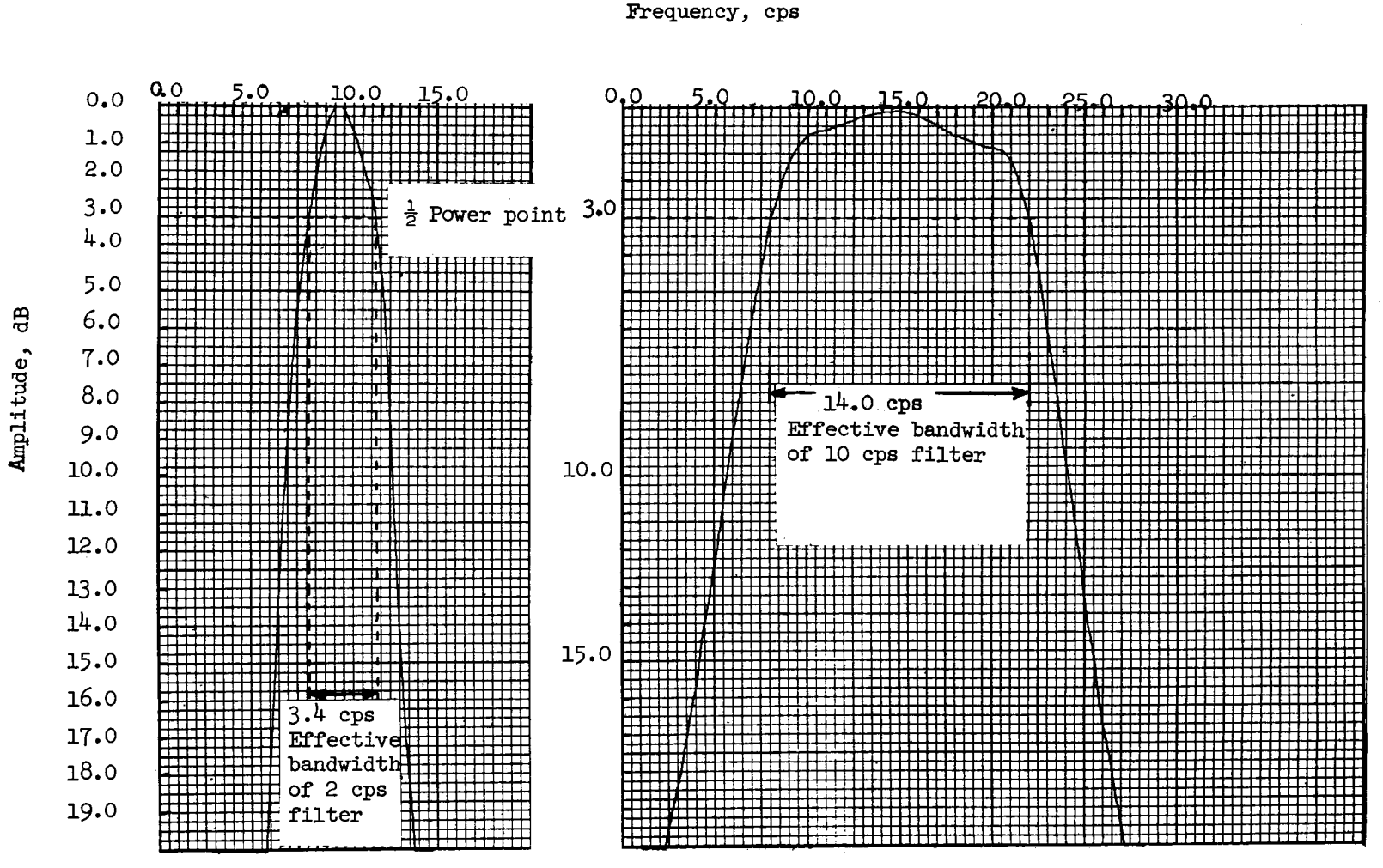

Figure 92.- Filter response curves. 2 and 10 cps narrow band filters.

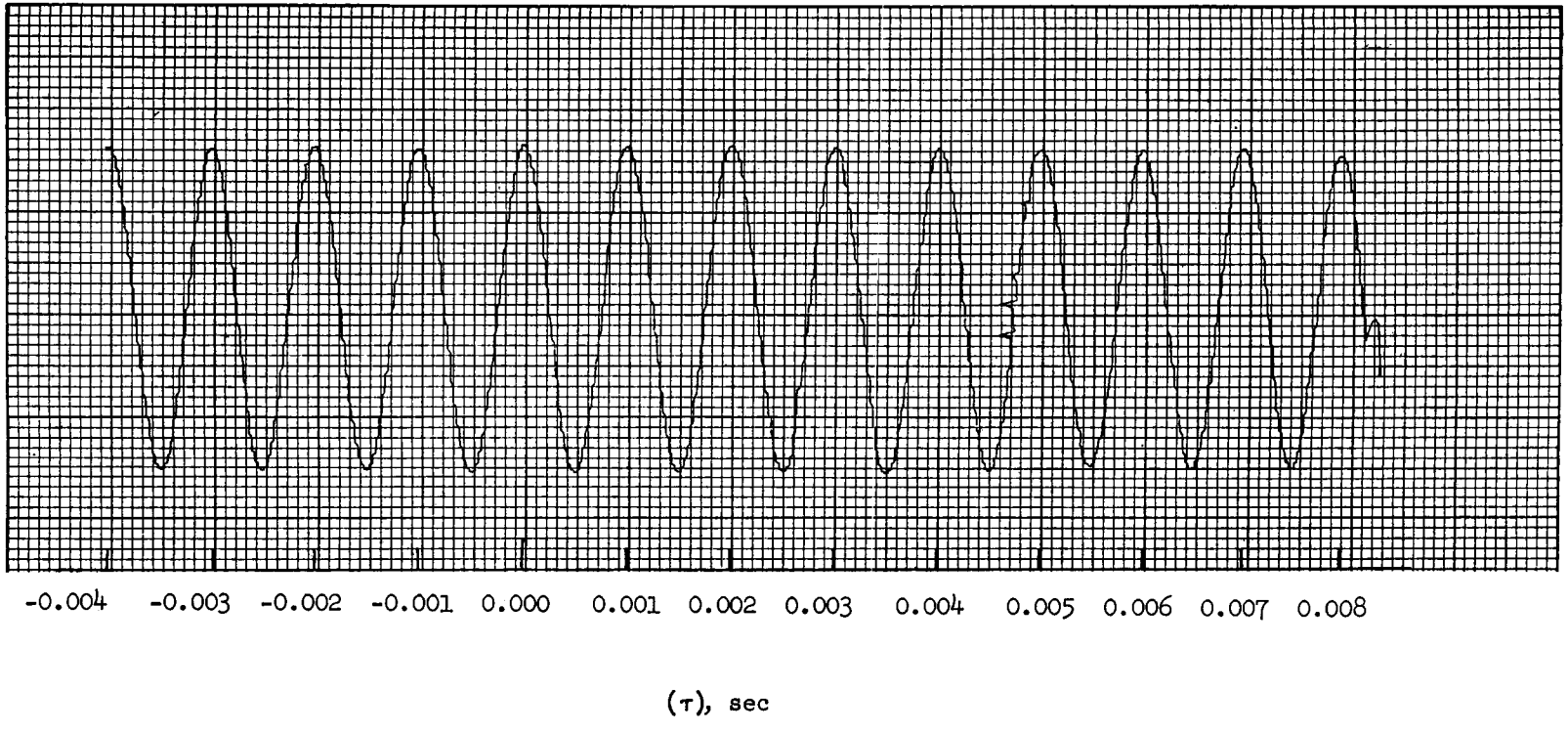

Figure 93.- 1000 cps calibration signal for auto- and cross-correlation analyses.

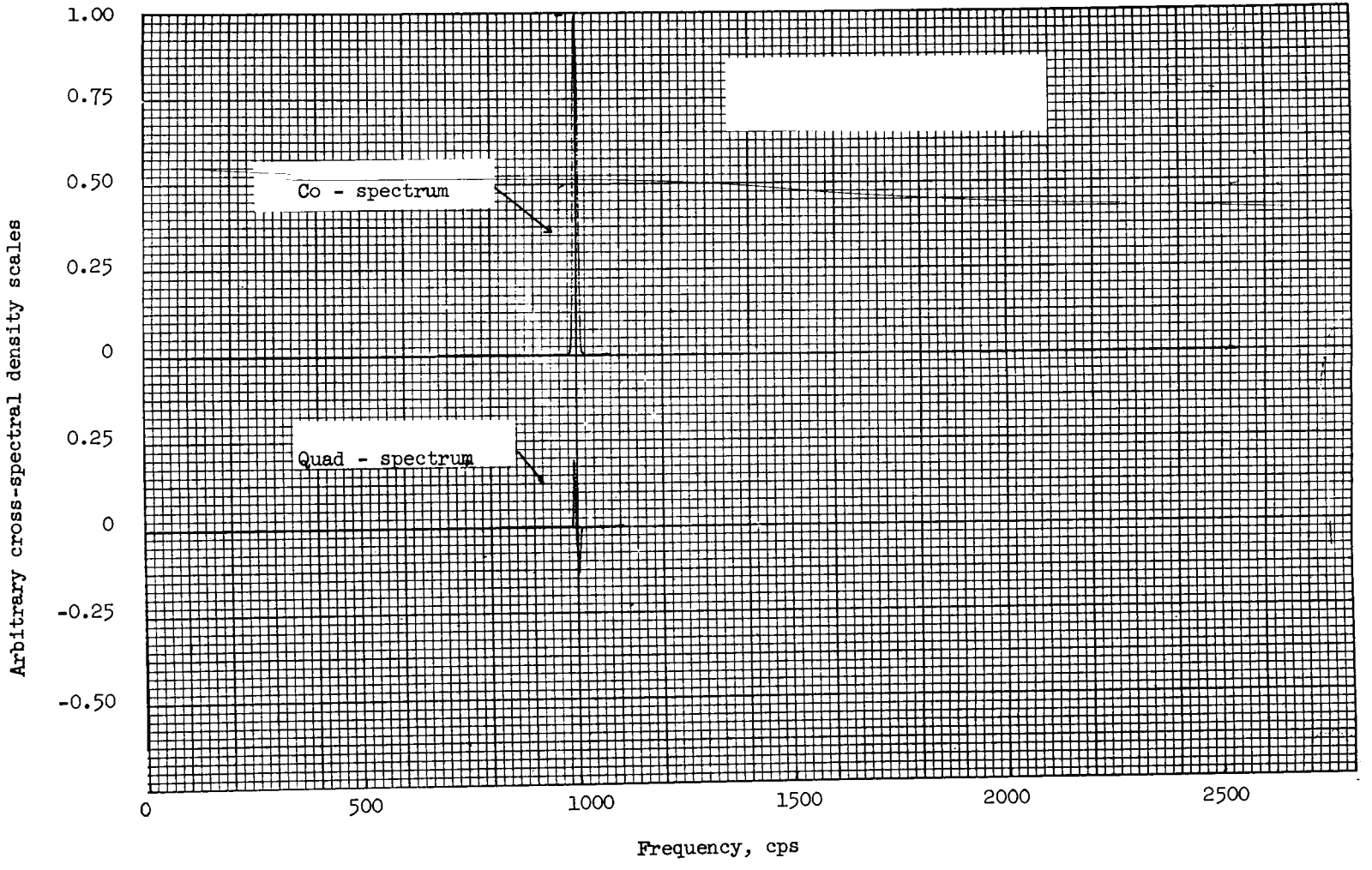

Figure 94.- 100 percent sinusoidal calibration signal for cross-spectral density analysis.